VI. Applications

In this chapter we will study such important topics as heat exchangers, flowmeters, and turbomachines. We will also evaluate the thermal hydraulics response of systems to transients and heat generation from nuclear energy.

VIa. Heat Exchangers

Heat exchanger (HX) is a generic term applied to a wide range of mechanical systems, which are designed for the purpose of exchanging thermal energy between two streams of fluids separated by a solid surface. Some heat exchangers are used as heat sinks including automotive inter-coolers, containment air coolers, cooling towers, automotive radiators, and power plant condensers. Some other heat exchangers are used as a heat source including boilers, radiators for space heating, and steam generators. For example, a nuclear plant utilizes many heat exchangers. In a typical plant, feedwater heaters are employed in the balance of plant to improve plant thermal efficiency. Also, other heat exchangers, such as the component cooling water and shutdown cooling (also known as the residual heat removal) system, provide a heat sink for the reactor during the shutdown period. Finally, the service water heat exchanger provides a heat sink for the balance of plant equipment. Heat exchangers have a hot side and a cold side separated by tubes or plates. Heat transfer between the fluids in each side takes place through the surface dividing the hot side and the cold side. Heat transfer may take place between liquid and liquid, liquid and gas, and gas and gas. Heat exchangers may also carry two-phase flow resulting in boiling or in condensation. Heat exchangers may be operating at steady-state or transient conditions. Due to such design variations, heat exchangers require careful analysis in design optimization as well as in performance evaluation. In this chapter we will deal primarily with the thermal aspects of tubular heat exchangers.

1. Definition of Heat Exchanger Terms

Concentric parallel flow heat exchanger consists of a tube surrounded by a shell. In parallel flow heat exchangers, both hot and cold streams flow in the same direction as shown in Figure VIa.1.1.

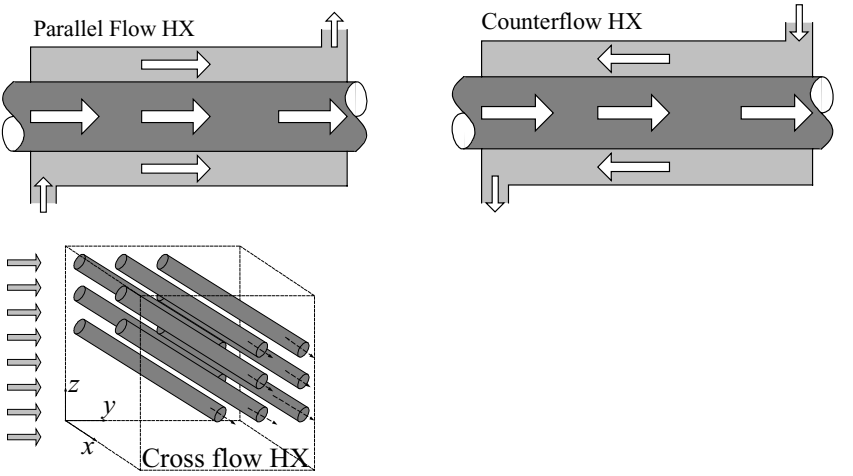

Figure VIa.1.1. Schematics of parallel, counterflow, and cross flow heat exchangers

Concentric counter flow heat exchanger consists of a tube surrounded by a shell. In counter flow heat exchangers, the hot and cold streams flow in opposite directions as shown in Figure VIa.1.1.

Cross flow heat exchangers are generally used in gas-liquid applications. They include tubes with a stream flowing parallel to the *xy*-plane and cross flow parallel to the the *yz*-plane and perpendicular to the tube axis. The cross flow may be mixed, as shown in Figure VIa.1.1, or unmixed by passing cross flow through parallel plates.

Shell and tube heat exchanger is similar to the concentric heat exchanger. However, shell and tube heat exchangers consist of multi tubes held in place by baffle plates. These plates prevent tube vibration and enhance the rate of heat transfer by diverting the shell-side fluid in a cross flow manner, as shown in Figure VIa.1.2. Shell and tube heat exchangers may be arranged in series to obtain

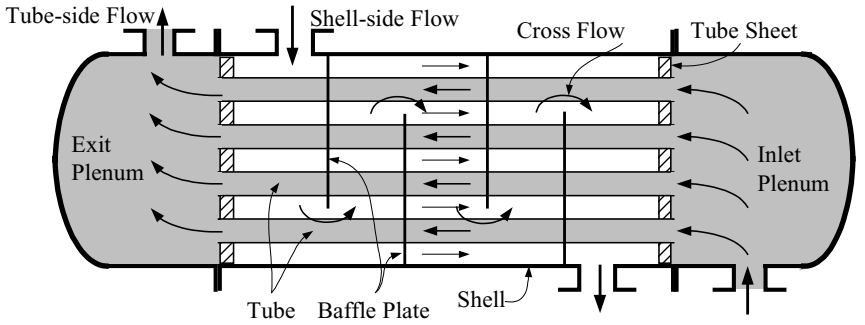

Figure VIa.1.2. Schematic of a shell and tube heat exchanger

several cascaded shells. Each heat exchanger has a minimum of four ports. As shown in Figure VIa.1.2, there is an inlet port and an outlet port in the hot side. Similarly, there is an inlet and an outlet port in the cold side. Tubes are either straight or bent in the form of a U. Heat exchangers including straight tubes have an inlet *plenum* and an outlet plenum. Tubes are installed inside tube sheets, which also act as barriers between the plenum fluids and the shell-side fluid.

Fouling factor f, is a measure of cleanliness of heat exchangers. Fluid streams generally carry impurities. Sedimentation of the impurities over time leads to a layer of deposit. This poses a resistance to heat transfer across the solid surface. The sedimentation may also consist of sludge that would pit and corrode solid surfaces. Maintaining a closely monitored chemistry of the fluid stream and periodic cleaning of heat exchangers is essential in ensuring proper operation of the device. In a shell and tube heat exchanger, for example, cleaning of the shell side is especially challenging due to the presence of the baffle plates. In such cases, the cleaner stream flows in the shell side, as cleaning the inside of the tubes is by far easier. In power plants using large bodies of water as the heat sink, steam always condenses on the tubes with river, lake, bay, or ocean water flowing in the tubes. Fouling may be categorized as particulate fouling, crystallization fouling, corrosion fouling, biofouling, and chemical reaction fouling (Kakac). One way to account for fouling in the design process of heat exchangers is to increase the surface area for heat transfer. Fouling factor has units of thermal resistance $ft^2 \cdot h \cdot F/Btu$ or $m^2 \cdot K/W$. Some typical values are as follows:

Fluid	f ($m^2 \cdot K/W$)	f ($ft^2 \cdot h \cdot F/Btu$)
Transformer oil	0.000176	0.0010
Engine lube oil	0.000176	0.0010
Crude oil	0.000352	0.0020
Heavy gas oil	0.000881	0.0050
Heavy fuel oil	0.001233	0.0070
Vegetable oil	0.000528	0.0030
Seawater	0.000176	0.0010
Brackish water	0.000528	0.0030
Muddy or silt water	0.000705	0.0040
River water (< 50 C)	0.001000	0.0060
Refrigerating liquid	0.000200	0.0011

From: Standards of Tubular Exchangers Manufacturers Association

Overall heat transfer coefficient is given in Equation IVa.6.8 for a clean concentric heat exchanger. To account for fouling resistance, Equation IVa.6.8 should be modified as follows:

$$UA = \left[\frac{1}{\pi d_i L h_i} + \frac{f_i}{\pi d_i L} + \frac{\ln(d_o / d_i)}{2\pi k L} + \frac{f_o}{\pi d_o L} + \frac{1}{\pi d_o L h_o} \right]^{-1} = U_i A_i = U_o A_o \qquad \text{VIa.1.1}$$

where subscripts *i* and *o* stand for tube inside and tube outside, respectively. Tube outside is also known as the *tube bundle*, *shell side*, or *secondary-side*. In Equation VIa.1.1, f_i and f_o are the tube-side and shell-side fouling factors, respectively. Typical values of *U* for various streams are as follows.

Stream A / Stream B	U (W/m^2·K)	U (Btu/ft^2·h·F)
Condensing Steam / Water (Condenser & FWH)	1100 – 5500	200 – 1000
Freon 12 Condenser / Water	300 – 850	50 – 150
Water / Water	850 – 1700	150 – 300
Water / Oil	100 – 350	20 – 60
Gas / Gas	10 – 40	2 – 8

Cleanliness factor, C_F is another measure of heat exchanger cleanliness and is defined as the ratio of the overall heat transfer coefficient when a heat exchanger is fouled, to the overall heat transfer coefficient of the clean heat exchanger, $C_F = U_{fouled}/U_{clean}$. When defining C_F, we need not to consider any fouling (f_i and f_o) in Equation VIa.1.1, rather calculate U_{clean} and find U_{fouled} from $U_{fouled} = C_F U_{clean}$.

Heat Capacity, *C* is the product of mass flow rate and specific heat, $C = \dot{m}c_p$ having units of Btu/s·F or W/C.

2. Analytical Solution

In this section we discuss steady-state operation of heat exchangers. As shown in Figure VIa.2.1, we can assign control volumes to the entire hot-side, the cold-side and the solid surface separating the hot and cold sides. In steady state conditions, flow rates at the inlet and outlet ports for each control volume are equal hence:

$$\dot{m}_{h,in} = \dot{m}_{h,out} = \dot{m}_h \qquad \text{VIa.2.1a}$$

$$\dot{m}_{c,in} = \dot{m}_{c,out} = \dot{m}_c \qquad \text{VIa.2.1b}$$

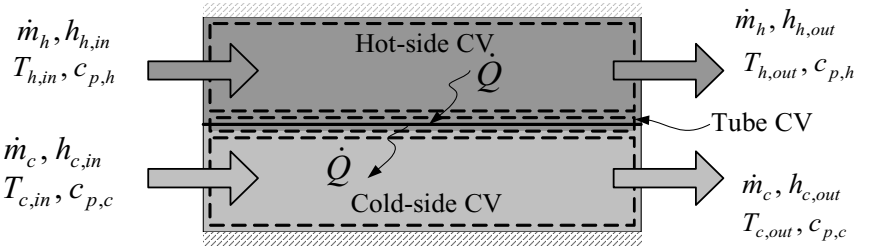

Figure VIa.2.1. Control volumes for the primary and secondary sides

The hot stream enters at an enthalpy of $h_{h,in}$ and leaves at an enthalpy of $h_{h,out} < h_{h,in}$. If the heat exchanger shell is fully insulated so that there is no heat loss to the environment, then under steady-state operation:

$$\dot{Q}_h = \dot{Q}_s = \dot{Q} \qquad \text{VIa.2.2a}$$

On the other hand, the cold side fluid enters at an enthalpy of $h_{c,i}$ and leaves at an enthalpy of $h_{c,o} > h_{c,i}$. The gain in the cold stream energy is due to the transfer of heat from the solid surface. In steady-state:

$$\dot{Q}_c = \dot{Q}_s = \dot{Q} \qquad \text{VIa.2.2b}$$

Substituting for the rate of heat transfer while assuming negligible potential and kinetic energies, we find:

$$\dot{Q} = \dot{m}_h (h_{h,in} - h_{h,out}) \qquad \text{VIa.2.3a}$$

$$\dot{Q} = \dot{m}_c (h_{c,out} - h_{c,in}) \qquad \text{VIa.2.3b}$$

For a special case where each stream exits at the same phase as it entered the heat exchanger, we may replace $\Delta h \approx c_p \Delta T$. Assuming variations in specific heat are small and using $c_p = f(T_{in} + T_{out})/2$, we can write the axial energy equations as:

$$\dot{Q} = C_h (T_{h,in} - T_{h,out}) \qquad \text{VIa.2.4a}$$

$$\dot{Q} = C_c (T_{c,out} - T_{c,in}) \qquad \text{VIa.2.4b}$$

So far we used the conservation equations of mass and energy in the axial direction. In the next section we use the conservation equation of energy in the transverse direction for elemental control volumes to tie the hot-side and cold-side temperatures by applying the overall heat transfer coefficient. The reason for using elemental control volume is that axial temperature profiles are generally not linear functions of the heat exchanger length. As a result, we cannot generally use average temperatures for the hot and cold side as:

$$\overline{\Delta T} = \left[\frac{T_{h,in} + T_{h,out}}{2} - \frac{T_{c,in} + T_{c,out}}{2}\right] \qquad \text{VIa.2.5}$$

If it were possible, the rate of heat transfer would have been calculated from $\dot{Q} = UA\overline{\Delta T}$. The simple relation given in Equation VIa.2.5 provides only an estimation of ΔT. In the next section we will see that ΔT is a logarithmic function of the inlet and outlet temperatures referred to as the *logarithmic mean temperature difference* (LMTD).

2.1. LMTD Method of Analysis

The analysis performed below applies to parallel flow heat exchangers as shown in Figures VIa.2.2(a). Similar analysis can be performed for counterflow heat exchangers, shown in Figure VIa.2.2(b).

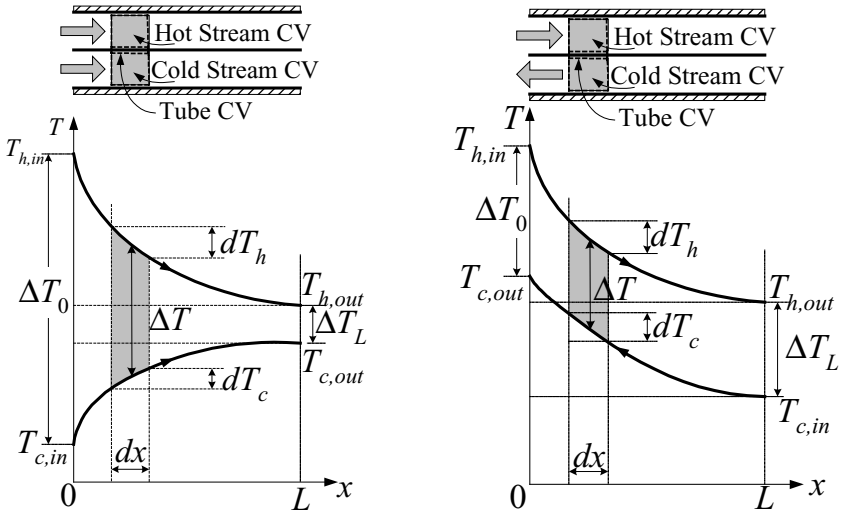

Figure VIa.2.2. Hot and cold temperature profiles for (a) parallel and (b) counterflow heat exchangers

Consider three elemental control volumes, one for the hot side, one for the tube surface, and one for the cold side of a heat exchanger, Figure VIa.2.2(a) and VIa.2.2(b). These figures show the temperature profiles as a function of the heat exchanger length. Similar to Equations VIa.2.4a and VIa.2.4b, we can write axial energy equations for the hot side and cold side of the elemental control volumes:

$$d\dot{Q} = -C_h dT_h \qquad \text{VIa.2.6a}$$

$$d\dot{Q} = C_c dT_c \qquad \text{VIa.2.6b}$$

We now write the transverse energy equation assuming negligible axial heat conduction in the tube. Such thermal resistances as flow, tube wall, and fouling are taken into account by the use of an overall heat transfer coefficient:

$$d\dot{Q} = [U(x)dA(x)]\Delta T \qquad \text{VIa.2.7}$$

Note that the term ΔT in Equation VIa.2.7 represents the difference in the average temperatures of the hot and cold side elemental control volumes (i.e. $\Delta T = T_h - T_c$). To relate Equations VIa.2.6a and VIa.2.6b to Equation VIa.2.7, we differentiate ΔT and substitute for terms:

$$d(\Delta T) = dT_h - dT_c = -\frac{d\dot{Q}}{C_h} - \frac{d\dot{Q}}{C_c} = -d\dot{Q}\left(\frac{1}{C_h} + \frac{1}{C_c}\right) \qquad \text{VIa.2.8}$$

If we integrate Equation VIa.2.8 from $x = 0$ to $x = L$, we get:

$$\Delta T_0 - \Delta T_L = \dot{Q}\left(\frac{1}{C_h} + \frac{1}{C_c}\right) \qquad \text{VIa.2.9}$$

We may also substitute in Equation VIa.2.8 for $d\dot{Q}$ from Equation VIa.2.7 and divide by ΔT to obtain:

$$\frac{d(\Delta T)}{\Delta T} = -[U(x)dA(x)]\left(\frac{1}{C_h} + \frac{1}{C_c}\right)$$

Integrating the above equation from $x = 0$ to $x = L$, yields:

$$\int_0^L \frac{d(\Delta T)}{\Delta T} = -\left[\frac{1}{C_h} + \frac{1}{C_c}\right]\int_0^L U(x)dA(x) \qquad \text{VIa.2.10}$$

We now define an overall heat transfer coefficient, which is averaged over the heat exchanger length:

$$U = \frac{\int_0^L U(x)dA(x)}{A}$$

where A is the heat exchanger surface area. By defining the average U, Equation VIa.2.10 becomes:

$$\ln\frac{\Delta T_0}{\Delta T_L} = UA\left(\frac{1}{C_h} + \frac{1}{C_c}\right) \qquad \text{VIa.2.11}$$

Substituting for $1/C_h + 1/C_c$ from Equation VIa.2.9 we find:

$$\dot{Q} = UA\frac{\Delta T_0 - \Delta T_L}{\ln(\Delta T_0 / \Delta T_L)} = UA\Delta T_{LMTD} \qquad \text{VIa.2.12}$$

Note that in applying Equation VIa.2.12 to parallel and counterflow heat exchangers, we must recall that (see Figure VIa.2.2):

Parallel Flow: $\Delta T_0 = T_{h,in} - T_{c,in}$ and $\Delta T_L = T_{h,out} - T_{c,out}$
Counterflow: $\Delta T_0 = T_{h,in} - T_{c,out}$ and $\Delta T_L = T_{h,out} - T_{c,in}$

For the same inlet and outlet temperatures, $(\Delta T_{LMTD})_{\text{Counterflow}} > (\Delta T_{LMTD})_{\text{Parallel}}$. This implies that for the same U and A, a counterflow heat exchanger has a higher rate of heat removal than a parallel flow heat exchanger. Comparing Equation VIa.2.5 with Equation VIa.2.12, we note that the temperature difference unfortunately contains a logarithmic term. This complicates analysis when unknown temperatures must be found from Equation VIa.2.12.

Example VIa.2.1. Use the given data to find a) ΔT_{LMTD} if the heat exchanger uses a parallel flow arrangement and b) ΔT_{LMTD} if the heat exchanger uses a counterflow arrangement. Data: $T_{h,i}$ = 195 F, $T_{h,o}$ = 160 F, $T_{c,i}$ = 65 F, and $T_{c,o}$ = 105 F.

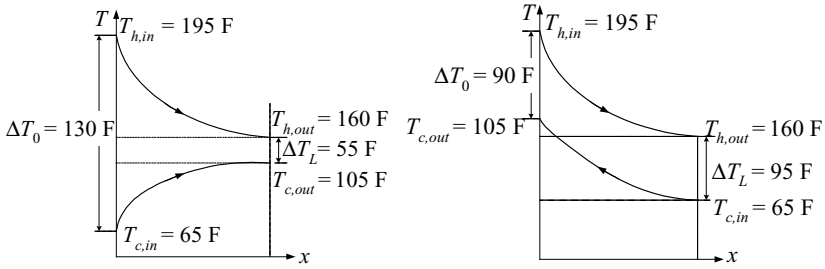

Solution: a) For parallel flow, $\Delta T_0 = T_{h,i} - T_{c,i}$ = 195 – 65 = 130 F, and $\Delta T_L = T_{h,o} - T_{c,o}$ = 160 – 105 = 55 F

$[\Delta T_{LMTD}]_{\text{Parallel}}$ = [130 – 55]/ln(130/55) = 87.2 F

b) For counterflow, $\Delta T_0 = T_{h,i} - T_{c,o}$ = 195 – 105 = 90 F, and $\Delta T_L = T_{h,o} - T_{c,i}$ = 160 – 65 = 95 F

$[\Delta T_{LMTD}]_{\text{Counterflow}}$ = [90 – 95]/ln(90/95) = 92.5 F

Comment: Two observations can be made from this example. First, as discussed earlier and shown above $(\Delta T_{LMTD})_{\text{Counterflow}} > (\Delta T_{LMTD})_{\text{Parallel}}$. In this example, for the same U and A, the counterflow HX is more efficient than the parallel flow HX by about 6%. Second, an average temperature difference per Equation VIa.2.5 is ΔT = [(195 + 160) – (105 + 65)]/2 = 92.5 F, which happens to agree with $(\Delta T_{LMTD})_{\text{Counterflow}}$.

Equations and Unknowns. For a concentric heat exchanger, we derived three equations, namely two axial energy equations (Equations VIa.2.4a and VIa.2.4b) and a transverse energy equation (Equation VIa.2.12). The number of unknowns, being nine, exceeds the number of equations by a wide margin. The unknowns are $\dot{Q}, \dot{m}_h, \dot{m}_c, T_{h,in}, T_{c,in}, T_{h,out}, T_{c,out}, U$, and A. Note that $c_{p,h}$ and $c_{p,c}$ are not unknowns as they are functions of the related temperatures. We have an additional equation for U given by Equation VIa.1.1, which introduces h_i, h_o, f_i, f_o, d_i, d_o, and L. However, the heat transfer coefficients are functions of Re, Pr, fluid temperature, d_i, and d_o. Also the heat exchanger surface area is related to tube diameter and tube length as $A = \pi dL$. An additional unknown is the shell diameter, which can be calculated from an appropriate equation. We increased the number of equations to eight. These are Equations VIa.2.4a, VIa.2.4b, VIa.2.12, VIa.1.1, V.3.4 (for h_i and a similar equation for h_o), the relation for $A = f(d, L)$, and the relation for D_{shell}. However, we increased the number of unknowns to seventeen! To have a consistent set, we must then specify nine of the unknowns. This argu-

ment indicates that, from the thermal analysis point of view, heat exchangers have a large degree of freedom. On the other hand, constraints for design optimization include:

- structural considerations (tube outside diameter to stand internal pressure)
- hydraulic considerations (tube inside diameter for pumping power and pressure drop in tube)
- performance (fouling characteristics of the working fluids)
- tube material (conductivity, erosion, and corrosion characteristics)
- size and weight limitations
- cost

Returning to the three equations and nine unknowns discussion, let's consider a case where two inlet temperatures ($T_{h,in}$ and $T_{c,in}$), two flow rates ($\dot{m}_h$, and $\dot{m}_h$), the heat transfer coefficient U, and the surface area A are specified. We solve for the two exit temperatures ($T_{h,out}$ and $T_{c,out}$) and the rate of heat transfer $\dot{Q}$. We substitute for the two exit temperatures from Equations VIa.2.4a and VIa.2.4b into Equation VIa.2.12 to solve for $\dot{Q}$:

$$\dot{Q} = \frac{(T_{h,in} - T_{c,in})(\beta - 1)}{(\beta / C_h) - (1 / C_c)} \qquad \text{VIa.2.13}$$

where $\beta = e^{UA[1/\dot{m}_h c_{p,h} - 1/\dot{m}_c c_{p,c}]}$. This equation is applicable to counterflow heat exchangers. See Section 2.2 for generalization of this method.

Example VIa.2.2. Water flows in both sides of a counterflow heat exchanger. Find the rate of heat transfer $\dot{Q}$, and exit temperatures ($T_{h,out}$ and $T_{c,out}$) for the following data: $T_{h,i}$ = 130 F, $T_{c,i}$ = 95 F, $\dot{m}_h = 1.5\text{E}6$ lbm/h, $\dot{m}_c = 2.41\text{E}6$ lbm/h, U = 259 Btu/ft^2·h·F, A = 5,790 ft^2, and c_p = 1 Btu/lbm·F.

Solution: To use Equation VIa.2.13, we find
β = exp[259 × 5,790(1/1.5E6 – 1/2.41E6)] = 1.4586

$\dot{Q} = C_h(T_{h,in} - T_{h,out})$ = (130 –95) × (1.4586 – 1)/[1.4586/1.5E6 – 1/2.41E6] = 28.8E6 Btu/h

$T_{h,out} = T_{h,in} - (\dot{Q} / C_h)$ = 130 – (28.8E6/1.5E6) = 111 F

$T_{c,out} = T_{c,in} + (\dot{Q} / C_c)$ = 95 + (28.8E6/2.41E6) = 107 F.

Special Modes of Operation. Shown in Figure VIa.2.3 are three different modes of operations. Figure VIa.2.3(a) shows one stream is boiling while the other stream is cooling down. In this case (i.e., in the case of a steam generator) $\Delta T \to 0$ and $C_c \to \infty$. Figure VIa.2.3(b) shows one stream is condensing

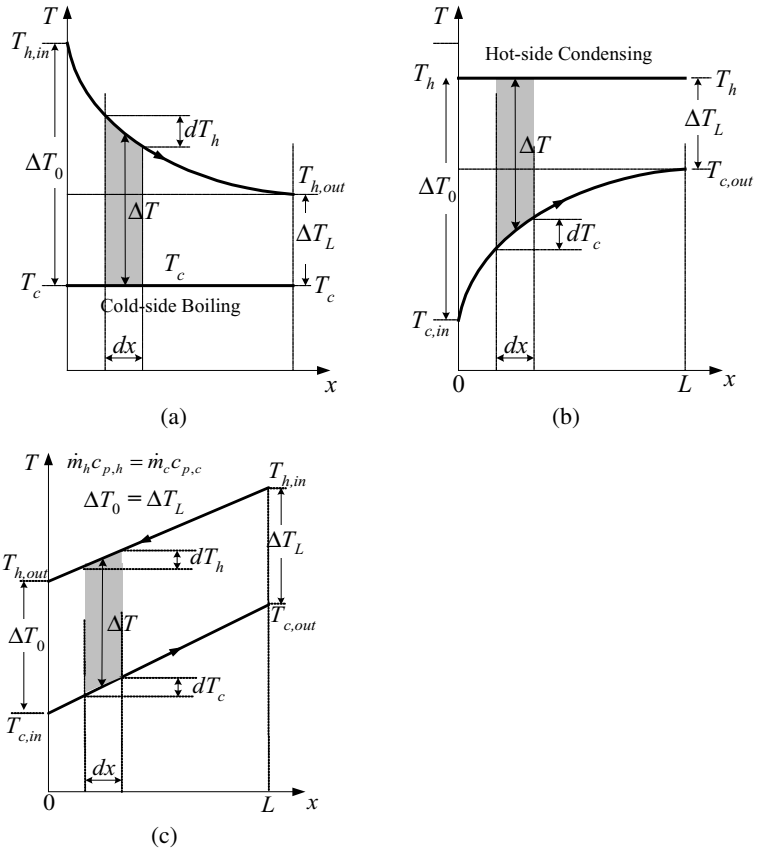

Figure VIa.2.3. (a) Steam generator, (b) Condenser, and (c) Special case of $\Delta T_h = \Delta T_c$

while the other stream is heating up. In this case (i.e. in the case of a condenser), we have $\Delta T \to 0$ and $C_h \to \infty$. Note that in these cases we should use Equations VIa.2.3a and VIa.2.3b. Finally, Figure VIa.2.3(c) shows a special case in which $C_h = C_c$. This requires that $\Delta T_h = \Delta T_c$.

Multi-pass Heat Exchangers. The LMTD method outlined above and the result culminated in Equation VIa.2.12 apply to concentric heat exchangers (Figure IVa.6.3). The same results can be applied to the shell and tube heat exchangers with multi-pass tubes and shell, by applying a correction factor $F_{multi\text{-}pass}$ so that:

$$\dot{Q} = F_{Multi-pass} UA \Delta T_{LMTD} \qquad \text{VIa.2.12a}$$

The $F_{Multi\text{-}pass}$ factor is given in Figure VIa.2.4 for two cases. The left side figure is for any multiples of two tube pass (four, six, etc.) and one shell pass. The right

side figure is for any multiple of four tube and two shell passes. In these figures, the tube-side inlet and outlet temperatures are shown by t_i and t_o whereas the shell-side inlet and outlet temperatures are shown by Ti and T_o, respectively. The correction factor obtained from Figure VIa.2.3 should be used in conjunction with the ΔT_{LMTD} calculated for a counterflow configuration. The correction factor for one shell path, as shown in the left side plot of Figure VIa.2.4 is obtained from:

$$F_{Multi-pass} = \frac{\sqrt{R^2+1}}{R-1} \times \frac{\ln[(1-P)/(1-PR)]}{\ln\{[2-P(R+1-\sqrt{R^2+1})]/[2-P(R+1+\sqrt{R^2+1})]\}} \qquad \text{VIa.2.14}$$

Parameters P and R in Figure VIa.2.4 and in Equation VIa.2.11 are known as *capacity ratio* and *effectiveness*, respectively and are given as:

$$\text{Capacity Ratio: } P = \frac{C_c}{C_h} = \frac{t_0 - t_i}{T_i - t_i}$$

$$\text{Effectiveness: } R = \frac{C_c(T_i - T_o)}{C_h(t_o - t_i)} = \frac{T_i - T_o}{t_o - t_i}$$

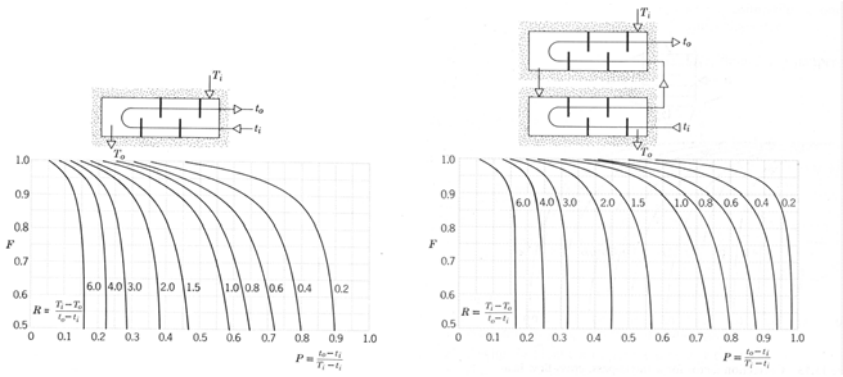

Figure VIa.2.4. Correction factor for multiple tube and shell passes

The LMTD correction factor (F) for multi-pass shell and tube heat exchangers can be calculated by using the software on the accompanying CD-ROM.

Example VIa.2.3. Seawater is used to cool the lubricating oil of a ship's diesel engine. The shell and tube heat exchanger has one shell and two tube passes. Tube surface area is 100 ft^2 and the overall heat transfer coefficient is given as U = 250 Btu/ft^2·h·F. Oil enters at 160 F and leaves at 125 F. Water enters the tube at 75 F and leaves at 100 F. Find the total rate of heat transfer.

Solution: We find the capacity ratio and the effectiveness as follows,
$P = (100 - 75)/(160 - 75) = 0.294$. $R = (160 - 125)/(100 - 75) = 1.4$

Using the left plot of Figure VIa.2.3, we find $F_{Multi\text{-}pass} \approx 0.95$

$\Delta T_{LMTD} = [(160 - 100) - (125 - 75)]/\ln[(160 - 100)/(125 - 75)] = 54.85$ F

$\dot{Q} = F_{Multi\text{-}pass} UA\Delta T_{LMTD} = 0.95 \times 250 \times 100 \times 54.85 = 1.3\text{E}6$ Btu/h ≈ 0.4 MW.

Cross Flow Heat Exchangers. Equation VIa.2.12 is also applicable to cross flow heat exchangers:

$$\dot{Q} = F_{CrossFlow} UA\Delta T_{LMTD} \qquad \text{VIa.2.12b}$$

where $F_{Cross\ Flow}$ is given in Figure VIa.2.5 for two cases. The left figure is for a case where both streams are unmixed and the right figure is for one stream mixed and other stream unmixed.

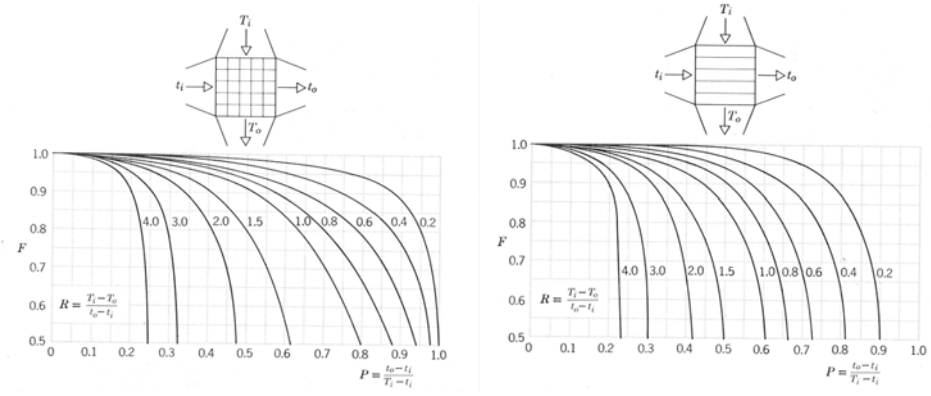

Figure VIa.2.5. Cross flow heat exchangers

2.2. NTU Method of Analysis

In cases where exit temperatures are unknown, we have to solve an equation involving the logarithmic term for ΔT_{LMTD}. An alternative method of analyzing heat exchangers is the $\varepsilon - NTU$ method where $NTU = UA/C$ stands for *number of transfer units,* and effectiveness (now represented by ε) is given as:

$$\varepsilon = \frac{\dot{Q}_{actual}}{\dot{Q}_{ideal}} = \frac{\dot{Q}_{actual}}{C_{\min}(T_{h,in} - T_{c,in})}$$

where $C_{\min}$ is the minimum of C_h and C_c. The ideal or maximum rate of heat transfer is associated with maximum ΔT, which is $\Delta T_{\max} = T_{h,in} - T_{c,in}$. If we find ε, then we can calculate $\dot{Q}_{actual}$ from:

$$\dot{Q}_{actual} = \varepsilon C_{\min} \Delta T_{\max}$$

Therefore, in the ε-*NTU* method, rather than calculating ΔT_{LMTD} we calculate ε, which depends on the type of heat exchanger and flow configuration. Since $\dot{Q}_{actual} = C_h (T_{h,in} - T_{h,out}) = C_c (T_{c,out} - T_{c,in})$, then

$$\varepsilon = \frac{C_h (T_{h,in} - T_{h,out})}{C_{\min} (T_{h.in} - T_{c,in})} \qquad \text{VIa.2.15a}$$

and

$$\varepsilon = \frac{C_c (T_{c,out} - T_{c,in})}{C_{\min} (T_{h.in} - T_{c,in})} \qquad \text{VIa.2.15b}$$

We use Equations VIa.2.15a, VIa.2.15b, and VIa.2.11 to derive relations for ε for various types of heat exchangers. For example, for a parallel flow heat exchanger, we can write Equation VIa.2.11 as:

$$\frac{\Delta T_L}{\Delta T_0} = \frac{T_{h,out} - T_{c,out}}{T_{h,in} - T_{c,in}} = \exp[-UA(1/C_h + 1/C_c)]$$

We now solve Equation VIa.2.15a for $T_{h,out}$ and substitute in the above equation to get:

$$1 - \frac{T_{c,out} - T_{c,in}}{T_{h,in} - T_{c,in}} (1 + \frac{C_c}{C_h}) = \exp[-UA(1/C_h + 1/C_c)]$$

Substituting for the temperature ratio term in the above equation from Equation VIa.2.15b yields:

$$\varepsilon = \frac{1 - \exp[-UA(1/C_h + 1/C_c)]}{C_{\min}/C_c + C_{\min}/C_h}$$

If it happens that $C_c < C_h$, then $C_{min} = C_c$ and the denominator becomes $1 + C_c/C_h$. Conversely, for the case of $C_h < C_c$, the denominator becomes $1 + C_h/C_c$. We can write the result in compact form of $1 + C_r$ where $C_r = C_{\min}/C_{\max}$. Similarly, in the numerator, we factor out $C_{\min}$ and substitute for $UA/C_{\min} = NTU$:

$$\varepsilon = \frac{1 - \exp[-NTU(1 + C_{\min}/C_{\max})]}{1 + C_{\min}/C_{\max}} \qquad \text{VIa.2.16}$$

Equation VIa.2.16 gives the effectiveness as a function of NTU, $\varepsilon = f(NTU, C_r)$. We may also solve Equation VIa.2.16 for NTU as a function of ε, $NTU = f(\varepsilon, C_r)$. The same method used to derive Equation VIa.2.16 for the parallel flow heat exchangers can be applied to other types of heat exchangers and obtain similar relations for effectiveness (Kays). The results for ε as a function of NTU and $C_r = C_{\min}/C_{\max}$ are summarized in Table VIa.2.1. This is followed by the results obtained from Kays for $NTU = f(\varepsilon)$, as shown in Table VIa.2.2.

Example VIa.2.4. Water flows in both sides of a counterflow heat exchanger. Find the rate of heat transfer $\dot{Q}$, and exit temperatures, $T_{h,out}$, and $T_{c,out}$ for the following data: $T_{h,in} = 55$ C, $T_{c,in} = 30$ C, $\dot{m}_h = 200$ kg/s, $\dot{m}_c = 300$ kg/s, $U = 1.5$ kW/m^2·C, and $A = 540$ m^2, $c_p = 4.18$ kJ/kg·K.

Solution: In this example, $C_{\min} = C_h = 200 \times 4.18 = 836$ kW/C

$$NTU = \frac{UA}{C_{\min}} = \frac{1.5 \times 540}{836} = 0.97$$

$$C_r = \frac{200 \times 4.18}{300 \times 4.18} = 0.667$$

$$\varepsilon = \frac{1 - \exp[-NTU(1 - C_r)]}{1 - C_r \exp[-NTU(1 - C_r)]} = \frac{1 - \exp[-0.97 \times (1 - 0.667)]}{1 - 0.667 \times \exp[-0.97 \times (1 - 0.667)]} = 0.534$$

$$\dot{Q}_{\max} = C_{\min}(T_{h,in} - T_{c,in}) = 200 \times 4.18 \times (55 - 30) = 20{,}900 \text{ kW}$$

$$\dot{Q}_{\text{actual}} = \varepsilon \dot{Q}_{\max} = 0.534 \times 20{,}900 = 11{,}161 \text{ kW}$$

Having $\dot{Q}_{\text{actual}}$, we can find exit temperatures as:

$$T_{h,out} = 55 - \frac{11{,}161}{200 \times 4.18} = 42 \text{ C}$$

$$T_{c,out} = 30 + \frac{11{,}161}{300 \times 41.8} = 39 \text{ C}.$$

Table VIa.2.1. Heat exchanger effectiveness for various flow arrangements

Flow Arrangement	Effectiveness
Parallel Flow:	$\varepsilon = \dfrac{1-\exp[-NTU(1+C_r)]}{1+C_r}$
Counterflow:	$\varepsilon = \dfrac{1-\exp[-NTU(1-C_r)]}{1-C_r\exp[-NTU(1-C_r)]}$
Shell & tube (1 shell pass, 2, 4, … *n* tubes passes):	$\varepsilon_1 = 2\left\{1+C_r+(1+C_r^2)^{1/2}\dfrac{1+\exp[-NTU(1+C_r^2)^{1/2}]}{1-\exp[-NTU(1+C_r^2)^{1/2}]}\right\}^{-1}$
Shell & tube (*n* shell pass, 2*n*, 4*n*,… tube passes):	$\varepsilon = \left[\left(\dfrac{1-\varepsilon_1 C_r}{1-\varepsilon_1}\right)^n - 1\right]\left[\left(\dfrac{1-\varepsilon_1 C_r}{1-\varepsilon_1}\right)^n - C_r\right]^{-1}$
Cross flow (single path, both streams unmixed):	$\varepsilon = 1-\exp[(1/C_r)(NTU)^{0.22}\{\exp[-C_r(NTU)^{0.78}]-1\}]$
Cross flow (C_{max} mixed, C_{min} unmixed):	$\varepsilon = (1/C_r)(1-\exp\{-C_r[1-\exp(-NTU)]\})$
Cross flow (C_{max} unmixed, C_{min} mixed):	$\varepsilon = 1-\exp(-C_r^{-1}\{1-\exp[-C_r(NTU)]\})$
Heat exchangers with $C_r = 0$:	$\varepsilon = 1-\exp(-NTU)$

Table VIa.2.2. Heat exchanger *NTU* for various flow arrangements

Flow Arrangement	Number of Transfer Units
Parallel Flow:	$NTU = -\dfrac{\ln[1-\varepsilon(1+C_r)]}{1+C_r}$
Counterflow:	$NTU = -\dfrac{1}{C_r-1}\ln\left(\dfrac{\varepsilon-1}{\varepsilon C_r-1}\right)$
Shell & tube (1 shell pass, 2, 4, … *n* tubes pass):	$NTU = -(1+C_r^2)^{-1/2}\ln\left(\dfrac{E-1}{E+1}\right)$, $E = \dfrac{2/\varepsilon_1-(1+C_r)}{(1+C_r^2)^{1/2}}$
Cross flow (C_{max} mixed, C_{min} unmixed):	$NTU = -\ln[1+(1/C_r)\ln(1-\varepsilon C_r)]$
Cross flow (C_{max} unmixed, C_{min} mixed):	$NTU = -(1/C_r)\ln[C_r\ln(1-\varepsilon)+1]$
Heat exchangers with $C_r = 0$:	$NTU = -\ln(1-\varepsilon)$

3. Analysis of Shell and Tube Heat Exchanger

Shell and tube heat exchangers are the most widely used type of heat exchanger. They are used as steam generators, condensers, feedwater heaters, and in single-phase processes. In this section we consider shell and tube heat exchangers with subcooled water flowing in both tubes and the shell. In the next section, we consider shell and tube heat exchangers as condensers, followed by the section for shell and tube heat exchangers as steam generators. A schematic of a straight tube heat exchanger in shown in Section 1. Shown in Figure VIa.3.1 is the schematic of a U-tube heat exchanger of the shell and tube type. This figure shows a one-shell and two-tube pass. Shown on the right are examples of the tube arrangements. Tubes may be arranged in triangular, square, or other types of arrays. Earlier, it was mentioned that the chemically controlled stream should flow in the shell as tubes are easier to clean. Straight tube cleaning is generally performed with projectile guns to scrape tubes of deposits. There are other factors to consider in the allocation of the streams to the tube or the shell side. For example, high-pressure fluid should flow through tubes due to tube capability to withstand higher pressures. The stream with lower mass flow rate and heat transfer coefficient should generally flow in the shell. As discussed by Kakac, this facilitates installation of fins on the outside of the tubes. Also, mixing and redirecting flow by the baffle plates would enhance heat transfer. In the analysis that follows, subscripts *i* and *o* refer to the tube side and shell side, respectively.

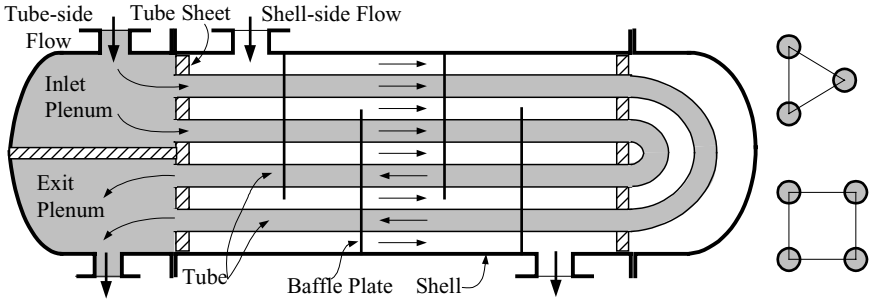

Figure VIa.3.1. Schematic of a one-shell, two-tube pass shell and tube heat exchanger and tube arrays

3.1. Performance Evaluation

Heat exchangers are designed for a rated or nominal condition. Often we need to find the performance of a heat exchanger operating at conditions different than nominal. In such circumstance, we generally know the shell and tube mass flow rates and inlet temperatures. The goal is to determine the outlet temperatures as well as the rate of heat transfer and the overall heat transfer coefficient. Hence, performance evaluation of a shell and tube heat exchanger for which d_i, d_o, L, and N are known includes finding $\dot{Q}$, $T_{h,out}$, $T_{c,out}$, and U for given $\dot{m}_h$, $\dot{m}_c$, $T_{h,in}$, and

$T_{c,in}$. The solution requires iteration since properties must be evaluated at an average temperature while outlet temperatures are unknown. In the first trial, we assume either the outlet temperatures or determine fluid properties based on the known inlet temperatures. The solution steps are outlined as follows:

1- find A_o having d_o, L, and N
2- find h_h and h_c having $\dot{m}_h$, $\dot{m}_c$, and the thermophysical properties
3- find U_o having h_h, h_c, tube data, f_i, and f_o
4- find C_{min}, C_{max}, and C_r having $\dot{m}_h$, $c_{p,h}$ and $\dot{m}_c$, $c_{p,c}$
5- find NTU having UA and C_{min}
6- find ε having NTU and C_r
7- find $\dot{Q}$, $T_{h,o}$, $T_{c,o}$ having ε, $T_{h,in}$, and $T_{c,in}$
8- find F and the average temperatures having $T_{h,out}$, $T_{c,,out}$, $T_{h,in}$, and $T_{c,in}$.

Repeat the above steps using updated properties until the required convergence criterion is met. These steps can be implemented in a spreadsheet or simple FORTRAN program, as shown in the next example.

Example VIa.3.1. Hot water flows inside tubes of a shell and tube heat exchanger. Find the total rate of heat transfer for the following data (k_s = 10 Btu/h·ft·F):

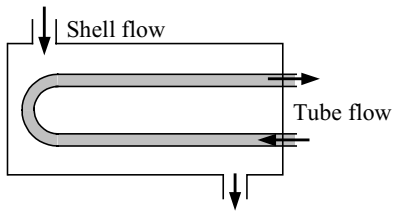

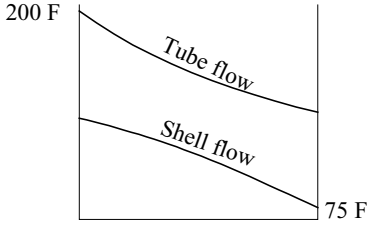

d_i (in)	d_o (in)	L (ft)	N (-)	$\dot{m}_h$ (lbm/h)	$\dot{m}_c$ (lbm/h)	$T_{h,in}$ (F)	$T_{c,in}$ (F)	f_i (ft²·h·F/Btu)	f_o (ft²·h·F/Btu)
0.652	0.75	40	1000	2E6	3E6	200	75	0.0005	0.0005

Solution: We follow the above solution steps. Since we do not have $T_{h,out}$ and $T_{c,out}$, we use an approximation and find properties at $T_{h,in}$ and $T_{c,in}$:

	T (F)	ρ (lbm/ft³)	c_p tu/lbm·F)	μ (lbm/h·ft)	k (Btu/h·ft·F)	Pr (-)
Tube:	200	60.1	1.0	0.7293	0.392	1.87
Shell:	75	62.3	1.0	2.225	0.352	6.32

$a_i = \pi d_i^2 / 4 = 3.14 \times 0.0543^2 / 4 = 2.32\text{E-}3 \text{ ft}^2$

$a_o = \pi d_o^2 / 4 = 3.14 \times 0.0625^2 / 4 = 3.07\text{E-}3 \text{ ft}^2$

$\text{Re}_i = \dot{m}_i d_i / (\mu_i a_i) = 2\text{E}3 \times 0.0543/(0.7293 \times 2.32\text{E-}3) = 64{,}225$

$\mathrm{Re}_o = \dot{m}_o d_o /(\mu_o a_o)$ = 3E3 × 0.0625/(2.225 × 3.07E-3) = 27,144

$h_i = (k_i/d_i)\mathrm{Nu}_i = (k_i/d_i)(0.023\,\mathrm{Re}_i^{0.8}\,\mathrm{Pr}_i^{0.3})$ = (0.392/0.0543)(0.023 × 64,225$^{0.8}$ × 1.87$^{0.3}$ = 1406 Btu/h·ft^2·F

$h_o = (k_o/d_o)\mathrm{Nu}_o = (k_o/d_o)\,(0.023\,\mathrm{Re}_o^{0.8}\,\mathrm{Pr}_o^{0.4})$ = (0.352/0.0625)(0.023 × 27,144$^{0.8}$ × 6.32$^{0.4}$ = 954 Btu/h·ft^2·F

$$U_o = [\frac{d_o}{d_i h_i} + \frac{d_o f_i}{d_i} + \frac{d_o \ln(d_o/d_i)}{2k_s} + f_o + \frac{1}{h_o}]^{-1}$$
$$= [R_i + R_{fi} + R_s + R_{fo} + R_o]^{-1}$$

$R_i = d_o/(d_i h_i)$ = 0.0625/(0.0543 × 1406) = 8.1864E-4 h·ft^2·F/Btu
$R_{fi} = d_o f_i/d_i$ = 0.0625 × 0.0005/0.0543 = 5.7551E-4 h·ft^2·F/Btu
$R_s = d_o \ln(d_o/d_i)/(2k_s)$ = 0.0625 × ln(0.0625/0.0543)/(2 × 10) = 8.7901E-4 h·ft^2·F/Btu
$R_{fo} = f_o$ = 0.0005 h·ft^2·F/Btu
$R_o = 1/h_o$ = 1/954 = 1.0482E-4 h·ft^2·F/Btu

ΣR = 8.1864E-4 + 5.7551E-4 + 8.7901E-4 + 5.00E-4 + 1.0482E-4 = 3.382E-3 h·ft^2·F/Btu

$U_o = 1/\Sigma R$ = 1/3.382E-3 = 295.7 Btu/h·ft^2·F

C_{min} = 2E6 Btu/F and C_{max} = 3E6 Btu/F. We find C_r as: $C_r = C_{min}/C_{max}$ = 0.667

$NTU = U_o A_o/C_{min}$ = 295.7 $(\pi d_o NL)$/2E6 = 295.7 × 3.14 × 0.0625 × 1000 × 40/2E6 = 1.161

Having NTU = 1.161 and C_r = 0.667, the effectiveness is found as: ε = 0.55
$\dot{Q} = \varepsilon C_{min}(T_{h,,in} - T_{c,in})$ = 0.55 × 2E6 × (200 – 75) = 1.375E8 Btu/h.

We should now use the calculated $\dot{Q}$ to update tube and shell average temperature and repeat the steps that were performed above. These are implemented in the following FORTRAN program, which is also included on the accompanying CD-ROM.

```
c                                  Shell & Tube Heat Exchanger
c This program finds Th_o, Tc_o, Qdot, e, NTU, and DTlmtd Given:
c dmh, dmc, Th_i, Tc_i as well as di, do, aL, aN, fi, and fo for a Shell & Tube
c heat exchanger with water in both sides
c      implicit real*8 (a-h,o-z)
c
c  Nomenclature:
c  aa:   tube flow area (ft2)                ab:  shell flow area (ft2)
c  aL:   total tube length (ft)              aN:  total number of tubes
c  cpa:  tube-side specific heat (Btu/lbm-F) cpb: shell-side specific heat
c                                                (Btu/lbm-F)
c  di:  tube inside diameter (in)          do: tube outside diameter (in)
c  ha:  tube-side HTC. (Btu/hr-ft2-F)      hb: shell-side HTC (Btu/hr-ft2-F)
c  Thi: tube-sdie inlet temperature (F)  Tbi: shell-side inlet temperature (F)
```

```
c
      data pi/3.1415927/
      open(5,file='hx1.in')
      open(6,file='hx1.out')
      read(5,*) dmi,dmo
      read(5,*) Ti_in,To_in
      read(5,*) dip,dop,aL,aN
      read(5,*) aks
      read(5,*) fi,fo
c
      di=dip/12.00
      do=dop/12.00
      fai=pi*di*di/4.
      fao=pi*do*do/4.
      Ao=pi*do*aL*aN
c     Only for the first trial, find properties based on the inlet temps.
      iter=0
      Ti_out=Ti_in
      To_out=To_in
100   continue
      iter=iter+1
      Ti_avg=0.5*(Ti_in+Ti_out)
      To_avg=0.5*(To_in+To_out)
      Ts=0.5*(Ti_avg+To_avg)
      call intrpl(Ti_avg,cpfi,cpgi,amufi,amug,akfi,akg,Prfi,Prg,
     1            sigf,betaf,rofi,rog,anuf,anug,vf,vfg,vg)
      call intrpl(To_avg,cpfo,cpgo,amufo,amug,akfo,akg,Prfo,Prg,
     1            sigf,betaf,rofo,rog,anuf,anug,vf,vfg,vg)
      call htc(Ti_avg,Ts,dmi,aN,di,fai,hi)
      call htc(To_avg,Ts,dmo,aN,do,fao,ho)
c
      Call Uover(di,do,hi,ho,fi,fo,aks,Uo)
      Call NTU(dmi,cpfi,dmo,cpfo,Ao,Uo,Cmin,Cr,aNTU,eff)
      Qdot=eff*Cmin*abs(Ti_in-To_in)
      If(Ti_in.lt.To_in) go to 1
      Ti_out=Ti_in-(Qdot/(dmi*cpfi))
      To_out=To_in+(Qdot/(dmo*cpfo))
      go to 2
1     continue
      Ti_out=Ti_in+(Qdot/(dmi*cpfi))
      To_out=To_in-(Qdot/(dmo*cpfo))
2     continue
      DTlmtd=Qdot/(Uo*Ao)
      if(iter.eq.1) go to 100
      Tsn=0.5*(Ti_avg+To_avg)
      eps=abs(Tsn-Ts)/Tsn
      if(eps.le.1.e-6) go to 101
      if(iter.lt.30) go to 100
      print *,'Steady-State Iteration Did Not Converge'
      stop
101   continue
      write(6,3) dip,dop,aL,aN,dmi,dmo,Ti_in,To_in,Ti_out,To_out,Ts,
     1           DTlmtd,hi,ho,Qdot,Uo,aNTU,eff
3     format(
     1' Tube inside diameter (in):.....',f8.3,5x,
     1' Tube outside diameter (in):....',f8.3,5x,/,
     1' Tube total length (ft):........',f8.1,5x,
     1' Total number of tubes (-):.....',f8.1,5x,/,
     1' Tube mass flow rate (lbm/h):...',e8.0,5x,
     1' Shell mass flow rate (lbm/h):..',e8.0,5x,/,
     1' Tube inlet temperature (F):....',f8.0,5x,
     1' Shell inlet temperature (F):...',f8.0,5x,/,
     1' Tube outlet temperature (F):...',f8.1,5x,
     1' Shell outlet temperature (F):..',f8.1,5x,/,
     1' Tube surface temperature (F):..',f8.1,5x,
     1' Log mean temp. difference (F):.',f8.1,5x,/,
     1' Tube-side HTC (Btu/ft2 h F):...',f8.1,5x,
```

```
    1' Shell-side HTC (Btu/ft2 h F):..',f8.1,5x,/,
    1' Rate of heat transfer (Btu/h):.',e8.1,5x,
    1' Overall HTC (Btu/ft2 h F):.....',f8.1,5x,/,
    1' Number of transfer units (-):..',f8.1,5x,
    1' Heat exchanger effectiveness:..',f8.3,5x,/)
     stop
     end

c.....................................................................
     subroutine htc(Tflow,Ts,dm,aN,diam,fa,h)
     implicit real*8 (a-h,o-z)
     call intrpl(Tflow,cp,cpg,amu,amug,ak,akg,Pr,prg,sigf,betaf,
1    ro,rog,anuf,anug,vf,vfg,vg)
     Re=dm*diam/(amu*aN*fa)
     if(Re.gt.4000.) go to 1
     h=(48/11)*ak/diam
     return
1    continue
c n=0.4 for fluid being heated up and n=0.3 for fluid being cooled down
      b=0.4
      if(Ts.lt.Tflow) b=0.3
      h=(ak/diam)*0.023*(Re**0.8)*(Pr**b)
      return
      end
c.....................................................................
      Subroutine NTU(dmi,cpfi,dmo,cpfo,Ao,Uo,Cmin,Cr,aNTU,eff)
      implicit real*8(a-h,o-z)
      Cmin=dmi*cpfi
      Cmax=dmo*cpfo
      If(Cmax.gt.Cmin) go to 1
      Cmin=dmo*cpfo
      Cmax=dmi*cpfi
      continue
      Cr=Cmin/Cmax
      aNTU=Uo*Ao/Cmin
      arg=exp(-aNTU*sqrt(1.+Cr*Cr))
      ratio=(1.+arg)/(1.-arg)
      eff=2./(1.+Cr+sqrt(1.+Cr*Cr)*ratio)
      return
      end
c.....................................................................
         Subroutine Uover(di,do,hi,ho,fi,fo,aks,Uo)
         implicit real*8(a-h,o-z)
         Resi=do/(di*hi)
         Resfi=do*fi/di
         Ress=do*alog(do/di)/(2.*aks)
         Reso=1./ho
         Uo=1./(Resi+Resfi+Ress+fo+Reso)
         return
         end
c.....................................................................
```

The results for the above data are obtained in 5 iterations as follows:

Tube inside diameter (in):	0.652	Tube outside diameter (in):	0.750
Tube total length (ft):	40.0	Total number of tubes (-):	1000
Tube mass flow rate (lbm/h):	2E+6	Shell mass flow rate (lbm/h):	3E+6
Tube inlet temperature (F):	200.	Shell inlet temperature (F):	75.
Tube outlet temperature (F):	131.6	Shell outlet temperature (F):	120.8
Tube surface temperature (F):	131.9	Log mean temp. difference (F):	58.6
Tube-side HTC (Btu/ft^2·h·F):	1145.4	Shell-side HTC (Btu/ft^2·h·F):	1186
Rate of heat transfer (Btu/h):.	1.37E8	Overall HTC (Btu/ft^2·h·F):	297.6
Number of transfer units (-):..	1.2	Heat exchanger effectiveness:	0.547

3.2. Performance Monitoring

Performance of heat exchangers degrades over time primarily due to fouling. Two methods can be used to evaluate heat exchanger performance. The first method is to measure pressure drop and the second is to use measured flow rates and temperatures to calculate the fouling factor. The second method is accomplished by calculating the heat transfer coefficients in the tubes and in the shell (i.e., h_i and h_o). The fouling factor is then obtained from Equation VIa.1.1 and VIa.1.12:

$$\frac{f_i}{A_i}+\frac{f_o}{A_o}=\frac{F(\Delta T_{LMTD})_{Fouled}}{\dot{Q}_{Fouled}}-[\frac{1}{h_i A_i}+\frac{\ln(d_o/d_i)}{2\pi L k_s}+\frac{1}{h_o A_o}] \qquad \text{VIa.3.1}$$

where in steady-state operation,

$$\dot{Q}=\dot{m}_c c_{p,c}(T_{c,out}-T_{c,in})=\dot{m}_h c_{p,h}(T_{h,in}-T_{h,out})\,.$$

The software on the accompanying CD-ROM can be used to analyze the performance of the shell and tube heat exchangers including the calculation of the tube-side pressure drop.

Example VIa.3.2. The rate of heat transfer in a shell and tube heat exchanger is 11.72 MW or about 4E7 Btu/h. Water flows in both tube and shell. The design values for the clean heat exchanger are as follows:

	T_{in} (F)	T_{out} (F)	$\dot{m}$ (lbm/h)	d (in)	L (ft)	N
Tube:	150	130.0	2.0E6	0.652	13	773
Shell:	90	102.5	3.2E6	0.750	18	1

The data for the same heat exchange in a fouled condition are:

	T_{in} (F)	T_{out} (F)	$\dot{m}$ (lbm/h)	d (in)	L (ft)	N
Tube:	150	133.0	2.0E6	0.652	13	773
Shell:	90	100.6	3.2E6	0.750	18	1

a) Find the overall heat transfer coefficient for the clean heat exchanger. (k_s = 8 Btu/h·ft·F)
b) Find the cleanliness factor for the fouled heat exchanger
c) Find the fouling factor, assuming that the fouling occurs primarily in the tubes.

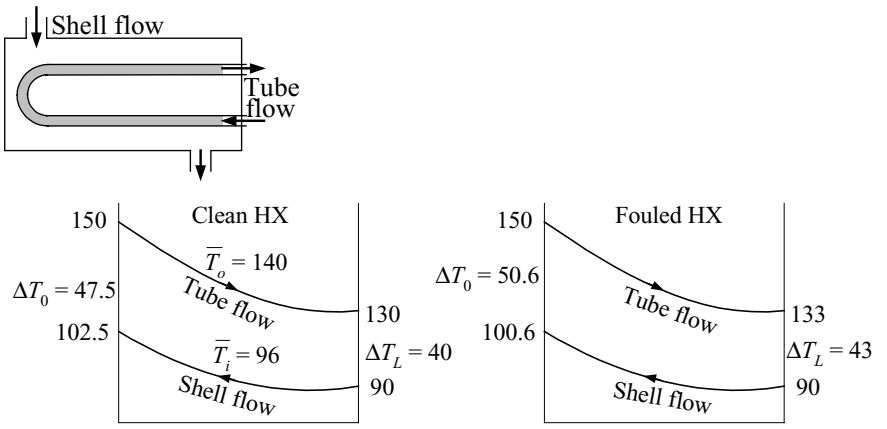

Solution: a) We find ΔT_{LMTD} for the clean heat exchanger and follow the steps outlined below:

$[\Delta T_{LMTD}]_{Clean} = (47.5 - 40)/\ln(47.5/40) \approx 44$ F
$P = (102.5 - 90)/(150 - 90) = 0.2$ and $R = (90 - 102.5)/(130 - 150) = 0.21$
Figure VIa.2.3 gives $F \approx 0.97$
$A_o = \pi d_o LN = 3.14 \times (0.75/12) \times 13 \times 773 = 1973$ ft^2
$\dot{Q}_{Clean} = F(U_o)_{Clean} A[\Delta T_{LMTD}]_{Clean}$
$(U_o)_{Clean} = 4E7/(0.97 \times 1973 \times 44) \approx 475$ Btu/h·F

To confirm, $(U_o)_{\text{Clean}}$, we perform the following calculation:

	$\overline{T}$ (F)	ρ (lbm/ft^3)	c_p (Btu/lbm·F)	μ (lbm/ft·h)	k (Btu/ft·h·F)	Pr
Tube	140	61.37	1.0	1.13	0.378	2.99
Shell	96	62.03	1.0	1.73	0.362	4.77

We use the Dittus-Boelter correlation to find heat transfer coefficient in both tube and shell:

$d_i = 0.652/12 = 0.0543$ ft $\rightarrow$ $a_i = \pi d_i^2/4 = 3.14 \times 0.0543^2/4 = 2.32$E-3 ft^2.

$d_o = 0.75/12 = 0.0625$ ft $\rightarrow$ $a_o = \pi d_o^2/4 = 3.14 \times 0.0625^2/4 = 3.06$E-3 ft^2.

$\text{Re}_i = 4\dot{m}_i/(\pi N \mu_i d_i) = 4 \times 2.0\text{E}6/(3.14 \times 773 \times 1.13 \times 0.0543) = 53{,}688$

$\text{Re}_o = 4\dot{m}_o/(\pi N \mu_i d_o) = 4 \times 3.2\text{E}6/(3.14 \times 773 \times 1.73 \times 0.0625) = 48{,}748$

$h_i = (k_i/d_i)[0.023\text{Re}^{0.8}\text{Pr}^{0.3}] = (0.378/0.0543) \times [0.023 \times 53{,}688^{0.8} \times 2.99^{0.3}] = 1352$ Btu/h·ft^2·F
$h_o = (k_o/d_o)[0.023\text{Re}^{0.8}\text{Pr}^{0.4}] = (0.362/0.0625) \times [0.023 \times 48{,}748^{0.8} \times 4.77^{0.4}] = 1401$ Btu/h·ft^2·F

$1/(U_o)_{\text{Clean}}$ = [0.0625/(0.0543 × 1352)] + [0.0625ln(0.0625/0.0543)/(2 × 8)] + [1/1401] = 2.1126E-3
$(U_o)_{\text{Clean}}$ = 1/2.1145E-3 = 473 Btu/h·ft^2·F

b) For the fouled exchanger, the average temperatures and related properties are as follows:

	$\overline{T}$ (F)	ρ (lbm/ft^3)	c_p (Btu/lbm·F)	μ (lbm/ft·h)	k (Btu/ft·h·F)	Pr
Tube	141.5	61.35	1.0	1.16	0.378	2.95
Shell	95.3	62.03	1.0	1.75	0.361	4.82

The related Re numbers, Nu numbers, and heat transfer coefficients become:

	$\overline{T}$ (F)	Re	Nu	h (Btu/h·ft^2·F)
Tube	141.5	53,023	191.5	1333
Shell	95.3	49,311	245.8	1420

$[\Delta T_{LMTD}]_{Fouled}$ = (50.6 – 43)/ln(50.6/43) ≈ 46.7 F.
P = (100.6 – 90)/(150 – 90) = 0.17 and R = (90 – 100.6)/(133 – 150) = 0.62
Figure VIa.2.3 gives F = 1.0
$\dot{Q}_{Fouled}$ = 2E6 × 1 (150 – 133) = 3.4E7 Btu/h
$(U_o)_{Fouled} = \dot{Q}_{Fouled} / [FA_o(\Delta T_{LMTD})_{Fouled}]$ = 3.4E7/(1973 × 46.7) = 369 Btu/h·F
$C_F = U_{Fouled}/U_{Clean}$ = 369/475 ≈ 78%

c) To find the fouling factor, we solve Equation VIa.1.1 for f_i as f_o is specified to be negligible:

$$\frac{d_o f_i}{d_i} = \frac{FA_o(\Delta T_{LMTD})_{Fouled}}{\dot{q}_{Fouled}} - \left[\frac{d_o}{d_i h_i} + \frac{d_o \ln(d_o/d_i)}{2k_s} + \frac{1}{h_o}\right]$$

Substituting values

$$\frac{d_o f_i}{d_i} = \frac{1}{369} - \left[\frac{0.0625}{0.0543 \times 1333} + \frac{0.0625 \ln(0.0625/0.0543)}{2 \times 8} + \frac{1}{1420}\right]$$

= 2.71E-3 – 2.1E-3

This results in f_i = 0.0005 h·ft^2·F/Btu. Note that the calculation of h_o was simplified in this problem.

As noted in the conclusion of Example VIa.3.1, calculation of the heat transfer coefficient for the tube bundle was based on a simplistic approach. Generally, the design of a heat exchanger shell depends on several factors including the number of tube passes, tube layout (type of array for tube bundle), baffle type, geometry, baffle spacing, operational pressure, weight, and size limitations. As a result, calculation of the shell-side h_o and ΔP_o is much more involved than h_i and ΔP_i for the tube side. For example, the baffle plates force fluid, which without the baffles flows parallel to the tube axis, to flow in a cross-flow manner over the tube bundle. Also, the diameter used in a correlation for h_o should be an appropriate hydraulic diameter. For a concentric or a double-pipe heat exchanger, the hydraulic diameter is found from:

$$D_c = 4\frac{A_f}{C_w} = 4\frac{\pi[D_{Sh}^2 - d_o^2]/4}{\pi(D_{Sh} + d_o)} = D_{Sh} - d_o$$

where A_f is the flow area, C_w the wetted perimeter, D_{sh} the shell diameter, and d_o the tube outside diameter. The hydraulic diameter found above can then be used in a suitable correlation such as Dittus-Boelter to find the heat transfer coefficient. For shell and tube heat exchangers, the hydraulic diameter is calculated for the tube array. Perry suggests correlations for calculation of h_o and Kakac provides related examples.

4. Analysis of Condensers

Power plant condensers generally use coolant from large bodies of water such as a lake or bay to cooldown the condensing steam. The temperature difference between the condensing steam saturation temperature and circulating water inlet temperature is referred to as *ITD*, the initial temperature difference. The temperature difference at the tube exit is referred to as *TTD*, the terminal temperature difference (Figure VIa.4.1).

In condenser design, in addition to the steam pressure, hence steam saturation temperature (T_o), and the cooling water inlet temperature ($T_{c,in}$), we need to select an appropriate tube-side flow velocity to meet the heat transfer requirement while minimizing pumping power and tube erosion. Tube velocity may range from 3 to 12 ft/s. The tube side heat transfer coefficient can be found from the Dittus-Boelter correlation (Equation IVb.3.4) and the bundle-side heat transfer coefficient from condensation on horizontal tubes, given by Equation Vc.3.4. Temperature rise of the cooling water for large power plants is generally in the range of 12 to 15 F to minimize thermal pollution. Having the temperature rise, the flow rate of the cooling water is then found from $\dot{m}_c = \dot{Q}/\Delta T_i$. Knowing the heat sink water temperature, we can then find the temperature of the cooling water at the outlet. Selection of the tube diameter (tube flow area) combined with the cooling water density and velocity give the mass flow rate per condenser tube. The total number of tubes (N_{tube}) is obtained by dividing the cooling water mass flow rate by the mass flow rate of a tube. We then find the average tube length (L_{tube}) from $\dot{Q}$, ΔT_{LMTD}, and Equation VIa.2.12a.

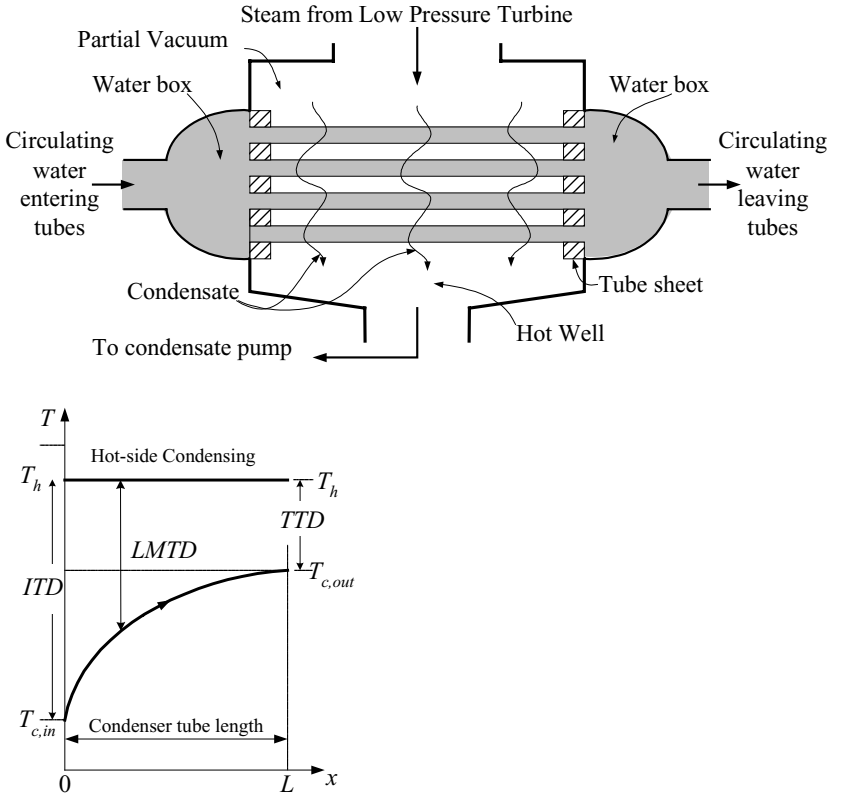

Figure VIa.4.1. Schematic of a condenser

Example VIa.4.1. A power plant produces 855 MWe at a thermal efficiency of $\eta_{\text{Thermal}} = 30\%$. Find: a) N_{tube} and L_{tube}, b) tube side pressure drop and c) Shell-side flow rate. Use the following data: $d_i = 0.93$ in, $d_o = 1$ in, $T_{c,in} = 68$ F, $\Delta T_c = 20$ F, $T_h = 123$ F, $V_i = 9$ ft/s, $k_s = 26$ Btu/ft·h·F, $c_{p,c} = 1$ Btu/lbm·F.

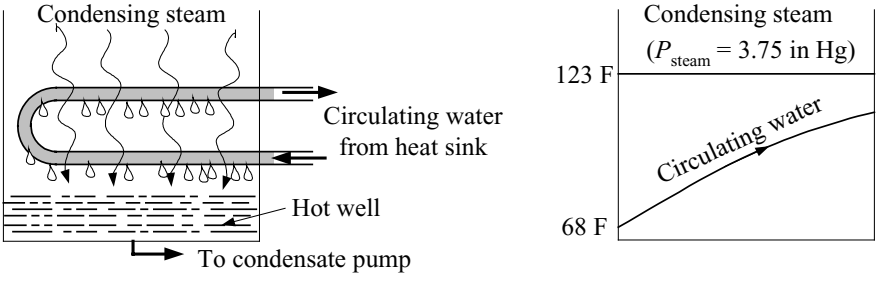

Solution: a) First we calculate the rate of heat to be removed by the condenser. Total power produced is:

$\dot{Q}_H = \dot{W} / \eta_{Thermal}$ = 855/0.3 = 2850 MWth. The rate of heat to be removed in the condenser is:

$\dot{Q}_C$ = 2850 – 855 = 1995 MWth = 6.8069E9 Btu/h

- Tube-side mass flow rate: $\dot{m}_i = \dot{Q}_C /(c_{p,c}\Delta T_c) \cong 6.8069E9/(1 \times 20) = 3.4E8$ lbm/h

- Since $T_{c,out}$ = 68 + 20 = 88 F, the tube-side average temperature becomes T_c = 0.5(68 + 88) = 78 F.

- To find U we need h_i and h_o. To find h_o, we need tube temperature T_s, which varies along the tube length. We use T_s calculated at average temperatures to represent the entire tube temperature. Since we do not have tube surface area, for now we guess T_s from T_c and T_h: $T_s = 0.5(T_c + T_h)$ = 05(78 + 123) = 100.5 F

- Properties for both tube-side and shell-side at the related film temperatures are: $(T_{film})_c = 0.5(T_c + T_s)$ = 89.25 F. $(T_{film})_h$ = 0.5(100.5 + 123) = 111.75 F

	$\overline{T}$ (F)	ρ (lbm/ft^3)	c_p (Btu/lbm·F)	μ (lbm/ft·h)	k (Btu/ft·h·F)	Pr
Shell	111.75	61.82	0.998	1.466	0.368	-
Tube	89.25	62.12	0.998	1.868	0.358	5.207

For tube bundle (shell-side) we also find h_{fg}(123 F) = 1023.9 Btu/lbm and ρ_g(111.75 F) = 0.004 lbm/ft^3

- Since $T_{sat} > T_s$, we find Ja = $c_{p,h}(T_h - T_s)/h_{fg}$ = 0.998 × (123 – 100.5)/1023.9 = 0.0219. Thus h'_{fg} = 1023.9(1 + 0.68 × 0.0219) 1039.17 Btu/lbm

$$h_o = 0.729[\frac{g\rho_f(\rho_f - \rho_g)k_f^3 h'_{fg}}{\mu_f(T_h - T_s)d_o}]^{1/4} = 0.729[\frac{4.173E8 \times 61.82^2 \times 0.368^3 \times 1039.17}{1.466 \times (123 - 100.5) \times (1./12)}]^{1/4}$$

= 1707 Btu/ft^2·h·F

- To calculate h_i we need to find $\mathrm{Re}_i = \dot{m}_i d_i/(\mu_i N a_i)$. This in turn requires N and a_i, which are found as:

$a_i = \pi d_i^2 / 4$ = 3.14 × (0.93/12)^2/4 = 0.004717 ft^2.

$N = \dot{m}_i /(\rho_i V_i a_i)$ = 3.41E8/[62.12 × (9 × 3600) × 0.004717] = 35918

Re_i = 3.41E8 × (0.93/12)/(1.868 × 35918 × 0.004717) = 83,500

$h_i = (k_i/d_i)[0.023\,\mathrm{Re}_i^{0.8}\,\mathrm{Pr}_i^{0.4}]$ = (0.358 × 12/0.93) × [0.023 × 83500$^{0.8}$ × 5.207$^{0.4}$] = 1779.5 Btu/ft^2·h·F

- We now calculate U_o:

$$U_o = [\frac{d_o}{d_i h_i} + \frac{d_o \ln(d_o/d_i)}{2k_s} + \frac{1}{h_o}]^{-1} = [\frac{1}{0.93\times 1779.5} + \frac{(1/12)\ln(1/0.93)}{2\times 26} + \frac{1}{1707}]^{-1}$$

$= 765.5$ Btu/ft^2·h·F

- We also calculate $\Delta T_{LMTD} = \dfrac{(123-68)-(123-88)}{\ln[(123-68)/(123-88)]} = 44.25$ F

- To find total tube length, we use the overall energy balance $\dot{Q}_C = U_o A_o \Delta T_{LMTD}$ $= U_o (\pi d_o N L)\, \Delta T_{LMTD}$

- $L = \dfrac{\dot{Q}_C}{U_o(\pi d_o N)\Delta T_{LMTD}} = \dfrac{6.8069\text{E}9}{765.5\times\pi\times(1/12)\times 35918\times 44.25} = 21.2$ ft.

- For two-tube pass per shell, $L_{pass} = 21.2/2 = 10.68$ ft.

b) The tube-side pressure drop is found from Equation III.6.7:

$$\Delta P_i = f\frac{L}{d_i}\frac{\dot{m}_i^2}{2\rho_i g_c a_i^2} = (\frac{0.184}{\text{Re}_i^{0.2}})\frac{21.2}{(0.93/12)}\frac{(3.41\text{E}8/35918)^2}{2\times 62.12\times(32.2\times 3600^2)(0.004717)^2}$$

$= 408$ lbf/ft$^2 = 2.83$ psi.

c) The rate of steam condensation is found from:

$$\dot{m}_o = \dot{Q}_C / h'_{fg} = 6.8069\text{E}9/1039.17 = 6.55\text{E}6 \text{ Btu/h}$$

The results are summarized below:

d_i (in)	d_o (in)	h_i (Btu/h·ft^2·F)	h_o (Btu/h·ft^2·F)	U_o (Btu/h·ft^2·F)	L (ft)	ΔT_{LMTD} (F)	ΔP_i (psi)
0.93	1	1779.5	1707	765.5	21.2	44.25	2.83

Comment: we may use a transverse heat balance $h_i A_i (T_s - T_c) = h_o A_o (T_h - T_s)$ to update tube temperature, T_s. Note that due to high tube thermal conductivity, we assumed $T_{si} = T_{so}$. The updated average tube temperature becomes $T_s = [T_h + (h_i d_i/h_o d_o)T_c]/[1 + (h_i d_i/h_o d_o)] = 101.66$ F. This is 1% larger than T_s used in the above analysis.

The above example shows the theoretical aspects of a condenser design. In practice, such problems as tube fouling and the ingress of non-condensable gases in the tube bundle need to be dealt with. The gas leakage in the tube bundle not only increases the hot well total pressure but also, as discussed by Harpster, tends to collect around some tubes, degrading condensation.

4.1. Condenser Design Optimization

For a given rate of heat transfer ($\dot{Q}$) and bundle-side pressure [$T_h = T_{sat}(P_{steam})$], we are interested in evaluating the effects of such parameters as tube velocity (V_i), tube diameter (d_i and d_o) and tube length (L) on the tube-side pressure drop and subsequently the required pumping power. To perform this parametric evaluation, we rearrange Equation VIa.3.1, noting that $F = 1$ for condensers:

$$\frac{1}{h_i(\pi d_i NL)} + \frac{\ln(d_o / d_i)}{2\pi k_s NL} + \frac{1}{h_o(\pi d_o NL)} = \frac{\Delta T_{LMTD}}{\dot{Q}} \qquad \text{VIa.4.1}$$

where h_o may be calculated from Equation Vc.3.4. Hence, it is treated here as a constant. This is because the value of h_o depends only on the properties of the condensing fluid and the outside diameter of the tube. In Equation VIa.4.1, we need to substitute for h_i in terms of V_i and d_i. For this purpose, we use the definition of the Nusselt number:

$$\begin{aligned} h_i d_i &= k_i Nu_i = k_i \left[0.023 \left(\rho_i V_i d_i / \mu_i \right)^{0.8} \mathrm{Pr}_i^{0.4} \right] \\ &= \left(0.023 k_i \, \mathrm{Pr}_i^{0.4} \, \rho_i^{0.8} / \mu_i^{0.8} \right) \left(d_i V_i \right)^{0.8} \end{aligned}$$

Substituting for $h_i d_i$ in Equation VIa.4.1 and rearranging, we obtain:

$$\left(\frac{\pi \Delta T_{LMTD}}{\dot{Q}} \right) NL = \frac{1}{\left(0.023 k_i \, \mathrm{Pr}_i^{0.4} \, \rho_i^{0.8} / \mu_i^{0.8} \right) \left(d_i V_i \right)^{0.8}} + \left[\frac{\ln\left(d_o / d_i \right)}{2k_s} - \frac{1}{d_o h_o} \right] \qquad \text{VIa.4.2}$$

Equation VIa.4.2 provides a relation between N and L. We can find N in terms of d_i and V_i from an energy balance for the tube side:

$$N = \frac{4\dot{m}_i}{\rho_i V_i (\pi d_i^2)} = \left[\frac{4\dot{Q}}{(\pi d_i^2) c_{p,c} (T_{c,out} - T_{c,in})} \right] \frac{1}{\rho_i V_i} \qquad \text{VIa.4.3}$$

Substituting N from Equation VIa.4.3 into Equation VIa.4.2, we find tube length L as:

$$L = \frac{\left[\dfrac{d_i^{1.2} V_i^{0.2}}{0.023 k_i \, \mathrm{Pr}_i^{0.4} \, \rho_i^{0.8} / \mu_i^{0.8}} \right] - \left[\dfrac{\ln\left(d_o / d_i \right)}{2k_s} - \dfrac{1}{d_o h_o} \right] d_i^2 V_i}{\left[\left(\dfrac{4}{\rho_i c_{pi}} \right) \left(\dfrac{\Delta T_{LMTD}}{\Delta T_i} \right) \right]} \qquad \text{VIa.4.4}$$

As shown in Tables A.III.1 and A.III.2, the selection of tube or pipe outside diameter and the specification of tube gage or pipe schedule results in the determination of the inside diameter. Equation VIa.4.3 shows that, for a specified tube size, the number of tubes is inversely proportional to the coolant velocity in the tubes. On the other hand, Equation VIa.4.4 shows that tube length is nearly a

tubes. On the other hand, Equation VIa.4.4 shows that tube length is nearly a linear function of tube-side velocity.

Using the above equations and the data of Example VIa.4.1, plots of tube length and number of tubes versus tube diameter are obtained as shown in Figure VIa.4.2. As expected, the plots show that for a specified flow velocity, the number of tubes increases, whereas tube length decreases with decreasing tube diameter. Also, for a given tube diameter, tube length increases and number of tubes decreases with increasing tube velocity. The same conclusion can be made for tube-side pressure drop and pumping power. The pumping power is given as:

$$\dot{W}_{pump} = \Delta P(\dot{m}_i / \rho) \qquad \text{VIa.4.5}$$

For a given tube diameter, the required pumping power decreases as the number of tubes increases. This reduces operational cost. On the other hand, as shown by Nahavandi, the initial capital cost increases with an increasing number of tubes. Therefore, an optimized value for the number of tubes should be found to satisfy cost criterion.

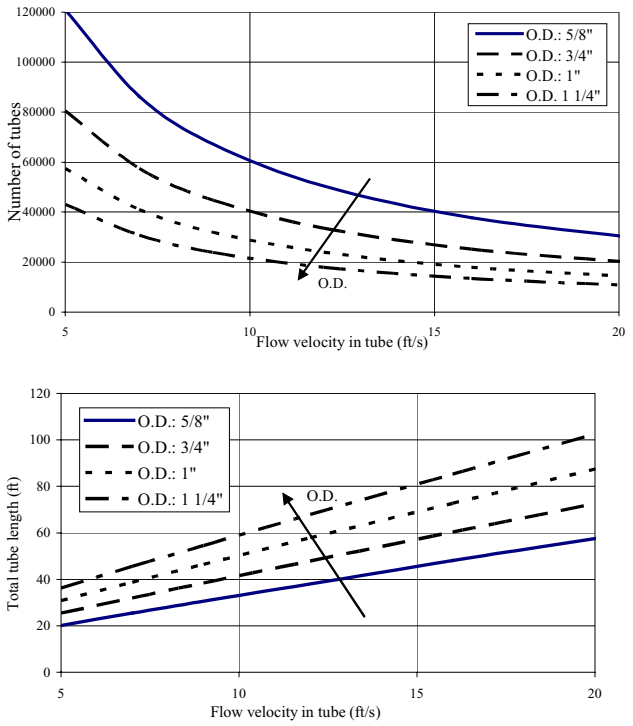

Figure VIa.4.2. Tube length and tube number versus flow velocity for various tube diameters

5. Analysis of Steam Generators

In the design of steam generators, the rate of heat transfer, inlet and outlet temperatures, and flow rates are generally known quantities (Figure VIa.5.1). The goal, therefore, is to calculate the heat transfer area of the tubes. In steam generators, the hot fluid generally flows in the tubes with water boiling in the tube bundle. In this analysis we consider the secondary side to be at saturation condition along the entire length of the tubes whether tubes are oriented horizontally or vertically. To be consistent, we show tube side values with subscript i and secondary-side values with subscript o, respectively. Also, $T_{h,in}$, $T_{h,out}$, and T_c are tube inlet, tube exit, and shell-side saturation temperatures, respectively. Known values are $\dot{Q}$, $\dot{m}_i$, $T_{h,in}$, $T_{h,out}$, T_c, f_i, f_o, d_i and d_o. We calculate the steam generator effectiveness from:

$$\varepsilon = \frac{T_{h,in} - T_{h,out}}{T_{h,in} - T_c} \qquad \text{VIa.5.1}$$

Having ε from Equation VIa.5.1, we can calculate NTU from $NTU = UA/C_{\min} = -\ln(1-\varepsilon)$ Therefore,

$$UA = -\dot{m}_i c_{p,i} \ln(1-\varepsilon) \qquad \text{VIa.5.2}$$

Combining Equations VIa.1.1 and VIa.5.2, writing the total tube length as $L = A_o/(\pi d_o)$, and the surface area of the inside of the tubes as $A_i = d_i A_o/d_o$ yields:

$$\left[\frac{d_o}{d_i}\frac{1}{h_i A_o} + \frac{d_o}{d_i}\frac{f_i}{A_o} + \frac{d_o}{2k_s}\frac{\ln(d_o/d_i)}{A_o} + \frac{f_o}{A_o} + \frac{1}{h_o A_o}\right]^{-1} = -\dot{m}_i c_{p,i} \ln(1-\varepsilon) \qquad \text{VIa.5.3}$$

Total tube surface area, A_o is obtained from Equation VIa.5.3 provided h_i and h_o are substituted in terms of known quantities. We use the Dittus-Boelter correlation (Equation IVb.3.4) for turbulent flow inside tubes to find h_i:

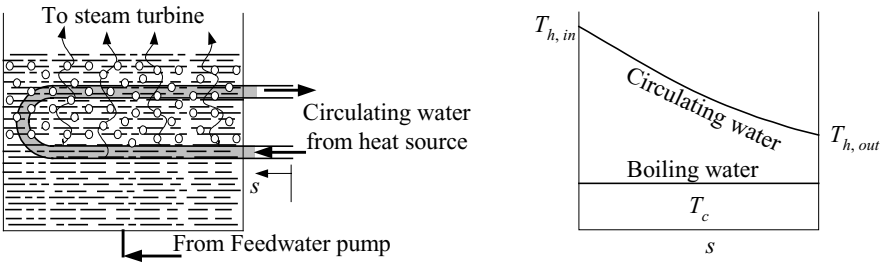

Figure VIa.5.1. Schematic of a steam generator

$$h_i = 0.023 \frac{k_i}{d_i} \left(\frac{4\dot{m}_i}{\pi \mu_i N d_i}\right)^{0.8} \mathrm{Pr}_i^{0.3} \qquad \text{VIa.5.4}$$

where the exponent of the Pr number is changed to 0.3 as the fluid is cooling down. Also physical properties in Equation VIa.5.4 are developed at the fluid bulk temperature. The secondary side heat transfer coefficient h_o may be found from Rohsenow's pool boiling correlation or the Chen correlation (Equations Vb.4.1a and Vb.5.1b, respectively). Selecting the Rohsenow correlation, we find:

$$T_s - T_c = \frac{C_{fs} h_{fg}}{c_{p,o}} \left[\frac{\dot{Q}/A_o}{\mu_o h_{fg}} \sqrt{\frac{g_c \sigma_o}{g(\rho_{f,o} - \rho_{g,o})}}\right]^{1/3} \mathrm{Pr}_o^{1.7} \qquad \text{VIa.5.5}$$

We now correlate the surface superheat to the secondary-side thermal resistance as

$$T_s - T_c = \left(\frac{f_o}{A_o} + \frac{1}{h_o A_o}\right) \dot{Q}$$

and substitute the result in Equation VIa.5.5:

$$\left(\frac{f_o}{A_o} + \frac{1}{h_o A_o}\right) = \left\{\frac{C_{fs} h_{fg}}{c_{p,o}} \left[\frac{1}{\mu_o h_{fg}} \sqrt{\frac{g_c \sigma_o}{g(\rho_{f,o} - \rho_{g,o})}}\right]^{1/3} \mathrm{Pr}_o^{1.7}\right\} \frac{1}{\dot{Q}^{2/3} A_o^{1/3}} \qquad \text{VIa.5.6}$$

Substituting Equation VIa.5.6 into Equation VIa.5.3 results in:

$$C_1 A_o + C_2 A_o^{2/3} + C_3 = 0 \qquad \text{VIa.5.7}$$

where $C_1 = \left[\dot{m}_i c_{p,i} \ln(1-\varepsilon)\right]^{-1}$,

$$C_2 = \left\{\frac{C_{fs} h_{fg}^{2/3}}{c_{p,o}} \left[\frac{1}{\mu_o} \sqrt{\frac{g_c \sigma_o}{g(\rho_{f,o} - \rho_{g,o})}}\right]^{1/3} \mathrm{Pr}_o^{1.7}\right\} \frac{1}{\dot{Q}^{2/3}} \text{ and}$$

$$C_3 = \left[\frac{d_o}{d_i}\frac{1}{h_i} + \frac{d_o}{d_i} f_i + \frac{d_o}{2} \frac{\ln(d_o/d_i)}{k_s}\right],$$

where g_c is given in Chapter IIa. Equation VIa.5.7 is a non-linear algebraic equation that may be solved by Newton-Raphson iteration. The first guess for tube area is obtained from an approximate solution (i.e., by assuming that the secon-

dary-side thermal resistance is negligible $(A_o)_{\text{Guess}} = C_3/C_1$). Upon solving Equation VIa.5.7, we can find the average tube length from $L = A_o/(\pi d_o N)$.

Example VIa.5.1. The following data are given for a steam generator. Find a) the average tube length L_{tube}, b) tube side pressure drop, and c) shell side flow rate. Data: $d_i = 0.654$ in, $d_o = 0.75$ in, $T_{h,in} = 604$ F, $T_{h,out} = 550$ F, $P_h = 2250$ psia, $P_c = 850$ psia, $k_s = 11.00$ Btu/ft·h·F, $N_{tube} = 8485$, $\dot{m}_i = 61$E6 lbm/h, $C_{fs} = 0.015$, $c_{p,o} = 1.24$ Btu/lbm·F, $f_i = 0.0002437$ ft^2·h·F/Btu, $f_o = 0.0$ ft^2·h·F/Btu.

Solution: The solution, in a FORTRAN program, is included on the accompanying CD-ROM.

The input data and results of calculation are summarized below.

Table VIa.5.1. Pertinent steam generator thermal hydraulic data

Total rate of heat transfer (Btu/h - MW):	4.386E9 - 1285.5
Tube inlet temperature (F - C):	604 - 318
Tube exit temperature (F - C):	550 - 288
Tube-side pressure (psia - MPa):	2250 - 15.51
Tube bundle-side pressure (psia - MPa):	850 - 5.86
Tube bundle-side temperature (F - C):	525.2 - 274
Total number of tubes:	8485
Tube outside diameter (in - mm):	0.75 - 19.05
Tube wall thickness (in - mm):	0.048 - 1.22
Tube inside diameter (in - mm)	0.654 - 16.61
Tube average heated length (ft - m):	54.16 - 16.5
Tube heat transfer area (ft^2 - m^2):	90,232 - 8383
Overall heat transfer coefficient (Btu/h·ft^2·F - W/m^2·C):	1041 - 183.3
The log mean temperature difference, ΔT_{LMTD} (F - C):	46.7 - 25.9
Effectiveness:	0.684
Tube-side thermal resistance (h·ft^2·F/Btu - m^2·C/W):	0.0001744 - 0.00099
Tube-wall thermal resistance (h·ft^2·F/Btu - m^2·C/W):	0.0003950 - 0.00224
Tube bundle-side thermal resistance (h·ft^2·F/Btu - m^2·C/W):	0.0001475 - 0.00084
Tube-side fouling resistance (h·ft^2·F/Btu - m^2·C/W):	0.000 - 0.000
Tube bundle-side fouling resistance (h·ft^2·F/Btu - m^2·C/W):	0.0002437 - 0.00138

An alternative derivation for determination of the required surface area for the tubes takes into account the energy balance for an elemental control volume due to the change in temperature from tube inlet to tube exit (Nahavandi). Similar correlations can then be used for heat transfer coefficients and the resulting differential equation is integrated from tube inlet to tube outlet to obtain the required surface area. (see Problem VIa.18).

In steam generators, we often need to find the temperature of the hot fluid as it moves inside the tubes and transfers energy to the secondary side. This is shown in the next example.

Example VIa.5.2. Hot liquid is flowing steadily at a rate of $\dot{m}$ inside the tubes of a steam generator having N tubes of outside diameter d_o. The secondary side is boiling, resulting in an overall heat transfer coefficient of U_o that remains uniform along the tube. Find the tube-side temperature profile as a function of flow path.

Solution: Applying Equation IIa.6.4-1 to the single-phase liquid inside the tubes over element ds, results in:

$$\frac{dT_h}{ds} = -\frac{N\pi d_o U_o}{\dot{m} c_p}\left(T_h - T_{sat}\right)$$

where s is an element of length in the flow direction and T_{sat} is the secondary-side saturation temperature. Since $\dot{m}$, U_o, and T_{sat} remain constant, we can integrate from $T_{h,in}(s = 0)$ to $T(s)$ to find:

$$T_h(s) = T_{h,in} - \left(T_{h,in} - T_{sat}\right)\left(1 - e^{-s/l^*}\right) \qquad \text{VIa.5.8}$$

where s is an element of length along the tube and l^* is given by $l^* = \dot{m}\, c_p/(\pi N d_o U_o)$. This result is not applicable if liquid boils in the tube-side or liquid does not boil in the secondary side.

6. Transient Analysis of Concentric Heat Exchangers

A transient during heat exchanger operation is generally caused by throttling a valve located on the discharge line of the pump feeding the tube or the shell side. Heat exchanger transients also take place during starting or stopping the pump. Transients imposed by valves and pumps affect flow rate. Inlet temperatures to tube or shell may also change due to the loss of a feedwater heater if located upstream of the heat exchanger. In this analysis we consider concentric parallel and counterflow heat exchangers and divide the exchanger along its length to several nodes. Both streams are assumed to be incompressible and average fluid properties are used. By explicitly modeling the tube region, thermal inertia of the tube material would then appear in the formulation. Shown in Figure VIa.6.1 is the schematic of a concentric heat exchanger, divided into N nodes but only three nodes are shown. Node i, for example, receives mass and energy from node i - 1, as carried by the mass flow rate of stream A and, in turn, delivers mass and enthalpy to node i + 1. Due to the liquid incompressibility, mass flow rate into node i equals the mass flow rate into node i + 1, as only energy would accumulate in

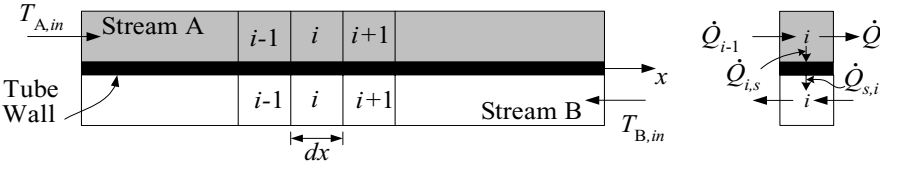

Figure VIa.6.1. Nodalization of a concentric heat exchanger

node *i*. There is also a transverse energy transfer out of node *i* of stream A, through the tube surface into node *i* of stream B. Hence, the energy balance in the axial direction for element *i* in stream A yields:

$$\dot{Q}_{i-1} - \dot{Q}_i - d\dot{Q}_{i-s} = \frac{\partial}{\partial t}\left(m_i c_v T_i\right) \qquad \text{VIa.6.1}$$

where in Equation VIa.6.1, m_i is the mass of stream A fluid in control volume *i*. Note that in this derivation, we ignored heat conduction in the fluid compared with the rate of energy transfer by convection. Replacing $m_i = \rho_i A_i dx$, where A_i is the flow area of stream A, and expanding the second term in the left side, Equation VIa.6.1 becomes:

$$\dot{Q}_{i-1} - \left(\dot{Q}_{i-1} + \frac{\partial \dot{Q}_{i-1}}{\partial x}dx\right) - d\dot{Q}_{i-s} = \frac{\partial}{\partial t}\left[\left(\rho A dx\right)_i c_{v,i} T_i\right]$$

Since fluid is incompressible, we express enthalpy in terms of specific heat and temperature. Parameters ρ_i, $c_{p,i}$, and A_i are also constant. The formulation for stream A becomes:

$$-\frac{\partial}{\partial x}\left(\rho V A c_p T\right)_{\mathrm{A}} dx - d\dot{Q}_{i-s} = \frac{\partial}{\partial t}\left(\rho A dx c_v T\right)_{\mathrm{A}}$$

Substituting for the transverse energy term, yields:

$$-\frac{\partial}{\partial x}\left(\rho V A c_p T\right)_{\mathrm{A}} dx - (\mathrm{P}h dx)_{\mathrm{A}}\left(T_{\mathrm{A}} - T_s\right) = \frac{\partial}{\partial t}\left(\rho A dx c_v T\right)_{\mathrm{A}}$$

where P is the perimeter ($\mathrm{P} = \pi d$) and *h* is the heat transfer coefficient. Note that we have represented the elemental tube since we are using average values for properties, ρ, c_p, c_v, and *h* remains constant. Since A_{A} and V_{A} are also assumed to be constant, we can write:

$$\frac{\partial T_{\mathrm{A}}}{\partial t} + \left(V\frac{c_p}{c_v}\right)_{\mathrm{A}}\frac{\partial T_{\mathrm{A}}}{\partial x} + \left(\frac{\mathrm{P}h}{\rho A c_v}\right)_{\mathrm{A}}\left(T_{\mathrm{A}} - T_s\right) = 0 \qquad \text{VIa.6.2}$$

Similarly, the differential equation describing axial energy of stream B becomes:

$$\frac{\partial T_{\mathrm{B}}}{\partial t} + \lambda\left(V\frac{c_p}{c_v}\right)_{\mathrm{B}}\frac{\partial T_{\mathrm{B}}}{\partial x} - \left(\frac{\mathrm{P}h}{\rho A c_v}\right)_{\mathrm{B}}\left(T_s - T_{\mathrm{B}}\right) = 0 \qquad \text{VIa.6.3}$$

where in this equation, $\lambda = 1$ for parallel flow and $\lambda = -1$ for counterflow heat exchangers. The rate of change of energy in the *i*th node of the tube material is due to the exchange of energy with streams A and B, hence the energy equation for the heat exchanger tube material becomes:

$$\frac{\partial T_s}{\partial t} - \frac{(\mathrm{P}h)_\mathrm{A}}{(\rho cA)_s}(T_\mathrm{A} - T_s) + \frac{(\mathrm{P}h)_\mathrm{B}}{(\rho cA)_s}\left(T_s - T_\mathrm{B}\right) = 0 \qquad \text{VIa.6.4}$$

Equations VIa.6.2, VIa.6.3, and VIa.6.3 constitute an approximate formulation for transient analysis of parallel and counterflow heat exchangers. Various solution methods are proposed for this set of equations. For example, Li finds an exact solution for the parallel flow heat exchanger by using Laplace transforms. Lorenzini applies the finite element method while Romie uses several dimensionless ratios to describe the exit temperature response to a unit step change in the inlet temperatures. The following solution is based on the finite difference method. The energy equations for stream A, in finite difference form is:

$$\frac{T_{\mathrm{A},i}^{n+1} - T_{\mathrm{A},i}^{n}}{\Delta t} + \left(V\frac{c_p}{c_v}\right)_\mathrm{A} \frac{T_{\mathrm{A},i}^{n+1} - T_{\mathrm{A},i-1}^{n+1}}{\Delta x} + \left(\frac{\mathrm{P}h}{\rho A c_v}\right)_\mathrm{A} \left(T_{\mathrm{A},i}^{n+1} - T_{s,i}^{n+1}\right) = 0$$

The finite difference form of the tube wall energy equation becomes:

$$\frac{T_{s,i}^{n+1} - T_{s,i}^{n}}{\Delta t} - \frac{(\mathrm{P}h)_\mathrm{A}}{(\rho cA)_s}\left(T_{A,i}^{n+1} - T_{s,i}^{n+1}\right) + \frac{(\mathrm{P}h)_\mathrm{B}}{(\rho cA)_s}\left(T_{s,i}^{n+1} - T_{\mathrm{B},i}^{n+1}\right) = 0$$

and the finite difference form of stream B energy equation, considering a counterflow heat exchanger is:

$$\frac{T_{\mathrm{B},i}^{n+1} - T_{\mathrm{B},i}^{n}}{\Delta t} - \left(V\frac{c_p}{c_v}\right)_\mathrm{B} \frac{T_{\mathrm{B},i}^{n+1} - T_{\mathrm{B},i+1}^{n+1}}{\Delta x} - \left(\frac{\mathrm{P}h}{\rho A c_v}\right)_\mathrm{B} \left(T_{s,i}^{n+1} - T_{\mathrm{B},i}^{n+1}\right) = 0$$

These equations can be simplified by introducing dimensionless constants for stream A:

$$\alpha_1 = \left(\frac{c_p}{c_v}\right)_\mathrm{A} \frac{V_\mathrm{A}}{(\Delta x/\Delta t)}; \qquad \alpha_2 = 1 + \alpha_1 + \alpha_3; \qquad \alpha_3 = \left(\frac{\mathrm{P}h}{\rho A c_v}\right)_\mathrm{A} \Delta t$$

for the tube material:

$$\sigma_1 = \frac{(\mathrm{P}h)_\mathrm{A}}{(\rho cA)_s}\Delta t; \qquad \sigma_2 = 1 + \sigma_1 + \sigma_3; \qquad \sigma_3 = \frac{(\mathrm{P}h)_\mathrm{B}}{(\rho cA)_s}\Delta t$$

and for stream B:

$$\beta_1 = \left(\frac{\mathrm{P}h}{\rho A c_v}\right)_\mathrm{B} \Delta t; \qquad \beta_2 = 1 + \beta_1 + \beta_3; \qquad \beta_3 = \lambda\left(\frac{c_p}{c_v}\right)_\mathrm{B} \frac{V_\mathrm{B}}{(\Delta x/\Delta t)}.$$

Definition of these dimensionless coefficients reduces the finite difference equations to:

$$-\alpha_1 T_{\mathrm{A},i-1}^{n+1} + \alpha_2 T_{\mathrm{A},i}^{n+1} - \alpha_3 T_{s,i}^{n+1} = T_{\mathrm{A},i}^{n}$$
$$-\sigma_1 T_{\mathrm{A},i}^{n+1} + \sigma_2 T_{s,i}^{n+1} - \sigma_3 T_{\mathrm{B},i}^{n+1} = T_{s,i}^{n}$$
$$-\beta_1 T_{\mathrm{B},i-1}^{n+1} + \beta_2 T_{\mathrm{B},i}^{n+1} - \beta_3 T_{\mathrm{B},i+1}^{n+1} = T_{\mathrm{B},i}^{n}$$

Writing similar equations for node $i = 1$ through $i = N$, the following set of equations is obtained:

$$A^n \underline{Y}^{n+1} = \underline{C}^{n+1} \qquad \text{VIa.6.5}$$

where vector $\underline{Y}$ in Equation VIa.6.5 contains all unknown temperatures:

$$\underline{Y} = \left[\left(T_{\mathrm{A},1}^{n+1} \cdots T_{\mathrm{A},i}^{n+1} \cdots T_{\mathrm{A},N}^{n+1}\right), \left(T_{s,1}^{n+1} \cdots T_{s,i}^{n+1} \cdots T_{s,N}^{n+1}\right), \left(T_{\mathrm{B},1}^{n+1} \cdots T_{\mathrm{B},i}^{n+1} \cdots T_{\mathrm{B},N}^{n+1}\right)\right]^T$$

vector $\underline{C}$ contains known temperatures and the boundary terms, added to the first and last terms:

$$\underline{C} =$$
$$\left[\left(T_{\mathrm{A},1}^{n} + \alpha_1 T_{\mathrm{A},in} \cdots T_{\mathrm{A},i}^{n} \cdots T_{\mathrm{A},N}^{n}\right), \left(T_{s,1}^{n} \cdots T_{s,i}^{n} \cdots T_{s,N}^{n}\right), \left(T_{\mathrm{B},1}^{n} \cdots T_{\mathrm{B},i}^{n} \cdots T_{\mathrm{B},N}^{n} + \beta_3 T_{\mathrm{B},in}\right)\right]^T$$

and matrix A is a $3N \times 3N$ matrix having the structure shown in Figure VIa.6.2 (all other terms are zeroes). The left matrix is for parallel and the right matrix is for counterflow heat exchangers.

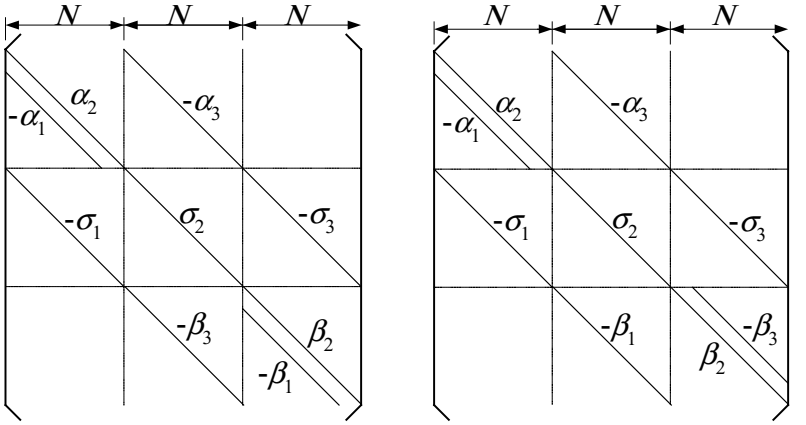

Figure VIa.6.2. Structure of the coefficient matrix for a parallel and a counterflow heat exchanger

Equation VIa.6.5 is written in a semi-implicit form where the terms of coefficient matrix A are developed at the previous time step. This prevents linearization of terms and formation of a Jacobian matrix. The initial conditions for the speci-

fied boundary conditions (inlet flows and temperatures) are obtained from the steady state solution to Equation Va.6.5:

$$(A - I)\underline{Y}^{o} = \underline{C}$$

where I is the identity matrix and Y^o includes the steady-state temperature distribution in stream A, in tube material, and in stream B.

QUESTIONS

- What types of heat exchangers can be found in a house?
- What is the difference between a concentric heat exchanger and a shell and tube heat exchanger?
- Why a counterflow HX is more efficient than a parallel flow heat exchanger?
- What is the purpose of the baffle plates in a shell and tube heat exchanger? What are the advantages and disadvantages of baffle plates?
- Two streams are exchanging heat in a heat exchanger. One stream is cleaner than the other. Which stream should flow in the tubes and which stream should flow in the shell?
- What is the difference between fouling factor and the cleanliness factor (C_F)?
- If a heat exchanger has $C_F = 0.8$ and $U_{dirty} = 2000$ W/m^2.K what is U_{clean}?
- Why does tube temperature not appear in the steady-state formulation of heat exchangers?
- In a counterflow heat exchanger, can the outlet temperature of the cold stream be greater than the outlet temperature of the hot stream?
- What are the six major assumptions made in the derivation of the equations in Section 2 of this chapter?
- What heat exchanger design constraints are affected by the selection of tube diameter?
- What advantages and drawbacks can you identify for a horizontal versus a vertical steam generator?
- Why does the shell side of a power plant condenser operate at a partial vacuum?
- What effects does the ingress of non-condensable gases have on a condenser performance?

PROBLEMS

1. The following temperatures are obtained at the inlet and exit ports of a counterflow heat exchanger. Find ΔT_{LMTD} and compare it with $\overline{\Delta T}$ as given by Equation VIa.2.5. Data: $T_{h,i}$ = 130 F, $T_{h,o}$ = 111.9 F, $T_{c,i}$ = 95 F, and $T_{c,o}$ = 106.3 F [Ans.: ΔT_{LMTD} = 20.1 F, $\overline{\Delta T}$ = 20.3 F. Temperature profiles are flat]

2. A concentric counterflow heat exchanger is used to cool oil by water. The oil flow rate is 0.1 kg/s and enters at 100 C. Water enters at 30 C and a flow rate of

0.2 kg/s. The heat transfer area is 5.223 m^2 and the overall heat transfer coefficient is 37.8 W/m^2·K. Find the rate of heat transfer and exit temperatures. Data: $c_{p,h}$ = 2131 J/kg·K and $c_{p,c}$ = 4178 J/kg·K. [Ans.: $\dot{Q}$ = 8524 W, T_{ho} = 60 C, and T_{co} = 40 C].

3. A one-shell, two-tube pass shell and tube heat exchanger has 1580 tubes with d_i = 13 mm and d_o = 16 mm. Tubes have an average length of 6 m per pass. Cold water enters the tubes at 30 C and a rate of 110 kg/s and hot water enters shell at 90 C and a rate of 125 kg/s. Find the rate of heat transfer, ΔT_{LMTD}, and the overall heat transfer coefficient. Use stainless steel tubes and f_i = 0.001 m^2·K/W. [Ans.: 13 MW, 10.7 C, and 493 W/m^2·K].

4. A shell and tube heat exchanger uses 600 tubes of ¾ in B.W.G 20 (d_o = 0.75 in and d_i = 0.68 in) and 17.5 ft per pass. Hot water enters the tubes at 1.5E6 lbm/h and 180 F. The heat exchanger has one shell and two-tube pass per shell. Cold water enters the shell at 1.5E6 lbm/h and 70 F. The fouling factors happen to be equal for both tube and shell sides, $f_i = f_o$ = 0.0003 h·ft^2·F/Btu. Find the tube and shell outlet temperatures and the heat exchanger effectiveness. [Ans.: 130 F, 120 F, and 0.456].

5. A shell and tube heat exchanger uses 650 tubes of 5/8 in B.W.G 18 (d_o = 0.625 in and d_i = 0.527 in) and 7.5 ft per pass. Tubes are stainless steel. The heat exchanger has one shell and two-tube passes per shell. Cold water enters the tubes at a velocity of 6.818 ft/s and a temperature of 75 F. Hot water enters the shell at 195 F and at a rate of 2.5E6 lbm/h. The fouling factors happen to be equal for both tube and shell sides, $f_i = f_o$ = 0.0005 h·ft^2·F/Btu. Find $T_{h,out}$, $T_{c,out}$, U_o, ε, total rate of heat transfer, and the tube-side pressure drop. [Ans.: 173.67 F, 110.75 F, 373.2 Btu/h·ft^2·F, 0.298, and 2.38 psi].

6. Consider the steady-state operation of a counterflow heat exchanger. The energy balance for an elemental control volume in the cold stream is shown below. Write a similar energy balance for an elemental control volume in the hot stream. Then for each stream, derive the differential equation for temperature as function of the exchanger length. [Ans.: $dT_c/dx = (U\mathrm{P}/C_c)(T_h - T_c)$ and $dT_h/dx = (U\mathrm{P}/C_h)(T_h - T_c)$].

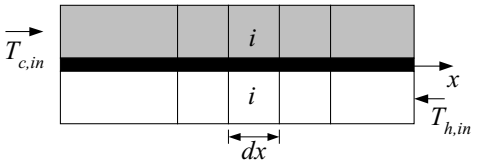

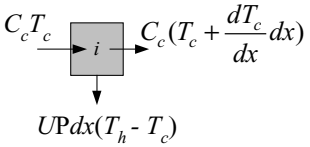

7. Solve the differential equations obtained in Problem VIa.6 using the following boundary conditions, $T_h(x = 0) = T_{h,o}$ and $T_h(x = L) = T_{h,i}$ for the hot and $T_c(x = 0) = T_{c,i}$ and $T_c(x = L) = T_{c,o}$ for the cold stream. [Ans: if $C_c = C_{min}$, $T_h = \{T_{h,o} - C_r T_{c,i} - C_r(T_{h,o} - T_{c,i})\exp[-(1/C_c - 1/C_h)U\mathrm{P}x]\}/(1 - C_r)$ similar relation for T_c].

8. Show that for condensers, $T_{c,out} = T_{c,in} + (T_h - T_{c,in})[1 - e^{-UA/C_c}]$.

9. In Example VIa.5.2, we derived the primary-side temperature profile for a steam generator. Derive a similar temperature profile but for a counter-current heat exchanger in terms of tube length, area, flow rates, and inlet temperatures. [Ans.: $T_h(s) = T_{h,in} - (T_{h,in} - T^*)\left(1 - e^{(\beta-\alpha)s/L}\right)$ where in this relation parameters α, β, and T^* are given as $\alpha = UA/\dot{m}_h c_{p,h}$, $\beta = UA/\dot{m}_c c_{p,c}$, and $T^* = \left(\beta T_{h,in} - \alpha T_{c,o}\right)/(\beta - \alpha)$. Note, $T_{c,o}$ is obtained from Problem VIa.6 in terms of $T_{h.in}, T_{c,in}, \dot{m}_h, \dot{m}_c$, and UA].

10. In Example VIa.5.2, we derived the primary-side temperature profile for a steam generator. Now consider a case where fluid in the primary side is also boiling. Derive the profile for steam quality.

11. A shell and tube condenser uses saturated steam at 1 atm and 212 F (100 C) in the shell to heat water in the 18 tubes from 100 F (38 C) to 120 F (49 C). The tubes are thin wall with $d_o \approx d_i$ = 1 in (2.54 cm) and are arranged in a triangular pitch. The velocity of water inside the tubes is 8 ft/s (2.44 m/s). Find a) the mass flow rate of water in the tubes, b) the heat transfer coefficient on the inside and outside of the tubes, c) the overall heat transfer coefficient for the tubes neglecting any fouling, d) the length of the tubes, and e) the rate of steam condensation in this condenser. Use carbon steel tubes.

12. In a tubular condenser, steam condenses on the tube bank at 50.5 C (123 F) while cooling water enters the tubes at a rate of 42.966 kg/s (3.41E8 lbm/h) and a temperature of 20 C (68 F). There are 35918 tubes having an outside diameter of 2.54 cm (1 inch) and a length of 6.5 m (21.3 ft). The overall heat transfer coefficient for the clean condenser is 4346 W/m·C (765.5 Btu/h·F). Find the cooling water temperature at the outlet. Use copper tubes. [Ans.: 31 C (88 F)]

13. A condenser is used to reject 2000 MW to a large lake. Pressure of the condensing steam is 3 in Hg. Cooling water enters at 75 F. The maximum allowed temperature rise of the cooling water is 15 F. Tube velocity is 7 ft/s. Tubes are 1 ¼ in 18 BWG (d_o = 1.250 in and d_i = 1.152 in). Find the number of tubes, total tube length, and the tube-side pressure drop. Tubes are stainless steel. [Ans.: N = 40276, L = 16.8 ft, ΔP_i = 4.88 psi].

14. A condenser is used to reject 2000 MW to a large lake. Pressure of the condensing steam is 3 in Hg. Cooling water enters at 75 F. The maximum allowed temperature rise of the cooling water is 15 F. Tube velocity is 7 ft/s. Tubes diameters are d_o = 1.50 in and d_i = 1.402 in. Find number of tubes, total tube length, and tube-side pressure drop. Tubes are stainless steel. [Ans.: N = 23756, L = 19.6 ft, ΔP_i = 0.93 psi].

15. The core of a PWR produces 2,778.43 MWth. The PWR is equipped with two recirculating U-tube steam generators. Hot water leaves the core and enters the hot leg at 312.8 C (595.1 F). The system is fully insulated. Colder water

leaves the steam generator tubes and enters the cold legs at 286.7 C (548 F). Water is boiling in the shell-side at the saturation temperature of 277.6 C (531.64 F), corresponding to a pressure of 6.2 MPa ($P_o \cong$ 900 psia). There are a total of 8471 tubes, each having an inside and outside diameter of 1.685 cm (0.6635 in) and 1.904 cm (0.7495 in), respectively. Use f_o = 3.522E-6 C·m^2/W (0.00002 F·h·ft^2/Btu) and C_{sf} = 0.012 to find A_o, ΔT_{LMTD}, h_i, h_o, U_o, L, ε, NTU, and ΔP_i. [Ans.: 8548 m^2 (92010 ft^2), 19.3 C (34.75 F), 43420 W/m^2·C (7647 Btu/ft^2·h·F), 46877 W/m^2·C (8256 Btu/ft^2·h·F), 8417 W/m^2·C (1482.4 Btu/ft^2·h·F), 16.87 m (55.35 ft), 74.2%, 1.356, 0.2 MPa (29.67 psi)].

16. The design of a steam generator as described in Section 5 of this chapter uses the Rohsenow pool boiling correlation. Derive a relation for the calculation of the tube surface area using the Chen correlation.

17. The design of a steam generator as described in Section 5 ignores the preheating section of the tube bundle. a) Determine the expected tube length within which the feedwater reaches saturation, and b) revise the formulation to include the preheating calculation of the tube heat transfer area.

18. The steam generator design procedure outlined in Section 5 is based on the effectiveness. In this problem we want to design the steam generator by using a differential approach. [Hint: Writing a steady state energy balance in the axial and transverse directions for an element of length alongside the tubes gives:

$$\dot{q}'' = \frac{d\dot{Q}}{dA} = \dot{m}_i c_{p,i} \frac{dT_i}{dA} = U(T_i - T_o) = \frac{T_s - T_o}{R_s} \qquad 1$$

where subscripts i, s, and o stand for tube side, tube, and tube-bundle-side. Use Equation IVa.6.8-2 to relate the various thermal resistances, as shown below, to the overall heat transfer coefficient.

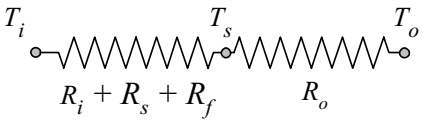

From the last two terms of Equation 1 conclude that $T_i - T_o = \dot{q}''(R_c + R_o)$. Use Equation VIa.5.5, to find $T_s - T_o = f(P_o)\dot{q}''^{1/3}$ and from Equation 1 obtain $R_o = f(P_o)(\dot{q}'')^{-2/3}$. Substitute in Equation 1 and find:

$$T_i - T_o = \dot{q}''R_c + \dot{q}''R_o = \dot{q}''R_c + (\dot{q}'')^{2/3} f(P_o) \qquad 2$$

Integrate Equation 1 to find

$$A = \int_{inlet}^{exit} \dot{m}_i c_{p,i} \frac{dT_i}{\dot{q}''} = \dot{m}_i c_{p,i} \int_{inlet}^{exit} \frac{d(T_i - T_o)}{\dot{q}''}$$

Substitute for $T_i - T_o$ from Equation 2 and integrate from inlet (I) to exit (E) to obtain:

$$A = \dot{m}_i c_{p,i} \{ R_c \ln \frac{\dot{q}''_E}{\dot{q}''_I} + f(P_o)[(\dot{q}''_E)^{-2/3} - (\dot{q}''_I)^{-2/3}] \} \qquad 3$$

To find the required tube surface area, you need to find the heat fluxes at the inlet and exit of the tubes. These are determined from Equation 2 by using the Newton-Raphson method].

19. A cylindrical reflecting lens focuses direct solar light on a collector pipe through which fluid circulates. The heated fluid is used as the heat source for a heat engine producing mechanical power. The collector tube is surrounded by a glass tube to reduce heat loss to the ambient atmosphere. The collector tube diameter is larger than the solar image formed by the reflecting lens. Use the given data and:

a) Find an analytical expression for the efficiency of the solar collector (i.e., the ratio of heat collected by the circulating fluid to the solar flux intercepted by the reflecting lens) as a function of the ratio $(T_c - T_a)/\dot{Q}_i$ and the fixed parameters listed below,

b) if the thermodynamic efficiency of the heat engine is a fixed fraction of the Carnot efficiency of a reversible heat engine operating between heat reservoirs having temperatures equal to the collecting fluid temperature and the ambient temperature, find an analytical expression for the collector temperature which will maximize the power output of the heat engine, and determine its nominal value.

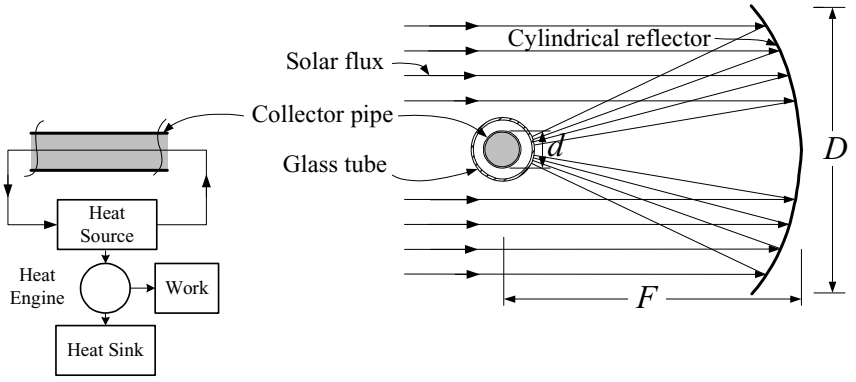

Data:

Cord of cylindrical lens (D = 1 m), focal length of cylindrical lens (F = 2 m), collector tube outer diameter (d = 0.03 m), design direct solar flux ($\dot{q}''_i$ = 950 W/m^2), ambient atmospheric temperature (T_a = 20 C), temperature of the collecting fluid (T_c), absorptivity-transmissivity product for the incident solar radiation focused on the collector tube ($\alpha\tau$ = 0.75), reflectivity of lens surface for solar spectrum (ρ = 0.9).

VIb. Fundamentals of Flow Measurement

Flow measurement is an interesting application of the principals of fluid mechanics. Measurements in fluid mechanics are performed for a variety of properties including local (such as velocity, pressure, temperature, density, viscosity) and integrated (volume and mass flow rates) properties. In this section only measurement of local velocity and integrated properties are discussed. However, first some fundamental terms are defined.

1. Definition of Flow Measurement Terms

Invasive is a term applied mostly to classical flowmeters such as the Bernoulli obstruction meters, turbine meter, rotameter and even some modern instruments as vortex meter. Most modern flowmeters such as electromagnetic, ultrasonic, and laser Doppler anemometer are noninvasive instruments. The invasive meters must be integrated in the piping system. The invasive flowmeters generally disturb the flow.

Noninvasive flowmeters have several advantages compared with the invasive flowmeters including the lack of any moving parts, ease of installation, longevity as the instrument is not affected by the flow condition, cost savings, and capability to be bi-directional. Since the noninvasive flowmeters are not exposed to the fluid flow, they do not cause any pressure drop to the flow hence, there is no need for any *flow straightener*.

Error is the difference between the measured value and the true value. Error may be expressed as absolute error or relative error. If the true value of a ruler is 3 m, a measurement of 2.98 m has an absolute error of 0.02 m or relative error of 0.02/2.98 = 0.7%.

Fixed error is referred to as the amount of error appearing in repeated measurement by practically the same amount. In flow measurement, a leak upstream of the flowmeter introduces a fixed error regardless of the number of the times flow is measured. Similarly, in temperature measurements by thermometers, some heat is lost to the surroundings by the instrument itself. This additional heat transfer would cause the thermometer to read a lower temperature than the fluid temperature.

Random error is due to such factors as personal fluctuations, mechanical friction associated with certain processes, and electronic fluctuations.

Uncertainty refers to the *errors* associated with the measured data. Uncertainty is expressed in terms of percentage of the true value. An instrument reading with an uncertainty of ±1% implies that the reading falls within 1% of the true value in each direction.

Accuracy is the degree of proximity of the measurement to the actual value and refers to the fractional *error* in the instrument. Accuracy is a qualitative term to describe an instrument and is often confused with *uncertainty*.

Resolution of an instrument is the minimum change in output that the instrument can detect. As such, resolution can be defined as the smallest quantity that the instrument can measure.

Repeatability refers to the maximum difference between the same outputs for the same input, obtained in separate measurements but under similar test conditions. Any difference is generally due to *random error*.

Precision of an instrument is a measure of its repeatability with a specified degree of accuracy.

Calibration is a process to determine accuracy and resolution. Hence, the calibration of an instrument involves the measurement of known values. Such known values are primary standards or a previously calibrated instrument used as a reference. The calibration may also include the application of a primary measurement. Calibration of a flowmeter for example, may be based on a bucket and stop watch.

Drift is an undesirable change in the output of the instrument over a period of time. Drift is usually caused by the electronics of the device and not the process under measurement.

Hysteresis is a property of the instrument and is the difference in output when the measured value is approached with increasing and then with decreasing values. Hysteresis may be caused by friction, elastic deformation, thermal or magnetic effects.

Range refers to the domain within which the instrument works properly and beyond which the outputs are not reliable and the device may be damaged.

Response time is the time required for the output to rise to the value corresponding to the step change of the input.

Sensitivity is the ratio of change in the instrument output to the change in the value of the input.

Span is the difference between the limits of the range.

2. Repeatability, Accuracy, and Uncertainty

2.1. Repeatability and Accuracy

Due to the importance of repeatability and accuracy in measurement, we use an example dealing with throwing darts at a dartboard (Baker). In Figure VIb.2.1(a), 10 out of 10 darts are in the bulls-eye. Since the darts in this case have been accu-

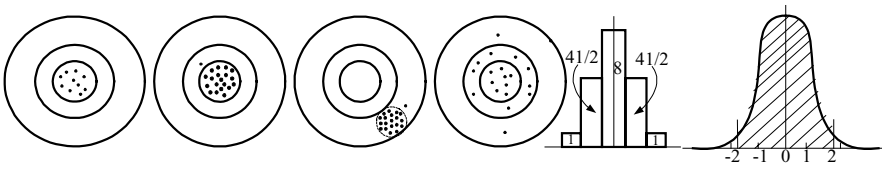

Figure VIb.2.1. Accuracy and repeatability in hitting a dart board

rate, the number of bulls-eyes is therefore, repeatable. In Figure VIb.2.1(b), 19 out of 20 (19/20 = 95%) shots have hit the bulls-eye. Statistically this is a low value of uncertainty (±1%) with a 95% confidence level or within 2 standard deviations. In Figure VIb.2.1(c), the same repeatability is reached as in case (b) but with a certain bias causing all the shots to be off target. This indicates that good accuracy also means good repeatability whereas good repeatability does not necessarily imply good accuracy. In Figure VIb.2.1(d) 19 out of 20 have hit the target (±5% uncertainty with 95% confidence level) but 8 out of 20 darts have hit the bulls-eye. Figure VIb.2.1(e) shows a depiction of case (d) on a linear plot. Figure VIb.2.1(f) shows the normal distribution, a good representation of flow measurement readings.

2.2. Uncertainty Analysis

Due to the importance of the uncertainty in measurement, more details are necessary for full understanding. During any measurement, there is always the possibility of errors entering the data acquisition process, and distorting data. This may be due to human error, fixed error, systematic error, or random error. It is therefore customary to express data along with some degree of uncertainty to clarify accuracy in the measurement. Uncertainties in the data are usually expressed as a percentage of the full-scale output of the instrument. Measurement of physical values consisting of several parameters, where each parameter is measured by separate instrument, is affected by the uncertainty associated with each instrument. One way to calculate the associated uncertainty in the result is to find the worst-case uncertainty. To explain, suppose that we are interested in calculating the uncertainty associated with pumping power from the flow rate and pressure rise over the pump:

$$\dot{W} = \Delta P \dot{\mathrm{V}}$$

For a flow rate of 800 ft^3/h ± 12 ft^3/h and a pressure rise of 45 psi ± 1 psi, the nominal pumping power is $\dot{W}$ = 36000 ft·lbf/h. Applying the worst case uncertainty, pumping power can be calculated as $\dot{W}_{max}$ = (800 + 12)(45 + 1) = 37352 ft·lbf/h and $\dot{W}_{min}$ = (800 – 12)(45 –1) = 34,672 ft·lbf/h:

$$\dot{W} = 36000 \pm 3.7\%$$

However, it is very unlikely indeed that the highest measurement of pressure rise occurs at the highest measurement of flow rate as these are independent instruments. The same is true for the value of flow rate to coincide with the lowest measurement of pressure rise. The more accurate means of calculating the resulting uncertainty is the method referred to as the *mean squared error*. If output *F* is a function of *n* independent variables as:

$$F = f(x_1, x_2, \cdots x_i, \cdots x_n)$$

Then the uncertainty in *F*, also known as the *expected error*, is given by (Kline):

$$e_F = \pm\left[(\frac{\partial F}{\partial x_1} e_{x_1})^2 + (\frac{\partial F}{\partial x_2} e_{x_2})^2 + \cdots (\frac{\partial F}{\partial x_i} e_{x_i})^2 + \cdots + (\frac{\partial F}{\partial x_n} e_{x_n})^2 \right]^{1/2} \qquad \text{VIb.2.1}$$

where e_{x_i} is the uncertainty associated with each independent variable x_i.

Example VIb.2.1. The rated pressure rise and flow rate of a pump are given as $\Delta P_{pump} = 45 \pm 2\%$ psi and $\dot{\mathrm{V}} = 800 \pm 1.5\%$ ft^3/h, respectively. Find the uncertainty in pumping power using the mean squared error method.

Solution: The pumping power is found as $\dot{W} = \Delta P \dot{\mathrm{V}}$. We first find the nominal pumping power as:

$\dot{W} = 800 \times 45 = 36000$ ft·lbf/h. To find the uncertainty in $\dot{W}$, we find:

$\partial \dot{W} / \partial(\Delta P) = \dot{\mathrm{V}} = 800$ ft^3/h.

The corresponding uncertainty is:

$e_{\dot{\mathrm{V}}} = 800 \times (1.5/100) = 12$

$\partial \dot{W} / \partial \dot{\mathrm{V}} = \Delta P = 45$ psi.

The corresponding uncertainty is:

$e_{\Delta P} = 45 \times (2/100) = 0.9$ psi.

Thus the uncertainty in $\dot{W}$ is calculated as:

$$e_{\dot{W}} = \pm\left[\left(\frac{\partial \dot{W}}{\partial(\Delta P)} e_{\Delta P} \right)^2 + \left(\frac{\partial \dot{W}}{\partial \dot{\mathrm{V}}} e_{\dot{\mathrm{V}}} \right)^2 \right]^{1/2} = \pm\left[(800 \times 0.9)^2 + (45 \times 12)^2 \right]^{0.5} = \pm 900 \text{ft} \cdot \text{lbf/h}$$

Therefore the pumping power is found as $\dot{W}$ = 36000 ± (900/36000) = 36000 ± 2.5% ft·lbf/h. Earlier, the uncertainty was found as 3.7%.

To minimize the random error, several readings must be made. Such multiple observations allow the estimation of the *most probable error* from a normal probability distribution around an average value. For example, in the case of a ruler having an average length of $\overline{L}$, we take *N* measurements so that:

$$\overline{L} = \sum_{i=1}^{N} L_i / N$$

or σ being the standard deviation given by:

$$\sigma^2 = \sum_{i=1}^{N} (L_i - \overline{L})^2 / N$$

the error in measurement is estimated from $e_{\overline{L}} = \sigma / \sqrt{N-1}$ where the error is enhanced by subtracting unity from the number of observations to account for the fact that the true value of the length is not known.

Example VIb.2.2. The length of a ruler is measured 10 times and the following readings are obtained. Find the most probable error.

Reading:	1	2	3	4	5	6	7	8	9	10
Length (m):	3.97	3.82	4.10	4.01	4.16	3.87	4.15	4.05	3.89	3.92

Solution: Arithmetic average of the readings is $\overline{L} = 39.94/10 = 3.994$ m. Set up the following table:

Reading:	1	2	3	4	5	6	7	8	9	10
$L_i - \overline{L}$:	-0.024	-0.174	0.106	0.016	0.166	-0.124	0.156	0.056	-0.104	-0.074
$(L_i - \overline{L})^2 \times 100$:	0.058	3.030	1.12	0.026	2.75	1.54	2.43	0.314	1.08	0.55

Standard deviation is then found as σ = $(0.1047/10)^{1/2}$ = 0.102 m. Hence, $e_{\overline{L}} = 0.135/\sqrt{9} = 0.034$ m.

3. Flowmeter Types

Recall that for fully developed flow, velocity varies as a function of pipe radius across the flow area and mass flow rate is given by (Equation IIb.2.3):

$$\dot{m} = \int_A \rho \vec{V} \cdot d\vec{A}$$

This equation was simplified for a stationary control surface, flow area normal to the control surface, and the uniform thermodynamic state uniform over the flow area at any instant to obtain Equation IIa.5.2, $\dot{m} = \rho \vec{V} A = \rho \dot{\mathrm{V}}$. A flowmeter may then measure local flow velocity ($\vec{V}$), volumetric flow rate ($\dot{\mathrm{V}} = \vec{V} A$) or mass flow rate ($\dot{m}$).

Flowmeters can be divided into several categories based on such factors as type of flow parameter to measure, cost, induced pressure drop, type of fluid, accuracy,

etc. A large class of flowmeters includes those meters that measure a change in the flow momentum. Examples of this class include the Bernoulli obstruction meters such as venturi, nozzle, and thin plate orifice as discussed in Section IIIb.4.2.

Also included in this class are such devices as rotameter, pitot tube, and 90 degree elbows. Another large class of flowmeters includes instruments that measure the volumetric flow rate. Examples of this class include positive displacement of fluid and such devices as electromagnetic, vortex shedder and turbine meters. Devices that also measure volumetric flow rate and are noninvasive include the Laser Doppler anemometer, ultrasonic flowmeter, and pulsed neutron activation meters. To measure mass flow rate directly, such techniques as thermal mass flow measurement, Coriolis force meter, and angular momentum measurement are used. A summary of various types of flowmeters is shown in Table VIb.3.1, which provides information useful in the selection of flowmeters.

Depending on the application, as shown in Table VIb.3.1, the disadvantage of invasive floweters is the associated pressure loss. The invasive flowmeters are defined as those that cross the flow boundary. On the other hand, the noninvasive flowmeters, measure the flow by indirect means and are not associated with any head loss nor do they need to be integrated in the piping. For invasive flowmeters, it is important to install the device so that flow entering and leaving the instrument is not disturbed by the presence of fittings and valves. Manufacturers generally specify the minimum distance required upstream and downstream of the pipe. This distance is specified in terms of the diameter of the pipe on which the device would be installed. On occasions that such a possibility does not exist due to space limitations, a flow straightener is used to streamline the flow.

3.1. Momentum Sensing Flowmeters

Orifice, Nozzle, Venturi. The most famous momentum sensing instruments are Bernoulli obstruction meters as were discussed in Section IIIb.4.2. Table VIb.3.1 shows that the orifice has the highest and the venturi has the lowest pressure loss. The cost of these devices is inversely proportional to the pressure drop they introduce to the flow. Hence, a venturi is the most expensive and a thin-plate orifice is the least expensive. The Bernoulli obstruction meters are found in various sizes. Thin plate orifices can be found as small as 1 inch in diameter. On the other hand the world's largest flowmeter is a venturi made for Southern Nevada Water authority. The diameter of this flowmeter is 180 inches (4.6 m), having a dry weight of 60,000 lbm and a volume of 6400 ft^3 to measure a water flow rate in excess of 555,000 GPM (35 m^3/s). The venturi flowmeter is 52 ft (15.85 m) long (Flow Control Magazine).

Rotameter: the trade name of a manufacturer has been applied to the variable area meter. Such meters consist of a tapered tube oriented vertically and a float as shown in Figure VIb.3.1(a). There are three forces acting on the float, the drag force (F_D), as a result of the external flow of fluid over the float, the buoyancy force (F_B) and the float weight (F_W). When $F_W = F_B + F_D$ then the float is at equilibrium and the flow rate is read from a calibrated scale.

Table VIb.3.1. Comparison of Various Flowmeters

Class	Type	Fluid	Accu-racy	Head Loss	Cost	UD/ DD	Advantages & Disadvantages
Momen-tum	Orifice	L/G	M	h	l	20/5	Corrosion & wear: su
	Nozzle	L/G/T	M	m	m	20/5	High temp. & velocity: su
	Venturi	L/G/S/T	M	l	h	15/5	High temp. & velocity: su
	Rotameter	L/G	L	m	l	n	Low flow: st, Pulsating flow: li
	Ave. Pitots	L/G	L	l	l	30/5	Probe flow eparation: su
	Laminar	G	L	h	m	15/5	Pulsating flow: st, Dirty fluid: li
	Elbow	L/G/S	L	l	l	25/10	Available performance data: li
Volume	Turbine	L/G	H	h	h	15/5	Bearing wear: su
	Paddle wheel	L/G	M	l	l	15/5	Bearing wear: su
	Vortex	L/G	H	h	h	20/5	Low flow: ns, Vibration: su
	Electro-magnetic	L/S/T	M	n	h	5/3	Non-conducting fluid: su
	Ultrasonic	L/G/T	H	n	h	15/5	Change in temperature: st
	Laser Doppler	L/G/S/T	M	n	h	15/5	Reynolds Number: li
	Positive displacement	L/G	H	h	l	n	Dirty fluid: su, Wear: su
Mass	Thermal	L/G	L	m	m	5/3	Dirty fluid: su, Low flow: st
	Angular	L	M	m	m	n	Aircraft fuel flow: st
	Coriolis	L/G/S	H	m	h	N	Pipe size: li, Fouling: su

Table abbreviations:

L: liquid, n: None
G: gas, ns: Not suitable
S: slurry, st: Suitable
T: two-phase su: Susceptible
h: high, li: Limitation
m: medium UD: Straight piping, as multiples of pipe Diameter, required Upstream
l: low DD: Straight piping, as multiples of pipe Diameter, required Downstream

Substituting for weight in terms of float volume and density, for buoyancy in terms of float volume and liquid density, and for drag in terms of specific kinetic energy:

$$\rho_F \mathrm{V}_F g = \rho_f \mathrm{V}_F g + C_D A_F \left(\rho_f \overline{V}^2\right)/2$$

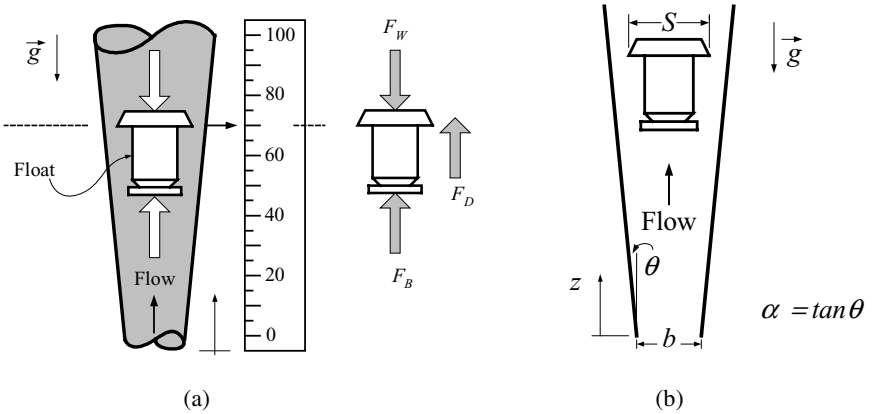

Figure VIb.3.1 A variable area flowmeter

where V is the float volume, $\overline{V}$ is the mean flow velocity, and subscripts *f* and *F* stand for liquid and float, respectively. In this equation, C_D is the drag coefficient, which is pertinent to external flow over immersed bodies. For spherical floats, the drag coefficient is readily available as a function of the Reynolds number. For example, experimental data indicate that the drag coefficient for spheres remains practically constant at 0.5 if the Reynolds number is between 2000 to 200,000. At higher Reynolds number, the drag coefficient is even smaller. Solving the above equation for flow velocity:

$$\overline{V} = \left[\frac{1}{C_D} \frac{2g\mathrm{V}_F}{A_F} \left(\frac{\rho_F}{\rho_f} - 1 \right) \right]^{1/2} \qquad \text{VIb.3.1}$$

The volumetric flow rate can then be calculated from $\dot{\mathrm{V}} = \overline{V} A(z)$ where $A(z) = \pi\left[(b+\alpha z)^2 - S^2\right]/4$. Although rotameters are generally made of glass or other special transparent materials, there are variable area flow meters made of metal where the reading is obtained by magnetic coupling so that the signal can be received and recorded remotely.

Elbow meter, as shown in Figure VIb.3.2(a), takes advantage of the centrifugal force applied on fluid elements when moving around a bend. The top and the bottom of the 90-degree elbow are drilled at 45 degrees for the insertion of the pressure taps. These pressure taps provide input to a differential-pressure measuring device (DP-cell), which, upon calibration, would show flow rate in the 90-degree elbow.

Laminar flowmeters, also known as viscous flowmeters, shown in Figure VIb.3.2(b), are used to measure gas flow rate based on Equation IIIb.2.3:

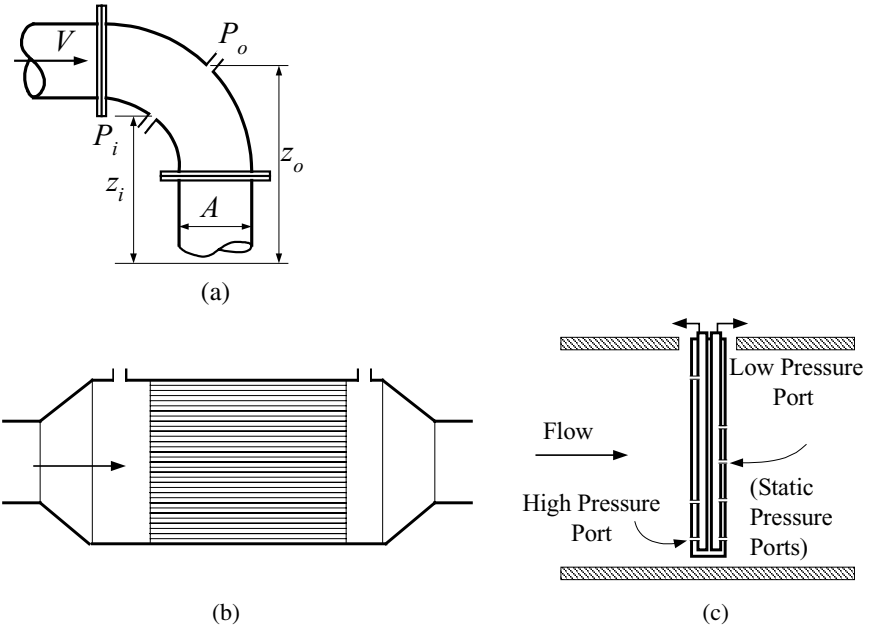

Figure VIb.3.2. (a) Elbow meter; (b) Laminar flowmeter; (c) Averaging pitot flowmeter

$$\dot{V} = \frac{\pi D^4}{128 \mu L} \Delta P \qquad \text{VIb.3.2}$$

To change the flow regime from turbulent to laminar so that the viscous effects become dominant, a laminar flow element is used. The laminar flow element consists of capillary tubes with inside diameter as small as 0.01 inches (about 0.23 mm). The pressure taps for differential pressure measurement are located upstream and downstream of the laminar flow element.

Averaging Pitot device works on the basis of differential pressure. A bar that spans the pipe is inserted perpendicular to the flow. The bar may be a circular cylinder or have other profiles such as hexagonal, square, diamond, or elliptic cross section. Holes are drilled in the side facing the flow and in the downstream side of the bar, as shown in Figure VIb.3.2(c). The inputs to the pressure taps are carried to individual pressure sensors to be sent to a DP-cell. The advantage of an averaging pitot tube is its ease of installation and low impact on the flow. Underestimating the flow rate is its main disadvantage. This is because of a suction effect at the static pressure ports, due to the vortices created downstream of the probe. This is generally taken into account by a flow coefficient in calibration.

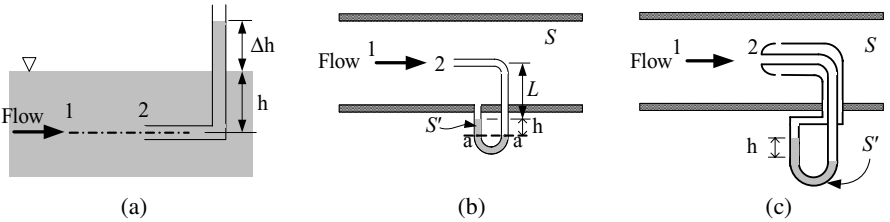

Figure VIb.3.3. (a) Simple pitot tube; (b) Differential pitot tube; (c) Pitot-static tube

It should be added that a pitot tube, invented by Henri Pitot in 1732, is itself a device for measuring flow velocity. Shown in Figure VIb.3.3(a), is a glass pitot tube in an open channel. Points 1 and 2 are on a streamline where point 2 is at the entrance to the tube, hence is at rest. Point 2 is called the *stagnation point*. Pressure at point 1 is $P_1 = \rho gh$. Pressure at point 2 is $P_2 = \rho g(h + \Delta h)$. From the Bernoulli equation between point 1 and point 2 we have; $P_1 + (\rho V_1^2/2) = P_2$. Substituting, we get $V_1 = \sqrt{2g\Delta h}$. We derived pressure at point 2 in terms of pressure at point 1 and pressure related to velocity head. Pressure at point 2 is *total* or *stagnation pressure* as it consists of static and dynamic heads of the flowing fluid. Shown in Figure VIb.3.3(b) is the differential pitot tube. If the flowing fluid has a specific gravity of S and the manometer liquid has a specific gravity of S', a force balance at the level a-a gives:

$$P_1 + \rho_w g(LS + \mathrm{h}S') = P_2 + \rho_w g(L + \mathrm{h})S \qquad \text{VIb.3.3}$$

This simplifies to $P_2 - P_1 = \rho_w gS[(S'/S) - 1]\mathrm{h}$. On the other hand, $P_1 + (\rho_w V_1^2/2) = P_2$. We find that $V_1 = V = \sqrt{2g\mathrm{h}\left[(S'/S) - 1\right]}$. A more compact system is the pitot-static tube as shown in Figure VIb.3.3(c). For this case, similar expression can be derived.

3.2. Volume Measuring Flowmeters

Turbine flowmeter, Figure VIb.3.4(a), and its various forms have been in use for flow measurement for centuries. The turbine meter consists of a shaft equipped

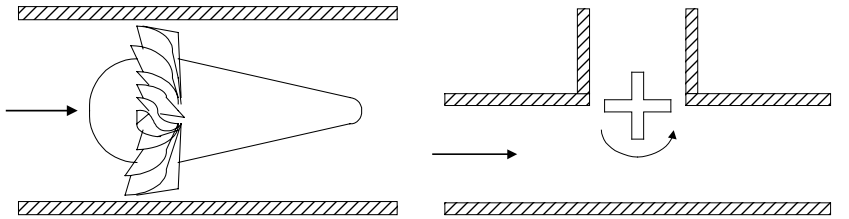

Figure VIb.3.4. (a) Turbine meter and (b) Paddle wheel

with blades and located centrally against the flow. The shaft and the blades are designed to minimize the adverse effect on the flow. The flow of fluid through the blades imparts momentum, causing rotation of the blade, which, in a magnetic field, produces current proportional to the flow volume passing over the shaft. In the absence of friction, this proportionality would have been a linear function. However, various frictional forces result in non-linearity. These forces include bearing friction, drag on the rotor and the blades, and friction due to the electromagnetic effects. Like the turbine meter, there are similar flowmeters, which work on the transfer of momentum from the flow to a turning wheel. These are paddle wheel or vane-type and the Pelton-wheel flowmeter, Figure VIb.3.4(b).

Vortex meter is a relatively new concept in flow measurement as the idea was introduced in the mid 1950s. The device become available in the mid 1970s. In a vortex meter, a bluff body is placed in the flow field to cause some flow separations downstream of the bluff body, Figure VIb.3.5(a). As flow increases, so does the rate of flow separation to a point that the separated flow is rolled back in the low-pressure area developed behind the bluff body. This backward curl is called a vortex. As the flow rate is increased, these vortexes grow in size and begin to travel downstream to form a so-called *vortex street*. The notable feature of such vortex-shedding instruments is that the vortexes are formed and depart in alternate manner from each side of the bluff body. This causes an alternating pressure gradient across the body. The frequency of vortex generation and pressure oscillations is proportional to flow rate.

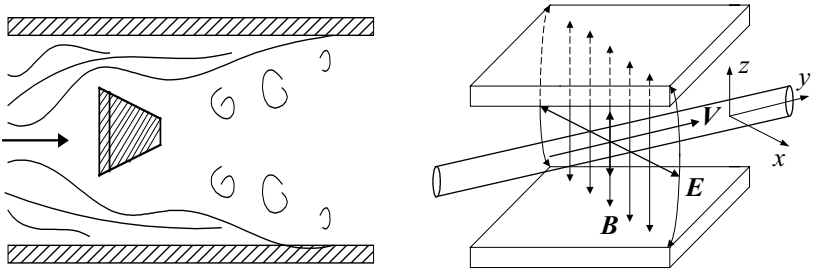

(a) (b)

Figure VIb.3.5. (a) Schematics of Vortex flowmeter (b) Electromagnetic flowmeter

Electromagnetic flowmeter works on the basis of Michael Faraday's law of electromagnetic induction. As shown in Figure VIb.3.5(b), a magnetic field is created in the coil surrounding the pipe carrying a conducting liquid. The magnetic field may be created by an alternating current. The pipe carrying the conducting liquid is made of nonmagnetic material to allow penetration of a magnetic field. We now envision molecules of the conduction liquid on a line parallel to the vector *E*. Since these lines are moving with flow velocity *V* inside the coil, they cut through the magnetic lines, which, in turn, induce electrical current in these lines of fluid. Electrodes attached to both sides of the pipe pick these electric signals and transfer them to a signal processor. The flow of fluid is proportional with

the generated signals. Major advantages of this flowmeter are lack of moving parts and that it is noninvasive, resulting in no pressure loss. The major disadvantage is the limitation to electrically conducting liquids. It is not suited for such non-conducting fluids as hydrocarbons, hence is not widely used in petroleum industry.

Ultrasonic flowmeter, as shown in Figure VI3.6(a), is based on the travel time of acoustic waves in a flow field. Some clarification is needed regarding the term ultrasonic. Some flowmeters, such as a vortex-shedding meter, use ultrasonic sensing in their data acquisition systems. Ultrasonic flowmeters are of two types: ultrasonic doppler meter and ultrasonic transit-time meter. The ultrasonic transit time meter works on the basis that sound waves in the flow direction travel at a speed faster by $2V$ compared with the sound waves travelling against the flow. The time it takes for the wave to travel from the transmitter to the receiver is $t_1 = L/(c + V\cos\alpha)$. Similarly, the time it takes for the wave to travel from the receiver back to the transmitter is $t_2 = L/(c - V\cos\alpha)$. This results in:

$$\Delta t = \frac{2LV\cos\alpha}{c^2 - V^2\cos\alpha^2} \cong \frac{2LV\cos\alpha}{c} \qquad \text{VIb.3.4}$$

indicating that the measured time is linearly proportional with the measured flow velocity. Note that V is the flow velocity and c the speed of sound in the fluid. The transit-time meter is by far more accurate than a Doppler meter, Figure VIb.3.6(b). The latter works on the basis of the Doppler frequency shift. This occurs when sound waves are reflected from an impurity in the fluid. If sound waves are reflected from stationary objects, there is no change in their wave characteristics wavelength and frequency. However, upon reflection from a moving target, there will be a shift in the wave characteristics hence the wave would have new amplitude, period, and frequency. The flow velocity by Doppler flowmeter is found from $V = c\Delta f/(2f\cos\alpha)$ where f is the transmission frequency and Δf is the doppler shift in frequency. Generally noninvasive flowmeters have the advantage of no moving parts, no induced pressure drop, no need for integration in the piping system, ease of use, capability to be bi-directional, and associated cost savings.

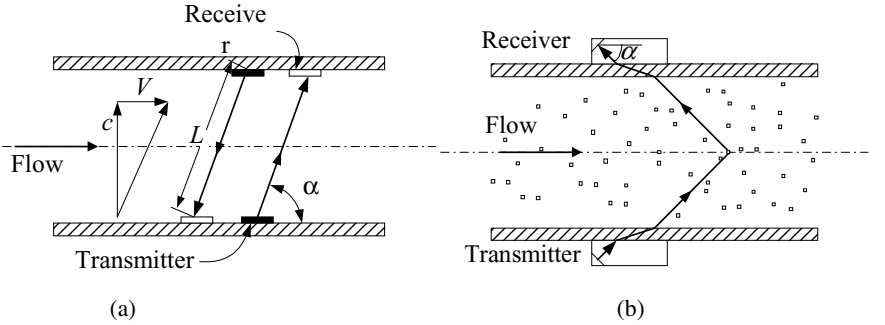

Figure VIb.3.6. (a) Ultrasonic Transit-Time flowmeter and (b) Ultrasonic Doppler flowmeter

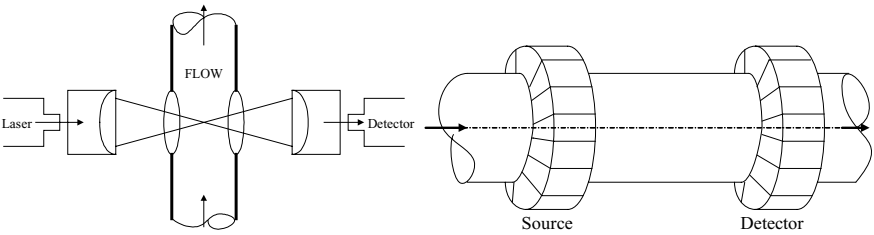

Figure VIb.3.7. Schematics of (a) Laser Doppler flowmeter; (b) Pulsed Neutron Activation Flowmeter

Laser Doppler anemometer or LDA is also used to measure flow rate using the concept of doppler shift. In this method a laser - a coherent monochromatic light beam - passes through the fluid flow and is highly focused in an LDA. Solid particles, in the order of 25 microns in the fluid will scatter the light beam. The scattered light would have a different frequency than the incident light. This is the Doppler shift. A photo multiplier device receives the scattered beam to electronically sense the change in frequency with respect to a reference (non-scattered) beam. Shown in Figure VIb.3.7(a) is a dual-beam LDA with α being the angle between the incident rays. If l is the frequency of the incident ray, the flow velocity is then given by $V = \lambda \Delta f/[2\sin(a/2)]$. The disadvantage of this method is the fact that it requires a glass window for light to pass through.

Pulsed neutron activation or PNA is another non-invasive means of measuring flow rate and is included in the class of radioisotope tracer technique. As shown in Figure VIb.3.7(b), an energetic neutron source is used to induce radioactivity into the flow field. The field velocity is determined by detecting the γ-ray emitted from the irradiated liquid, in a detector located downstream of the neutron source. There are disadvantages associated with this method. PNA uses high-energy neutrons. For example, for the O^{16} (n, p) N^{16} reaction, which has a half-life of 7.14 seconds, the neutron activation threshold is 10.24 MeV. Such high levels of energy require extensive shielding. Additionally, the neutron source and the detector should be circumferencially distributed to minimize radiation bias. Indeed radiation bias occurring due to beam attenuation is another drawback of this method.

Elbow meter is another means of measuring volumetric flow rate, using the change of flow momentum and the associated centrifugal force. Lansford correlated the resulting differential pressure to volumetric flow rate to obtain a formula similar to Equation IIIb.4.3:

$$\dot{V} = CA\sqrt{2g\{[(P_o - P_1)/\rho g] + (z_o - z_i)\}} \qquad \text{VIb.3.5}$$

where, in this relation, value of C ranges from 0.56 - 0.88 depending on the size and shape of the elbow.

Positive Displacement (PD) is the most widely used flowmeter for flow measurement of liquid and gas for industrial, commercial and residential applications. A recent survey indicates that the worldwide sale of the positive displacement flowmeters constituted half of all the flowmeters sold in 2001. Thus more PD flowmeters are sold than all other types, such as Ultrasonic, Electromagnetic, ΔP meter, Vortex meter and mass measuring flowmeters combined (Control magazine). The PD flowmeters are of various types. All function on the same principle of measuring a known volume of the fluid in a distinct compartment that is accurately measured by the manufacturer. The number of these measurements (i.e. the number of times these compartments are filled and emptied per unit time) would determine the flow rate. The PD flowmeters are suitable for viscous fluids (such as oil, paint, varnish, and cosmetics), for low flow rates (as low as about 2 liter/m), and for corrosive products.

3.3. Mass Measuring Flowmeters

There is no need to measure density in these flowmeters, as mass flow rate is directly measured. Several such instruments are discussed below.

Coriolis flowmeters are used in the flow measurement of liquids, suspensions, emulsions, and gases. The coriolis flowmeter is named after the French mathematician Gustave Coriolis who in 1835 showed that an inertial force must be taken into account when describing the motion of bodies in non-inertial frames. The

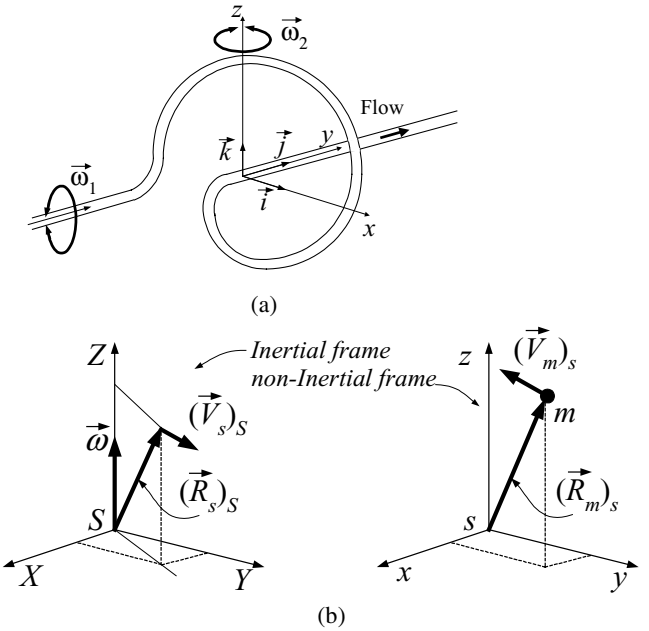

Figure VIb.3.8. (a) A Coriolis flowmeter; (b) Depiction of an inertial and a non-inertial frame

coriolis flowmeter is an instrument consisting of a twisted tube resting on two flexible couplings. Figure VIb.3.8(a) shows the tube being alternatively rotated by a motor along the *y*-axis with an angular velocity of $\vec{\omega}_1 = \omega_1 \vec{j}$. Vibration of the tube coupled with the flow of fluid induces acceleration, causing the Coriolis force to deflect the tube ($\vec{\omega}_2 = \omega_2 \vec{k}$). Tube deflection is accurately measured. Since the applied rotation to the tube is known, the induced rotation can be used to find mass flow rate. To show the relation between the tube deflection and mass flow rate, let's consider mass *m* moving at a velocity *V* with respect to frame *s* $(V_m)_s$. In general, frame *s* is a non-inertial frame, having its own linear velocity $(V_s)_S$ and angular velocity ($\vec{\omega}$) with respect to an inertial frame *S*. Vectors in frame *s* can be expressed in frame *S* using the following mathematical operator:

$$\left(\frac{d}{dt}\right)_S = \left(\frac{d}{dt}\right)_s + \vec{\omega}\times \qquad \text{VIb.3.6}$$

Having the position vector $(\vec{R}_m)_s$ and velocity $(\vec{V}_m)_s$ of mass *m* in frame *s*, velocity of mass *m* in frame *S* (i.e., $(\vec{V}_m)_S$) is found by applying the operator given by Equation VIb.3.6 to the position vector of mass *m*:

$$\left(\vec{V}_m\right)_S = \frac{d(\vec{R}_m)_S}{dt} = \frac{d}{dt}\left[(\vec{R}_s)_S + (\vec{R}_m)_s\right] + \vec{\omega}\times(\vec{R}_m)_s$$

which simplifies to $(\vec{V}_m)_S = (\vec{V}_s)_S + (\vec{V}_m)_s + \vec{\omega}\times(\vec{R}_m)_s$. Similarly, the acceleration of mass *m* in frame *S* is:

$$(\vec{a}_m)_S = \left(\frac{d(\vec{V}_m)_S}{dt}\right)_S = \left[\left(\frac{d}{dt}\right)_s + \vec{\omega}\times\right]\left[(\vec{V}_s)_S + (\vec{V}_m)_s + \vec{\omega}\times(\vec{R}_m)_s\right] \qquad \text{VIb.3.7}$$

carrying out an operation on each of the three terms of the right-hand side bracket in Equation VIb.3.7, we find:

$$(\vec{a}_m)_S = \frac{d}{dt}\left[(\vec{V}_s)_S + (\vec{V}_m)_s + \vec{\omega}\times(\vec{R}_m)_s\right] + \vec{\omega}\times\left[(\vec{V}_s)_S + (\vec{V}_m)_s + \vec{\omega}\times(\vec{R}_m)_s\right] \qquad \text{VIb.3.8}$$

taking the derivative of the terms in the first bracket and performing multiplication in the second bracket yields:

$$(\vec{a}_m)_S = \left[\frac{d(\vec{V}_s)_S}{dt} + \frac{d(\vec{V}_m)_s}{dt} + \vec{\omega}\frac{d(\vec{R}_m)_s}{dt} + \frac{d\vec{\omega}}{dt}\times(\vec{R}_m)_s\right] + \left[\vec{\omega}\times(\vec{V}_s)_S + \vec{\omega}\times(\vec{V}_m)_s\right] + \vec{\omega}\times\left[\vec{\omega}\times(\vec{R}_m)_s\right]$$

Finally;

$$(\vec{a}_m)_S = (a_s)_S + (\vec{a}_m)_s + 2\vec{\omega}\times(\vec{V}_m)_s + \frac{d\vec{\omega}}{dt}\times(\vec{R}_m)_s + \vec{\omega}\times\vec{\omega}\times(\vec{R}_m)_s$$

Newton's second law of motion applies to the absolute acceleration; $\sum\vec{F} = m(\vec{a}_m)_S$. Alternatively:

$$\sum\vec{F} = m\left[(\vec{a}_s)_S + (\vec{a}_m)_s + 2\vec{\omega}\times(\vec{V}_m)_s + \frac{d\vec{\omega}}{dt}\times(\vec{R}_m)_s + \vec{\omega}\times\vec{\omega}\times(\vec{R}_m)_s\right] \qquad \text{VIb.3.9}$$

where;

$m(\vec{a}_s)_S$:	Force due to frame *s* acceleration
$m(\vec{a}_m)_s$:	Force due to local acceleration
$m\left[2\vec{\omega}\times(\vec{V}_m)_s\right]$:	Force due to Coriolis acceleration
$m\left[\frac{d\vec{\omega}}{dt}\times(\vec{R}_m)_s\right]$:	Force due to angular acceleration
$m\left[\vec{\omega}\times\vec{\omega}\times(\vec{R}_m)_s\right]$:	Force due to centripetal acceleration

Thermal mass flowmeters may be used for both liquids and gases to measure mass flow rate. For gases, a resistance heater is wrapped around a thin-wall pipe. Fluid temperatures upstream and downstream of the heater are measured. Having the rate of heat transferred to the fluid and the temperature difference, flow rate of the fluid is then calculated. For liquids, the instrument consists of a U-tube. A heat sink in addition to a heat source is used to bring the liquid temperature down to the inlet temperature at the exit. The obvious error is associated with axial heat transfer in the pipe wall.

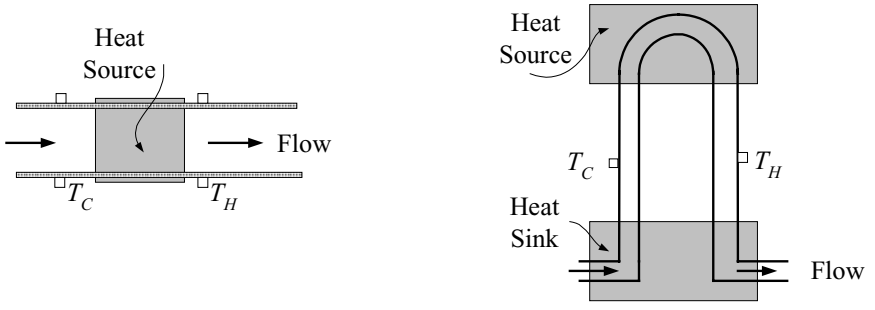

Figure VIb.3.9. Schematics of a thermal mass flow meter for (a) gas; (b) liquid

4. Flowmeter Installation

Since the majority of flow meters measure the average flow velocity and require fully developed flow, such meters should be installed in a way that ensures a symmetric and undisturbed velocity profile through the instrument (Figure VIb.4.1). Flow disturbance is primarily caused by valves and fittings in a piping system.

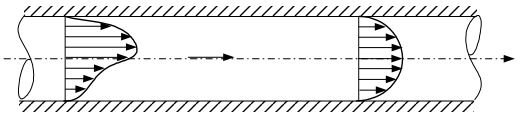

Figure VIb.4.1. Comparison of disturbed and unperturbed velocity profiles

Therefore, flow meter manufacturers require a minimum length of straight pipe to be considered upstream and downstream of the instrument. For example, the required lengths of straight pipe for a vortex meter for various fittings are show in Figure VIb.4.2. When space is at a premium and the recommended straight pipelength cannot be accommodated, various flow straighteners, as shown in Figure VIb.4.3 are used to enforce a symmetric profile. This, however, is achieved at the cost of higher induced pressure drop.

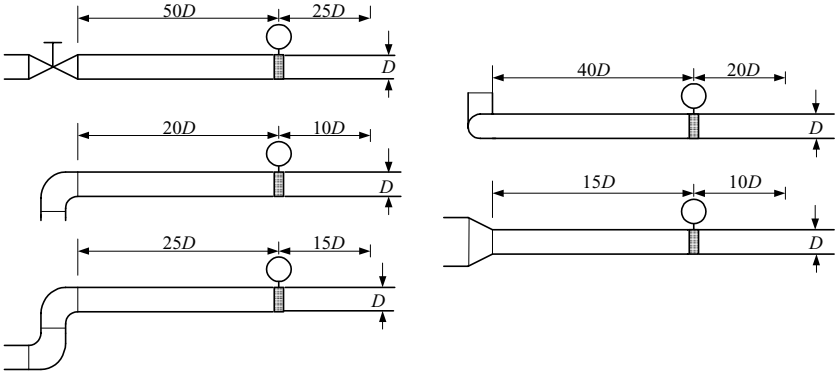

Figure VIb.4.2. Required straight pipe length upstream and downstream of a vortex meter

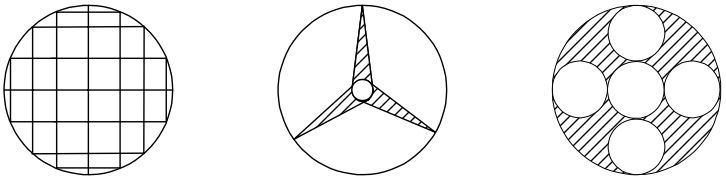

Figure VIb.4.3. Various flow straightner designs

QUESTIONS

- What is the difference between fixed errors and random errors?
- If an experiment has high degree of repeatability are the results necessarily highly accurate?
- List 5 types of noninvasive flowmeters.
- List 5 advantages associated with non-invasive flowmeters.
- Why are flow straightners used? What is the major component of a laminar flowmeter?
- How does a positive displacement flowmeter measure flow?
- What type of flowmeter should be used when fluid flows at a low velocity?
- Why is a rotameter tube tapered?
- What are the advantages of the mass flowmeter?
- How do we measure the flow rate of slurry?
- What are the advantages of the electromagnetic flowmeter?
- What is the principle upon which a vortex flowmeter operates?
- What is the major drawback of the pulsed neutron activation flowmeter?

PROBLEMS

1. Two electric resistors are connected in series, thus $R = R_1 + R_2$. Find the uncertainty in power dissipated in these resistors noting that $E = RI$ where I is the electric current passing through each resistor.
Data: $R_1 = 0.005 \pm 0.25\%$, $R_2 = 0.008 \pm 0.20\%$, and $I = 150 \pm 1$ A.

2. The mass flow rate from a Bernoulli obstruction meter is given as:

$$\dot{m} = CA\sqrt{2P_1\Delta P/(RT_1)}$$

Find the percent uncertainty in the mass flow rate for the following data:
$C = 0.9 \pm 0.0075$, $P_1 = 30$ psia $\pm$ 0.8 psia, $T_1 = 85$ F $\pm$ 1 F, $\Delta P = 1.5$ psi $\pm$ 0.0035 psi, $A = 1.5$ in^2 $\pm$ 0.001 in^2

3. In a shell & tube heat exchanger, total rate of heat transfer between the shell-side and the tube-side is given as $\dot{Q} = UA\Delta T$. Find the uncertainty percent in total rate of heat transfer using the following data:
$U = 500$ Btu/ft^2·h $\pm$ 5 Btu/ft^2·h, $A = 1000$ ft^2 $\pm$ 2.5 ft^2, $\Delta T = 75$ F $\pm$ 2 F.

4. In the measurement of the water mass flow rate in a pipe, the following data are obtained: $A = 100$ cm^2 $\pm$ 0.5%, $\rho = 950 \pm 5$ kg/m^3, and $V = 6$ m/s $\pm$ 7%. Using Equation VIb.2.1, show that the uncertainty in mass flow rate is dominated by the uncertainty in the velocity measurement. What conclusion can then be made from attempts in reducing the uncertainties in area and density measurement?

5. A variable area flowmeter (rotameter) is used to find the flow rate of water at room temperature. The rotameter is 18 inches log with the smallest and largest diameters of 1.75 and 4 inches, respectively. The floater is a stainless steel ball,

2 inches in diameter. Find the volumetric flow rate when the floater mid-plane is at 1 foot from the entrance to the meter. [Ans.: 27 GPM].

6. Apply the Bernoulli equation and the equation of state for an ideal gas to derive a relation similar to Equation IIIb.1.8 for velocity of compressible fluids flowing in the pipe.

(Ans.: $V = \sqrt{2c_p T_1 \left[(P_2 / P_1)^{(k-1)/k} - 1 \right]}$).

7. Suppose we want to use a small probe equipped with a camera at the end of the probe to measure the flow of a liquid. The probe is inserted in a pipe perpendicular to the flow. Attached to the wall opposite to the probe is a light sensitive patch consisted of solar cells, shown as cross-hatched regions in the figure. When inserted in the pipe, the probe behaves as a cantilever, bending in the direction of the flow. The device (i.e., the probe and the patch) is calibrated so that activation of each strip (i.e., solar cell) is associated with a certain flow rate. Comment on applicability, advantages, and disadvantages associated with the use of this flowmeter design.

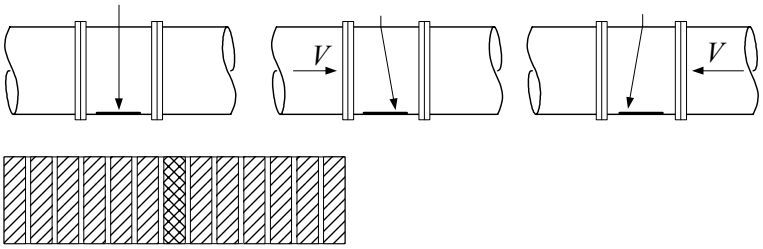

8. Consider the pitot tube of Figure VIb.3.3-b. Gas is flowing over the tube at 40 C and 1 atm. The dynamic pressure is measured as 2 in-H_2O. Find the flow velocity. (Ans.: 29.7 m/s).

9. A hot-wire anemometer is a heated electric resistance placed in the pipe carrying the flow. King showed that the rate of heat transfer is proportional to the flow velocity as:

$$\dot{Q} = \left(a + bV^{0.5}\right)\left(T_{wire} - T_f\right)$$

where constants a and b are determined from a calibration of the anemometer. The rate of heat transfer is also given by the electric power consumed to heat up the resistance:

$$\dot{Q} = R_{wire} I^2 = R_o \left[1 + \alpha (T_{wire} - T_o\right] I^2$$

where I is the electric current, a is the temperature coefficient of resistance, and R_o is the wire resistance at temperature T_o. Obtain flow velocity as a function of the electric current.

VIc. Fundamentals of Turbomachines

Turbomachines are mechanical devices that exchange momentum and energy with a fluid. Machines in which energy is transferred to the fluid are called pumps, compressors, blowers, and fans depending on the type of the fluid and pressurization. In turbines, transfer of energy is from the fluid to the rotating shaft. Such machines, depending on the type of working fluid, are called hydraulic turbine, steam turbine, or gas turbine. If a turbomachine contains a blade or vane, momentum is exchanged with a fluid by changing the direction and the velocity of the flow. The rate of change of fluid momentum results in a force that leads to transfer of work due to fluid displacement. Next, some fundamental terms are defined which help in the discussion of turbomachine operation.

1. Definition of Turbomachine Terms

Dimensional analysis is a third technique to analyze a flow field with the first and second techniques being the integral and differential methods that were discussed in Chapter IIIa. Dimensional analysis, being a means of reducing the number of variables that affect a physical phenomenon, is based on the identification of the pertinent *dimensionless groups*. In this chapter we make extensive use of dimensionless groups.

Scaling laws are a direct result of using the dimensional analysis technique. Scaling laws allow us to extrapolate the results of the study regarding the effects of fluid flow on a *model* to the *prototype*. When the scaling law is valid, it is said that a condition for *similarity* between model and prototype exists.

Velocity vector diagram refers to fluid velocity vector in the impeller of pumps or turbines. Figure VIc.1.1. shows the velocity vector diagrams for a pump impeller rotating clockwise and for a centrifugal compressor rotating counterclockwise. The fluid absolute velocity, whether at the blade inlet or outlet, has two components. One component is always perpendicular to the position vector

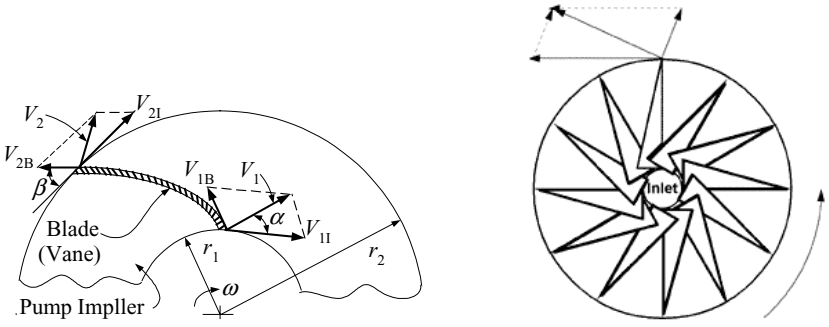

Figure VIc.1.1. Velocity vector diagrams of impellers of a pump and a compressor

hence, tangent to the impeller (V_I) and another component tangent to the blade (V_B). The component tangent to the impeller is the peripheral speed of the impeller at that location ($r\omega$). The velocity component tangent to the blade is fluid velocity relative to the blade. The geometric similarity between the two systems requires that angle α, referred to here as the velocity angle, and angle β, known as the blade angle, are equal in both systems.

Homologous systems are any two systems that are geometrically similar and have a similar velocity vector diagram. For example, if a given pump (say pump A) is to be homologous with another pump (say pump B), the geometrical symmetry requires that $\alpha_A = \alpha_B$ and $\beta_A = \beta_B$. For angle α to be constant, it requires that $\dot{V} / \omega D^3 = \text{constant}$.

Dimensionless groups are generated by identifying pertinent parameters in the operation of turbomachines. For example, there are three groups containing pertinent pump parameters. Group one contains pump performance consisting of flow rate and pressure rise ($\dot{V}$, ΔP). Group two contains pump geometry data given by the impeller diameter, speed, and roughness (D, ω, ε). Group three contains fluid properties, the most pertinent being density and viscosity (ρ, μ). According to the *Buckingham Pi theorem*, the number of dimensionless groups between N independent variables is equal to $N - N'$ where N' is equal to the number of primary dimensions, such as Mass, Length, and Time (m, L, t).

Pump performance curve is a term applied to the head delivered by the pump versus the flow rate. A more comprehensive pump performance curve, discussed later in this chapter, includes head versus flow curves for a given rotor speed and various rotor sizes. The pump performance curve is constructed by the pump manufacturer from a wide range of data and generally includes plots of pump efficiency.

Classification of pumps. There are many types of pumps in various shapes and forms for different industrial, residential, and medical applications. Hence, pumps may be classified in various ways. Here we classify pumps based on the means of momentum transfer to the working fluid. This classification results in only two types of pumps, positive displacement and dynamic.

Positive displacement pumps are devices delivering fluid that, in each cycle, fills a known volume or closed compartment of the pump. This type of pump delivers periodic or pulsating flow. The means of delivering varies depending on a specific design. For example, fluid delivery may take place by the action of sliding vanes, rotating gears and screws, or moving plungers and pistons. Schematic of a piston-cylinder positive displacement pump is shown in Figure VIc.2.1.

Dynamic pumps basically deliver momentum to the fluid through the rotation of vanes or impellers. The momentum is converted to pressure head as the liquid passes through the pump diffuser. Dynamic pumps may in turn be divided into two major categories; rotary and special applications.

Dynamic pumps for special applications include such pumps as electromagnetic pumps for the delivery of liquid metals such as sodium and mercury, jet pumps for mixing two streams of fluids, and fluid actuated pumps. The electromagnetic pumps are of either direct-current (also known as the dc-Faraday pumps) or of the alternating-current type. The electromagnetic pumps operate on the same principle as electromagnetic flowmeters.

Dynamic rotary pumps are also referred to as *rotodynamic* pumps. They consist of radial, mixed, and axial flow designs. The design refers to the flow inside the pump. The rotor of the radial flow pump is generally referred to as an impeller and the rotor of the axial flow pump as a propeller. The impeller of the radial flow pumps, consists of vanes and the propeller of the axial flow pump consists of blades. In the radial flow pump, flow enters the inlet of the pump impeller and primarily flows in the radial direction until exiting the impeller. In the axial flow pumps, flow direction is along the axis of the pump propeller. The most widely used dynamic pump is the centrifugal pump.

2. Centrifugal Pumps

We begin the introduction of the centrifugal pump by comparing its characteristic curve with that of a positive displacement pump. As shown in Figure VIc.2.1, positive displacement pumps deliver nearly constant flow at a wide range of pressure while rotodynamic pumps deliver nearly constant pressure at a range of flow rate. Rotodynamic pumps provide high rate of flow rates (as high as 700 ft^3/s) but with rather low head (in the range of 100 psi). On the other hand, positive displacement pumps supply high head (up to 3000 psia) but rather low flow rate (in the range of 2 ft^3). For example, a typical PWR plant uses positive displacement pumps, each delivering about 45 GPM (3.5 lit/s) at 2250 psia (15.5 MPa).

To investigate the design and operation of rotodynamic pumps we consider centrifugal pumps as shown in Figure VIc.2.2. A centrifugal pump is a mechanical device, combining centrifugal force with mechanical impulse to produce an increase in pressure. In such pumps, kinetic energy is produced by the action of centrifugal force and then the energy is partially converted to pressure by efficiently reducing its velocity. Centrifugal pumps consist of rotating and stationary

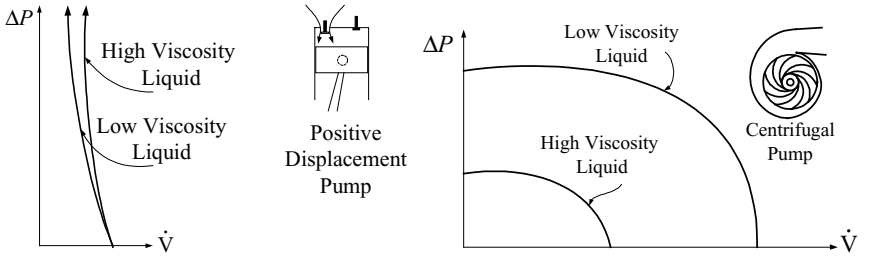

Figure VIc.2.1. Characteristic curve comparison of positive displacement and rotodynamic pumps (White)

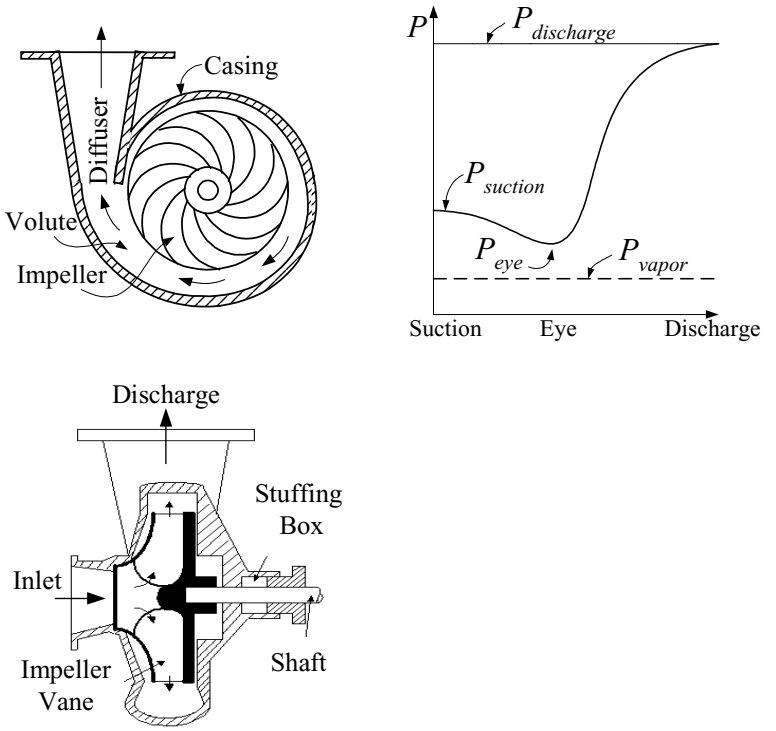

Figure VIc.2.2. Cross-section of a single-stage centrifugal pump

parts. Rotating parts include the impeller, mounted on a shaft, which, in turn, rests in the pump bearings. The impeller contains blades or vanes. Liquid enters the pump through the central hole or *eye* of the impeller, at the inlet to the blades. Stationary parts include the casing and the diffuser. Some casings are equipped with stationary blades acting as a diffuser. Note that we must have the liquid pressure at the eye of the pump greater than the liquid vapor pressure as described in Section 1.4 of Chapter IIa and Section 2.1 of this chapter.

Generally, casings have spiral shape, referred to as a volute, to change the liquid velocity to pressure head at the discharge. The casing may be solid with an opening in one side to access the impeller or may be split either axially or radially. In the latter case, bolts are used to fasten the two parts of the casing together.

Power to rotate the pump shaft is provided by the pump driver also referred to as the *prime mover*, which may be a reciprocal engine, a steam turbine, or an electrical motor. A pump coupling provides connection between the two units. Pressurized liquid in the pump has the tendency to leak at the shaft access through the casing. This is prevented by a pump seal, which also prevents air leakage into the pump in the case of a suction lift when pressure drops below atmospheric. The pump seal generally consists of a series of packing rings, the housing of which is

referred to as the *stuffing box*. Pumps may also use mechanical seals as are used in reactor coolant pumps. In such cases, the mechanical seals are cooled by the plant component cooling system. Seal cooling is required due to the high pumping power of such pumps (about 5 MW per pump for a typical 1000 MWe PWR).

2.1. Definition of Terms for Centrifugal Pumps

In the definitions below, reference is made to Figure IIIb.4.1, but subscript *i* is used for suction- and *e* for discharge-side.

Useful work of a pump is defined as the product of two terms. The first term is the rate at which fluid passes through the pump. The second term is the height of a column of fluid equivalent, under adiabatic conditions, to the total pressure differential measured immediately before entering and right after leaving the pump. The first term is referred to as *capacity*, *discharge*, *volumetric flow rate*, *flow rate*, or simply *flow*. The second term is referred to as *pump pressure head*.

Velocity head is the vertical distance a body would have to fall to acquire the velocity V, $\mathrm{h}_V = \dfrac{V^2}{2g}$.

Static suction head is the absolute pressure at the free level (Z_i) of the suction reservoir in feet of liquid plus the vertical distance from the pump centerline to this level. This definition applies only if $Z_i > Z_P$:

$$\mathrm{h}_{ss} = \frac{P_i}{\rho g} + (Z_i - Z_P)$$

If $Z_i < Z_P$, the term is referred to as the static-suction lift.

Static discharge head is the absolute pressure at the pump discharge plus the elevation head with respect to the pump centerline:

$$\mathrm{h}_{sd} = \frac{P_e}{\rho g} + (Z_e - Z_P)$$

Total static head is the difference between the static discharge and the static suction head.

$$\mathrm{h}_{sd} = \frac{P_e - P_i}{\rho g} + (Z_e - Z_i)$$

Total dynamic suction head is the static suction plus the velocity head minus the suction friction head.

$$\mathrm{h}_s = \left(\frac{P_i}{\rho g} + \frac{V_i^2}{2g} + Z_i - Z_P \right) - \mathrm{h}_{sf}$$

Total dynamic discharge head is the static discharge head plus the velocity head plus the discharge friction head.

$$\mathrm{h}_d = \left(\frac{P_e}{\rho g} + \frac{V_e^2}{2g} + Z_e - Z_P \right) + \mathrm{h}_{df}$$

Total dynamic head is the difference between total dynamic discharge and total dynamic suction head:

$$\mathrm{H} = \left(\frac{P_e}{\rho g} + \frac{V_e^2}{2g} + Z_e \right) - \left(\frac{P_i}{\rho g} + \frac{V_i^2}{2g} + Z_i \right) + \mathrm{h}_f = \mathrm{h}_s$$

where $\mathrm{h}_f = \mathrm{h}_{df} + \mathrm{h}_{sf}$

Vapor pressure of a liquid is the absolute pressure at which liquid vaporizes and is in equilibrium with its vapor phase. If the liquid pressure drops below the vapor pressure, the liquid boils. If liquid pressure is greater than the vapor pressure, then the liquid vaporizes at the interface between the two phases. The vapor pressure of water at 80 F (27 C), for example, is P_V = 0.50683 psia (3.5 kPa). Similar definition is given in Section IIa.1.4. If pressure at the eye of the pump drops below the vapor pressure then the pump begins to cavitate.

Cavitation is the major cause of damage to pumps and valves where liquid experiences a large and sudden pressure drop. Cavitation is defined as formation, via vaporization, and subsequent collapse, via condensation, of vapor bubbles in a liquid. A pressure drop to or below the liquid vapor pressure coupled with existing nuclei (tiny voids containing vapor or gas) results in liquid vaporization. These voids appear as tiny bubbles that will grow if the surrounding pressure remains at or below the vapor pressure of the liquid or they will collapse at higher pressures. Pressure drop occurs at such locations as tip of a propeller, edges of a thin-plate orifice, or seats of a valve. These unrecoverable pressure losses in these places are associated with dissipation of energy, which constitutes the loss coefficient of valves and fittings. Collapse of bubbles in higher-pressure regions is associated with rapid pressure fluctuations that will eventually result in erosion and pitting of the hydraulic structure.

There are various means of preventing cavitation, primarily depending on the type of the hydraulic system. Prevention of cavitation in a pump is discussed in Section 3. In some hydraulics systems, it may be possible to introduce a gradual pressure drop to the flow. Cavitation control valves may use a tortuous flow path, cascaded orifices, or a combination of both to cause high velocity hence, large local frictional losses. Another means of preventing material erosion due to cavitation is to use erosion resistant materials at locations prone to cavitation, such as the use of stainless steel for a turbine blade, valve seat, or pump impeller. As shown in Figure VIc.2.2, during operation we must ensure that $P_{eye} > P_{vapor}$.

Best efficiency point (BEP) is an operation mode at which the pump efficiency is a maximum. While pumps should be operated at their BEP, it is especially im-

portant for pumps that operate with liquids with abrasive contents. At the BEP, the angle at which the impeller and the liquid meet is optimized, helping to reduce impingement and minimize erosion. In this chapter, the pump parameters at BEP are shown with subscript "o".

Net positive suction head as required by the pump is usually given for the best efficiency point by the pump manufacturer. The available net positive suction head ($NPSH_A$) defined as $P_P + (V_P^2/2) - P_v$ is obrained from:

$$NPSH_A = \frac{P_i}{\rho g} - (Z_P - Z_i) - \frac{P_v}{\rho g} - \mathrm{h}_{fs} \qquad \text{VIc.2.1}$$

where point i is on the surface of the source reservoir and point P is at the pump inlet. However, for large pumps, point P should be taken at the top of the impeller. Pressure at the source reservoir is P_i. If the reservoir is open to atmosphere then $P_i = P_{atm}$. In Equation VIc.2.1, P_v shows the vapor pressure of the liquid at operating temperature. For example, water vapor pressure at P = 14.7 psia and T = 80 F is about P_v = 0.5 psia. Finally, h_{fs} represents frictional head loss in the suction piping and is found from Equation IIIb.3.12 with $L = s + \delta$ as depicted in Figure VIc.1.1 where h_{fi} is friction head loss between the suction-side reservoir and pump inlet and P_v is the working liquid saturation pressure at operating temperature.

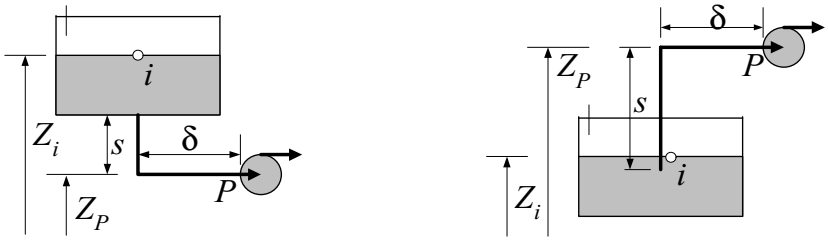

(a) Arrangement Helps $NPSH_A$ (b) Arrangement Hurts $NPSH_A$

Figure VIc.1.1. Two arrangements for pump suction (P_i is maintained throughout the pumping process)

Shutoff head is the maximum head a pump develops corresponding to the minimum flow rate.

Runaway speed is the speed a centrifugal pump would reach when the pump impeller runs in the reverse direction. This occurs upon failure of the discharge valve to close when a running pump is stopped under a high static head.

Design pressure is the maximum pressure the pump casing can be exposed to before being structurally damaged.

Rated conditions are the values of pump head and pump flow rate corresponding to maximum pump efficiency. For all practical purposes, pumps should be operated at the BEP. However, we recognize that deviations will occur from

pump conditions during operations primarily variations in demand for flow rate. The more the operating conditions deviate from the BEP, the more a pump would be subject to degradation in performance and long-term deterioration of its components.

Hydraulic horsepower is the power transferred to the fluid to deliver a flow rate of $\dot{\mathrm{V}}$ at a total dynamic head of H. To calculate the pumping power, we use $\dot{W}_{HYD} = FV = (\Delta PA)(\dot{\mathrm{V}}/A) = \rho g \mathrm{H}\dot{\mathrm{V}} = \dot{m}\, g\mathrm{H}$.

Brake horsepower is the power delivered by the prime mover to drive the pump ($\dot{W}_{BHP} = \omega \mathrm{T}$), where ω is the shaft angular velocity (radian/s) and T is the shaft torque delivered by the prime mover.

Pump efficiency is the ratio of hydraulic horsepower to brake horsepower, $\eta = \dfrac{\dot{W}_{HYD}}{\omega \mathrm{T}} = \eta_v \eta_h \eta_m$.

Substituting values, efficiency can be found from $\eta = \rho g \mathrm{h}\dot{\mathrm{V}}/(2\pi N \mathrm{T})$ where head is in ft, flow rate in GPM, torque in ft·lbf, and impeller speed in rpm.

Volumetric efficiency, as a component of pump efficiency, is defined as $\eta_v = \dot{\mathrm{V}}/(\dot{\mathrm{V}} + \dot{\mathrm{V}}_L)$ where $\dot{\mathrm{V}}_L$ is the leakage flow rate to the casing from the impeller-casing clearance.

Hydraulic efficiency is defined by three types of losses occurring in the pump. The first type is the *shock* loss at the impeller inlet (eye) due to imperfect match between inlet flow and the impeller entrance. The second type is due to *frictional* losses in the impeller. The third type is the *circulation* loss caused by the imperfect match between the exit flow and the impeller outlet. Hence, we find $\eta_h = 1 - (\mathrm{h}_f / \mathrm{h}_s)$.

Mechanical efficiency is defined by the losses in pump bearings, packing-glands, or mechanical seals and other contact points. If $\dot{W}_f$ is the power wasted in all the contact points, $\eta_m = 1 - (\dot{W}_f / \dot{W}_{BHP})$. Improvement of the pump seal and the bearing material may increase pump efficiency by as much as 2%.

Priming refers to the inability of rotodynamic pumps to operate if non-condensable gases have leaked into the pump. In positive displacement pumps, the moving element, whether piston, gear, screw, or sliding vane, readily evacuates gases from the pump. For this reason, positive displacement pumps are considered to be *self-priming*.

3. Dimensionless Centrifugal Pump Performance

Earlier in this section we identified three groups containing pertinent pump parameters, ($\dot{V}$, ΔP), (D, ω, ε), and (ρ, μ). To obtain a relation for $\Delta P_{pump} = \rho g H = f\left(\dot{V}, \rho, \mu, N, D, \varepsilon\right)$ with H being total dynamic head, we note that there are a total of seven variables. Choosing ρ, D, and ω to represent the three primary dimensions mass, length, and time, we can identify four dimensionless ratios. Two obvious ones are ε/D for roughness ratio and $\rho ND^2/\mu$ for the Reynolds number. The non-dimensional flow rate and head rise become $\dot{V}/ND^3$ and gH/N^2D^2, respectively. Hence, we can write:

$$\frac{gH}{N^2D^2} = f_1\left(\frac{\dot{V}}{ND^3}, \frac{\rho ND^2}{\mu}, \frac{\varepsilon}{D}\right)$$

Similar analysis can be performed for break horsepower and pump efficiency with dimensionless ratios of $\dot{W}_{BHP} / \rho N^3 D^5$ and η, respectively. The dimensionless ratios for flow, head, and break horsepower are referred to as *capacity coefficient* ($C_{\dot{V}} = \dot{V}/ND^3$), *head coefficient* ($C_H = gH/N^2D^2$), and *power coefficient* ($C_{\dot{W}} = \dot{W}_{BHP} / \rho N^3 D^5$), respectively. Similar to the power coefficient, we may also define a *torque coefficient* ($C_T = T/\rho N^2 D^5$). If we assume that head and power coefficients are weak functions of Reynolds number and surface roughness, for all practical purposes we can then write:

$$C_H \cong C_H(C_{\dot{V}}) \qquad C_{\dot{W}} \cong C_{\dot{W}}(C_{\dot{V}}) \qquad \eta = \eta(C_{\dot{V}}) \qquad \text{VIc.3.1}$$

Hence for two pumps to be homologous, we must have $C_{\dot{V}1} = C_{\dot{V}2}$, $C_{H1} = C_{H2}$, $C_{\dot{W}1} = C_{\dot{W}2}$, and $\eta_1 = \eta_2$. These conditions are known as the similarity rules. Using the similarity rules, not only can we predict the performance of other homologous units of pumps but we can also predict the performance of the same pump at various speeds.

Example VIc.3.1. A performance curve of a typical centrifugal pump having an impeller diameter of 41.5 inches at 710 rpm (pump A) is shown in the figure. Find the performance curve of the homologous pump (pump B) having a head and flow rate of 325 ft and 3000 GPM at the point of best efficiency.

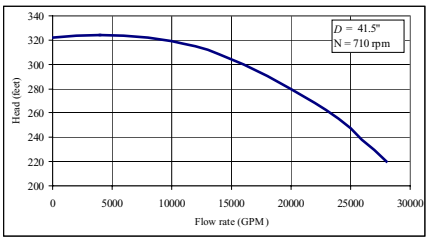

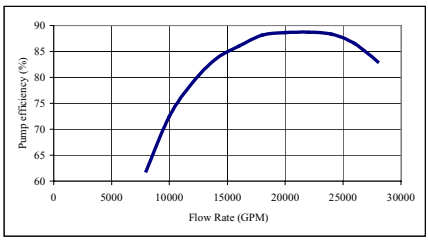

Solution: We use the conditions for dynamic similarity given by three relations in Equation VIc.3.1. Since head and flow rate of pump B are specified at the point of best efficiency, to satisfy the third condition, we also use the head and flow rate of pump A in the first and the second relations at the point of best efficiency. Flow rate and head for pump A at the point of best efficiency (i.e. at $\eta \cong 88\%$) are about $\dot{V}_o =$ 22000 GPM and H_o = 270 ft, respectively. Hence, from $\dfrac{\dot{V}_B}{N_B D_B^3} = \dfrac{\dot{V}_A}{N_A D_A^3}$ and $\dfrac{gH_B}{N_B^2 D_B^2} = \dfrac{gH_A}{N_A^2 D_A^2}$ we solve for D_B and N_B, to find $D_B = (H_A / H_B)^{1/4} (\dot{V}_B / \dot{V}_A)^{1/2} D_A$ and $N_B = \sqrt{\dot{V}_A / \dot{V}_B}\,(H_B/H_A)^{3/4} N_A$. Substituting for flow rates, heads, and D_A, we get D_B = 14.63 inches and N_B = 2209 rpm. Having, D_B and N_B, other points of the pump B characteristic curve at other efficiencies can be obtained by using similar points of pump A.

In the next example, we compare pump A of Example VIc.3.1 with another pump, which belongs to the same homologous series of pumps (say pump C). Our intention is to verify if the homologous pumps can be represented only with the non-dimensional groups.

Example VIc.3.2. A performance curve of Pump C, which is homologous to pump A of Example VIc.3.1, is shown below in the left-hand side plot. Find the head versus the flow coefficient for these pumps.

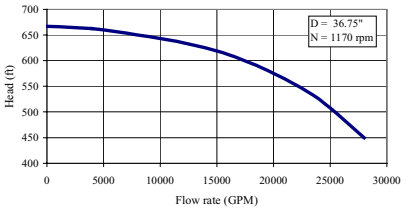

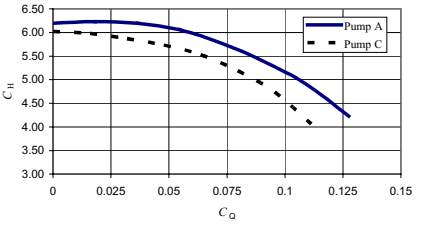

Solution: Having N and D for each pump, as well as the characteristic curves (H versus $\dot{V}$) for both pumps A and C, we find the head and flow coefficients as plotted in the right graph in the above figure. This figure shows that for geometrically similar pumps, the head coefficient is almost a unique function of the capacity coefficient. The reason for the slight difference is due to the assumptions we

made namely, ignoring the viscosity effects and the surface roughness. Similar comparison can be made for the brake horsepower coefficient and efficiency of pumps A and C.

Even with ignoring the effects of viscosity and surface roughness to find the two independent variables H and $\dot{W}_{BHP}$, we need to know the values of three independent variables: $\dot{V}$, *N*, and *D*. Shown in Figure VIc.3.1(a) are head and brake horsepower (also efficiency and NPSH) versus flow rate for a specified diameter and a specified impeller speed. These data, referred to as the pump characteristic curves, are produced empirically by the pump manufacturer. Due to the complexity of dealing with a multi-variable system, it is essential, especially for computer analysis, to use single graphs to represent the pump characteristic curves. Example VIc.3.1 showed that dimensionless homologous curves allow us to make such single graph representations, as shown in Figure VIc.3.1(b).

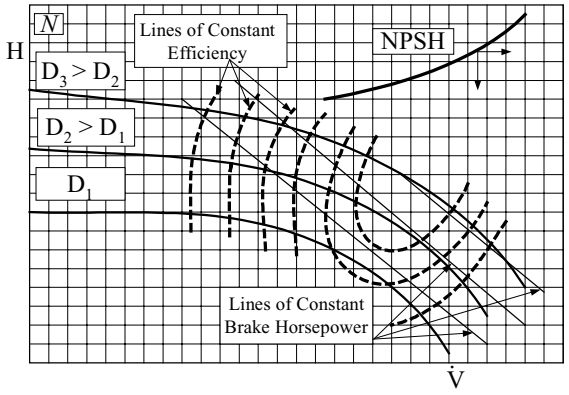

(a)

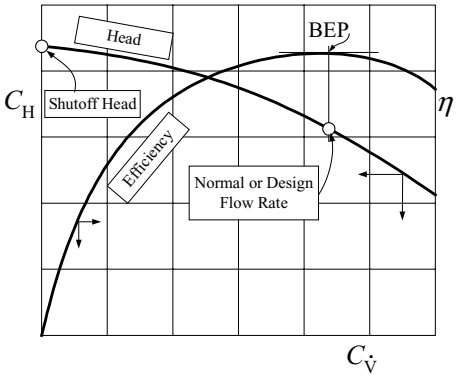

(b)

Figure VIc.3.1. Representation of (a) pump characteristic curves by (b) homologous curves

Example VIc.3.3. Use the similarity rules and compare the performance of a series of homologous pumps for various impeller diameters and impeller speeds.

Solution: The similarity rules require that;

$$\frac{\dot{V}_2}{\dot{V}_1} = \frac{N_2}{N_1}\left(\frac{D_2}{D_1}\right)^3, \quad \frac{H_2}{H_1} = \left(\frac{N_2}{N_1}\right)^2\left(\frac{D_2}{D_1}\right)^2, \text{ and } \frac{\dot{W}_2}{\dot{W}_1} = \frac{\rho_2}{\rho_1}\left(\frac{N_2}{N_1}\right)^3\left(\frac{D_2}{D_1}\right)^5$$

These relations indicate that brake horsepower varies significantly with impeller size, as it depends on the diameter to the power of 5. The impeller size also affects flow rate since for the same total dynamic head, we get higher flow rate with higher diameter. Pump performance curves for various diameters and speed are plotted on the comparative diagrams where $D_1 < D_2 < D_3$ and $N_1 < N_2 < N_3$. Note that the similarity rules require that we also have $\eta_1 = \eta_2$. In reality however, larger pumps generally have higher efficiency than smaller pumps due to the smoother surfaces and tighter clearances.

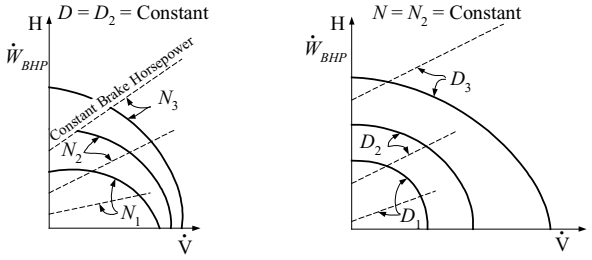

3.1. Specific Speed

In Example VIc.3.1, we eliminated the impeller diameter and obtained $N_B = \left(\dot{V}_A / \dot{V}_B\right)^{1/2}\left(H_B/H_A\right)^{3/4} N_A$. If we now assume that for pump B, $\dot{V}_B = 1$ GPM and H_B = 1 ft, then N_B is known as specific speed of the pump (N_s) given by:

$$N_s = N\dot{V}_o^{1/2} / H_o^{3/4} \qquad \text{VIc.3.2}$$

Therefore, for a homologous series of pumps, the specific speed is the pump speed that delivers a unit discharge at unit head at the BEP since N_s is generally calculated at the point of peak efficiency (shown by subscript o). Specific speed expressed in the *U.S. customary units* is calculated assuming speed in RPM, flow rate in GPM and head in feet. The advantage of specific speed is that it is associated with a particular range of values for each class of pumps. For example, high-head and low-flow pumps have a specific speed in the range of about 500 in U.S. customary units. As flow rate increases and dynamic head drops, the specific speed increases. Wislicenus showed (Figure VIc.3.2) that pump peak efficiency increases with increasing flow rate and specific speed.

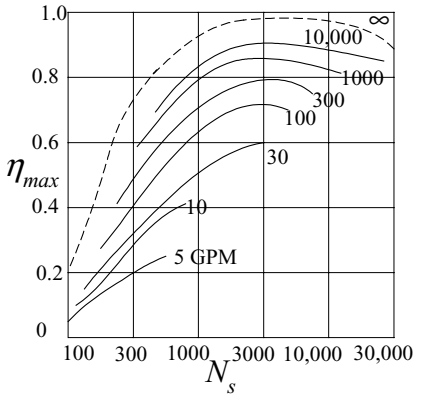

Figure VIc.3.2. Pump peak efficiency versus specific speed

Example VIc.3.4. Use the pump performance data of Example VIc.3.1 to find specific speed.

Solution: Specific speed is found at the point of peak efficiency. Therefore, given an impeller speed of 710 RPM, a flow rate of 22,000 GPM (8248 lit/s), and head of 270 ft (82.3 m), we find:

$$N_s = \frac{710 \times (22{,}000)^{0.5}}{(270)^{0.75}} = 1581$$

Example VIc.3.5. Find the specific speed of a pump with flow rate of 50,000 GPM and head of 23 ft. For this pump the capacity coefficient and the head coefficient at the BEP are 0.1 and 5.0, respectively.

Solution: Flow rate in ft^3/s is 50,000 GPM × (1 ft^3/7.481 gallon) × (1 min/60) = 111.4 ft^3/s.

$C_{\dot{V}} = \dot{V}/ND^3$, therefore, $ND^3 = \dot{V} / C_{\dot{V}} = 111.4/0.1 = 1114$

$C_H = gH/N^2D^2$, therefore, $N^2D^2 = gH/C_H = 32.2 \times 23/5 = 148.12$

Solving for N and D, we find $D = 9.6$ ft and $N = 1.3$ revolution/s = 76 RPM. Since high flow rate is pumped at a low head, the impeller diameter becomes too large and the impeller speed too slow. The specific speed is found as $N_s = 76(50{,}000)^{1/2}/(23)^{3/4} = 1619$.

The disadvantages associated with large diameter impeller and slow speed pumps include size accommodation and cost associated with parts (bearings, shaft, impeller, mechanical seals, and casing) in manufacturing and operation. As seen from the above example, the centrifugal pumps are well suited for low flow and

high head applications. Delivering high flow rates at lower head is better accomplished with pumps that reduce the radial component and increase the axial flow component. Figure VIc.3.3 shows that the large diameter radial flow impeller should be used for low specific speed. As specific speed increases, the shape of the impeller changes to reduce the centrifugal component in favor of the axial flow component. At very high specific speeds, pumps equipped with propeller should be used.

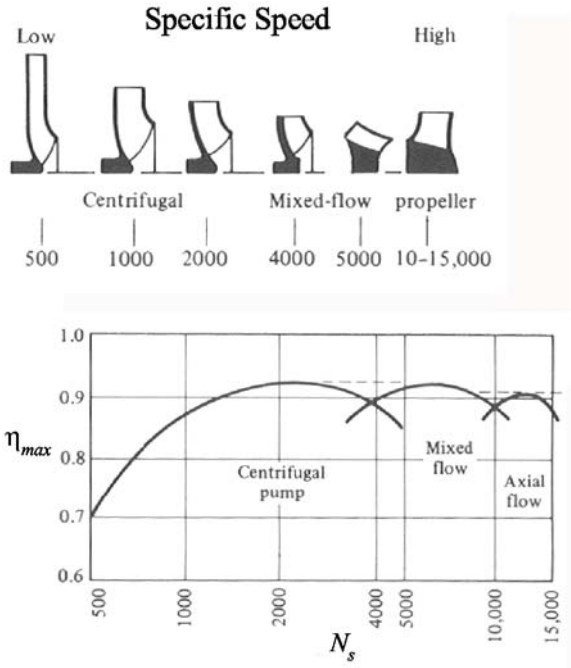

Figure VIc.3.3. Depiction of type and efficiency versus specific speed (White)

3.2. Prevention of Pump Cavitation

The required NPSH to avoid cavitation ($NPSH_R$) is specified by the pump manufacturer. As shown in Figure VIc.3.4, NPSH is a function of flow rate and impeller speed. Installation of the pump must ensure that the available NPSH remains always greater than the required NPSH. Therefore, to avoid cavitation, we must ensure that $NPSH_A > NPSH_R$ holds during pump operation. In fact, to enhance the margin to the onset of cavitation, it is recommended (Kreith) to increase the $NPSH_R$ by an additional 2 to 3 m (6.5 to 10 ft).

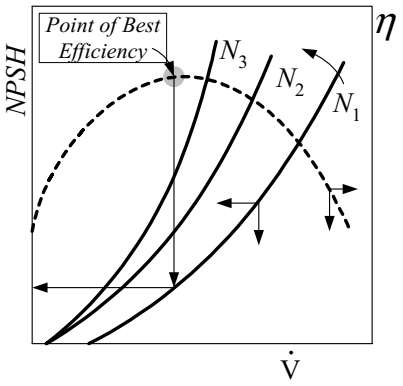

Figure VIc.3.4. Effect of flow rate and speed on the required NPSH

Example VIc.3.6. A centrifugal pump is used to deliver water at a rate of 250 GPM. The pump manufacturer has specified a minimum NPSH of 17 ft. The source reservoir is open to the atmosphere. The suction piping has a diameter of 3.5 in. with a total loss coefficient of K = 8. Find the maximum height that the pump can be placed above the reservoir to prevent cavitation. Water in the reservoir is at 14.7 psia and 75 F. The horizontal suction pipe run is 18 ft.

Solution: We use Equation VIc.2.1. Water is at P_i = 14.7 psia, and 75 F. The vapor pressure is about P_v = 0.43 psia. Total head loss in the suction piping is:

$$\mathrm{h}_{fs} = \left(f\frac{s+\delta}{D} + \mathrm{K} \right)\frac{V^2}{2g}$$

where s is the height we are looking for and δ = 18 ft is the specified horizontal pipe run to pump intake. To find velocity, we use $\dot{V}$ = 250/(7.481 × 60) = 0.557 ft^3/s and $A = \pi D^2/4$ = 3.14 × (3.5/12)^2/4 = 0.0668 ft^2. Hence, V = 0.557/0.0668 = 8.34 ft/s and Re = $\rho VD/\mu$ = 62.4 × 8.34 × (3.5/12)/6.25E-4 = 0.243E6. Assuming a smooth pipe, f = 0.184/Re$^{0.2}$ = 0.0154. Using Equation VIc.2.1:

$$\frac{14.7\times144}{62.4} - s - \left(0.0154\frac{s+18}{(3.5/12)} + 8 \right)\frac{8.34^2}{2\times32.2} - \frac{0.43\times144}{62.4} \geq NPSH_R = 17$$

From here $s = Z_p - Z_i$ = 6 ft. Hence, $Z_P = Z_i$ + 6 ft. This is the maximum elevation for the pump to avoid cavitation. Note that in this example head loss due to skin friction (h_1 = 1.4 ft) is by far smaller than losses due to valves, filters, and fittings (h_2 = 8.64 ft) on the suction line. In general, the suction line must be located as close to the source reservoir as possible with as few valves and fittings on the suction line as absolutely necessary. Head loss due to skin friction can become noticeable in cases where pumps cannot be located near the source reservoir with only few fittings on the suction line.

The likelihood for cavitation increases with increasing specific speed conservatively beyond about 8000.

Example VIc.3.7. The available NPSH for a pump delivering 50,000 GPM water is 40 ft. Find the maximum impeller speed to avoid cavitation.

Solution: We find N from Equation VIc.3.2 with NPSH substituted for H_o:
$N = N_s(\text{NPSH})^{3/4}/\dot{V}^{1/2}$:
$N = 8000 \times (40)^{0.75}/(50{,}000)^{1/2} = 569$ RPM.

4. System and Pump Characteristic Curves

The challenge of selecting a pump is to meet the required capacity while providing the required head at the point of best efficiency. Equation IIIb.4.8-1 (or IIIb.4.8-2) gives serial-path system curves for laminar and turbulent flows. This is also plotted in Figure VIc.4.1(b). Pump head and flow rate is obtained from the intersection of the pump characteristic and system curves. If this point does not correspond with the point of peak efficiency, the pump speed should be adjusted otherwise alternate pumps should be sought. We may try an analytical solution for turbulent flow in pipes, for example where $H_{System} = c_1 + c_3\dot{V}^2$. Representing pump head versus flow rate with a parabola, we find $H_{Pump} = a + b\dot{V}^2$. Setting the system head equal to the pump head, we find $(b - c_3)\ \dot{V}^2 + (a - c_1) = 0$. Flow rate is then found as

$$\dot{V} = \left(\frac{a - c_1}{c_3 - b}\right)^{1/2} = \left(\frac{H_{Pump}(\dot{V}=0) - (Z_e - Z_i)}{\sum fL'/(2gDA^2) + [H_{Pump}(\dot{V}=0)/\dot{V}^2(H_{Pump}=0)]}\right)^{1/2} \qquad \text{VIc.4.1}$$

where the two points to describe the $H_{Pump} = f(\dot{V})$ are taken at maximum H and maximum $\dot{V}$. The flow rate calculated above should be checked against $\dot{V}_o$, flow rate corresponding to best efficiency point. If significant difference exists, pump speed should be changed. If the change in speed still does not increase efficiency, an alternate pump should be sought. To find if a change in speed brings efficiency to its peak value, we use the homologous relations $C_{\dot{V}} = C_{\dot{V}'}$ and $C_H = C_{H'}$. If at N_o rpm, the flow rate and head corresponding to peak efficiency are $\dot{V}_o$ and H_o, then at any other speed these are given by $\dot{V} = \dot{V}_o(N/N_o)$ and $H = H_o(N/N_o)^2$. We now substitute the new head and flow rate into the system curve to get $H_o(N/N_o)^2 = c_1 + c_3\left[\dot{V}_o(N/N_o)\right]^2$. We solve this equation for N to get:

$$N = \left(\frac{C_1}{H_o - C_3 \dot{V}_o^2} \right) N_o = \left\{ \frac{Z_e - Z_i}{H_o - [\sum fL'/(2gDA^2)]\dot{V}_o^2} \right\}^{1/2} N_o \qquad \text{VIc.4.2}$$

Equation VIc.4.2 yields an acceptable answer only if the argument is greater than zero. To increase accuracy, the pump curve should be represented by a higher order polynomial.

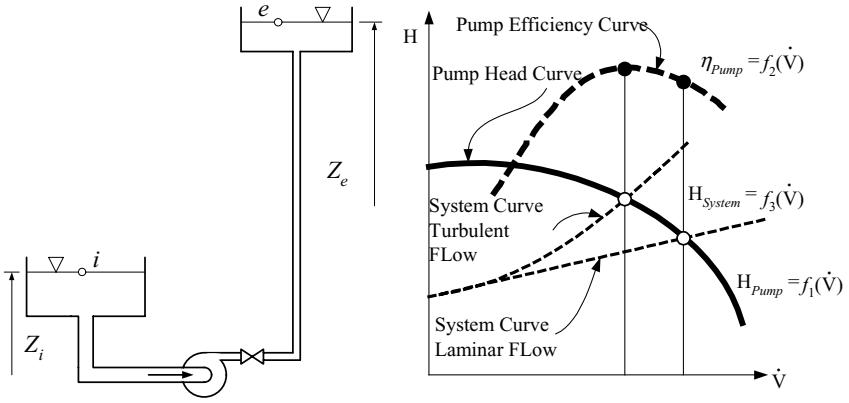

Figure VIc.4.1. (a) Pump in a single-path system (b) Pump and system curves

Example VIc.4.1. The pump in Example VIc.3.1 is used to deliver water to a height of 100 ft from the source reservoir. Total pipe length is 2000 ft and the pipe diameter is 14 in. The pipe run includes a swing check valve, a fully open gate valve, and a fully open globe valve as well as a total of 4 threaded 90° elbows. a) Find flow rate and efficiency. b) How do you maximize efficiency in part (a)?

Solution: a) We first find the system curve from $H_{system} = c_1 + c_3 \dot{V}^2$ where c_1 = 100 and c_3 is given by $c_3 = fL'/(2gDA^2)$.
However, $L' = L + L_e$. From Table III.6.3 (b), $L_e = 4 \times 30 + 50 + 8 + 340 = 518$ and from Table III.3.2, $f = 0.013$. Flow area becomes $A = \pi(14/12)^2/4 = 1.069$ ft^2. Finally, $c_3 = 0.013 \times (2000 + 518)/[2 \times 32.2 \times (14/12) \times 1.069^2] = 0.38$. Therefore, $H_{system} = 100 + 0.38\ \dot{V}^2$, where flow rate is in ft^3/s.

Approximating the pump head versus flow as a parabola ($H_{Pump} = a + b\ \dot{V}^2$), we find coefficients a and b by using two points. The first point is at $\dot{V} = 0$, H_{Pump} = 322 ft. Picking the second point at the best efficiency gives $\dot{V}$ = 22000 GPM/(7.481 × 60) = 49 ft^3/s and H_{Pump} = 270 ft. This results in, a = 322 and b = –0.0216 or $H_{Pump} = 322 - 0.0216\,\dot{V}_o^2$. From Equation VIc.4.1:

$\dot{V} = \sqrt{(c_1 - a)/(b - c_3)} = \sqrt{(100 - 322)/(-0.0216 - 0.38)} = 23.51$ ft^3/s = 10552 GPM.
This corresponds to a head of 310 ft and an efficiency of about 73%, far from the peak efficiency of 88%.

b) To increase the pump efficiency we may change the pump speed. To find the new pump speed, we use homologous relations to get $\dot{V}' = (N/710)\dot{V}_o$ and H' = $(N/710)^2 H_o$. We now substitute the new head and flow rate into the system curve to get: $(N/710)^2 \times 270 = 100 + 0.38\ \{(N/710)\ [22000/(7.481 \times 60)]\}^2$. Thus, -1.275E-3 $N^2 = 100$. It is clear we cannot reach peak efficiency for the operational condition using this pump.

4.1. Compound Pumping System

Pumps may be used in serial or parallel arrangements depending on the flow or head requirement. Pumps combined in series, as shown in Figure VIc.4.2(a) provide a higher head for the same flow rate and pumps combined in parallel, provide the same head at higher flow rate. For optimum performance, not only the head and flow rate of the compound pumping system must meet the demand but they must also correspond to the point of best efficiency of each participating pump. Compound pumping systems are not always used to meet the head and flow rate demand. In many cases pumps are arranged in parallel to increase system availability.

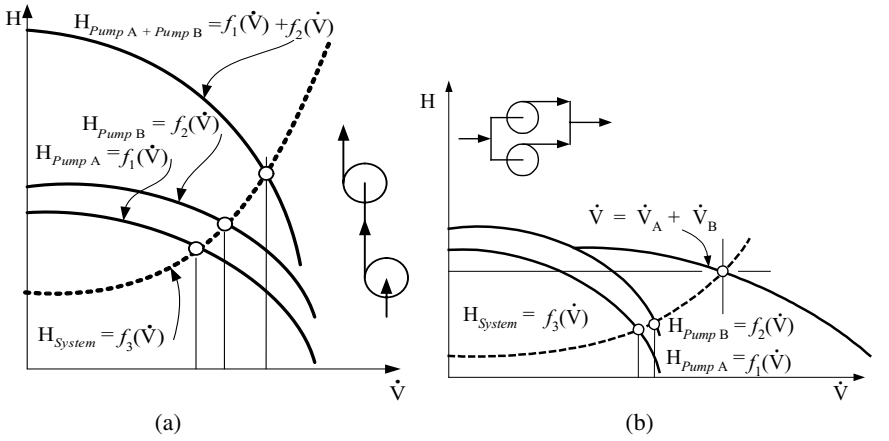

Figure VIc.4.2. Compound pumping system in (a) serial and (b) parallel arrangements

4.2. Extension of Pump Characteristic Curves

Earlier we discussed pump characteristic curves and the representation of the family of such curves with the pump homologous curves. While it is desired that pumps operate steadily at their rated condition, there are cases where pumps must be analyzed for such off normal conditions as flow reversal in the pump and reverse rotation of the impeller. Such off normal operations require the extension of the first-quadrant pump characteristic curves (positive flow rate and positive speed) to all four quadrants where any combination of positive and negative flow rate and speed exists. Unlike Figure VIc.3.1, where head and volumetric flow rate are chosen as coordinates, as shown in Figure VIc.4.3(a), the coordinates are chosen to be volumetric flow rate and the impeller speed. The resulting plots, as empirically produced by the pump manufacturer, are known as the *synoptic curves*, which constitute the *Karman-Knapp circle diagram*. In this figure, the solid lines represent constant head and the dotted lines show the constant pump hydraulic torque. Figure VIc.4.3(b) shows possible modes of operation of a pump during a transient. The first quadrant is normal pump (N). The solid lines between H = 0 and the speed coordinate are the familiar head versus flow rate curves. Expectedly, for a constant flow rate, head increases with increasing impeller speed. There are also lines representing negative pump head in this quadrant for positive flow and positive impeller speed.

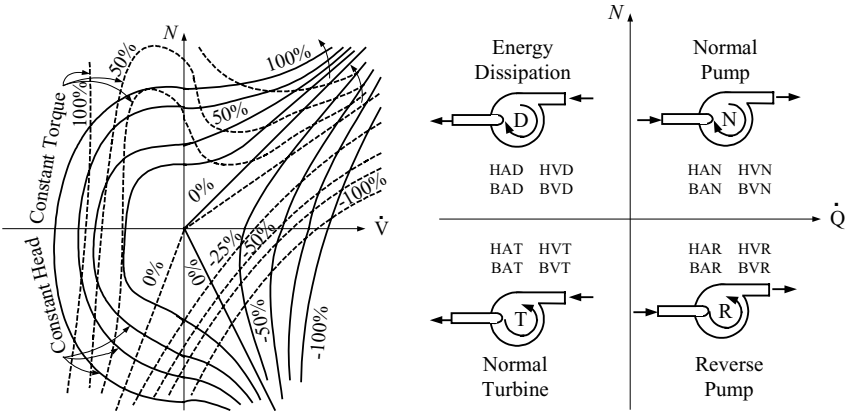

Figure VIc.4.3. (a) Pump characteristic curves in four quadrants and (b) Possible modes of operation

In the second quadrant (D), we find only positive pump head for positive impeller speed but negative flow rate. The third quadrant (T) is referred to as normal turbine where, for positive pump head, flow direction is into the pump with the impeller rotating in the reverse direction. Finally, in the forth quadrant (R) there are both positive and negative pump heads for positive flow and reverse impeller rotation. It is obvious that representation of such massive pump characteristic data

in computer analysis is impractical. Therefore, we resort to the non-dimensional homologous curves to represent the pump characteristic curves. This, in turn, requires the definition of some additional non-dimensional groups.

For a given pump, we use the rated data, which correspond to the point of best efficiency, to normalize variables. Hence, we obtain *speed ratio* ($a = \omega/\omega_o = N/N_o$), *flow ratio* ($v = \dot{V}/\dot{V}_o$), *head ratio* ($h = H/H_o$) and *torque ratio* ($b = T/T_o$). The flow, head, and torque coefficients now take the form of $C_{\dot{V}} = b/v$, $C_H = h/a^2$, and $C_T = b/a^2$, respectively. We then can find C_H and C_T as functions of $C_{\dot{V}}$. During analysis of pump response to a transient flow rate and impeller speed traverse positive and negative values. As such, both variables may encounter zero. In the case of the impeller speed, the values of the above coefficients would be undetermined. To avoid such conditions, we update our definition of the above coefficients and produce $C'_H = h/b^2$ and $C'_T = b/v^2$.

Generally, the head or torque coefficients (C_H and C_T or C'_H and C'_T) as independent variables are expressed in terms of flow and speed ratios (a and v). Since there are also four quadrants where these independent variables should be determined, it has become customary to use shorthand (a three-letter notation) to identify various variables in various quadrants. The first letter identifies the dependent variables (i.e., whether we are dealing with head or torque (h or b)). Hence, H designates head and T designates torque ratios. The second letter, as a representative of the independent variable, is such that A designates division by a for the independent variable, and division by a^2 for the dependent variable. Similarly, V designates division by v for the independent variable and division by v^2 for the dependent variable. Finally, the third letter indicates the mode in which the pump is operating, as shown in Figure VIc.4.3(b). These modes are N, R, T, and *D* for Normal pump, Reverse pump, normal Turbine, and energy Dissipation, respectively. These conventions are summarized in Table VIc.4.1, which defines 16 curves: 8 for head and 8 for torque. We now group similar curves of Table VIc.4.1 to obtain only four curves as summarized in Table VIc.4.2. These four homologous curves are shown for a typical centrifugal pump in Figure VIc.4.4(a) for homologous head and in Figure VIc.4.4(b) for homologous torque.

Table VIc.4.1. Summary of homologous curve notations

No.	a	v	v/a	Independent Variable	Dependent Variable		Dependent Variable	
					Type	Head	Type	Torque
1	>0	≥ 0	≤ 1	v/a	HAN	h/a^2	BAN	b/a^2
2	>0	>0	>1	a/v	HVN	h/v^2	BVN	b/v^2
3	>0	<0	≥ -1	v/a	HAD	h/a^2	BAD	b/a^2
4	>0	<0	<-1	a/v	HVD	h/v^2	BVD	b/v^2
5	<0	≤ 0	≤ 1	v/a	HAT	h/a^2	BAT	b/a^2
6	≤ 0	<0	>1	a/v	HVT	h/v^2	BVT	b/v^2
7	<0	>0	≥ -1	v/a	HAR	h/a^2	BAR	b/a^2
8	≤ 0	>0	<-1	a/v	HVR	h/v^2	BVR	b/v^2

Table VIc.4.2. Determination of pump homologous curves from pump characteristic curves

No.	Curves Paired		Independent Variable	v or a		Homologous Curve
	No.	No.				
I	3	1	$\lvert v/a \rvert \le 1$	$v < 0$	$v \ge 0$	$h/a^2 = f(v/a)$
			$a > 0$	HAD/BAD	HAN/BAN	$b/a^2 = f(v/a)$
II	7	5	$\lvert v/a \rvert \le 1$	$v > 0$	$v \le 0$	$h/a^2 = f(v/a)$
			$a < 0$	HAR/BAR	HAT/BAT	$b/a^2 = f(v/a)$
III	8	2	$\lvert a/v \rvert < 1$	$a < 0$	$a \ge 0$	$h/v^2 = f(a/v)$
			$v > 0$	HVR/BVR	HVN/BVN	$b/v^2 = f(a/v)$
IV	4	6	$\lvert a/v \rvert < 1$	$a > 0$	$a \le 0$	$h/v^2 = f(a/v)$
			$v < 0$	HVD/BVD	HVT/BVT	$b/v^2 = f(a/v)$

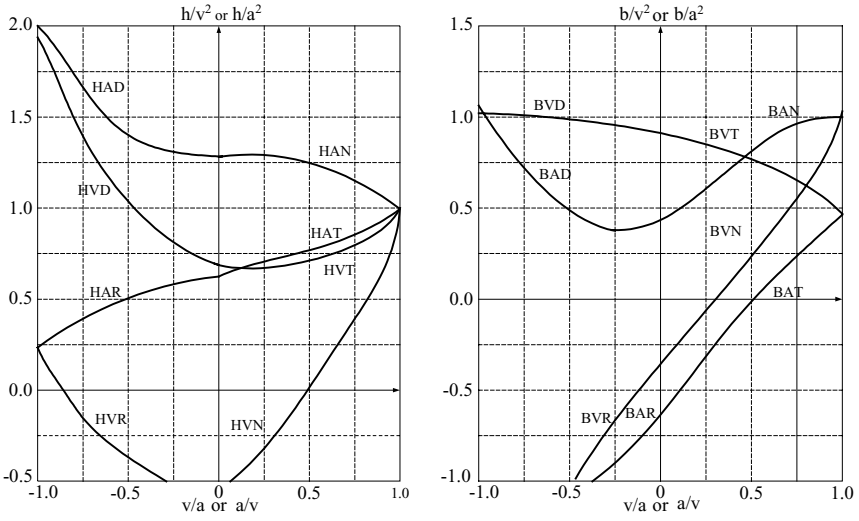

(a) (b)

Figure VIc.4.4. Dimensionless homologous (a) pump head and (b) hydraulic torque

Example VIc.4.2. In a transient, the speed and flow rate of a centrifugal pump are given as $N = -600$ rpm and $\dot{V} = -200{,}000$ GPM. Find a) pump head and torque, b) pump efficiency, and c) the temperature rise of the liquid across the pump for rated conditions. The rated values of the pump are:
$N_o = 900$ rpm, $\dot{V}_o = 370{,}000$ GPM, $H_o = 270$ ft, $T_o = 136{,}000$ ft·lbf, and
$\rho = 50$ lbm/ft^3.

Solution: a) Having $\dot{V}$ and N, we obtain $v = \dot{V} / \dot{V}_o = -200{,}000/370{,}000 = -0.54$ and $a = N/N_o = -600/900 = -0.67$. Hence, $a/v = -0.54/-0.67 = 0.81$.

From Figure VIc.4.4(a), using the HVT curve we find for a/v = 0.81, $h/v^2 = c_1 \cong 0.8$
From Figure VIc.4.4(b), using the BVT curve we find for a/v = 0.81, $b/v^2 = c_2 \cong 0.6$. Therefore,
$H = hH_o = 0.8 \times (0.54)^2 \times 270 = 63$ ft and $T = bT_o = 0.6 \times (0.54)^2 \times 136{,}000 = 24{,}588$ ft·lbf.

b) It can be easily shown that pump efficiency is related to the rated efficiency as $\eta/\eta_o = (c_1/c_2)(v/a)$
Having c_1 and c_2 from (a), and η_o, we can find η. However, pump efficiency is defined for the first quadrant. In the third quadrant for example, where the pump is in the turbine mode, efficiency should be redefined to fit the mode of operation.

c) Total power delivered to the liquid is $\dot{W}_{BHP} = \rho_o g \dot{V}_o H_o$. This is equal to the energy gained by the water as given by $\rho_o \dot{V}_o c_p \Delta T$. Hence, $\Delta T = H_o g/c_p$. If the liquid is water, c_p = 1 Btu/lbm F = 778 ft·lbf/lbm F. Hence, ΔT = 270/778 = 0.35 F.

Since production of the pump homologous curves is tedious, there are several attempts to represent these by polynomial curve fits. For example, Streeter recommends parabolic functions for the representation of these curves in various quadrants. The dimensionless head becomes:

$$h = c_{11} + c_{12}(v/a) + c_{13}(v/a)^2 \qquad 0 \le |v/a| \le 1 \qquad \text{VIc.4.1-1}$$

$$h = c_{13} + c_{12}(a/v) + c_{11}(a/v)^2 \qquad |v/a| > 1 \qquad \text{VIc.4.1-2}$$

and the dimensionless hydraulic torque:

$$b = c_{21} + c_{22}(a/v) + c_{23}(a/v)^2 \qquad 0 \le |v/a| \le 1 \qquad \text{VIc.4.2-1}$$

$$b = c_{21} + c_{22}(a/v) + c_{23}(a/v)^2 \qquad |v/a| > 1 \qquad \text{VIc.4.2-2}$$

using the coefficients c_{ij} given in Table VIc.4.3.

Table VIc.4.3. Coefficient for parabolic fit to pump homologous curves

Quadrant	Curve	c_{11}	c_{12}	c_{13}	Sign	Curve	c_{21}	c_{22}	c_{23}
Normal	HAN	1.30	–0.02	–0.28	–	BAN	–0.45	–0.85	–0.30
Pump	HVN	0.70	0.85	–0.55	–	BVN	0.480	0.880	–0.36
Energy	HAD	1.30	0.30	1.000	+	BAD	0.450	0.670	1.22
Dissipation	HVD	1.20	–0.10	0.700	–	BVD	–0.20	0.340	0.86
Normal	HAT	0.65	0.25	0.100	+	BAT	–0.65	1.420	–0.32
Turbine	HVT	0.50	–0.15	0.650	+	BVT	–0.18	–0.23	0.86
Reverse	HAR	0.65	0.15	–0.300	+	BAR	–0.65	1.250	0.28
Pump	HVR	0.90	0.15	–0.550	+	BVR	–1.44	0.700	–0.36

Having the curve fit coefficients and the rated values, flow rate and hydraulic torque are found from:

$$\dot{V} = (\dot{V}_o / 2c_{13})\left\{-c_{12}a + \text{sign}\left[\left(c_{12}^2 - 4c_{11}c_{13}\right)a + 4c_{13}h\right]^{1/2}\right\}$$

$$T_H = T_o\left(c_{21}a^2 + c_{22}av + c_{23}v^2\right)$$

Another example for curve fitting to the pump homologous curve is given by Kao as polynomials:

$$h/a^2 = \sum_{i=1}^{4} c_{3i}(v/a)^{i-1} \text{ and } b/a^2 = \sum_{i=1}^{4} c_{4i}(v/a)^{i-1}$$

where coefficients c_{31} through c_{34} for positive impeller speed are 1.80, –0.30, 0.35 and –0.85 and for negative impeller speed are 0.50, 0.51, –0.26, 0.25. For dimensionless torque, coefficients c_{41} through c_{44} for positive impeller speed are 1.37, –1.28, 1.61, and –0.70 and for negative impeller speed are –0.65, 1.9, –1.28, and 0.54. In a transient, if the impeller speed goes to zero when changing direction from positive to negative speed, the pump head versus flow for these sets of polynomial curves may be found from:

$$h = (-4.181E - 3)|v|v$$

While theoretically a centrifugal pump may operate in all four quadrants, in practice, pump operation in the first quadrant can be ensured by pump and system modification. For example, installing a non-reversing ratchet prevents the impeller from rotating in the reverse direction and a check valve on the discharge line prevents reverse flow into the pump.

5. Analysis of Hydraulic Turbines

Turbines are mechanical devices to convert the energy of a fluid to mechanical energy. Turbines can be classified in various ways based on process, head conversion, or rotor type. Regarding the process, energy transfer in turbines may take place in either an adiabatic or in an isothermal process. Regarding head conversion, turbines may be divided into the reaction and the impulse type for momentum exchange between fluid and the turbine rotor. Finally, turbines may be classified depending on the velocity vector resulting in an axial, radial, or mixed-flow rotor.

5.1. Definition of Terms for Turbines

Adiabatic process turbines, as were studied in Chapter IIb, include gas and steam turbines where the means of energy transfer from fluid to the turbine rotor is primarily through the change in the fluid enthalpy. In this type of turbine, changes

in the fluid potential and kinetic energy are generally negligible, compared with the change in fluid enthalpy.

Isothermal process turbines include turbines used in greenpower production such as hydropower and wind turbines. In this type of turbine, the transfer of mechanical energy to the turbine rotor is due to the fluid kinetic energy, while changes in enthalpy are generally negligible compared with the change in the fluid kinetic energy.

Reaction type turbines or simply reaction turbines, have rotors equipped with blades. In the reaction type turbines, fluid fills the blade passages of the rotor to deliver momentum. Thus, the head conversion in the reaction type turbines occurs within the turbine rotor where fluid pressure changes from inlet to outlet. Examples of the reaction type turbines include adiabatic, wind, and most hydropower turbines.

Impulse type turbines convert the head in an injector. Thus, in an impulse turbine, the head conversion takes place outside the turbine rotor. The high velocity jet then strikes individual buckets attached to the Pelton wheel at a constant pressure. Imparting the momentum of the jet to a bucket produces a force, which results in a torque to turn the wheel and brings the adjacent bucket to face the jet.

5.2. Specific Speed for Turbines

The same dimensionless groups defined in Section 3 for pumps are also applicable to turbines. Recall that for pumps we expressed the head and the power coefficient in terms of the capacity coefficient. However, for turbines, we express the capacity and the head coefficient in terms of the power coefficient. In the U.S., it is customary to find specific speed for turbines from:

$$N_s = \frac{(N, \text{rpm})(\text{bhp})^{1/2}}{(\text{H}, \text{ft})^{5/4}} \qquad \text{VIc.5.1}$$

5.3. Adiabatic Turbines, Steam Turbine

The adiabatic turbines, regardless of the type of working fluid, are generally of axial flow type. However, turbines used for turbo-charging are generally of radial flow type.

5.4. Isothermal Turbines, Pelton Turbine

As discussed in Chapter I, Pelton wheels are impulse turbines in which high head and low flow rate of water strikes the buckets attached to the wheel, as shown in Figure VIc.5.1. Our goal is to determine the Pelton wheel in terms of the jet velocity (V_j), the bucket velocity (V_t), and the bucket angle (β). This is shown in the example that follows.

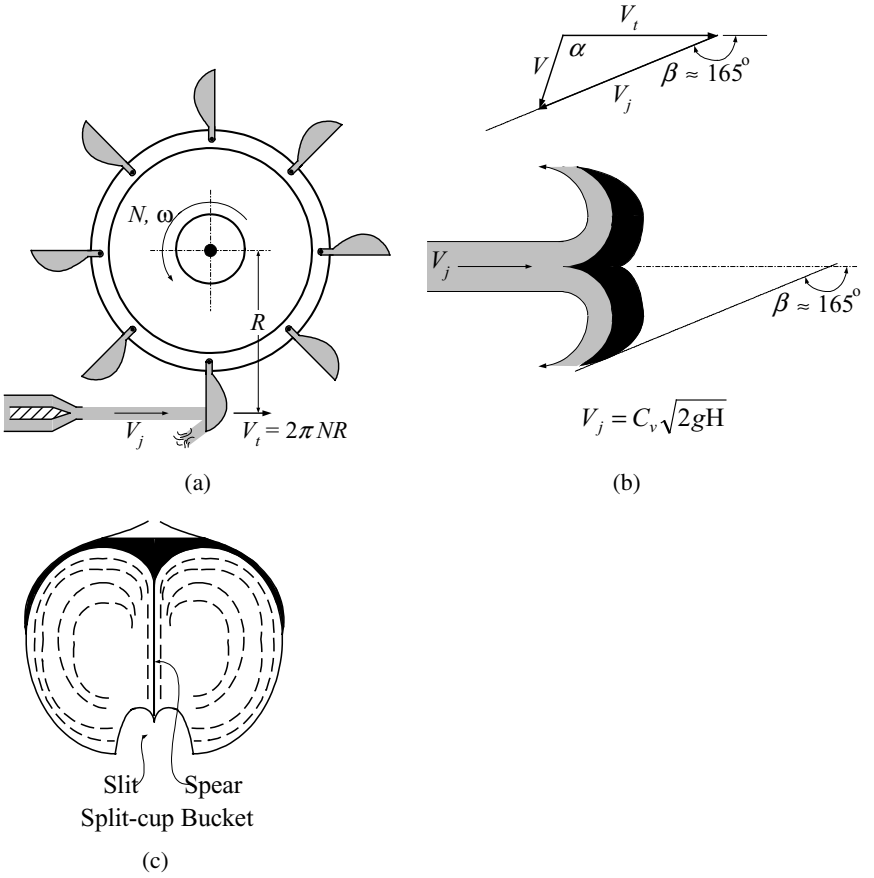

Figure VIc.5.1. Pelton wheel. (a) Side view of the wheel, (b) & (c) top and frontal views of the bucket.

Example VIc.5.1. Derive the efficiency of the Pelton wheel in terms of the constant velocities V_j, V_t, and the jet reflection angle of β.

Solution: Efficiency of the wheel is defined as the ratio of the power obtained from the wheel to the power delivered to the wheel $\eta = \dot{W}_{out} / \dot{W}_{in}$ (i.e., the break horsepower to the hydraulic horsepower).

$\dot{W}_{in} = dE_j / dt = d\left(mV_j^2 / 2\right)/ dt = (1/2)\left[(dm/dt)V_j^2 + m\left(dV_j^2 / dt\right)\right] = \rho\dot{\forall}V_j^2 / 2$

We find $\dot{W}_{out}$ from the rate of change of momentum for which we must consider the relative velocities.

$F = d(mV)/dt = (dm/dt)V + (dV/dt)m = \rho V\dot{\forall}$. Note that $V = V_j - V_t$. The net force applied on the wheel is

$$\Delta F = F_j - F_t = \rho\dot{\mathrm{V}}\left(V_j - V_t\right) - (\rho / g_c)\dot{\mathrm{V}}\left(V_j - V_t\right)\cos\beta =$$
$$\rho\dot{\mathrm{V}}\left(V_j - V_t\right)(1 - \cos\beta)$$
$$\dot{W}_{out} = \Delta F V = \left[\rho\dot{\mathrm{V}}\left(V_j - V_t\right)(1 - \cos\beta)\right]V_t$$
$$\eta_{theoretical} = \dot{W}_{out} / \dot{W}_{in} = \left[\rho\dot{\mathrm{V}}\left(V_j - V_t\right)(1 - \cos\beta)\right]V_t / \left(\rho\dot{\mathrm{V}} V_j^2 / 2\right) =$$
$$2(1 - \cos\beta)(V_j - V_t)V_t / V_j^2 .$$

To find $(\eta_{theoretical})_{\max}$ we set $d\eta_{theoretical}/dV_t = 0$ resulting in $V_t = V_j/2$. Hence, $(\eta_{theoretical})_{\max} = (1 - \cos\beta)/2$.

In the above example, we assumed an injector with maximum efficiency. In practice however, the bucket angle is about 165° and a velocity coefficient ($C_v \cong 0.94$) should also be considered for the nozzle. Hence, the efficiency becomes:

$$\eta = 2(1 - \cos\beta)(C_v - \phi)\phi \qquad \text{VIc.5.2}$$

where $\phi = V_t / \sqrt{2g\mathrm{H}}$. Maximum efficiency, considering the velocity coefficient, occurs when $\phi = C_v/2$. In practice, the Pelton wheel efficiency is even less than that given by Equation VIc.5.2 due to such losses as windage and mechanical friction. Additionally, the Pelton wheels suffer from two more losses, which are peculiar only to this type of turbine. The first has to do with the nature of a jet striking a turning wheel. As the bucket facing the jet moving away and the neighboring bucket approaches the jet, the back of the approaching bucket would first touch the jet before the front of the bucket faces the jet. Although a recess or a slit has been made in each bucket to minimize *back-splashing*, there are still some losses associated with this feature of the Pelton wheel. The second loss is due to the frontal structure of each bucket. Each bucket is made of two split cups, the common edge of which constitutes a spear, as shown in Figure VIc.5.1. The jet, upon entering the bucket, is divided up by the spear into two equal parts to pass the curvilinear surface of each cup and exit the bucket. Machining and surface finish of each split cup is essential for having a uniform flow in each cup of the bucket.

The Pelton wheel efficiency should, therefore, be calculated from experimentally obtained data such as the data shown in Figure VIc.5.2, which gives efficiency in terms of the turbine power specific speed. Figure VIc.5.2 indeed indicates that hydraulic turbines using the Pelton wheel have lower efficiency at their BEP than the Francis and the Kaplan turbines. Given this fact, it then appears that a Francis turbine is a better choice. Indeed Francis turbines, with radial-axial rotors, are used to harness the power of water at a height of up to 700 m (2,300 ft). However, the Pelton wheels are used for heads as high as 1500 m. Using a Francise turbine for such high heads, results in the rotor having to run at very high speeds. Furthermore, a thick casing is required to contain water at pressures that may exceed 2000 psia.

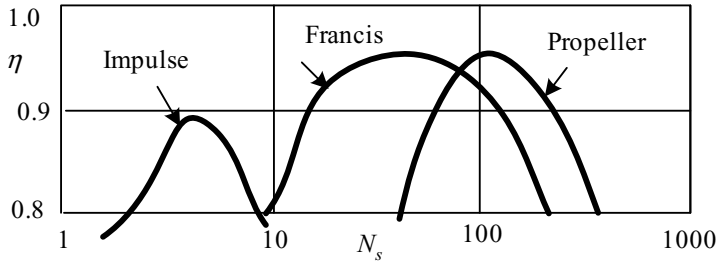

Figure VIc.5.2. Efficiency of hydraulic turbines as a function of specific speed (White)

Example VIc.5.2. The Pelton wheel of an impulse turbine has a wheel diameter of 4 m and an injector diameter of 10 cm. The turbine is operating at a net head of 600 m. Find the power output of this turbine for best efficiency.

Solution: We use a return angle of 165°, a velocity coefficient of 0.94, and perform the following steps:

$V_j = C_v\sqrt{2g\mathrm{H}}$ = 0.94(2 × 9.8 × 600) = 102 m/s and $(V_j)_{max}$ = 108.4 m/s.

Find flow rate from:

$\dot{\mathrm{V}} = \left(\pi d_j^2/4\right)V_j = \pi(10/100)^2 \times 102/4 = 0.8$ m^3/s = 12700 GPM.

Find η from Figure VIc.5.2.

To use Figure VIc.5.2, we need N_s. Recall that at best efficiency, $\phi = C_v/2$, where $C_v \cong 0.94$, therefore

$\phi = 0.94/2 \equiv 2\pi RN/(V_j)_{\max} = \pi \times 4 \times N/108.4$.

Solving for N, we obtain N = 4 RPS = 240 RPM.

We need to calculate the bhp:

bhp = $\left[(\rho/g_c)\dot{\mathrm{V}}\left(V_j - V_t\right)\left(1-\cos\beta\right)\right]V_t$ = 999 × 0.8 [102 – (102/2)](1 – cos165) × (102/2) = 5480 hp

$N_s = N(\mathrm{bhp})^{0.5}/\mathrm{H}^{5/4} = 240 \times (5480)^{0.5}/(600 \times 3.2808)^{5/4} = 1.355$.

From Figure VIc.5.2, $\eta \approx 0.73\%$

$\dot{W}_{out}$ = 5480 × 0.73 = 3993 hp.

5.5. Classification of Hydraulic Turbines

Classification of the hydraulic turbines in terms of specific speed and head is shown in Figure VIc.5.3. As shown in this figure, axial flow turbines are suitable for low head and high flow. As the available head of water increases, the runner is shaped so that the flow of water becomes mixed with respect to the axis of the turbine runner. Still at higher heads, the Francis wheel is used. At low flow rates and very high head, the Pelton wheel is the obvious choice.

As seen from Figure VIc.5.3, for reaction turbines, low specific speeds are associated with radial turbines and high specific speed with axial turbines. Similar association applies to pumps as shown in Figure VIc.3.2 for specific speed ranging from 500 –15,000. Mott indicates that axial flow pumps may be used for pump specific speed in the range of 7,000 – 60,000.

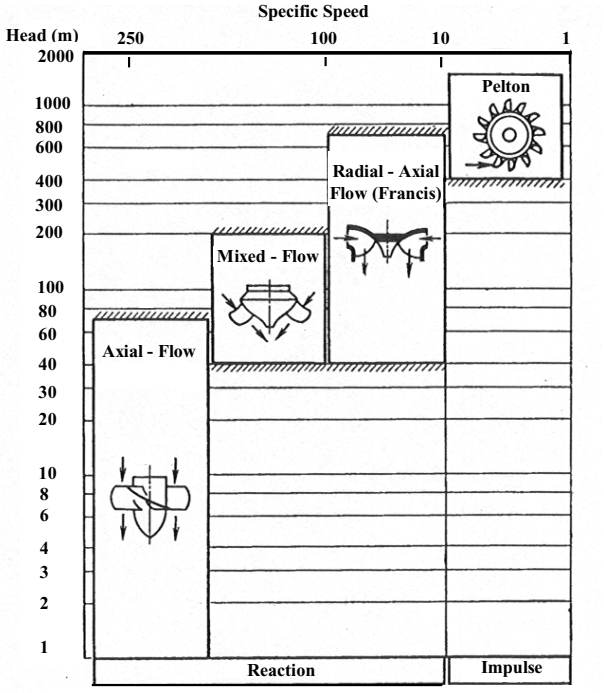

Figure VIc.5.3. Classification of hydraulic turbines (Krivchenko)

5.6. Isothermal Turbines, Wind Turbine

As was discussed in Chapter I, there are a variety of wind turbines in operation today. The most widely used is the wind turbine type of horizontal axis design equipped with propellers, as shown in Figure I.4.21. To derive the efficiency for the wind turbine, we use the method applied by White. For this purpose, we use the mass, momentum, and energy equations for the control volume consisting of a stream tube and a propeller, as shown in Figure VIc.5.4. We note that location 1 is the upstream of the propeller at velocity V_1 and pressure $P_1 = P_{atm}$. Locations 2 and 3 are right before and right after of the propeller. Air velocity and pressure at these locations are V_2, P_2, V_3, and P_3, respectively. Finally, location 4 is downstream of the propeller at which air velocity is V_4 and air pressure reaches the atmospheric pressure, $P_4 = P_{atm}$. In the following derivation we assume uniform

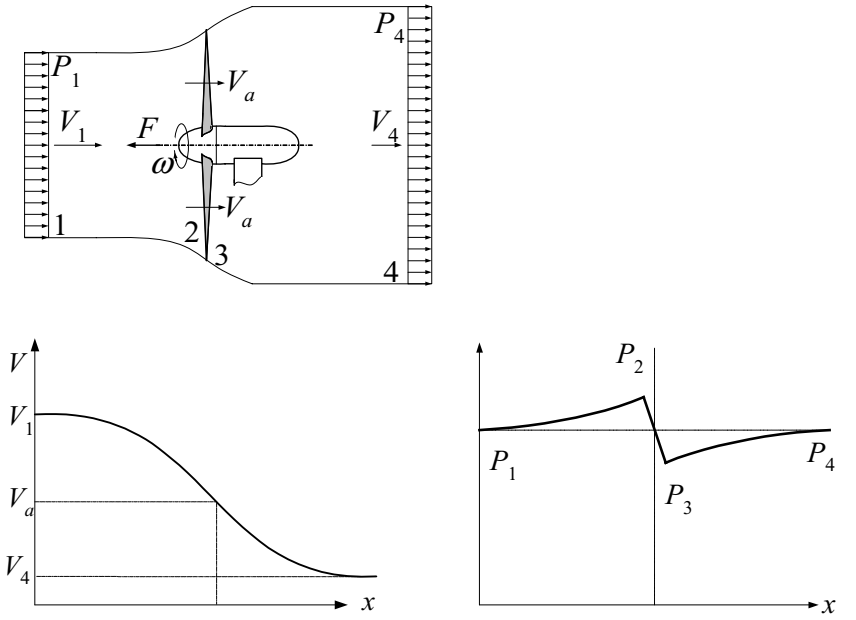

Figure VIc.5.4. The stream-tube for the flow of air through a wind turbine (White)

wake and ideal flow. There are reasonable assumptions for V_1 < 20 mph (32 km/h).

The continuity and the momentum equations. Regarding the continuity equation, we note that the mass flow rate of air through the propeller is found as $\dot{m} = \rho V_a A$ where A is the area swept by the propeller and V_a is the air velocity at the blade. As for the momentum equation, we apply the Bernoulli equation between locations 1 and 2 and between locations 3 and 4. Adding these equations and noting that $P_1 = P_4 = P_{atm}$ and $V_2 = V_3 = V_a$ we conclude:

$$P_2 - P_3 = \Delta P = \rho\left(V_1^2 - V_4^2\right)/2 \qquad \text{VIc.5.3}$$

We now use the momentum equation over the turbine (i.e. between locations 2 and 3). A free-body diagram for the turbine shows that the net force applied in the wind direction to the turbine is equal to the rate of the change of air momentum passing through the propeller:

$$F = \left(P_2 - P_3\right)A = \rho V_a A\left(V_1 - V_4\right) \qquad \text{VIc.5.4}$$

where we assume an ideal wind turbine for which no frictional losses exist. In reality, however, we must also include the friction force.

From Equation VIc.5.4, we find ΔP in terms of the turbine upstream and downstream velocities $\Delta P = \rho V_a(V_1 - V_4)$. Substituting ΔP in Equations VIc.5.3, we find:

$$V_a = (V_1 + V_4)/2 \qquad \text{VIc.5.5}$$

If we define parameter $\alpha = V_a/V_1$, we note that for wind turbines, $0.5 < \alpha < 1$. For $\alpha < 1$, the wake flows towards the turbine. In an airplane equipped with a propeller, $\alpha > 1$.

The energy equation. To obtain the maximum power delivered to the wind turbine, we treat the incoming wind toward the blades as a jet having a flow area equal to the swept area of the propeller. Hence, the maximum power delivered to the impeller is:

$$\dot{W}_{available} = \frac{dE_{wind}}{dt} = \frac{d}{dt}\left(\frac{mV_1^2}{2}\right) = \left(\frac{1}{2}\right)\left[\frac{dm}{dt}V_1^2 + \cancel{m\frac{dV_1^2}{dt}}\right] = \frac{\dot{m}V_1^2}{2} \qquad \text{VIc.5.6}$$

where the derivative of the wind velocity, for constant flow of wind, is zero. If we substitute for the wind mass flow rate, we find the wind power delivered to the propeller as:

$$\dot{W}_{available} = \frac{\rho A V_1^3}{2} \qquad \text{VIc.5.7}$$

Having the rate of energy delivered to the propeller, we need to find the rate of energy extracted by the propeller to find the turbine efficiency. To find the latter, we use Equation VIc.5.4 in conjunction with the definition of power:

$$\dot{W}_{extracted} = FV = \left[\rho V_a A\left(V_1 - V_4\right)\right]V_a \qquad \text{VIc.5.8}$$

where F is substituted from Equation VIc.5.4.

Turbine efficiency. We may find efficiency by dividing Equation VIc.5.8 by Equation VIc.5.7. However, we are more interested in finding the maximum efficiency, which requires the calculation of the maximum extracted work. The latter is found by taking the derivative of Equation VIc.5.8 and setting it equal to zero. To take the derivative of Equation VIc.5.8, we first substitute for V_a from Equation VIc.5.5:

$$\dot{W}_{extracted} = \left[\rho A\left(V_1 - V_4\right)\right]\left(V_1 + V_4\right)^2/4 \qquad \text{VIc.5.9}$$

By taking the derivative of Equation VIc.5.9 with respect to V_4 and setting it equal to zero, we find that the maximum power is extracted if $V_4 = V_1/3$. The maximum extracted power is then obtained by substituting this result into Equation VIc.5.9:

$$\left(\dot{W}_{extracted}\right)_{\max} = \frac{8}{27}\rho A V_1^3 \qquad \text{VIc.5.10}$$

Having the maximum extracted power, we can now find the maximum efficiency from Equations VIc.5.7 and VIc.5.10:

$$\left(\eta_{\max}\right)_{windmill} = \left(\frac{8}{27}\rho A V_1^3\right) / \left(\frac{1}{2}\rho A V_1^3\right) = \frac{16}{27} = 59.3\%$$

The result indicates that even at the ideal conditions (i.e., with no friction) this wind turbine can only extract about 60% of the wind energy.

Example VIc.5.3. A wind turbine is exposed to 50 mile/h wind. Wind speed downstream of the propeller is 40 mile/h. The propeller, consisting of two blades, has a diameter of 40 ft. Assume ideal gas and standard condition for air to find a) the thrust on the wind turbine, b) the power delivered to the wind turbine, c) the maximum power extracted by the wind turbine, and d) the wind turbine maximum efficiency.

Solution: First find the air speed in ft/s; $V_1 = 50 \times 5280/3600 = 73.3$ ft/s and $V_2 = 58.7$ ft/s. Next we find:
$V_a = 0.5 \quad (73.3 + 58.7) = 66$ ft/s.
The swept area is $A = \pi D^2/4 = \pi \times 40^2/4 = 1256.6$ ft^2 and the air density is:
$\rho = P/RT = 14.7 \times 144/[(1535/28.97) \times (460 + 60)] = 0.077$ lbm/ft^3.

a) $F = \rho V_a A(V_1 - V_4) = 0.077 \times 66 \times 1256.6(73.3 - 58.7)/32.2 = 2896$ lbf

b) $\dot{W}_{available} = \rho A V_1^3 / 2 = 0.077 \times 1256.6 \times 73.3^3/64.4 = 0.592\text{E}6$ ft·lbf/s = 0.8 MW

c) $\dot{W}_{extracted} = \left[\rho V_a A\left(V_1 - V_4\right)\right] V_a =$ [0.077 × 66 × 1256.6(73.3 − 58.7)] × 66/32.2 = 0.26 MW

d) $\eta = 0.26/0.8 = 32\%$

6. Analysis of Turbojets for Propulsion

In Chapter I, various types of gas turbines for aircraft propulsion were described. In Chapter IIb, we discussed the air-standard cycle for reaction engines, and in Example IIb.1.7, we used the processes of an air-standard cycle to find the gas velocity at the exit of a turbojet for a specified sets of conditions. Our goal in this chapter is to find the thrust developed by various types of turbojets.

Derivation of Thrust for Aircraft Propulsion:
Shown in Figure VIc.6.1 are schematics of a turbojet, a turbofan, and a turboprop. The free stream properties are shown with subscript *i*. Let's first consider the control volume representing the turbojet. Air enters this control volume at velocity V_i,

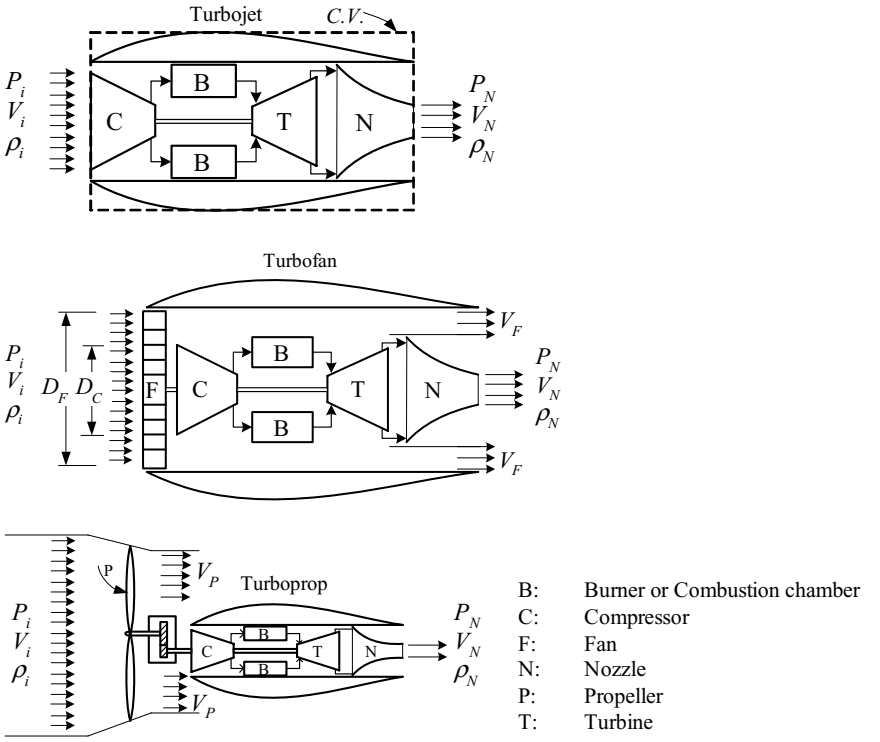

Figure VIc.6.1. Schematics of turbojet, turbofan, and turboprop

pressure P_i, and density ρ_i. These properties at the exit of the nozzle are V_N, P_N, and ρ_N, respectively. To obtain the thrust developed by this engine, we use the integral form of the conservation equations of mass (Equation IIa.5.1) and linear momentum (Equation IIIa.3.6). In this derivation, we are interested in calculating the engine thrust for steady state conditions. Therefore, the time dependent terms cancel out. Thus, the net forces acting on the control volume are balanced by the momentum flux. The net forces include such surface forces as the thrust on the engine and the pressure force at the inlet and exit of the control volume. We then write Equation IIIa.3.6 as:

$$F_x + (P_i - P_{atm})A_C - (P_N - P_{atm})A_N = \dot{m}_e V_e - \dot{m}_i V_i$$

Note that we assumed fuel enters the combustion chamber normal to the flow of air, hence it does not contribute to the momentum along the x-axis. The difference between the mass flow rates at the inlet and exit is due to the contribution of the fuel injected into the combustion chamber.

Example VIc.6.1. Air enters a turbojet at 500 km/h, 90 kPa, and a mass flow rate of 22 kg/s. Fuel enters the combustion chamber at a rate of 0.45 kg/s. The exhaust gases leave the nozzle at 2000 km/h and 130 kPa. Find the thrust on this engine. Other data: P_{atm} = 100 kPa, A_C = 0.16 m^2, A_N = 0.08 m^2. Ignore the momentum of the fuel entering the control volume.

Solution: For the control volume encompassing the engine:

$$F_{x,E} + (P_i - P_{atm})A_C - (P_N - P_{atm})A_N = (\dot{m}_i + \dot{m}_f)V_e - \dot{m}_i V_i$$

where subscripts E and f stand for engine and fuel, respectively. Substituting values, we find:

$$F_{x,E} = -(90-100)\times 0.16 + (130-100)\times 0.08 + (22+0.45)\times(2\text{E}6/3600) - 22\times(0.5\text{E}6/3600) = 9417 \text{ N}$$

In turbofans and turboprops, the thrust developed by the engine is primarily due to the action of the fan and the propeller, respectively. Thus, in the case of turbofans and turboprops, we use the conservations of energy in addition to the conservation equations of mass and momentum. We write the conservation equation of energy for a control volume encompassing the fan or the propeller. The flow velocity exiting the fan or the propeller is then calculated from the energy equation for the specified rate of shaft work based on the power delivered to the fan or the propeller.

QUESTIONS

- To pump highly viscous liquids, do you use rotodynamic pumps or positive displacement pumps?
- Is a centrifugal pump a radial-type or an axial-type pump?
- What is a driver or a prime mover? Give three examples of a prime mover.
- What does total dynamic head of a pump represent?
- When are two centrifugal pumps homologous?
- Why do we try to find non-dimensional groups and what are the applications of the similarity rules?
- What is the significance of specific speed? A centrifugal pump has a specific speed of 500. What is the relation of head and flow to a similar pump but with specific speed of 1000?
- Why are the reactor coolant pumps in PWRs located on the cold legs and not the hot legs?
- Is it fair to say that operating the centrifugal pumps at the best efficiency point reduces impeller erosion?
- What are the four quadrants for pump operation? In which quadrant does a pump act like a turbine?

- What is the difference in head and flow rate between the impulse and the reaction type turbines?
- What type of turbine is a Pelton wheel?
- A hydropower plant has 100 m of head available to be used for power production. Is a Pelton wheel suitable for this purpose? What type of hydraulic turbine do you recommend?
- Consider two turbines producing identical power. Once uses a Pelton wheel and the other a Kaplan type propeller. Which turbine has higher flow rate?
- What type of turbine do you use for a flow rate of 50 m^3/s at a head of 10 m?
- Can a wind turbine of horizontal axis design achieve an efficiency of 65%?
- How is the engine thrust calculated in turbofans?
- How is the engine thrust calculated in turboprops?

PROBLEMS

1. A charging pump in a PWR plant operates at a volumetric flow rate of $\dot{V} = 44$ GPM (166.5 lit/min) at a head of H = 7000 ft (2134 m). What is the type of this pump?

2. A pump delivers water from a reservoir, which is open to atmosphere. Water level in the reservoir and the pump centerline are at elevations of 40 ft and 35 ft, respectively. Find the static suction head of the pump. [Ans.: 39 ft].

3. A pump is delivering water at atmospheric pressure to an elevation of 400 m. Elevation of the pump centerline is –10 m. Find the static discharge head. [Ans.: 444 ft].

4. The main feedwater pump of a PWR delivers water to the steam generator at a rate of 15,000 GPM (946.3 lit/s). The steam generator pressure is 900 psia (6.2 MPa). The difference between the discharge and the pump centerline elevation is 100 ft (30.48 m). Find the pump static discharge head. Water temperature is 450 F (232.2 C). [Ans.: 2600 ft (792.5 m)].

5. A pump delivering water at a temperature of 400 F (204.4 C) and a rate of 12,000 GPM (757 lit/s) to a pressurized vessel at 1000 psia. The discharge piping is 135 ft (41.15 m) long schedule 40 stainless steel, and nominal pipe size of 20 in (7.874 cm). Find the total dynamic discharge head.

6. A 3 horsepower compressor, circulating air at 20 C and a head of 20 m. Find the mass flow rate of the circulating air.

7. Use the data of Example VIc.3.1 and the definition of flow coefficient, head coefficient, and power coefficients to show that: $\eta_{pump} = C_{\dot{V}} C_H / C_{\dot{W}}$.

8. The rigorous way of calculating the pump specific speed is to use:

$$N_s' = C_{\dot{V}_o}^{1/2} / C_{H_o}^{3/4}$$

where $C_{\dot{V}_o}$ and C_{H_o} are the flow and head coefficients corresponding to the point of best efficiency. Use Equation VIc.3.2 to show that the specific speed, using the

customary definition (N_s) is related to N_s' as $N_s = 17182 N_s'$. Also show that N_s or N_s' represents an entire family of pumps regardless of size or speed.

9. Using the performance curve of pump A given in Example VIc.3.2 (41.5" and 710 rpm) and find:
a) total dynamic head of a similar pump (pump B), at peak efficiency, having a diameter of 35 inches. Assume that both pumps A and B are operating at the same speed.
b) pump head if pump B is now operating at 1170 rpm. [Ans.: a) H = 192 ft and b) H = 521.5 ft].

10. A pump delivers 500 GPM water with a suction line 6 in. diameter. The reservoir is pressurized with to 17 psia. The required $NPSH_R$ is 15 ft. Due to the use of a filter and several bends on the suction line, the total loss coefficient adds up to K = 35. a) Find the maximum distance between pump centerline and water surface in the tank. Water is at 80 F for which, ρ = 62.5 lbm/ft^3 and μ = 2.1 lbm/ft·h. b) Find the $NPSH_A$ if the pump is located 5 ft below the source reservoir water level. [Ans.: a) 5 ft and b) 25 ft].

11. The rated conditions (at the point of best efficiency) of a centrifugal pump, having an impeller diameter of 40 in, are $\dot{V}_1$ = 22000 GPM, N_1 = 700 rpm, N_s = 2000, and η_1 = 82%. To increase the flow rate, a 1000 rpm electric motor is suggested to replace the current prime mover. Find head brake horsepower and the size of the current and the replacement prime movers. ρ_{water} = 62.4 lbm/ft^3.
[Ans.: H_1 = 193.7 ft (59 m), $\dot{W}_{BHP-1}$ = 1077 hp, $\dot{W}_{PM-1}$ = 1313.4 hp, H_2 = 395.2 ft (120.5 m), $\dot{W}_{BHP-2}$ = 3139 hp, $\dot{W}_{PM-2}$ = 3832.6 hp. Note, the available electric motors may not necessarily match the horsepower calculated. In such cases, the next largest standard size motor should be selected.]

12. A centrifugal pump is used for water delivery through a pipe having a diameter of 15.25 cm and total length of 61 m. Water level elevations of the source and the receiving reservoirs, both measured from the sea level, are 100 m and 103 m, respectively. There are losses due to pipe entrance, pipe exit and an elbow fitting with related loss coefficients of 0.5, 1.0, and 1.5, respectively. For the pump characteristic data given below, find flow rate and if this is a reasonably appropriate pump for this application.

Flow Rate (lit/s):	0	25	38	50	76	88	114	140
Pump Head (m):	27	26	25.8	24.7	22.8	21.3	18.3	14.3
Efficiency (%):	0	30	42	53	73	80	84	80

[Ans. 101 lit/s at 24 m].

13. The pump in Example VIc.3.1 is used to deliver water to a height of 110 ft above the source reservoir. Total pipe length is 600 ft and the pipe diameter is 14 in. The pipe run includes a fully open gate valve and 2 threaded 90 elbows.

a) Find the flow rate, b) How do you maximize efficiency? [Ans. a) $\dot{\mathrm{V}}$ = 18,655, and b) N = 1432 rpm].

14. Solve problem 3 for ΔZ = 50 ft, D = 16 in, and L = 500 ft. All other data remain the same. [Ans. a) $\dot{\mathrm{V}}$ = 28,880, b) N = 392 rpm].

15. A pump delivering water at a rate of 100,000 GPM. The maximum available NPSH is 50 ft. Find the maximum speed to avoid cavitation.

16. In Example VIc.5.1, we derived the efficiency of a Pelton wheel in terms of V_w, V_t, and β. Use a deflection angle of 165°, $V_w = \sqrt{2g\mathrm{H}}$, and $V_t = \omega R$, as shown in Figure VIc.5.1 and show that the Pelton wheel works most effectively when running at half the speed of the jet of water. Find the maximum efficiency. Comment on the actual Pelton wheel efficiency.
[Ans.: $\eta_{\max} = 97\%$. $\eta_{\text{actual}} < \eta_{\max}$ due to the involved frictions].

17. Find the maximum power produced by a Pelton wheel. The jet diameter is 10.45 in and the available head is 2,200 ft. [Ans.: Maximum power is the power delivered to the jet at a C_v = 1. Hence, V_j = 376.4, A_j = 0.596 ft^2, $\dot{W}_{in}$ = 56,000 hp].

18. A screw-type reciprocating compressor having helically-grooved rotors is shown in the figure. Mention two advantages associated with this design. [Ans.: Pulse free and compact].

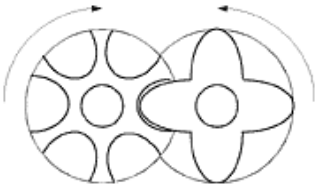

19. An impulse turbine is used to produce power from an available head of 500 m and flow rate of 100,000 GPM. Find the diameter of the jet and the maximum power that can conceivably be produced by the turbine.
[Ans.: $A_j = \dot{\mathrm{V}} / \sqrt{2g\mathrm{H}}$ and $\left(\dot{W}_j\right)_{\max} = \rho A_j V_j^3 / 2$].

20. An impulse turbine is operating at h = 700 m and $\dot{\mathrm{V}}$ = 150,000 gpm. The Pelton wheel has a diameter of 20 ft and rotating at 300 rpm. Find the power produced and the efficiency of the turbine. C_v = 0.94.
[Ans.: V_j = 385.6 ft/s, $V_t = V_j/2$.

21. An impulse turbine operating at a net head of 2000 ft uses a Pelton wheel of diameter 12 ft and a jet flow area of 5 in. Find the turbine power corresponding to the best efficiency. Use velocity coefficient of 0.94 and a bucket angle of 165°.
[Ans.: V_j = 337 ft/s, V_t = 169 ft/s, $\dot{\mathrm{V}}$ = 45.95 ft^3/s].

22. Use the Bernoulli equation and show that, for a wind turbine, the wind velocity is the arithmetic average of the velocity upstream and downstream of the propeller.

23. Wind is approaching a wind turbine at 27 mph, as shown in Figure VIc.5.3. The wake wind has a velocity of 15 mph. Find a) the wind velocity at the blade and b) the corresponding power extracted by the turbine.

24. A wind turbine has a diameter of 34 m and a power output of 350 kW at a wind velocity of 12.5 m/s. Find the efficiency of this turbine. Assume air at 27 C. [Ans. 33.6%].

25. A wind turbine having an efficiency of 35% and rotor diameter of 33 m is exposed to air flowing at a speed of 6 m/s. Find the power developed by the turbine. Assume $\rho = 1.2$ kg/m^3. [Ans.: 38.8 kW].

26. A two-blade wind turbine is exposed to 60 mile/h wind. Downstream of the propeller the wind speed is 45 mile/h. The propeller has a diameter of 45 ft. Assume ideal gas and standard condition for air to find a) the thrust on the wind turbine, b) the power delivered to the wind turbine, c) the maximum power extracted by the wind turbine, d) the maximum efficiency obtained from this wind turbine.

27. A two-blade wind turbine is installed on top of a hill experiencing winds of up to 80 mile/h. Downstream of the propeller the wind speed is 50 mile/h. Assume ideal gas and standard condition for air and find the tip to tip diameter of the propeller to obtain a theoretical efficiency of 50%.

VId. Simulation of Thermofluid Systems

In this chapter we study the response of such systems as reactor coolant pump (RCP), pressurizer, steam generator, containment, and the reactor coolant system (RCS) of a PWR to imposed transients. We begin by introducing some pertinent terms used in computer simulation and analysis of reactor thermal hydraulics.

1. Definition of Terms

Mathematical model refers to the application of the fundamental and constitutive equations to represent a physical phenomenon.

Computational cell is a control volume for which the physical phenomena are considered and mathematical models are developed. Since single-phase or two-phase fluid may flow through a computational cell, we need to identify the number of unknowns and set up a number of equations. For single-phase flow in a cell, there are five unknowns namely, P, T, V_x, V_y, and V_z. There are also five equations, conservation equation of mass, conservation equation of energy, and three conservation equations of momentum.

For two-phase flow through the cell, there are ten unknowns namely, P, T_l, T_v, $(V_x)_l$, $(V_y)_l$, $(V_z)_l$, $(V_x)_v$, $(V_y)_v$, $(V_z)_v$, and void fraction (α). Similarly, there are also ten equations consisting of two conservation equations of mass, two conservation equation of energy, and six conservation equations of momentum. Other unknowns are found from constitutive equations.

Node is the same as a computational cell. For the flow of water in a pipe, for example, we may divide the length L of the pipe into N sections. Therefore, the pipe now consists of N nodes, each having a length of $l = L/N$. For single-phase flow through the node, one pressure and one temperature would represent the entire node regardless of its size. Therefore, the higher the number of the nodes, the higher the amount of information obtained for the nodalized system. Pressure is generally calculated at the center of the node.

Node constituents in general may include several fluid fields such as continuous liquid, mixture of steam and gas, liquid droplets, and ice. The number of unknowns and equations increases with increasing number of the cell constituents. For example, if a cell contains liquid, steam, ice, drops, and 10 different noncondensable gases, there are as many as fourteen conservation equations of mass.

Nodalization. To determine the state parameters in a system, such as the primary side of a PWR, the system is broken down into several nodes. The process is generally referred to as nodalization. Figure VId.1.1 shows a section of a system, such as a hot leg, which is divided into N nodes with $1 \le k \le N$.

Control volume for mass and energy is shown in Figure VId.1.1(a). In this figure, nodes shown by $k-1$, k, and $k+1$ represent three sequential control volumes for calculation of mass and energy.

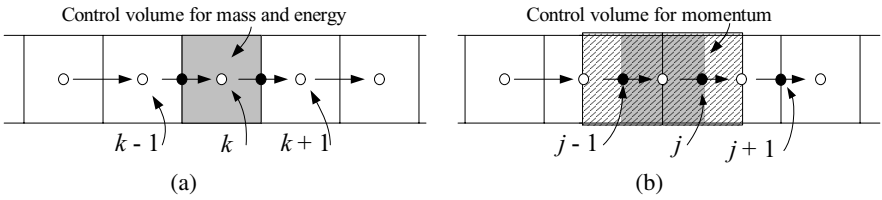

Figure VId.1.1. Nodalization of a horizontal pipe

Junctions or flow paths allow separate nodes to communicate. Hence, the mass and energy control volumes are connected together by junctions. Figure Id.1.1(b) shows junction j connecting the mass and energy control volume k to the mass and energy control volume $k + 1$.

Control volume for momentum. We may assign a control volume to node j extending from the center of node k to the center of node $k + 1$. This constitutes the control volume for the conservation of momentum for this one-dimensional flow. Momentum properties are calculated for this control volume. The most notable property calculated at node j is the flow velocity. Therefore, while pressure and temperature are calculated at the center of the mass and energy control volume, flow velocity is calculated at the junction.

Donor cell can be explained by considering two computational cells exchanging mass, momentum, and energy. The convective properties entering the receiving cell from the upstream cell are those of the upstream or so called donor cell. In Figure VId.1.1 for example, the enthalpy entering node k from node $k – 1$ is the enthalpy of node $k – 1$. Since there is no gradient inside a node, the enthalpy at the junction between nodes $k – 1$ and k is the same as enthalpy at the center of node $k – 1$.

Field, component, and phase. In Chapter IIIa and IIIb we dealt with homogenous fields (all water, all air, etc.) In general, fields may also be heterogeneous (Chapter IIIc). Consider for example, a vapor consisted of steam and several noncondensable gases. Each of the constituents is referred to as a component of the field. Phase, on the other hand, is the various forms of the same substance such as ice, water, steam, mist, and drop.

Two-flow field model (two-fluid model) refers to the treatment of the flow fields in a computational cell. Assuming only water and steam exist in the cell, ten conservation equations are used in the two-fluid model to describe the conditions in the cell. Thus, in this mathematical model, water and steam can be at different temperatures flowing at different velocities.

HEM or the homogenous equilibrium model, refers to the treatment of the fluid in a computational cell. Assuming only water and steam exist in the cell, the two phases are assumed to be at thermodynamic equilibrium. Thus, both phases flow at the same velocity in the same direction having the same temperature.

SEM or the separated equilibrium model refers to a deviation from the HEM, by the introduction of the slip ratio. This in turn requires the inclusion of the in-

ter-phase friction force in the momentum equation. In both HEM and SEM the mixture properties such as ρ and u are obtained through the use of void fraction.

2. Mathematical Model for a PWR Loop

Determination of such parameters as pressure, temperature, and velocity in systems involving fluid flow and heat transfer is generally an involved task. A nuclear reactor is an example of a thermofluid system for which it is important to determine such parameters by mathematical modeling. For this reason many computer codes are developed to study various operational aspects of a nuclear power plant. For example, several codes are devised to evaluate the thermal hydraulic characteristics of only the reactor core. Among the computer codes developed to analyze the reactor coolant system are RELAP, RETRAN, and TRAC. In this section, we study the mathematical model based on the HEM for analysis of the reactor coolant system. A nodalization example of a two-loop PWR is show in Figure VId.2.1.

Control volumes for mass and energy (shown with subscripts k and $k + 1$) and for momentum (shown with subscript j) are shown in Figure VId.2.2 for constant and variable area channels. The conservation equations of mass, momentum, and

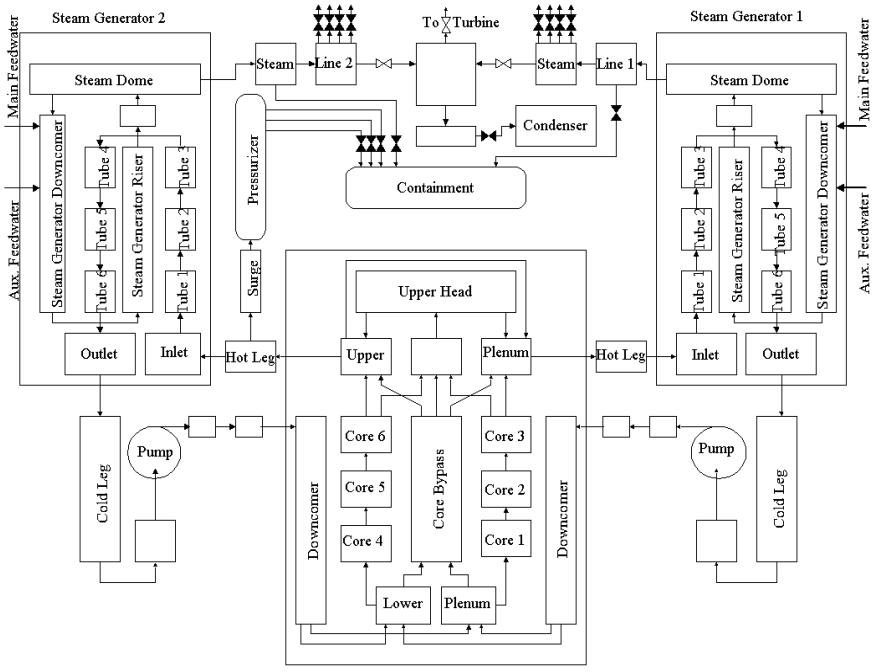

Figure VId.2.1. Nodal diagram of a two-loop PWR primary side

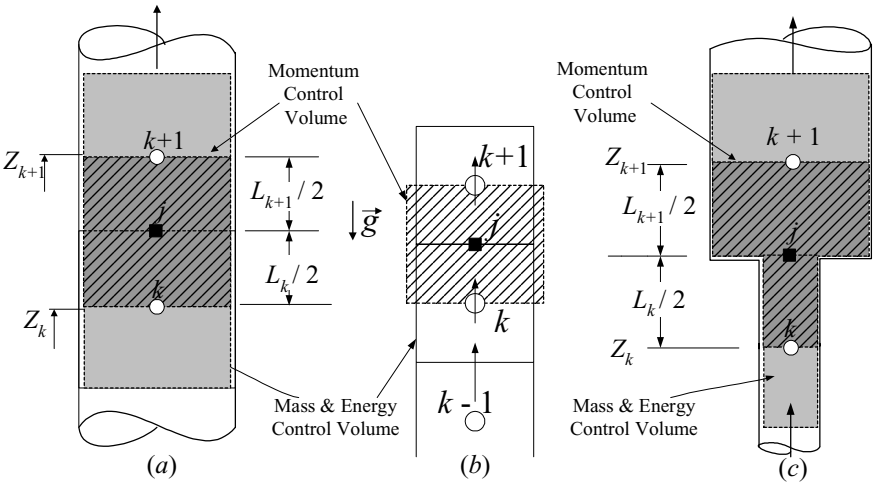

Figure VId.2.2. Mass, energy, and momentum control volume for channels with fixed or variable flow area

energy are described here. The area change plays no role for the conservation of mass and energy equations but the conservation equation of momentum, which is more involved, must consider the variable area channel. For node *k*, the conservation equation of mass, Equation IIa.5.1 can be written as:

$$\frac{d(\rho_m \mathrm{V})}{dt} = \sum_{inlet}(\rho VA) - \sum_{exit}(\rho VA) \qquad \text{VId.2.1}$$

where $\rho_m = (1 - \alpha)\rho_f + \alpha\rho_g$ and α is given by Equation Va.1.3. We may also write Equation VId.2.1 as:

$$\frac{dM_k}{dt} = \dot{m}_{j-1} - \dot{m}_j \qquad \text{VId.2.1-1}$$

The conservation equation of energy as given by Equation IIa.6.4 becomes:

$$\frac{dU_k}{dt} = \dot{m}_{j-1}\left[h_{j-1} + \frac{1}{2}\frac{\dot{m}_{j-1}^2}{\rho_{j-1}^2 A_{j-1}^2} + g(z_{j-1} - z_k)\right] - \dot{m}_j\left[h_j + \frac{1}{2}\frac{\dot{m}_j^2}{\rho_j^2 A_j^2} + g(z_k - z_j)\right] + \dot{Q}_k$$

VId.2.2

where in Equation VId.2.2, we ignored the rate of change in the kinetic energy as compared with the internal energy. Equation VId.2.2 includes enthalpy terms developed at the junctions. For fine nodalization, with good degree of approximation, we may use $h_{j-1} = h_{k-1}$ and $h_j = h_k$. This is consistent with the donor cell ap-

proach. However, there are certain nodes that require special treatment such as heated nodes within which density and enthalpy change substantially.

The one-dimensional momentum equation for the mixture can be readily obtained by applying Equation IIIa.3.44 to the variable channel area of Figure VId.2.2. The momentum control volume is centered at j and it extends from $L_k/2$ and $L_{k+1}/2$. Substituting for various pressure drop terms, for the lower segment we get:

$$\frac{L_k}{2A_k}\frac{d\dot{m}_j}{dt} = -[(P_j - P_k) + (\frac{\dot{m}_j^2}{\rho_k A_k^2} - \frac{\dot{m}_k^2}{\rho_k A_k^2}) + \frac{M_{k/2}}{A_k} g + f_k \phi \frac{L_k}{2D_k}\frac{\dot{m}_k|\dot{m}_k|}{2\rho_k A_k^2} + \mathrm{K}_j \phi \frac{\dot{m}_j|\dot{m}_j|}{2\rho_j A_j^2}]$$

where ϕ is the two-phase friction multiplier, as defined in Chapter VI. Now, we apply Equation IIIa.3.44 to the portion of the momentum control volume extending from j, right after the change in flow area to point $k + 1$:

$$\frac{L_{k+1}}{2A_{k+1}}\frac{d\dot{m}_j}{dt} = -[(P_{k+1} - P_j) + (\frac{\dot{m}_{k+1}^2}{\rho_{k+1} A_{k+1}^2} - \frac{\dot{m}_j^2}{\rho_{k+1} A_{k+1}^2}) + \frac{M_{(k+1)/2}}{A_{k+1}} + f_{k+1} \phi \frac{L_{k+1}}{2D_{k+1}}\frac{\dot{m}_{k+1}|\dot{m}_{k+1}|}{2\rho_{k+1} A_{k+1}^2} + \mathrm{K}_j \frac{\dot{m}_j|\dot{m}_j|}{2\rho_j A_j^2}]$$

Adding these equations, the result for the one dimensional momentum equation for variable area channel becomes:

$$\left[\frac{L_k}{2A_k} + \frac{L_{k+1}}{2A_{k+1}}\right]\frac{d\dot{m}_j}{dt} = \Delta P_{pump} - [(P_{k+1} - P_k) + (\frac{\dot{m}_{k+1}^2}{\rho_{k+1} A_{k+1}^2} - \frac{\dot{m}_k^2}{\rho_k A_k^2}) - (\frac{1}{A_{k+1}^2} - \frac{1}{A_k^2})\frac{\dot{m}_j^2}{2\rho_j} (\frac{M_{(k+1)/2}}{A_{k+1}} - \frac{M_{k/2}}{A_k}) g + \phi(f_k \frac{L_k}{2D_k}\frac{\dot{m}_k|\dot{m}_k|}{2\rho_k A_k^2} + f_{k+1}\frac{L_{k+1}}{2D_{k+1}}\frac{\dot{m}_{k+1}|\dot{m}_{k+1}|}{2\rho_{k+1} A_{k+1}^2} + \mathrm{K}_j \frac{\dot{m}_j|\dot{m}_j|}{2\rho_j A_j^2}]$$

VId.2.3

Example VId.2.1. Start with Newton's second law and derive Equation VId.2.3.

Solution: The momentum equation expresses that the net momentum flux to or from a control volume plus the rate of change of momentum in the control volume is equal to the net external forces acting on the control volume. We now apply this principle to a differential control volume located between z and $z + dz$. This control volume has a flow area of A and a hydraulic diameter of D_e. External

forces are the body force and the surface forces. Hence, the net force acting on the control volume becomes:

$$\sum dF = A(P_z - P_{z+dz}) - s\rho(Adz)g - \phi(f\frac{dz}{D_e} + \mathrm{K})\frac{\dot{m}|\dot{m}|}{2\rho A}$$

where s is introduced to account for the flow direction. For upward flow $s = +1$, for horizontal flow, $s = 0$, and for downward flow $s = -1$. The absolute value for flow rate signifies the fact that the friction force acts always opposite to the flow direction. Hence using the convention of $\dot{m} > 0$ for up-flow, the friction force becomes negative i.e., $\vec{F} = -|F|\vec{k}$. Similarly for down-flow ($\dot{m} < 0$), the friction force would act in the direction of the z-axis, $\vec{F} = |F|\vec{k}$. Accounting for the rate of change in momentum flux, the rate of change of momentum of the control volume is therefore given by:

$$\frac{\partial \dot{m}}{\partial t}dz = A(P_z - P_{z+dz}) - s\rho(Adz)g - \phi(f\frac{dz}{D_e} + \mathrm{K})\frac{\dot{m}|\dot{m}|}{2\rho A} - [(\frac{\dot{m}^2}{\rho A})_{z+dz} - (\frac{\dot{m}^2}{\rho A})_z]$$

We now divide both sides of this equation by Adz and let dz approach zero:

$$\frac{1}{A}\frac{\partial \dot{m}}{\partial t} = -\frac{\partial P}{\partial z} - s\rho g - \phi f\frac{1}{D_e}\frac{\dot{m}|\dot{m}|}{2\rho A^2} - \frac{1}{A}\frac{\partial(\dot{m}^2/\rho A)}{\partial z}$$

We may apply this equation to the control volume of Figure VId.2.2(c), which is located between elevations Z_k and Z_{k+1}. To obtain the momentum equation for this control volume, we multiply both sides of this equation by dz and integrate the resulting equation first over the portion of the momentum control volume extending from k to j right before the flow area changes. Integration over the lower portion of the control volume yields:

$$\int_k^j \frac{1}{A}\frac{d\dot{m}}{dt}dz = -(P_i - P_k) - \int_k^j (s\rho g dz) - \int_k^j \frac{\phi}{2}\frac{f}{D_e}\mathrm{v}_f\frac{\dot{m}^2}{A^2}dz - \int_k^j \frac{1}{A}d\left(\frac{\dot{m}^2\mathrm{v}}{A}\right)$$

Term by term integration is carried out as follows:

$$\int_k^j \frac{1}{A}\frac{d\dot{m}}{dt}dz \approx \frac{L_k}{2A_k}\frac{d\dot{m}_j}{dt}$$

$$\int_k^j s\rho g dz = \frac{sL_k g}{2\bar{\mathrm{v}}} = \frac{sM_k g}{2A_k}$$

$$\int_k^j \frac{\phi}{2}\frac{f}{D_e}\mathrm{v}_f\frac{\dot{m}^2}{A^2}dz = \frac{1}{2}\bar{\phi}(\bar{f}\frac{L_k}{2D_{e,k}} + \sum_k \mathrm{K})\bar{\mathrm{v}}_f\frac{\dot{m}_j|\dot{m}_j|}{A_k^2}$$

$$\int_k^j \frac{1}{A} d\left(\frac{\dot{m}\mathrm{v}}{A}\right) = \frac{\dot{m}_j^2 \mathrm{v}_j}{A_k^2} - \frac{\dot{m}_k^2 \mathrm{v}_k}{A_k^2}$$

Adding up terms we get:

$$\frac{L_k}{2A_k}\frac{d\dot{m}_i}{dt} = -(P_j - P_k) - \frac{sL_k g}{2\overline{\mathrm{v}}_k} - (f_k \frac{L_k}{2D_{e,k}} + \sum \mathrm{K}_k)\overline{\mathrm{v}}_k \frac{\dot{m}_k |\dot{m}_k|}{2A_k^2} - (\frac{\dot{m}_j^2 \mathrm{v}_j}{A_k^2} - \frac{\dot{m}_k^2 \mathrm{v}_k}{A_k^2})$$

We now apply the resulting equation to the portion of the momentum control volume extending from *j*, right after the change in flow area, to point *k*+1, yielding:

$$\frac{L_{k+1}}{2A_{k+1}}\frac{d\dot{m}_i}{dt} = -(P_{k+1} - P_j) - \frac{sL_{k+1}g}{2\overline{\mathrm{v}}_{k+1}} - (f_{k+1}\frac{L_{k+1}}{2D_{e,k+1}} + \sum \mathrm{K}_{k+1})\,\overline{\mathrm{v}}_{k+1}\frac{\dot{m}_{k+1}|\dot{m}_{k+1}|}{2A_{k+1}^2} - (\frac{\dot{m}_{k+1}^2 \mathrm{v}_{k+1}}{A_{k+1}^2} - \frac{\dot{m}_j^2 \mathrm{v}_j}{A_{k+1}^2})$$

Adding these equations, to get the one dimensional momentum equation for variable area channels:

$$\left[\frac{L_k}{2A_k} + \frac{L_{k+1}}{2A_{k+1}}\right]\frac{d\dot{m}_j}{dt} = \Delta P_{pump,k} - [(P_{k+1} - P_k) + \frac{s_i(L_k + L_{k+1})g}{2\overline{\mathrm{v}}_i} + (\frac{\dot{m}_{k+1}^2 \mathrm{v}_{k+1}}{A_{k+1}^2} - \frac{\dot{m}_k^2 \mathrm{v}_k}{A_k^2}) - (\frac{1}{A_{k+1}^2} - \frac{1}{A_k^2})\frac{\dot{m}_j^2 \overline{\mathrm{v}}_j}{2} + \phi(f_k \frac{L_k}{2D_{e,k}}\overline{\mathrm{v}}_{f,i}\frac{\dot{m}_k|\dot{m}_k|}{2A_k^2} + f_{k+1}\frac{L_{k+1}}{2D_{e,k+1}}\overline{\mathrm{v}}_{f,i}\frac{\dot{m}_{k+1}|\dot{m}_{k+1}|}{2A_{k+1}^2} + \sum \mathrm{K}_i \overline{\mathrm{v}}_i \frac{\dot{m}_j|\dot{m}_j|}{2A_j^2})]$$

This equation includes a pressure rise term in case there is a pump in the flow path. This equation while derived for single-phase flow is applied to two-phase mixture with the introduction of the multiplier ϕ and $\overline{\mathrm{v}}$.

Equations VId.2.1, VId.2.2, and VId.2.3 constitute a set of differential equations in mass, internal energy, and mass flow rate. Writing similar sets for the rest of the nodes would result in a system of differential equations, which upon solution would result in obtaining the key parameters versus time. The initial conditions are found from the steady state operation prior to the imposition of a transient.

3. Simplified PWR Model

The level of information obtained from a mathematical model depends on the extent of complexities used in the model such as the multi-dimensional analysis of multi-component flow. We may introduce a variety of simplifying assumptions to reduce the computational burden and obtain results with reasonable accuracy. However, simplifying assumptions impose limitations on the applicability of the model. An example of a simplifying assumption is the application of an integral or loop-wide momentum equation. This assumption decouples the solution of the momentum equation from the mass and energy equations. To see the saving in the number of equations, consider a case where there are N nodes in each loop of Figure VId.2.1. According to the model developed in Section 2, there are a total of $6N$ equations for the N nodes. By writing an integral momentum equation for each loop, the number of equations drops to $2N + N$' where N' is the number of loops. An integral momentum equation ignores the compressibility of fluid due to the local pressure changes and assumes that the pressure and velocity disturbances are propagated at infinite velocity. This allows us to assign one pressure to the entire RCS and one loop flow rate to each loop.

Let's now obtain the set of equations for node k (Figure VId.3.1) using the above simplifying assumption. For this purpose, we consider the various interactions with node k. Flow may enter this node from several inlet ports (shown with subscript i) and leaves from several exit ports (shown with subscript e). These are

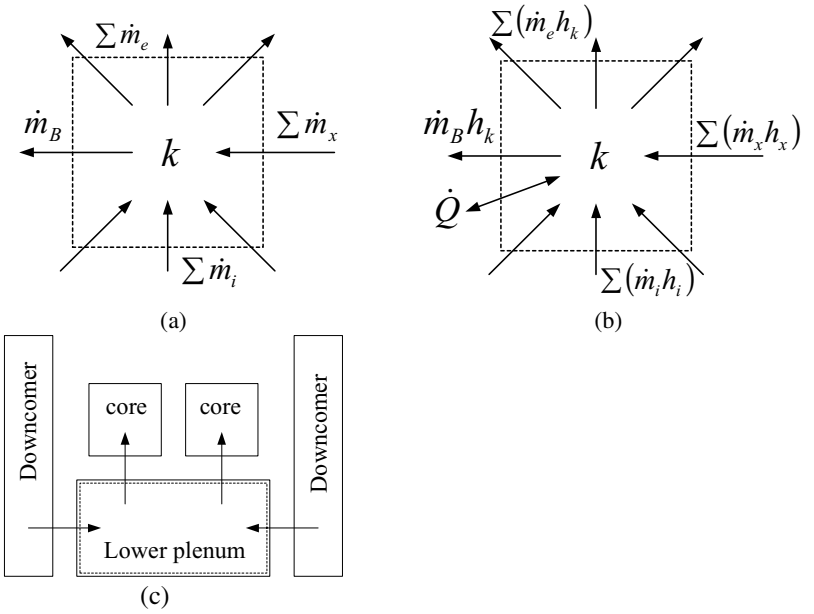

Figure VId.3.1. (a) mass and (b) energy transfer for a typical node. (c) Example of a multi-port node

the inter-nodal flow rates. Node k may also receive flow from external sources (shown by subscript x), such as safety injection. This node may also discharge flow if a pipe break (shown with subscript B) happens to occur at this node. Not all these flow rates exist simultaneously or for all the nodes. However, we are considering them for the sake of generality. The conservation equation of mass, Equation IIa.5.1 for node k becomes:

$$\frac{dm_k}{dt} = \sum(\dot{m}_i)_k - \sum(\dot{m}_e)_k + \sum(\dot{m}_x)_k - (\dot{m}_B)_k \qquad \text{VId.3.1}$$

Similarly, the conservation equation of energy, Equation IIa.6.4-1 for the node becomes:

$$\frac{d(m_k h_k)}{dt} = \sum(\dot{m}_i h_i)_k - \sum(\dot{m}_e h_k)_k + \sum(\dot{m}_x h_x)_k - \dot{m}_B h_k + \sum\dot{Q}_k + \mathrm{V}_k \dot{P}_{RCS}$$

VId.3.2

Note that the work term includes only the pressure work as there is no shaft work and the shear work is ignored. Taking the derivative of the left side, substituting from the conservation equation of mass, and rearranging, yields:

$$m_k \dot{h}_k = \left[\sum(\dot{m}_i h_i)_k - h_k \sum(\dot{m}_i)_k\right] - \left[\sum(\dot{m}_x)h_k - \sum(\dot{m}_x)_k h_x\right] + \sum\dot{Q}_k + c\mathrm{V}_k \dot{P}_{RCS}$$

VId.3.3

where c in Equation VId.3.3 is a conversion factor. We now use the volume constraint for node k, given the fact that V_k remains constant hence, $d\mathrm{V}_k/dt = 0$:

$$\frac{d\mathrm{V}_k}{dt} = \frac{d}{dt}\left(m_k \mathrm{v}_k\right) = \dot{m}_k \mathrm{v}_k + m_k \dot{\mathrm{v}}_k = 0$$

The derivatives can be expanded in terms of the RCS pressure (P_{RCS}) and the node enthalpy (h_k):

$$\dot{m}_k \mathrm{v}_k + m_k \left(\left.\frac{\partial \mathrm{v}_k}{\partial h_k}\right|_{P_{RCS}} \dot{h}_k + \left.\frac{\partial \mathrm{v}_k}{\partial P}\right|_{h_k} \dot{P}_{RCS} \right) = 0 \qquad \text{VId.3.4}$$

Substitute from Equations VId.3.1 and VId.3.3, we obtain:

$$(\mathrm{v}_k - h_k \frac{\partial \mathrm{v}_k}{\partial h_k})\sum(\dot{m}_i)_k + \frac{\partial \mathrm{v}_k}{\partial h_k}\sum(\dot{m}_i h_i)_k - \mathrm{v}_k \sum(\dot{m}_e)_k + (c\mathrm{V}_k \frac{\partial \mathrm{v}_k}{\partial h_k} + m_k \frac{\partial \mathrm{v}_k}{\partial P})\dot{P}_{RCS} =$$
$$(\dot{m}_B)_k \mathrm{v}_k - \left[\frac{\partial \mathrm{v}_k}{\partial h_k}\sum\dot{Q}_k + (\mathrm{v}_k - h_k \frac{\partial \mathrm{v}_k}{\partial h_k})\sum(\dot{m}_x)_k + \frac{\partial \mathrm{v}_k}{\partial h_k}\sum(\dot{m}_x h_x)_k\right]$$

VId.3.5

This is the general form of the *mass-energy algorithm* for loops using an integral momentum equation. In this relation, the unknowns are inter-nodal flow rates and RCS pressure. These can be determined for specified break flow rate, rate of heat transfer to the node, and the external flow rates and enthalpies.

3.1. Determination of Nodal Flow Rates In a One Loop PWR

To demonstrate the application of the mass-energy algorithm, Equation VId.3.5 is applied to a one-loop PWR as shown in Figure VId.3.2. By using the donor cell concept, the algorithm simplifies to:

$$\left[\mathrm{v}_k + \frac{\partial \mathrm{v}_k}{\partial h_k}(h_{k-1} - h_k) \right] \dot{m}_{k-1} - \mathrm{v}_k \dot{m}_k + \left(c\mathrm{V}_k \frac{\partial \mathrm{v}_k}{\partial h_k} + m_k \frac{\partial \mathrm{v}_k}{\partial P} \right) \dot{P}_{RCS} =$$

$$(\dot{m}_B)_k \mathrm{v}_k - \left[\frac{\partial \mathrm{v}_k}{\partial h_k} \sum \dot{Q} + \left(\mathrm{v}_k - \frac{\partial \mathrm{v}_k}{\partial h_k}(h_x - h_k) \right) \sum (\dot{m}_x)_k \right] \qquad \text{VId.3.6}$$

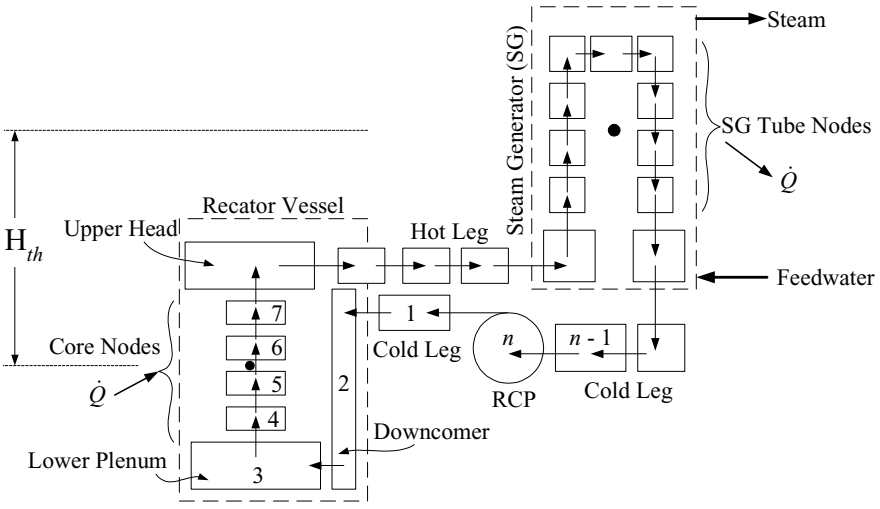

Figure VId.3.2. A one-loop PWR, obtained by collapsing all the loops into one loop

Equation VId.3.6 can be simply shown as:

$$\eta_k \dot{m}_{k-1} + \gamma_k \dot{m}_k + \delta_k \dot{P}_{RCS} = \varepsilon_k$$

where the coefficients η_k, γ_k, δ_k, and ε_k in this equation represent:

$$\eta_k = \mathrm{v}_k + \frac{\partial \mathrm{v}_k}{\partial h_k}(h_{k-1} - h_k)\,,$$

$$\gamma_k = -\mathrm{v}_k\,,$$

$$\delta_k = c\mathrm{V}_k \frac{\partial \mathrm{v}_k}{\partial h_k} + m_k \frac{\partial \mathrm{v}_k}{\partial P}\,, \text{ and}$$

$$\varepsilon_k = (\dot{m}_B)_k \mathrm{v}_k - \left\{ \frac{\partial \mathrm{v}_k}{\partial h_k} \sum \dot{Q}_k + \left[\mathrm{v}_k + \frac{\partial \mathrm{v}_k}{\partial h_k}(h_x - h_k) \right] \sum (\dot{m}_x)_k \right\}$$

We start from the discharge section of the cold leg as node 1. In this case, the flow entering this node is from the reactor coolant pump (RCP). Applying the mass-energy algorithm to all n nodes of the RCS, the following matrix equation is obtained:

$$\begin{bmatrix} \gamma_1 & 0 & 0 & 0 & \cdots & 0 & \delta_1 \\ \eta_2 & \gamma_2 & 0 & 0 & \cdots & 0 & \delta_2 \\ 0 & \eta_3 & \gamma_3 & 0 & \cdots & 0 & \delta_3 \\ 0 & 0 & \eta_4 & \gamma_4 & \cdots & 0 & \delta_4 \\ \vdots & \vdots & \vdots & \vdots & \ddots & \vdots & \vdots \\ \vdots & \vdots & \vdots & \vdots & \vdots & \gamma_{n-1} & \delta_{n-1} \\ 0 & 0 & 0 & 0 & \cdots & \gamma_n & \delta_n \end{bmatrix} \begin{bmatrix} \dot{m}_1 \\ \dot{m}_2 \\ \dot{m}_3 \\ \dot{m}_4 \\ \vdots \\ \dot{m}_{n-1} \\ \dot{P}_{RCS} \end{bmatrix} = \begin{bmatrix} \varepsilon_1 - \eta_1 \dot{m}_{RCP} \\ \varepsilon_2 \\ \varepsilon_3 \\ \varepsilon_4 \\ \vdots \\ \vdots \\ \varepsilon_n - \gamma_n \dot{m}_{RCP} \end{bmatrix} \qquad \text{VId.3.7}$$

At any time step, the thermodynamic properties and their derivatives are obtained from the equation of state by having the two independent variables of pressure and enthalpy of the previous time step. Hence, for a given pump flow rate, the RCS pressure and the inter-nodal flow rates are obtained from Equation VId.3.7 in an explicit manner. Subsequent to the calculation of the inter-nodal flow rates, nodal mass derivatives are found from back substitution of flow rates into the nodal conservation equations of mass. Upon integration over the time step this process yields the new nodal mass:

$$m_k^{N+1} = m_k^N + \left[\sum (\dot{m})_k + \sum (\dot{m}_x)_k - (\dot{m}_B)_k \right] \times \Delta t$$

Nodal enthalpy derivatives are determined from Equation VId.3.3 by using the calculated mass flow rates and the RCS pressure derivative as well as the updated nodal mass. The nodal enthalpies and the RCS pressure are then determined by explicit integration of the above quantities at the end of each time step. For example, the nodal enthalpy becomes $h_k^{N+1} = h_k^N + \dot{h}_k \times \Delta t$ and the RCS pressure $P_{RCS}^{N+1} = P_{RCS}^N + \dot{P}_{RCS} \times \Delta t$. This process is continued until the specified total

transient time is reached. In steady state operation, where no external flow or break flow rate exists, from Equation VId.3.1 we find:

$$\dot{m}_{k-1} = \dot{m}_k = \dot{m}_{RCP}$$

Similarly, for each node from Equation VId.3.2 we obtain the following energy balance:

$$\dot{Q}_k + \dot{m}_{RCP}(h_{k-1} - h_k) = 0$$

3.2. Integral Momentum Equation for a Multi-loop PWR

The primary side of a PWR may consist of two, three, four, or six loops. An integral momentum equation for loop *L*, for example, is obtained by integrating Equation IIIa.3.44 around the loop, which includes the reactor vessel:

$$\sum_L \left(\frac{L}{A}\right)_{\mathrm{L}} \frac{d\dot{m}_{\mathrm{L}}}{dt} + \sum_{\mathrm{V}} \left(\frac{L}{A}\right)_{\mathrm{V}} \frac{d\dot{m}_{\mathrm{V}}}{dt} = \left(\Delta P_{pump,\mathrm{L}}\right) - \left[\oint \left(\rho \vec{g}.d\vec{s}\right) + \sum_{loop} \left(\Delta P_{fric,\mathrm{L}}\right) + \Delta P_{fric,\mathrm{V}}\right] \qquad \text{VId.3.8}$$

where subscripts L and V stand for Loop and vessel, respectively. We now evaluate various terms in the right side of Equation VId.3.8, i.e. the friction pressure drop, the hydrostatic pressure head, and the pump head.

3.3. Friction Pressure Drop

The vessel and the rest of the loop friction pressure drops consists of skin friction and pressure losses at bends, the core support plate, the grid spacers, upper plenum, upper internals, entrance to hot leg, entrance to steam generator plenum, tubesheet, etc. As we did in Equation VId.2.3, we also consider a two-phase friction multiplier for cases where subcooling is lost and a two-phase mixture is flowing in the primary side. Calculation of the loss coefficients is discussed in Chapter IIIb. The loss coefficients for components used exclusively in the nuclear industry, such as the fuel rod grid spacers used in a specific design, are provided by the nuclear reactor vendor. However, we may use the correlation suggested by Rust to estimate pressure drop due to the fuel rod grid spacers as:

$$\Delta P_{grid} = \frac{C_v \varepsilon \dot{m} |\dot{m}|}{2\rho A^2}$$

where ε is the ratio of the projected grid spacer cross section to undisturbed flow cross section and C_v is the drag coefficient, in turn estimated from $C_v = 54.91|\dot{m}|^{-0.0245}$.

3.4 Hydrostatic Pressure Head

The hydrostatic head in Equation VId.3.8 represents the body force due to gravity. During normal operation when forced convection is the dominant flow regime, the hydrostatic force is negligible compared to such pressure forces as friction pressure drop and pressure rise over the pump. However, in thermal loops having natural circulation flow regime, the hydrostatic head is the driving force. The hydrostatic head then becomes:

$$\oint(\rho\vec{g}.d\vec{s}) = \sum_{L+V}[(\rho_k g\Delta Z_k)\cos(\alpha_k)] \qquad \text{VId.3.9}$$

where in Equation VId.3.9 the summation is over the vessel and other regions in the loop. These regions, as shown in Figure VId.3.2, include downcomer, lower plenum, core, upper plenum, hot leg, steam generator, and cold leg. In this equation, α is the angle between the velocity vector and the vector representing the acceleration of gravity. Hence, $\cos(\alpha_k)$ is the same as index s introduced in Example VId.2.1. For upward flow in the core, $\alpha_k = \pi$ and $\cos(\alpha_k) = -1$, for horizontal flow in the hot leg, $\alpha_k = \pi/2$ and $\cos(\alpha_k) = 0$, and for downward flow in the downcomer, $\alpha_k = 0$ and $\cos(\alpha_k) = 1$. In Equation VId.3.9, ΔZ_k is the difference between the exit and the inlet elevations to a given region hence, $\Delta Z_k = Z_e - Z_i$.

Determination of the hydrostatic head where change in the liquid is linear is straightforward. For example in the core, Figure VId.3.3(a), assuming a near linear density profile, the hydrostatic head becomes:

$$\int_{Core\ inlet}^{Core\ exit}(\rho\vec{g}.d\vec{s}) = [(\rho_{core} g\mathrm{H}_{core})\cos(\alpha_{core})]_i^e = -\frac{(\rho_i + \rho_e)}{2} g\mathrm{H}_{core}$$

Determination of the hydrostatic head in the steam generator is more involved. In the following example we evaluate the hydrostatic head for the single-phase flow inside the tubes of a U-tube steam generator. As shown in Figure VId.3.3(b), the height of each leg of the average tube is l and the length of the horizontal section is δ, so the average tube length becomes $L = 2l + \delta$.

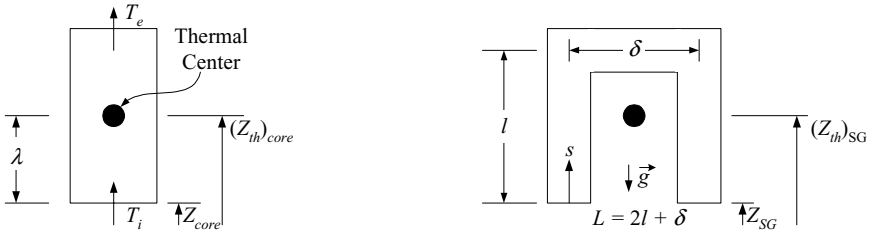

Figure VId.3.3. Nodes representing (a) core and (b) tubes of a U-tube steam generator

Example VId.3.1. Develop the hydrostatic head for flow of water in the tubes of a U-tube steam generator. Flow enters tubes at pressure P and temperature T_H and leaves at temperature T_C. The tube average length is L.

Solution: To find the hydrostatic head in the steam generator, we find the following:

$\int_0^L [\rho(s) - \rho_H]\vec{g} \cdot d\vec{s} = \int_0^l [\rho(s) - \rho_H]\vec{g} \cdot d\vec{s} + \int_{l+\delta}^L [\rho(s) - \rho_H]\vec{g} \cdot d\vec{s}$ with respect to Figure VId.3.3(b). Since in the upward leg $\cos(\pi) = -1$ and in the downward leg $\cos(0) = 1$, we can write:

$$\int_0^L [\rho(s) - \rho_H]\vec{g} \cdot d\vec{s} = -\int_0^l [\rho(s) - \rho_H] g ds + \int_{l+\delta}^L [\rho(s) - \rho_H] g ds$$

We do not have the density profile to integrate. However, we have the temperature profile from Equation VIa.5.8 given as $T(s) = T_{sat} + (T_H - T_{sat})\, e^{-s/l^*}$ where s is an element of length along the tube. To bridge the gap and relate the density difference to temperature difference, we use the definition of the thermal expansion coefficient of Chapter IIa, $\beta = -[(\partial\rho/\partial T)_P]/\rho$. It is assumed that β remains constant in the temperature range of T_C to T_H and β is approximated as $\beta \approx \Delta\rho/\Delta T)/\rho$ or $\Delta\rho = \rho\beta\Delta T$. Thus, the integral becomes:

$$\int_0^L [\rho(s) - \rho_H]\vec{g} \cdot d\vec{s} = \beta g \rho_H (T_H - T_{sat}) \left\{ -\int_0^l \left(1 - e^{-s/l^*}\right) ds + \int_{l+\delta}^L \left(1 - e^{-s/l^*}\right) ds \right\}$$

The integral of the argument is found as: $\int \left(1 - e^{-s/l^*}\right) ds = s + l^* e^{-s/l^*}$, subject to the limits 0 to l and $l + \delta$ to L:

$$\int_0^L [\rho(s) - \rho_H]\vec{g} \cdot d\vec{s} =$$
$$\beta g \rho_H (T_H - T_{sat}) \left\{ -\left(l + l^* e^{-l/l^*} - l^*\right) + \left(L + l^* e^{-L/l^*} - (l + \delta) - l^* e^{(l+\delta)/l^*}\right) \right\}$$

simplifies to:

$$\int_0^L [\rho(s) - \rho_H]\vec{g} \cdot d\vec{s} = \beta g \rho_H (T_H - T_{sat}) l^* \left(1 - e^{-l/l^*} - e^{(l+\delta)/l^*} + e^{-L/l^*}\right).$$

Substituting from Equation (2), we get:

$$\int_0^L [\rho(s) - \rho_H]\vec{g} \cdot d\vec{s} = \beta g \rho_H (T_H - T_{sat}) l^* \left(1 - e^{-l/l^*} - e^{(l+\delta)/l^*} + e^{-L/l^*}\right).$$

Replacing T_H - T_{sat} with T_H - T_C, yields:

$$\int_0^L [\rho(s) - \rho_H]\vec{g} \cdot d\vec{s} =$$
$$\beta g \rho_H (T_H - T_C) l^* \left(1 - e^{-l/l^*} - e^{(l+\delta)/l^*} + e^{-L/l^*}\right) / \left(1 - e^{-L/l^*}\right) \qquad \text{VId.3.10}$$

Two-Phase Flow in Tubes. In Example VId.3.1, we found the hydrostatic head for single-phase inside tubes. In the case of two-phase flow in the tubes, we must use the mixture density as defined in Chapter V, $\rho_m = (1 - \alpha)\rho_f + \alpha\rho_g$ where α is given by Equation Va.1.3 as $\alpha = X/(aX + b)$. Therefore, the hydrostatic head becomes:

$$\int_{SG}(\rho_m \bar{g}.d\bar{s}) = \int_0^L \left(\rho_f + \frac{(\rho_g - \rho_f)X}{aX + b} \right) \bar{g}.d\bar{s} \qquad \text{VId.3.11}$$

All we need to do now is to find the profile for flowing quality in the tubes. This is accomplished by using an energy balance in an elemental length of the tube, *ds* to obtain:

$$\dot{m}dh = -N\pi d_o U_o \left[T_{sat}(P_{primary}) - T_{sat}(P_{secondary}) \right] ds$$

Substituting for $dh = h_{fg}\, dX$ in the above equation allows us to solve for $dX/ds = -N\pi d_o U_o \left[T_{sat}(P_{primary}) - T_{sat}(P_{secondary}) \right] / \dot{m} h_{fg} = l^*_{2\,phase}$. We now integrate the result, which yields $X = l^*_{2\,phase}\, s + X_{in}$. Having the quality profile, we then substitute into Equation VId.3.11 and integrate. The final answer depends on the length of the boiling section (L_B) i.e. whether $L_B < l$, of $l < L_B < l + \delta$, or $l + \delta < L_B < L$. For example if $L_B < l$ then the hydrostatic head becomes:

$$\int_0^{L_B} (\rho_m \bar{g}.d\bar{s}) = -g \int_0^{L_B} \left(\rho_f + \frac{(\rho_g - \rho_f)\left(l^*_{2\,phase} s + X_{in}\right)}{a\left(l^*_{2\,phase} s + X_{in}\right) + b} \right) ds = g l^*_{2\,phase} \left[a_1 x - a_2 \ln \frac{aX_{in} + b}{b} \right]$$

where $a_1 = \rho_f - (\rho_g - \rho_f)/a$ and $a_2 = (\rho_g - \rho_f)b/a^2$. Then from L_B to L we use the single-phase integral of Equation VId.3.10. The solutions for all these cases are obtained by Kao.

Thermal Center. We now define a node property referred to as *thermal center*. In lumped nodes, the thermal center may be viewed as a point at which the heat transfer process takes place. For example, consider the node representing the core or the steam generator U-tubes in Figure VId.3.3. Thermal center for these nodes may be defined as:

$$\lambda = \frac{\int_0^L [T(s) - T_H]\, ds}{T_C - T_H} \qquad \text{VId.3.12}$$

where λ is measured from the entrance to the node. For the core node, it is trivial to show that for linear temperature rise in the core, the thermal center is located at $\lambda_{core} = L_{core}/2$. Determination of the thermal center for the steam generator node, where temperature profile is not linear, is similar to the method used in Example VId.3.1. For U-tube steam generators it can be shown (see Problem 2) that:

$$\lambda_{SG} = \frac{1 - e^{-l/l^*} - e^{-(l+\delta)/l^*} + e^{-L/l^*}}{1 - e^{-L/l^*}} l^* \qquad \text{VId.3.13}$$

If we now substitute λ_{SG} into Equation VId.3.10, we obtain the steam generator hydrostatic head as:

$$\int_0^L [\rho(s) - \rho_H] \vec{g} \cdot d\vec{s} = \int_0^L \rho(s) \vec{g} \cdot d\vec{s} = = \beta g \rho_H (T_H - T_C) \lambda_{SG}$$

Example VId.3.2. Find the distance to the thermal center of a steam generator from the tube sheet. Tube-side data: $\dot{m} = 61E6$ lbm/h, c_p = 1.4 Btu/lbm F, N = 8485, d_o = 0.75 in, U_o = 1040 Btu/h ft^2 F, L = 56 ft, l = 26 ft, average length of the U-tube horizontal section δ = 4 ft, cold leg temperature T_C = 550 F, hot leg temperature T_H = 600 F.

Solution: According to Example VIa.6.2, $l^* = \dot{m} c_p/(\pi N d_o U_o)$. Therefore, l^* is found as:

$l^* = 61E6 \times 1.4/[\pi \times 8485 \times (0.75/12) \times 1040] = 49.3$ ft.

We now use Equation VId.3.13:

$$\lambda_{SG} = \frac{1 - e^{-l/l^*} - e^{-(l+\delta)/l^*} + e^{-L/l^*}}{1 - e^{-L/l^*}} l^* =$$

$$\frac{1 - e^{-26/49.3} - e^{-(26+4)/49.3} + e^{-56/49.3}}{1 - e^{-56/49.3}} \times 49.3 = 13.57 \text{ ft}$$

This is almost equal to $l/2$. Indeed as $l^* \to \infty$, $\lambda_{SG} = 0.5(1 + \delta/L)l$.

Having the height of the core and the steam generator thermal centers, we can then find their corresponding elevations by adding the heights to the elevation of the bottom of the core and the tube sheet, respectively. Hence, $(Z_{th})_{core} = Z_{core} + \lambda_{core}$ and $(Z_{th})_{SG} = Z_{SG} + \lambda_{SG}$. These are shown in Figure VId.3.3.

The discussion on the hydrostatic head in a flow loop demonstrates that the hydrostatic head is primarily a function of the loop geometry and the working fluid density gradient. Therefore in flow loops, the hydrostatic force is given as:

$$\oint_{Loop} (\rho \vec{g} . d\vec{s}) = (\rho_C - \rho_H) g H_{th} \qquad \text{VId.3.14}$$

where H_{th} in Equation VId.3.14 is the difference between the steam generator and the core thermal centers given by $H_{th} = (Z_{th})_{SG} - (Z_{th})_{core}$. Note that elevations of the core and steam generator thermal centers are measured from a common reference.

Example VId.3.3. Find the pressure difference due to the buoyancy force in a flow loop. Data: $P = 2250$, $T_{Hot} = 600$ F, $T_{Cold} = 550$ F, $Z_{Heat\ Sink} = 61$ ft, $Z_{Heat\ Source} = 31$ ft. Working fluid is water.

Solution: We use Equation VId.3.14 to estimate $\Delta P_{gravity} = (47.2 - 43.1) \times (61 - 31) = 0.85$ psi.

3.5. Natural Circulation in Flow Loops

Natural circulation is the preferred mode of operation when the enhancement of the passive safety features, such as elimination of any pump failure, is a design requirement. Some high rise buildings use natural circulation for the heating of their units. This is accomplished by heating water in a boiler located in the basement resulting in warm water flowing upward inside the riser. As water passes various floors it deposits energy to heat the space. The colder and heavier water then flows downward and back to the boiler, pushing the warmer water upward. Hence, a necessary condition for establishment of natural circulation is that $H_{th} > 0$.

To estimate the natural circulation flow rate, we start with the single-loop of Figure VId.3.4 and use Equation VId.2.3. Since this equation is obtained for a single node, we integrate it over all the nodes comprising the loop. By doing so, the static pressure difference term cancels out. Integrating Equation VId.2.3 is equivalent to summing up all the terms of Equation IIIa.3.44 around the loop. This results in:

$$\sum_{k=1}^{n}\left(\frac{L}{A}\right)_k \frac{d\dot{m}}{dt} =$$

$$\Delta P_{pump} - \sum_{k=1}^{n} \overline{\rho}_k g \left(Z_{j+1} - Z_j\right)_k - \frac{\dot{m}^2}{2}\sum_{k=1}^{n}\frac{1}{\overline{\rho}_k}\left(\frac{1}{A_{j+1}^2} - \frac{1}{A_j^2}\right)_k - \frac{\dot{m}^2}{2}\sum_{k=1}^{n}\frac{1}{\overline{\rho}_k A_k^2}\left(f\frac{L}{D} + \mathrm{K}\right)_k \qquad \text{VId.3.15}$$

where in the case of Figure VId.3.4, $n = 5$. Equation VId.3.15 can be simplified by noting that in a natural circulation loop, the pump head is zero. Note that the pump head being zero does not necessarily mean that there is no pump in the loop. Rather, the pump is simply not operating. A loop without a pump has by far less frictional losses than an identical loop but equipped with a pump that is turned off. This is because in the latter case, the working liquid must flow through the pump volute and among the blades of the impeller. The losses due to friction in pumps depend on the type of the pump and whether the impeller is locked or is free to spin. For example, for the canned-motor pump of the LOFT (Reeder) experiment, the loss coefficient for the free spinning impeller with flow in forward direction (from pump suction to pump discharge) was estimated to be K = 3, for flow in the reverse direction K = 12, and for flow through the pump with impeller locked K = 20.

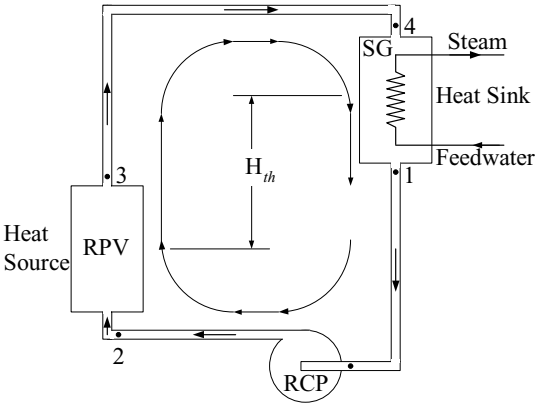

Number	Name	A (ft²)	L (ft)	D_h (ft)	K
1 - 2	Cold Leg	20	174	3.2	1
2 - 3	Heat Source	37	18	0.43	11
3 - 4	Hot Leg	20	75	3.0	1
4 - 1	Steam Generator	19.5	66	0.05	6

Figure VId.3.4. Schematics of a single-loop PWR primary side and related data

Returning to Equation VId.3.15, we may also ignore the pressure drop term due to the velocity change. Thus, in steady state operation, Equation VId.3.15 simplifies to:

$$\frac{\dot{m}^2}{2}\sum_{k=1}^{n}\frac{1}{\overline{\rho}_k A_k^2}\left(f\frac{L}{D}+\mathrm{K}\right)_k = -\sum_{k=1}^{n}\overline{\rho}_k g\left(Z_{j+1}-Z_j\right)_k \approx \left(\rho_c-\rho_H\right)g\mathrm{H}_{th} \qquad \text{VId.3.16}$$

The left side of Equation VId.3.16 may be shown as $\dot{m}R/2\overline{\rho}$ where $R=\sum[(f_k L_k/D_k)+\mathrm{K}_k]/A_k^2$, known as the loop *flow resistance*. In the right side of Equation VId.3.16, we made use of Equation VId.3.14 for the hydrostatic head. If we relate the density difference ($\Delta\rho$) to the corresponding temperature difference (ΔT) by $\Delta\rho \approx \beta\rho\Delta T$, assuming constant β in the temperature range of T_C to T_H, Equation VId.3.16 becomes:

$$\frac{1}{2}R\frac{\dot{m}^2}{\overline{\rho}} = \overline{\rho}\beta g\mathrm{H}_{th}\Delta T \qquad \text{VId.3.17}$$

The change in temperature in the loop is due to the rate of heat addition in the heat source (core) or the rate of heat rejection in the heat sink (steam generator). Therefore, from a steady state energy balance over the heat source, for example

we find that, $\dot{Q} = \dot{m} c_p (T_H - T_c)$. Substituting for ΔT we obtain the natural circulation flow rate in steady state operation as:

$$\dot{m}_{NC} = \left(\frac{2\beta g \bar{\rho}^2 \mathrm{H}_{th} \dot{Q}_{\mathrm{Core}}}{c_p R} \right)^{1/3} \qquad \text{VId.3.18}$$

Equation VId.3.18 provides a reasonable estimate for the natural circulation flow rate provided that the system resistances are closely approximated and the flow regime is turbulent (see Problem 16).

Example VId.3.4. Find the natural circulation flow rate using the data of the simplified PWR loop shown in Figure VId.3.4. Core power during shutdown is 5 MW. Data: $f = 0.01$, $\bar{\rho}$ = 45 lbm/ft^3, c_p = 1.3 Btu/lbm·F, β = 0.001 R^{-1}, $(Z_{th})_{SG}$ = 60 ft, $(Z_{th})_{RPV}$ = 30 ft.

Solution: We must first find the loop flow resistance using the specified friction factor of 0.01. Substituting values in $R_k = \left(f_k L_k / D_k + \mathrm{K}_k \right) / A_k^2$ yields:

$R_{1\text{-}2}$ = 3.86E-3 ft^{-4}, $R_{2\text{-}3}$ = 8.34E-3 ft^{-4}, $R_{3\text{-}4}$ = 3.12E-3 ft^{-4}, and $R_{4\text{-}1}$ = 0.05 ft^{-4}.

Thus, ΣR = 0.065 ft^{-4}. We now substitute values into Equation VId.3.18:

$$\dot{m}_{NC} = \left(\frac{2 \times 0.001 \times 32.2 \times 45^2 \times (60 - 30) \times (5{,}000 \times 3412 / 3600)}{1.3 \times 0.065} \right)^{1/3} = 603 \text{ lbm/s}$$

Having determined the hydrostatic pressure head and the natural circulation flow rate we now proceed to deal with the pump head.

4. Mathematical Model for PWR Components, Pump

In Section 3, we used the pump flow rate as a known function. In this section, we want to find how such a function can be obtained. To find the pump speed, we apply the conservation equation of angular momentum to the impeller of a centrifugal pump. Assuming the prime mover is an electric motor, the electric torque (T_E) must provide for the hydraulic torque (T) and the frictional torque (T_F). The net torque according to Newton's second law is then equal to the moment of inertia times the rate of change of the impeller angular velocity:

$$\mathrm{T}_E - \mathrm{T} - \mathrm{T}_F = I \frac{d\omega}{dt} \qquad \text{VId.4.1}$$

where I in Equation VId.4.1, represents the moment of inertia of the pump shaft, impeller, and flywheel. The electric torque delivered by the prime mover is a known quantity. If the pump is turned off, the electric torque drops exponentially as:

$$\mathrm{T}_E = \mathrm{T}_{E\mathrm{o}} \frac{\omega}{\omega_\mathrm{o}} e^{(-2t/\tau_e)}$$

where the rated electric torque, $\mathrm{T}_{E\mathrm{o}}$ is provided by the electric motor manufacturer. Also τ_e is the electric motor decay constant, which accounts for the inertia of the electric motor. To obtain an instantaneous loss of the applied torque, the decay constant may be set equal to a small value such as 0.1 μs. The hydraulic torque, T, due to the momentum transfer from the pump impeller to the liquid is obtained from the pump homologous curves as discussed in Chapter VIc. Finally, the frictional and windage torque, T_F accounts for all the losses in the contact points in such places as the bearings and the pump seals. The frictional and the windage torques may be correlated to the pump speed ratio by fitting a curve to pump coastdown data.

4.1. Implementation of Pump Model in Momentum Equation

Determination of flow rate as a function of time due to pump startup or shutdown in a multi-loop PWR requires simultaneous solution of the conservation equation of momentum, for the fluid, and conservation equation of angular momentum for the pump impeller. The momentum equation for the fluid is written as:

$$\sum_L \frac{L_k}{A_k} \frac{d\dot{m}_k}{dt} + \left(\frac{L}{A}\right)_\mathrm{V} \frac{d\dot{m}_\mathrm{V}}{dt} = F(\dot{m}_k, \omega_k, \dot{m}_\mathrm{V}) \qquad \text{VId.4.2}$$

where $\dot{m}_\mathrm{V}$ represents flow rate through the vessel, being the common flow path, i.e. $\dot{m}_\mathrm{V} = \sum_L \dot{m}_k$ where the summation is for the total number of loops. Function F, in Equation VId.4.2, is given by the right side of Equation VId.3.8 with pump head given by Equation VIc.4.1. Similarly, we may express Equation VId.4.1 as:

$$\frac{d\omega_k}{dt} = G(\dot{m}_k, \omega_k)$$

If the transient is due to pump shutdown then, without the imposed electrical torque, the flow rate drops to the natural circulation flow rate at a rate determined by the pump inertia, pump frictional resistance, and the hydraulic torque. This set of equations can be generalized, using matrix notation for the multi-loop configuration, as:

$$A\dot{Y} = B(Y)$$

In this relation, matrix *A* is a square matrix. Elements of vector *Y* consist of all of the unknowns including the unknown loop flow rate, vessel flow area, and the pumps angular velocities:

$$Y = \left[\dot{m}_1, \omega_1, ..., \dot{m}_n, \omega_n, \dot{m}_V\right]^T$$

and elements of vector *B* are:

$$B = \left[F_1, G_1, ..., F_n, G_n\right]^T$$

To solve this set by a semi-implicit finite difference scheme, we first linearize the differential equations to set up the Jacobian matrix, which is given as $A^N \Delta Y^{N+1} = \Delta t\left[B(Y^N) + J^N \Delta Y^{N+1}\right]$ where superscript *N* represents the previous time step and *J* represents the Jacobian matrix. This equation can be rearranged to get:

$$\left[A - \Delta t\, J\right]^N \Delta Y^{N+1} = \Delta t\, B^N Y^N \qquad \text{VId.4.3}$$

If we represent $\left[C\right] = \left[A - \Delta t\, J\right]$ then matrix [C] would have the following structure:

$$\left[C\right] = \begin{bmatrix} c_{11}(1) & c_{12}(1) & 0 & 0 & 0 & 0 & 0 & 0 & c_{13}(1) \\ c_{21}(1) & c_{22}(1) & 0 & 0 & 0 & 0 & 0 & 0 & 0 \\ 0 & 0 & c_{11}(2) & c_{12}(2) & 0 & 0 & 0 & 0 & c_{13}(2) \\ 0 & 0 & c_{21}(2) & c_{22}(2) & 0 & 0 & 0 & 0 & 0 \\ 0 & 0 & 0 & 0 & c_{11}(3) & c_{12}(3) & 0 & 0 & c_{13}(3) \\ 0 & 0 & 0 & 0 & c_{21}(3) & c_{22}(3) & 0 & 0 & 0 \\ 0 & 0 & 0 & 0 & 0 & 0 & c_{11}(4) & c_{12}(4) & c_{13}(4) \\ 0 & 0 & 0 & 0 & 0 & 0 & c_{21}(4) & c_{22}(4) & 0 \\ -1 & 0 & -1 & 0 & -1 & 0 & -1 & 0 & 1 \end{bmatrix}$$

where elements of matrix *C*, as calculated by Kao, are given in Table VId.4.1.

Table VIc.4.1. Elements of matrix *C*

Element	Mathematical Expression
$c_{11}(k)$	$\sum_k \left(L/A\right)_k - \Delta t\left(\partial F/\partial \dot{m}\right)_k^N$
$c_{12}(k)$	$-\Delta t\left(\partial F/\partial \omega\right)_k^N$
$c_{21}(k)$	$-\Delta t\left(\partial G/\partial \omega\right)_k^N$
$c_{22}(k)$	$1-\Delta t\left(\partial G/\partial \omega\right)_k^N$
$c_{13}(k)$	$\left(L/A\right)_V - \Delta t(\partial F/\partial \dot{m}_V)_k^N$

In this section we found numerical solution for the loop flow rate as a function of time. Next we find analytical solutions for the loop flow rate versus time in two cases of pump imposed transients. In the first case, we assume that the pump head remains constant and is independent of flow rate and in the second case, we account for pump head being a function of the loop flow rate.

4.2. Analytical Solution for Flow Transients, Constant Pump Head

Our goal is to find an analytical solution to the loop flow rate in such transients as pump shutdown or pump start up. For now, we assume that the pump head is a weak function of flow rate so that it can be treated as a constant in the loop momentum equation. Later in this chapter, this assumption is relaxed and the pump head is treated as a function of flow rate. The pump head being a constant is a reasonable assumption in certain cases. For example, at low flow rates as shown in Figure VIc.3.1, pump head remains relatively flat and it changes rather slightly with flow rate. Another example includes cases where the pump inertia is small as compared with the loop fluid inertia, which makes an analytical albeit approximate solution possible.

To derive the analytical solution for flow transients we start with the single-loop of Figure VId.3.4 and use Equation VId.2.3. Since this equation is obtained for a single node, we integrate it over all the nodes comprising the loop. By doing so, the static pressure differential term cancels out. The integration of Equation VId.2.3 is equivalent to summing up all the terms of Equation IIIa.3.44 around the loop. This results in:

$$\sum_{k=1}^{n}\left(\frac{L}{A}\right)_k \frac{d\dot{m}}{dt} = \Delta P_{pump} - \sum_{k=1}^{n}\overline{\rho}_k g\left(Z_{j+1}-Z_j\right)_k - \frac{\dot{m}^2}{2}\sum_{k=1}^{n}\frac{1}{\overline{\rho}_k}\left(\frac{1}{A_{j+1}^2}-\frac{1}{A_j^2}\right)_k - \frac{\dot{m}^2}{2}\sum_{k=1}^{n}\frac{1}{\overline{\rho}_k {A_k}^2}\left(f\frac{L}{D}+\mathrm{K}\right)_k \qquad \text{VId.4.4}$$

where an average density is used for each node. For example, in the core $\overline{\rho}_{core} = (\rho_{CL} + \rho_{HL})/2$. Since in this example, flow area remains constant within each control volume, the summation term for the geometric inertia is simplified and is made over the five primary side nodes. Equation VId.4.4 is a first order, linear differential equation of the following form:

$$\frac{d\dot{m}}{C_1^2 - C_2^2\dot{m}^2} = dt \qquad \text{VId.4.5}$$

where coefficients C_1^2 and C_2^2 represent:

$$C_1^2 = \left[g_c\Delta P_{pump} + \sum_{k=1}^{n}\overline{\rho}_k g\left(Z_{j+1}-Z_j\right)\right] \Bigg/ \sum_{k=1}^{n}\left(\frac{L}{A}\right)_k$$

$$C_2^2 = \frac{1}{2}\left[\sum_{k=1}^{n}\frac{1}{\overline{\rho}_k}\left(\frac{1}{A_{j+1}^2}-\frac{1}{A_j^2}\right)_k + \sum_{k=1}^{n}\frac{1}{\overline{\rho}_k {A_k}^2}\left(f\frac{L}{D}+\mathrm{K}\right)\right] \Bigg/ \sum_{k=1}^{n}\left(\frac{L}{A}\right)_k$$

To find an analytic solution for the above first order differential equation, we write it as

$$\frac{d\dot{m}}{C_1 - C_2\dot{m}} + \frac{d\dot{m}}{C_1 + C_2\dot{m}} = 2C_1 dt$$

this can be easily integrated to obtain:

$$\ln\frac{C_1 + C_2\dot{m}}{C_1 - C_2\dot{m}} = 2C_1C_2t + C_3 \qquad \text{VId.4.6}$$

Where C_3 is the constant of integration and is determined from the initial condition. The above solution applies to both cases of pump start up in a stagnant loop and pump shutdown in a forced flow loop. The difference is in the application of the boundary condition to obtain the constant C_3, as discussed next.

Case 1. Pump Start Up in a Stagnant Loop. Several conditions may lead to stagnation in flow loops. For example, there would be no flow if the thermal center of the heat sink is located below the thermal center of the heat source. Other examples include a flow loop with very high frictional losses resulting in insignificant rate of flow or an isothermal flow loop where $\rho_H = \rho_C$. In a stagnant loop, $\dot{m}$ ($t = 0$) = 0 hence, $C_3 = 0$. Equation VId.4.6 simplifies to:

$$\dot{m}(t) = \left(\frac{C_1}{C_2}\right)\frac{e^{2C_1C_2t} - 1}{e^{2C_1C_2t} + 1} \qquad \text{VId.4.7}$$

At steady state, when $t \to \infty$, forced circulation flow rate is found as $\dot{m}_{FC} = C_1 / C_2$.

Case 2. Pump Start Up in a Natural Circulation Loop. If a flow loop with pump turned off operates in natural circulation mode then $\dot{m}$ ($t = 0$) = $\dot{m}_{NC}$ hence, $C_3 = \ln[(C_1 + C_2\dot{m}_{NC})/(C_1 - C_2\dot{m}_{NC})]$. Substituting for C_3, Equation VId.4.6 becomes:

$$\dot{m}(t) = \left(\frac{C_1}{C_2}\right)\frac{y_{NC}e^{2C_1C_2t} - 1}{y_{NC}e^{2C_2C_2t} + 1} \qquad \text{VId.4.8}$$

where in Equation VId.4.8 $y_{NC} = (C_1 + C_2\dot{m}_{NC})/(C_1 - C_2\dot{m}_{NC})$. At steady state, when $t \to \infty$, forced circulation flow rate is found as $\dot{m}_{FC} = C_1 / C_2$.

Example VId.4.1. Consider the flow loop of Figure VId.3.4 as described in Example VId.3.4. We now start up the pump. Pressure rise over the pump is 50 psi. Find flow rate one second after start up and at steady state. $\rho_H = 44.5 \text{lbm/ft}^3$ and $\rho_C = 45.5 \text{ lbm/ft}^3$.

Solution: To calculate coefficients C_1 and C_2 of Equation VId.4.5 we find:

$\Sigma(L/A)_k = (174/20) + (18/37) + (75/20) + (66/19.5) = 16.3 \text{ ft}^{-1}$
$\Sigma(\rho g \Delta Z)_k = (\rho_C - \rho_H) g H_{th} = (45.5 - 44.5) \times 32.2 \times (60 - 30) = 966 \text{ lbm·ft/s}^2$
$\Sigma(R/\rho)_k = (3.86\text{E-}3/45.5) + (8.34\text{E-}3/45) + (3.12\text{E-}3/44.5) + (0.05/45) = 1.45\text{E-}3 \text{ (ft·lbm)}^{-1}$

$C_1 = [(32.2 \times 50 \times 144 + 966)/16.3]^{1/2} = 119.5$
$C_2 \cong [(0.5 \times 1.45\text{E-}3)/16.3]^{1/2} = 6.7\text{E-}3$
$C_1 C_2 = 0.8$ and $C_1/C_2 = 17{,}836$ lbm/s

$$y_{NC} = \frac{119.5 + 6.7\text{E} - 3 \times 603}{119.5 - 6.7\text{E} - 3 \times 603} = 1.07$$

$$\dot{m}(t) = 17{,}836 \frac{1.07 \exp(1.6t) - 1}{1.07 \exp(1.6t) + 1}$$

$\dot{m}(t=1) = 17{,}836 \times (1.07e^{0.8} - 1)/(1.07e^{0.8} + 1) = 17{,}836 \times 0.41 = 7{,}313$ lbm/s

$\dot{m}_{s-s} = 17{,}836$ lbm/s.

Case 3. Pump Shutdown in a Forced Circulation Loop. A similar solution can be found for the flow coast down due to the termination of pump operation. In this case, at time zero, the flow rate is equal to a specified steady state forced circulation flow. The intention is to obtain flow rate as a function of time after the pump is turned off. In this case, at time zero, $\dot{m} = \dot{m}_{FC}$, i.e., a known value. Therefore, for this case the constant C_3 can be determined as $C_3 = \ln[(C_1 + C_2\dot{m}_{FC})/(C_1 - C_2\dot{m}_{FC})]$. Substituting, the flow coastdown is found as:

$$\dot{m}(t) = \left(\frac{C_1}{C_2}\right) \frac{y_{FC} e^{2C_1C_2t} - 1}{y_{FC} e^{2C_2C_2t} + 1} \qquad \text{VId.4.9}$$

where in Equation VId.4.9, $y_{FC} = (C_1 + C_2\dot{m}_{FC})/(C_1 - C_2\dot{m}_{FC})$.

In both cases of pump startup and shutdown, the integration of Equation VId.4.6 was easily carried out due to our simplifying assumption that the pressure increase over the pump is independent of the flow rate. Next, we consider a more general case of pump pressure rise being a function of the loop flow rate.

4.3. Analytical Solution for Flow Transients, Pump Head a Function of Flow Rate

The rigorous approach that resulted in obtaining Equation VId.4.3 requires numerical solution. Here we seek an approximate but analytical solution to the flow coastdown in a thermalhydraulic loop. For this purpose we consider the reactor coolant pump in Figure VId.3.2 being turned off. We are interested in the early part of the transient when flow is coasting down. In steady state operation, identified with subscript o, we have:

$$\frac{1}{2}\sum f_{ko}\frac{L_k}{D_k A_k^2}\frac{\dot{m}_o^2}{\rho} = \rho g \mathrm{H}_{Po} + \oint \rho\left(\vec{g}\cdot\vec{ds}\right) \qquad \text{VId.4.10}$$

where H_{Po} is the pump head in steady state. Approximating the hydrostatic force by using the thermal expansion coefficient, we get:

$$\oint \rho\left(\vec{g}.d\vec{s}\right) = \rho_o g\left(\beta \Delta T_o Z_{th}\right) = \rho_o g \mathrm{H}_{So} \qquad \text{VId.4.11}$$

where Z_{th} is the difference in the elevations of the heat source and heat sink thermal centers, as shown in Figure VId.2.3, ρ_o is density at a reference temperature T_o, and H_{so} is the hydrostatic head at steady state. Assuming that the friction factors in the transient remain the same as in steady state and using an average flow rate for the entire loop, the momentum equation integrated over the loop yields:

$$\sum\left(\frac{L}{A}\right)\frac{d\dot{m}}{dt} = -\frac{\rho_o^2 g}{\rho}\left(\mathrm{H}_{Po}+\mathrm{H}_{So}\right)\left(\dot{m}/\dot{m}_o\right)^2 + \rho g\left(\mathrm{H}_P+\mathrm{H}_S\right) \qquad \text{VId.4.12}$$

As recommended by Burgreen, we further assume that both the pump head ratio and the torque ratio in the transient will follow the same homologous curves as in steady state operation. For the pump head, using the pump affinity laws, we can then write $\mathrm{H_P/H_{Po}} = (\omega/\omega_o)^2$. Also noting that for the early part of the pump shutdown transient, $\rho \cong \rho_o$ and $\mathrm{H_S} \cong \mathrm{H_{So}}$, Equation VId.4.12 simplifies to:

$$\sum\left(\frac{L}{A}\right)\frac{d\dot{V}}{dt} = -g\left(\mathrm{H}_{Po}+\mathrm{H}_{So}\right)\left(\dot{V}/\dot{V}_o\right)^2 + g\mathrm{H}_{Po}\left(\omega/\omega_o\right)^2 + g\mathrm{H}_{So} \qquad \text{VId.4.13}$$

For further simplification, we note that early in the flow coastdown event, the contribution to flow rate due to the natural circulation is exceedingly small. But as time goes on and the pump flywheel effect diminishes, the contribution of the hydrostatic force increases. Hence early in the event, we can assume that $\mathrm{H_{So}} \cong 0$ so that:

$$I_L\frac{d\dot{V}}{dt} = -g\mathrm{H}_{Po}\left(\dot{V}/\dot{V}_o\right)^2 + g\mathrm{H}_{Po}\left(\omega/\omega_o\right)^2 \qquad \text{VId.4.14}$$

where in Equation VId.4.14, I_L represents the loop inertia, $\Sigma(L/A)$. For pumps with negligible inertia, such as the canned motor and electromagnetic pumps, the third term in Equation VId.4.14 can be ignored compared with the other two terms and Equation VId.4.14 simplifies to $d\dot{V}/dt + (g\mathrm{H}_{Po}/I_L)\left(\dot{V}/\dot{V}_o\right)^2 = 0$. The so-

lution to this equation can be found as $t = (1/\dot{V} - 1/\dot{V}_o)\dot{V}_o^2 I_L / gH_{Po}$. The time for flow to decay to half of its initial value, $\dot{V}_o^2/2$ is, therefore, found as: $(t_{1/2})_L = I_L \dot{V}_o/(gH_{Po})$.

Returning to Equation VId.4.14, if we now define $\Phi = \dot{V}/\dot{V}_o$, $\theta = t/(t_{1/2})_L$, and $\Omega = \omega/\omega_o$ then Equation VId.4.14 simplifies to:

$$d\Phi/d\theta + \Phi^2 = \Omega^2 \qquad \text{VId.4.15}$$

Having obtained the simplified form of the loop momentum equation following pump shutdown, we now turn to the impeller angular momentum given by Equation VId.4.1. Neglecting the frictional losses and noting that the electric torque goes to zero upon pump trip, we find for hydraulic torque that;

$$-T = I_P d\omega/dt \qquad \text{VId.4.16}$$

Pump moment of inertia, I_P, typically consists of flywheel (≅ 75%), electric motor (≅ 23%), impeller (≅ 1.5%) and shaft (≅ 0.5%). Using the second approximation for pump break horsepower torque, $T/T_o = (\omega/\omega_o)^2$ where T_o is obtained from $T_o = \Delta P_o \dot{V}_o/(\eta_o \omega_o)$. Substituting, we find

$$d\omega/dt = -(1/I_P)T_o(\omega/\omega_o)^2 \qquad \text{VId.4.17}$$

this upon integration from time zero to any time results in:

$$\frac{1}{\omega} - \frac{1}{\omega_o} = \frac{1}{I_P}\frac{T_o}{\omega_o^2}t$$

If at $(t_{1/2})_P$ we have $\omega = \omega_o/2$, then $(t_{1/2})_P = I_P(\omega_o/T_o)$. Equation VId.4.17 can then be written as $d\Omega/dt + \Omega^2/(t_{1/2})_P = 0$. Changing variable from t to θ, similar to Equation VId.4.15, Equation VId.4.17 becomes:

$$d\Omega/d\theta + \alpha\Omega^2 = 0 \qquad \text{VId.4.18}$$

where parameter α in Equation VId.4.18 is given as $\alpha = (t_{1/2})_L/(t_{1/2})_P$. Equations VId.4.15 and VId.4.18 constitute a set of coupled first-order, nonlinear differential equations describing the effects of the pump on the loop flow rate. The solution to Equation VId.4.18 is obtained as:

$$\Omega = 1/(1 + \alpha\theta) \qquad \text{VId.4.19}$$

Upon substituting Equation VId.4.19 into Equation VId.4.15, we obtain the governing equation during pump coastdown as:

$$d\Phi/d\theta + \Phi^2 = 1/(1+\alpha\theta)^2 = 0 \qquad \text{VId.4.20}$$

The solution to Equation VId.4.20, as offered by Burgreen, is shown graphically in Figure VId.4.1. To get a better interpretation of α, we note that the initial en-

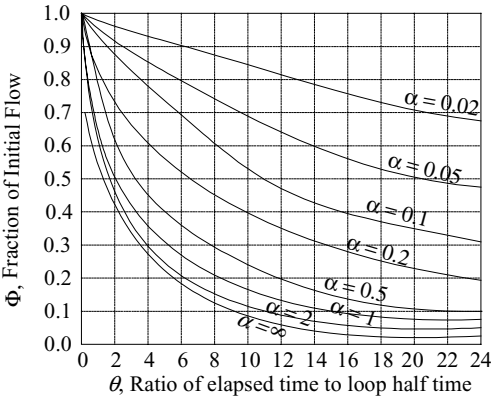

Figure VId.4.1. Approximate fluid coastdown curves following pump shutdown

ergy stored in the pump is $E_{Po} = \frac{1}{2} I_P \omega_o^2$. Similarly, the initial stored energy in the loop circulating fluid is $E_{Lo} = \frac{1}{2} \rho\Sigma(\dot{V}_o^2/A)LA = \frac{1}{2} \rho \dot{V}_o^2 I_L$. We can now express pump and fluid half-lives in terms of their corresponding initial stored energies as

$$(t_{1/2})_P = 2E_{Po}/(T_o\omega_o) \text{ and } (t_{1/2})_L = 2E_{Lo}/[\rho g \dot{V}_o H_{Po}]$$

Hence

$$\alpha = (t_{1/2})_P/(t_{1/2})_L = E_{Lo}/(\eta_o E_{Po})$$

where we also took advantage of the definition of pump efficiency. This relation indicates that the ratio of the fluid to pump half-lives is equal to the ratio of the fluid to pump effective initial stored energies. Expectedly, as shown in Figure VId.5.1, if the pump flywheel contains high initial energy ($\alpha << 1$), reasonable amount of fluid circulates the loop following termination of the pump operation, due to the pump inertial effects. For small or no initial pump stored energy, as in the case of canned motor or electromagnetic pumps, termination of the pump operation results in rapid flow decay due to the action of the friction forces.

Example VId.4.2. Find the coastdown flow fraction in a flow loop at 1, 5, 7 seconds into the event.
Loop Data: $I_L = \Sigma L/A = 108$ ft^{-1}, $\Delta P_o = 93$ psi, $\rho_o = 62.87$ lbm/ft^3.
Pump Data: $T_o = 636$ ft lbf, $I_P = 19.5$ lbm ft^2, $\omega_o = 375$ rad/s, $\eta_o = 0.86$.

Solution: We first find volumetric flow rate at steady state:

$$\dot{V}_o = \frac{T_o \eta_o \omega_o}{\Delta P_o} = \frac{636 \times 0.86 \times 375}{93 \times 144} = 15.3 \text{ ft}^3/\text{s}$$

To find $t_{1/2}$, we note that $H_{Po} = \Delta P_o/\rho_g = 93 \times 144/62.87 = 213$ ft

$$(t_{1/2})_L = \frac{I_L}{g}\frac{\dot{V}_o}{H_{Po}} = \frac{108}{32.2}\frac{15.3}{213} = 0.241 \text{ s}$$

To find α, we need to first find $(t_{1/2})_P$:

$(t_{1/2})_P = I_P(\omega_o/T_o) = (19.5/32.2)(375/636) = 0.357$ s. Therefore, $\alpha = 0.241/0.357 = 0.68$

We now find $\theta_1 = 1/0.241 = 4.15, \theta_2 = 2/0.241 = 8.3$, and $\theta_3 = 3/0.241 = 12.4$. From Figure VId.5.1, we obtain $\Phi_1 \cong 0.4$, $\Phi_2 \cong 0.25$, and $\Phi_3 \cong 0.18$

Hence, $\dot{V}_1 \cong 0.4 \times 15.3 \cong 6$ ft^3/s, $\dot{V}_2 \cong 0.25 \times 15.3 \cong 4$ ft^3/s, and $\dot{V}_3 = 0.18 \times 15.3 \cong 2.7$ ft^3/s.

5. Mathematical Model for PWR Components, Pressurizer

PWRs are filled with water, which remains subcooled during normal operation. Hence, a pressurizer is necessary to control water inventory and the system pressure. The volume of this tank is about 2% of the volume of the PWR primary system. A pressurizer is usually about half filled with water and half with steam. Since water and steam co-exist at equilibrium, both phases are saturated at the system pressure during normal operation. The pressurizer is attached to the hot leg through a pipe run referred to as the *surge line*. The vapor space allows for water to flow from the RCS into the pressurizer (in-surge) during transients that result in the expansion of the RCS water. The water region also allows water to flow from the pressurizer into the RCS (out-surge) during transients that result in contraction of the RCS inventory.

A pressurizer is equipped with spring loaded pressure safety valves (PSV), with pilot operated relief valves (PORV), with spray nozzles, and with two sets of heaters. The pressurizer design constraints include the existence of sufficient vapor space to prevent water from reaching the relief valves and sufficient water volume to prevent uncovering of the electric heaters. One set of heaters is designed to offset the heat loss through the insulation and maintain pressure. The other set of heaters is to produce steam following an out-surge, as shown in Figure VId.5.1.

Power increase. Events resulting in a power increase cause the RCS water temperature to rise. This is associated with an increase in water specific volume and subsequent expansion of water. The increase in water volume results in a rush of water from the surge line into the pressurizer and compression of steam in the bulk vapor region. The subsequent rise in the pressurizer pressure is controlled by

the spray control valve injecting colder water from the cold leg into the vapor space. Additional relief is provided by the chemical and volume control system (CVCS) by opening the letdown valve and allowing water to flow to the CVCS tank. Manual depressurization of the pressurizer is also possible by remote opening of the PORVs.

Power decrease. Events leading to a drop in the reactor power cause the water temperature, and hence, the water specific volume to decrease. The subsequent drop in the RCS water volume is compensated by the pressurizer water rushing to the RCS through the surge line. This results in the expansion of the bulk vapor space and a drop in the pressurizer pressure. Pressure is partially restored due to the flashing of water in the pressurizer. Additionally, the pressurizer heaters are activated by the pressure controller. If water drops below the low level set point, indicating the likelihood of heaters to be uncovered, the positive displacement charging pumps are automatically started to add coolant to the RCS from the CVCS tank.

Wall effect. The pressurizer wall also participates in the pressure control mechanism. During an in-surge, when steam may become superheated, the colder wall acts as a heat sink to condense some steam. In an out-surge, the warmer wall would heat up the expanding steam, which helps prevent excessive pressure drop. Also, during an out-surge, the warmer wall may result in boiling water adjacent to the wall. Hence, the heat transfer regime between wall and the fluid is either natural convection or results in the change of phase.

Mass and energy processes. Various mass and energy processes are discussed below. In this discussion, we use subscript l to represent the water region and v for the vapor region. To be consistent, we use subscripts f and g to represent the saturation properties. Hence, h_l stands for the enthalpy of water. If $h_l = h_f$ then the water is saturated. Otherwise, it is subcooled. Similarly, if $h_v = h_g$ then the steam is saturated. Otherwise, it is superheated. Figure VId.5.1 shows the various mass and associated energy transfer rates between regions. These include:

- surge flow rate to or from the water region, ($\dot{m}_{su}$, h_{su}). In an in-surge, $h_{su} = h_{HL}$ and in an out-surge $h_{su} = h_l$
- spray flow rate, to lower pressure, added to the water region ($\dot{m}_{sp}$, h_{sp})
- spray condensation flow from the steam region to the water region ($\dot{m}_{sc}$, h_f)
- flashing from the water to the steam region due to depressurization ($\dot{m}_{fl}$, h_g)
- rainout from the steam to the water region due to depressurization ($\dot{m}_{ro}$, h_f)
- wall condensation from steam to the water region ($\dot{m}_{wc}$, h_f)
- wall boiling from water to the steam region ($\dot{m}_{wb}$, h_g)
- safety and relief valve flow rate from the steam region ($\dot{m}_{rv}$, h_v)

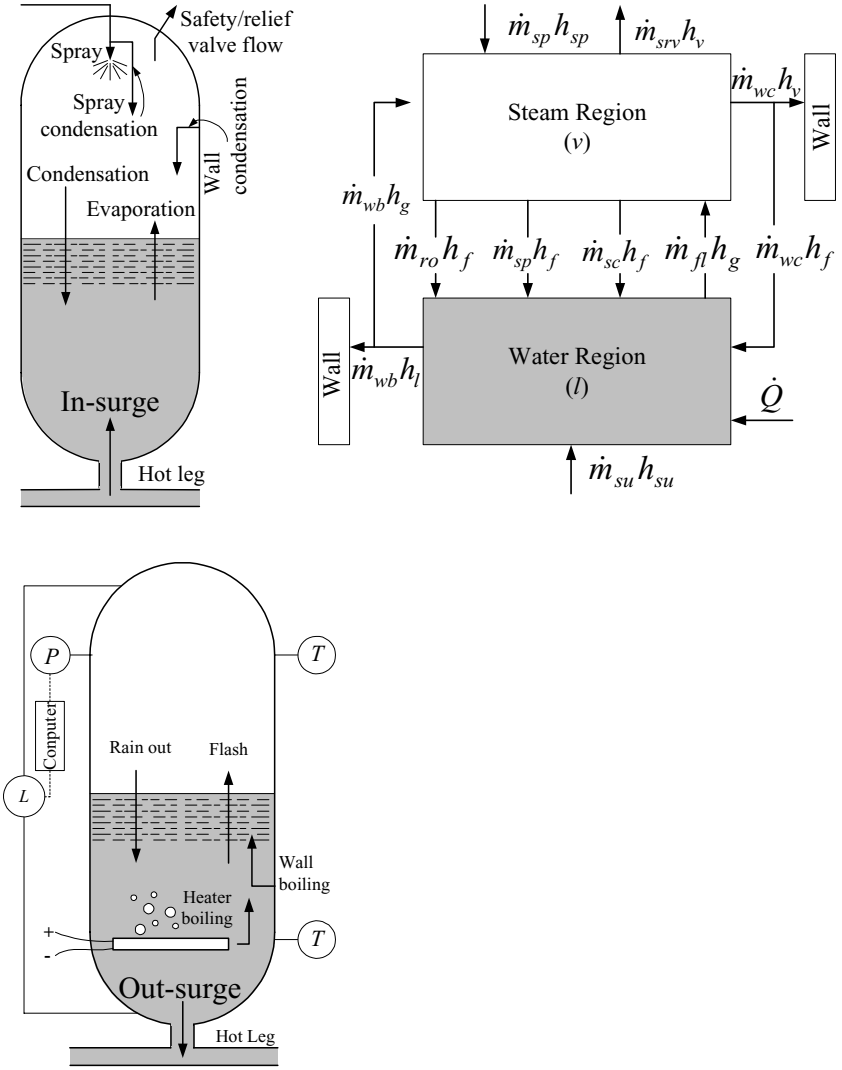

Figure VId.5.1. Various mass and energy processes in a PWR pressurizer

– condensation on and evaporation from the bulk interface ($\dot{m}_{ic}, h_f$ and $\dot{m}_{ie}, h_g$), not shown on Figure VId.5.1
– non-condensable gases, released into the steam region (-).

– heater power in the water region and heat transfer to wall from water and steam, ($\dot{Q}_h$),($\dot{Q}_{lw}$) and ($\dot{Q}_{vw}$).

Pressurizers use a surge sparger to dampen the momentum of the in-surge. The penetration depth of the in-surge water to the water region is generally limited to about 30 cm (1 ft).

Mathematical model. Generally, the extent of information obtained from a mathematical model depends on the degree of complexity of the model. While we may make reasonable assumptions to simplify a model, we should be careful about the effect of such assumptions on the accuracy of the results. For example, we may use one control volume to represent the entire pressurizer by assuming that water and steam are well mixed and remain at one pressure and temperature during a transient. While this approach simplifies the analysis it may actually lead to erroneous result in case of an in-surge into the pressurizer. During an in-surge, the bulk vapor region is compressed causing the pressurizer pressure to rise (condensation of steam on the colder wall somewhat reduces the rate of pressure increase). On the other hand, by using a one-node model in which the colder in-surge water mixes with the steam and water mixture, we would calculate a drop in the pressurizer pressure.

In a two-region model, we consider two deformable control volumes for the bulk water and bulk vapor region. We use the term "bulk" to distinguish the water droplets in the bulk vapor region from water in the bulk water region and steam bubbles in the bulk water region from steam in the bulk vapor region. A three region model could allocate another deformable control volume to the colder in-surge in the lower portion of the pressurizer and a four region model could allocate a deformable control volume to each of the bulk water region, bulk vapor region, drops in the bulk vapor region, and bubbles in the bulk water region.

Example VId.5.1. In a transient, water rushes into the pressurizer at 58.94 lbm/s for 17.5 seconds at an average pressure and temperature of 700 psia and 450 F. Estimate the pressurizer pressure. Ignore any interaction at the wall and at the bulk fluid interface. Assume that the pressurizer is a right circular cylinder, no spray or safety valve is actuated, and ignore condensation on the wall.
Data: $V_{Pressurizer} = 700$ ft^3, $V_{water} = 100$ ft^3, $T_{inital} = 500$ F ($P_{initial} = 680.86$ psia).

Solution: a) No mixing assumption: If the transient is fast and there is not sufficient time for perfect mixing, we may find the peak pressure by assuming isentropic compression of the steam region.

Initially, at P= 700 psia and T = 450 F, $v_{su} = 0.01939$ ft^3/lbm and $h_{su} = 430.38$ Btm/lbm. To find the steam volume after compression, we need the in-surge mass and total volume:
$m_{su} = \dot{m}_{su} \Delta t = 58.94 \times 17.5 = 1031.45$ lbm

Hence, $V_{su} = m_{su}v_{su} = (58.94 \times 17.5) \times 0.01939 = 20$ ft^3. The steam volume following compression is:
$(V_{steam})_2 = (V_{steam})_1 - V_{su} = 600 - 20 = 580$ ft^3
We find P_2 from Equation IIa.4.3:
$P_2 = P_1[(V_{steam})_1/(V_{steam})_2]^{(0.445/0.335)} = 680.86 \times (600/580)^{1.328} = 712.2$ psia.

b) Perfect mixing assumption: At $T_1 = 500$ psia, $v_{f1} = 0.0204$ ft^3/lbm, $v_{g1} = 0.6749$ ft^3/lbm
$m_1 = m_{f1} + m_{g1} = 4901 + 889 = 5790$ lbm and $x_1 = 0.153$ so that $u_1 = 486.1 + 0.153 \times 631 = 572.98$ Btu/lbm
Using Equation IIa.6.4 gives: $\dot{m}_i h_i = d(mu)/dt$. The integration of this equation yields: $m_2u_2 = m_1u_1 + m_{su}h_{su}$
$u_2 = [m_1u_1 + m_{su}h_{su}]/(m_1 + m_{su})$ and $v_2 = V/(m_1 + m_{su})$

$m_2 = m_1 + m_{su} = 5790 + 103.45 = 6821.7$ lbm

$u_2 = [5790 \times 572.98 + 500 \times 613]/6821.7 = 839$ Btu/lbm
$v_2 = 1000/22{,}222 = 0.045$ ft^3/lbm

Pressure corresponding to $v_2 = 0.045$ ft^3/lbm and $u_2 = 839$ Btu/lbm is $P_2 = 672.85$ psia. This model predicts a drop in pressure following the in-surge.

5.1. Two-Region Pressurizer Model

Development of the two-region mathematical model for the pressurizer is based on the Nahavandi method. We allocate one deformable control volume to the bulk water and another to the bulk vapor region. To find the various thermodynamic states of these two control volumes, we compare the enthalpy of each region (h_l and h_v) with $h_f(P)$ and $h_g(P)$. There are a total of 12 possible states as shown in Table VIc.5.2. However, we do not consider the meta-stable states where $h_l > h_f$ and $h_v < h_g$. These meta-stable states are shown in Figure VIc.5.2 for a depressurization process from an initial pressure of P_o to a final pressure of $P_o - \Delta P$. By not allowing such meta-stable states, we need to consider only four cases of a) saturated liquid, superheated vapor, b) saturated liquid, saturated vapor, c) subcooled liquid, saturated vapor, and d) subcooled liquid, superheated vapor. Selecting P and h as the state variables for each region, we begin with Equation IIa.5.1 and include all the transfer terms explicitly. For the water region we find:

Table VIc.5.2. Thermodynamic states in a 2-region model

$h_v < h_g$	$h_v = h_g$	$h_v > h_g$
$h_l < h_f$	$h_l < h_f$	$h_l < h_f$
$h_l = h_f$	$h_l = h_f$	$h_l = h_f$
$h_l > h_f$	$h_l > h_f$	$h_l > h_f$

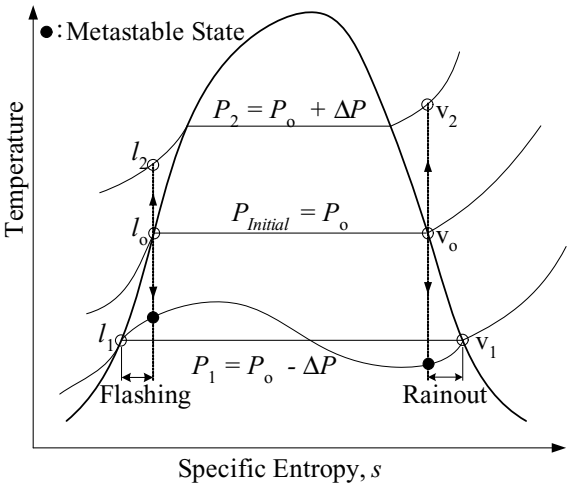

Figure VId.5.2. Isentropic rainout and flashing in a pressurizer during an out-surge transient (Todreas)

$$\frac{dm_l}{dt} = \dot{m}_{su} + \dot{m}_{sp} - \dot{m}_{fl} + \dot{m}_{ra} + \dot{m}_{wc} + \dot{m}_{sc} + \dot{m}_{ic} - \dot{m}_{ie} = \left(\sum_j \dot{m}_j\right)_l$$

and for the vapor region, the conservation equation of mass, Equation IIa.5.1 becomes:

$$\frac{dm_v}{dt} = \dot{m}_{fl} - \dot{m}_{ro} - \dot{m}_{wc} - \dot{m}_{sc} - \dot{m}_{rv} - \dot{m}_{ic} + \dot{m}_{ie} = \left(\sum_j \dot{m}_j\right)_v$$

We now use the conservation equation of energy for the water region, Equation IIa.6.4-1, to obtain:

$$\frac{d(m_l h_l)}{dt} = \dot{m}_{su}h_{su} + \dot{m}_{sp}h_f - \dot{m}_{fl}h_g + \dot{m}_{ro}h_f + \dot{m}_{wc}h_f + \dot{m}_{wc}h_f + \dot{m}_{ic}h_f - \dot{m}_{ie}h_g + \dot{Q}_h - \dot{Q}_{lw} + c\mathrm{V}_l\dot{P}$$

and apply Equation IIa.6.4-1 to the vapor region to obtain:

$$\frac{d(m_v h_v)}{dt} = \dot{m}_{sp}(h_{sp} - h_f) + \dot{m}_{fl}h_g - \dot{m}_{ro}h_f - \dot{m}_{wc}h_f - \dot{m}_{wc}h_f - \dot{m}_{rv}h_v - \dot{m}_{ic}h_f + \dot{m}_{ie}h_g - \dot{Q}_{vw} + c\mathrm{V}_v\dot{P}$$

Note that there is no shaft work and the shear work is ignored. Following the same method used in Chapter IIa to analyze the dynamics of gas-filled rigid vessels, we write the conservation equations as:

$$\frac{dm_k}{dt} = \left[\sum_j \left(\dot{m}_j\right)\right]_k$$

for mass in each control volume or region and as:

$$\frac{d\left(m_k h_k\right)}{dt} = \left[\sum_j \left(\dot{m}_j h_j + \dot{Q}_j + \dot{W}_{sj}\right)\right]_k + \mathrm{V}_k \dot{P}$$

for energy. Subscript *j* represents the various processes associated with a region and subscript *k* is a region index. We now make use of the volume constraint as $\mathrm{V}_l + \mathrm{V}_v = \mathrm{V}$ where V is the total volume of the pressurizer. Taking the derivative of the volume constraint relation and setting it to zero yields:

$$\frac{d(m_k \mathrm{v}_k)}{dt} = \sum\left(\dot{m}_k \mathrm{v}_k + m_k \dot{\mathrm{v}}_k\right) = \sum\left[\dot{m}_k \mathrm{v}_k + m_k\left(\frac{\partial \mathrm{v}_k}{\partial h_k}\dot{h} + \frac{\partial \mathrm{v}_k}{\partial P}\dot{P}\right)\right] = 0$$

VId.5.1

where in Equation VId.5.1, the summation is over the two regions of liquid and vapor. Hence, $k = l$ and v. Also in Equation VId.5.1 noting that $\mathrm{v} = f(P, h)$, the derivative of the specific volume of each region was expressed in terms of the partial derivatives with respect to pressure as well as the enthalpy of each region. We now carry out the derivatives of the energy equations. For the bulk liquid region we find:

$$\dot{h}_l = \left\{\left[\sum_j \left(\dot{m}_j h_j + \dot{Q}_j + \dot{W}_{sj}\right)\right]_l + \mathrm{V}_1 \dot{P} - \left[\sum_j \dot{m}_j\right] h_l\right\} / m_l$$

Similarly, for the bulk vapor region, the enthalpy derivative becomes:

$$\dot{h}_v = \left\{\left[\sum_j \left(\dot{m}_j h_j + \dot{Q}_j + \dot{W}_{sj}\right)\right]_v + \mathrm{V}_v \dot{P} - \left[\sum_j \dot{m}_j\right] h_v\right\} / m_v$$

Substituting the enthalpy derivatives ($\dot{h}_l$ and $\dot{h}_v$) into Equation VId.5.1 while also substituting from the conservation equations of mass we find the pressurizer pressure derivative as:

$$\dot{P} = -\frac{\sum_k \left\{\left(\sum_j \dot{m}_j\right)_{\mathrm{k}} \mathrm{v}_k + \left[\sum_j \left(\dot{m}_j h_j + \dot{Q}_j + \dot{W}_{sj}\right)_k - \left(\sum_j \dot{m}_j\right)_k h_k\right] \frac{\partial \mathrm{v}_k}{\partial h_k}\right\}}{\sum_k \left\{m_k \frac{\partial \mathrm{v}_k}{\partial P} + \mathrm{V}_k \frac{\partial \mathrm{v}_k}{\partial h_k}\right\}}$$

VId.5.2

Similar to the solution of Section 3, back substitution of pressure derivative results in finding the enthalpy derivatives. The mass and enthalpy of each region are then found by integration over each time step. As seen from Equation VIc.5.2, we also

need the derivatives of the properties. Such derivatives can be obtained by various means. For example, if properties are represented by least square fit to the data, we can then take the derivatives of the related functions.

This method of solution resulted in the explicit derivation for the control volume pressure. We used five equations (two conservation equations of mass, two conservation equations of energy, and one volume constraint) and we found five unknowns (P, h_l, h_v, m_l, and m_v). This in turn requires all other terms to be obtained from the related constitutive equations and the equations of state. Therefore, we need constitutive equations for such mass flow rates as flashing, rainout, spray condensation, wall condensation, surface evaporation, and condensation. If the pressurization of the vapor region results in the opening of a safety or relief valve, the corresponding flow rate is calculated from the momentum equation. If flow happens to be choked in a relief valve, the momentum equation appears in the form of the critical flow for the related valve.

5.2. Constitutive Models, Spray Condensation

To be able to find pressure from Equation VId.5.2, in general we need to find constitutive equations for various mass flow rates. Constitutive equations are also needed for the rate of heat transfer to or from a region. An example for such an equation includes a model for the estimation of the rate of steam condensation on the spray droplets injected into the steam region. If we assume that the subcooled spray flow rate reaches saturation to condense steam, a steady state energy balance predicts the rate of steam condensation as:

$$\dot{m}_{sc} = \frac{h_f - h_{sp}}{h_s - h_f} \dot{m}_{sp}$$

where h_{sp} and h_s are the spray and the steam enthalpy, respectively. In this relation, we assumed that steam is saturated, then $h_s = h_g$.

Example VId.5.2. A PWR pressurizer, operating at steady state condition at 15.51 MPa, is suddenly subject to a constant in-surge flow rate for 1 minute. Determine the pressurizer response to this event. For this purpose, use a two-region model for water and steam, ignore all transport processes at the fluid-fluid and solid fluid interfaces including water flashing to steam.
Data: D = 2.5 m, H = 10 m, V_{water} = 25 m^3, surge flow rate = 7 kg/s for 60 s, surge enthalpy = 1442 kJ/kg, A_{rv} = 1E-4 m^2, C_D = 0.61, $(P_{Actuation})_{rv}$ = 17 MPa, $(P_{Reset})_{rv}$ = 16 MPa. Subscript *rv* stands for relief valve.

Solution: The rate of pressurization is given by Equation VId.5.2, which for a two-region system becomes (subscripts i and e stand for into and exit from a region, respectively):

$$\dot{P} = -\frac{\left[\left(\Sigma\dot{m}_{i1} - \Sigma\dot{m}_{e1}\right)\mathrm{v}_1 + \left(\Sigma\dot{m}_{i2} - \Sigma\dot{m}_{e2}\right)\mathrm{v}_2\right] + \left[\Sigma\dot{m}_{i1}\left(h_{i1} - h_{e1}\right) + \Sigma\dot{Q}_{i1}\right]\frac{\partial \mathrm{v}_1}{\partial h_1} + \left[\Sigma\dot{m}_{i2}\left(h_{i2} - h_{e2}\right) + \Sigma\dot{Q}_{i2}\right]\frac{\partial \mathrm{v}_2}{\partial h_2}}{\left(m_1\frac{\partial \mathrm{v}_1}{\partial P} + m_2\frac{\partial \mathrm{v}_2}{\partial P}\right) + \left(\mathrm{V}_1\frac{\partial \mathrm{v}_1}{\partial h_1} + \mathrm{V}_2\frac{\partial \mathrm{v}_2}{\partial h_2}\right)}$$

In this equation $\Sigma\dot{m}_{i1} = \dot{m}_{su}$, $\Sigma\dot{m}_{e1} = 0$, $\dot{m}_{i2} = 0$ and $\dot{m}_{e2} = \dot{m}_{rv}$.

Since no heater power is given and there is no interface heat transfer $\dot{Q}_1 = \dot{Q}_2 = 0$. The FORTRAN program is included on the accompanying CD-ROM. The results for pressure and steam temperature are shown below.

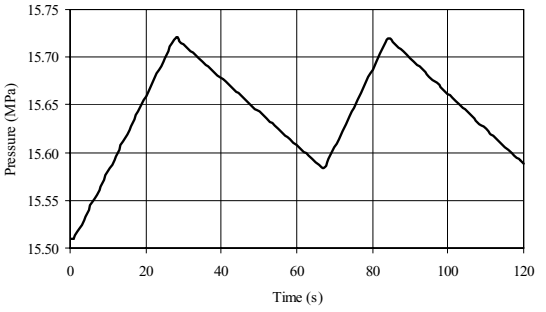

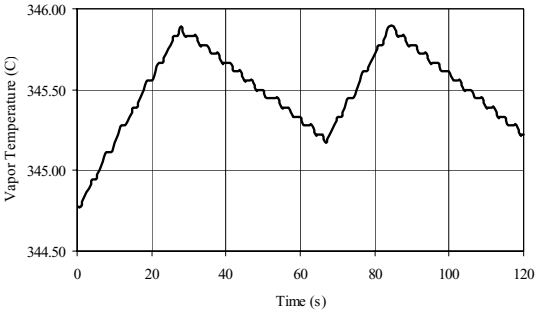

6. Mathematical Model for PWR Components, Containment

In addition to bulk water and bulk vapor regions, often control volumes may also include non-condensable gases in the bulk vapor region. Examples include the pressurizer with accumulated fission gases and the BWR and PWR plant containment. To solve for the pressures and temperatures, we use the method of Section 5. To simplify the formulation, we assign subscripts 1, 2, and 3 to water in the pool, steam in the bulk vapor region, and gas in the bulk vapor region. Figure VId.6.1(a) shows a system which consists of two control volumes, one for the bulk water region or the pool and one for the bulk vapor region. Various proc-

esses can take place for the system shown in Figure VId.6.1(a) including water addition to or removal from the pool region, steam and gas addition or removal from the bulk vapor region, heat addition or removal from each region, and spray addition to the bulk vapor region. Figure VId.6.1(b) shows steam injection into the bulk vapor region and the associated division of the injected two-phase into water and steam.

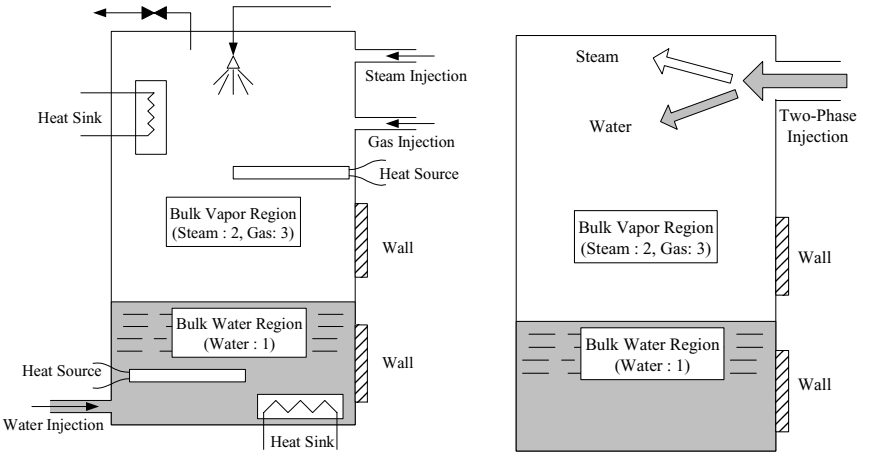

Figure VId.6.1. (a) A control volume with water and a mixture of steam and gas and (b) Division at the break

Following the method of Section 5, we write the conservation equations of mass for water in the bulk water region, steam in the bulk vapor region, and gas in the bulk vapor region:

$$\frac{dm_k}{dt} = \alpha_k \qquad \text{VId.6.1}$$

where for water in the bulk water region

$$\alpha_1 = \sum \dot{m}_{j,1} = \dot{m}_{in,1} + \dot{m}_{sp} + \dot{m}_{sc} + \dot{m}_{wc} + \dot{m}_{ro} - \dot{m}_{fl} - \dot{m}_{ev} - \dot{m}_{wb} \ ,$$

for steam in the bulk vapor region,

$$\alpha_2 = \sum \dot{m}_{j,2} = \dot{m}_{in_{,2}} + \dot{m}_{fl} + \dot{m}_{wb} + \dot{m}_{ev} - \dot{m}_{sc} - \dot{m}_{wc} - \dot{m}_{ro} - \dot{m}_{srv,2} \ ,$$

and for gas in the bulk vapor region, $\alpha_3 = \sum \dot{m}_{j,3} = \dot{m}_{in,3} - \dot{m}_{srv,3}$ where subscript *in* refers to the two-phase injection into the bulk vapor region. Other subscripts are the same as for pressurizer in Figure VId.5.1.

Unlike the conservation equation of mass, we write two conservation equations of energy, one for the water in the bulk water region and one for steam and gas in the bulk vapor region. For the pool region, we have:

$$\frac{d(m_1 h_1)}{dt} = \beta_1 + c\mathrm{V}_1 \dot{P}_1 \qquad \text{VId.6.2}$$

where $\beta_1 = \sum (\dot{m}h)_{j,1} + \sum \dot{Q}_1$. Similarly, for the steam and gas in the vapor region we write:

$$\frac{d(m_2 h_2 + m_3 h_3)}{dt} = \beta_{2-3} + c\mathrm{V}_2 (\dot{P}_2 + \dot{P}_3) \qquad \text{VId.6.3}$$

where P_1, P_2, and P_3 in Equations VId.6.1 through VId.6.3 are the control volume total pressure and steam and gas partial pressures, respectively. Similar to β_1, in Equation VId.6.3, $\beta_{2-3} = \sum (\dot{m}h)_{j,2-3} + \sum \dot{Q}_{2-3}$. Subscript 1 refers to the pool region and subscript 2-3 refers to the bulk vapor region.

In this formulation we have assumed only one non-condensable gas to exist in the bulk vapor region. If there are several gases in the bulk vapor region, we write as many conservation equations of mass as the number of gases in the bulk vapor region and include their effect in the related energy equation for the bulk vapor region (i.e., Equation VId.6.3).

There are a total of nine unknowns: m_1, m_2, m_3, h_1, h_2, h_3, P_1, P_2, and P_3. So far we have obtained five equations. We find the sixth equation from the volume constraint as $\mathrm{V}_1 + \mathrm{V}_2 = \mathrm{V}_{total}$. Substituting for $\mathrm{V} = m\mathrm{v}$ and taking the derivative of both sides we obtain:

$$\frac{d(m_1 \mathrm{v}_1)}{dt} + \frac{d(m_2 \mathrm{v}_2)}{dt} = 0 \qquad \text{VId.6.4}$$

Three more equations are needed for which we use the principles of the Dalton model. From $P_1 = P_2 + P_3$:

$$\dot{P}_1 = \dot{P}_2 + \dot{P}_3 \qquad \text{VId.6.5}$$

Also according to the Dalton model, $T_2 = T_3$ hence:

$$\dot{T}_2 - \dot{T}_3 = 0 \qquad \text{VId.6.6}$$

The last remaining equation is obtained by noting that according to the Dalton model the same volume in the bulk vapor region is occupied by steam and gas so $\mathrm{V}_2 = \mathrm{V}_3$ and, thus $\mathrm{V}_1 + \mathrm{V}_3 = \mathrm{V}_{total}$. Substituting and taking the derivative we get:

$$\frac{d(m_1 \mathrm{v}_1)}{dt} + \frac{d(m_3 \mathrm{v}_3)}{dt} = 0 \qquad \text{VId.6.7}$$

The set of nine equations may be reduced to six by substitution from the continuity equations into the energy equations. The resulting set at every time step is found as:

$$\begin{bmatrix} m_1 & 0 & 0 & -c\mathrm{V}_1 & 0 & 0 \\ 0 & m_2 & m_3 & -c\mathrm{V}_2 & 0 & 0 \\ m_1\dfrac{\partial \mathrm{v}_1}{\partial h_1} & m_2\dfrac{\partial \mathrm{v}_2}{\partial h_2} & 0 & m_1\dfrac{\partial \mathrm{v}_1}{\partial P_1} & m_2\dfrac{\partial \mathrm{v}_2}{\partial P_2} & 0 \\ m_1\dfrac{\partial \mathrm{v}_1}{\partial h_1} & 0 & m_3\dfrac{\partial \mathrm{v}_3}{\partial h_3} & m_1\dfrac{\partial \mathrm{v}_1}{\partial P_1} & 0 & m_3\dfrac{\partial \mathrm{v}_3}{\partial P_3} \\ 0 & \dfrac{\partial T_2}{\partial h_2} & -\dfrac{\partial T_3}{\partial h_3} & 0 & \dfrac{\partial T_2}{\partial P_2} & -\dfrac{\partial T_3}{\partial P_3} \\ 0 & 0 & 0 & 1 & -1 & -1 \end{bmatrix} \begin{pmatrix} \dot{h}_1 \\ \dot{h}_2 \\ \dot{h}_3 \\ \dot{P}_1 \\ \dot{P}_2 \\ \dot{P}_3 \end{pmatrix} =$$

$$\begin{pmatrix} \beta_1 - \alpha_1 h_1 \\ \beta_2 - \alpha_2 h_2 - \alpha_3 h_3 \\ -\alpha_1 \mathrm{v}_1 - \alpha_2 \mathrm{v}_2 \\ -\alpha_1 \mathrm{v}_1 - \alpha_3 \mathrm{v}_3 \\ 0 \\ 0 \end{pmatrix} \qquad \text{VId.6.8}$$

Equation VId.6.8 can be solved by Gaussian elimination. Having initial volumes, masses, enthalpies, physical properties and their derivatives, we can find enthalpy and pressure derivatives by solving the above set. The mass, enthalpy, pressure and volume derivatives are then integrated over a time step to find pressures, masses, volumes and enthalpies in a subsequent time step:

$$\begin{aligned} m_k^{N+1} &= m_k^N + \alpha_k \Delta t \\ h_k^{N+1} &= h_k^N + \dot{h}_k \Delta t \\ P_k^{N+1} &== P_k^N + \dot{P}_k \Delta t \\ \mathrm{V}_k^{N+1} &= \mathrm{V}_k^N + \dot{\mathrm{V}}_k \Delta t \end{aligned}$$

This process is repeated until the end of the specified transient is reached.

In addition to the constitutive equations required to represent many of the processes as discussed in Section 5, we use three equations of states for water, steam, and gas to obtain

$$\begin{aligned} \mathrm{v}_k &= f_{1,k}(P_k, h_k), \\ T_k &= f_{2,k}(P_k, h_k), \end{aligned}$$

$$\partial \mathrm{v}_k / \partial h_k = f_{3,k}(P_k, h_k),$$
$$\partial \mathrm{v}_k / \partial P_k = f_{3,k}(P_k, h_k),$$
$$\partial T_k / \partial h_k = f_{5,i}(P_k, h_k), \text{ and}$$
$$\partial T_k / \partial P_k = f_{65,k}(P_k, h_k),$$

where index k = 1, 2, and 3. Derivative of properties of the gas in the bulk vapor region, treated as an ideal gas, is readily obtained as:

$$\frac{\partial \mathrm{v}_3}{\partial h_3} = \frac{R_3}{c_{p,3} P_3}, \quad \frac{\partial \mathrm{v}_3}{\partial P_3} = -\frac{\mathrm{v}_3}{P_3}, \quad \frac{\partial T_3}{\partial h_3} = \frac{1}{c_{p,3}}, \text{ and } \frac{\partial T_3}{\partial P_3} = 0.$$

Recall that properties of saturated water and saturated steam are functions of either pressure or temperature. However, properties of subcooled water and superheated steam are functions of two variables. Thermal hydraulic computer codes use curve fits to the steam tables. However, to simplify analysis in the following example, we are assuming that superheated steam can be treated as an ideal gas. This assumption is reasonable, especially for specific volume (v = *RT*/*P*) at low pressures and high temperatures. This assumption is less accurate for enthalpy of the superheated steam, $dh = c_p dT$, if c_p is treated as a constant.

Example VId.6.1. A heavy load drop inside a containment ruptures two pipes. One carrying superheated steam and the other compressed air. Estimate the containment response for the first 10 minutes to this event. Treat steam and air as ideal gases. Data: $V_{containment}$ = 2E6 ft^3 (56.6 m^3), P_o = 14.7 psia (101.3 kPa), T_o = 120 F (49 C), ϕ_o = 59%, $\dot{m}_{steam}$ = 100 lbm/s (45.36 kg/s), h_{steam} = 1200 Btu/lbm (2791 kJ/kg), $\dot{m}_{air}$ = 50 lbm/s (22.68 kg/s), T_{air} = 350 F (177 F). Ignore all safety systems and steam condensation.

Solution: We calculate the initial masses, pressures, volumes, and enthalpies. Since no pool region is specified, hence, V_1 = 0, and $V_2 = V_3$ = 2E6 ft^3 (56.6 m^3)

$P_2 = 0.59 \times P_{sat}$(120 F) = 1 psia (6.9 kPa), P_3 = 14.7 – 1 = 13.7 psia (0.094 kPa) and P_1 = 14.7 psia (101.3 kPa)
$h_2 = h_{100} + c_{p,2}(T - 100)$ = 1105.3 + 0.445(120 – 100) = 1114 Btu/lbm (2591 kJ/kg)
h_3 = 0.24(120 +460) = 139.2 Btu/lbm (323.7 kJ/kg)
$\mathrm{v}_2 = R_2 T_2 / P_2$ = 345.7 ft^3/lbm (21.58 m^3/kg). Thus, $m_2 = V/\mathrm{v}_2$ = 1.0E6/345.7 = 5785 lbm (2624 kg)
$\mathrm{v}_3 = R_3 T_3 / P_3$ = 15.68 ft^3/lbm (0.978 m^3/kg). Thus, $m_3 = V/\mathrm{v}_3$ = 1.0E6/15.68 = 1.275E5 lbm (0.578E5 kg).

Since we have only the vapor region, Equation VId.6.8 simplifies to:

$$\begin{pmatrix} m_2 & 0 & -c\mathrm{V}_2 & 0 \\ 0 & m_3 & 0 & -c\mathrm{V}_3 \\ m_2\dfrac{\partial \mathrm{v}_2}{\partial h_2} & -m_3\dfrac{\partial \mathrm{v}_3}{\partial h_3} & m_2\dfrac{\partial \mathrm{v}_2}{\partial P_2} & -m_3\dfrac{\partial \mathrm{v}_3}{\partial P_3} \\ \dfrac{\partial T_2}{\partial h_2} & -\dfrac{\partial T_3}{\partial h_3} & \dfrac{\partial T_2}{\partial P_2} & -\dfrac{\partial T_3}{\partial P_2} \end{pmatrix} \begin{pmatrix} \dot{h}_2 \\ \dot{h}_3 \\ \dot{P}_2 \\ \dot{P}_3 \end{pmatrix} = \begin{pmatrix} \beta_2 - \alpha_2 h_2 \\ \beta_3 - \alpha_3 h_3 \\ -\alpha_2 \mathrm{v}_2 + \alpha_3 \mathrm{v}_3 \\ 0 \end{pmatrix}$$

Next, we find the forcing functions:
$\alpha_1 = 0$ lbm/s, $\alpha_2 = 100$ lbm/s, and $\alpha_3 = 50$ lbm/s
$\beta_2 = 100 \times 1200 = 1.2\text{E}5$ Btu/s, and $\beta_3 = 50 \times 0.24(350 + 460) = 0.972\text{E}4$ Btu/s

We now develop derivatives of specific volumes and temperatures:

$\partial \mathrm{v}_2/\partial h_2 = R_2/c_{p,2}P_2 = (1545/18)/(0.445 \times 144P_2) = 1.339/P_2$
$\partial \mathrm{v}_3/\partial h_3 = 1.543/P_3$
$\partial \mathrm{v}_2/\partial P_2 = -\mathrm{v}_2/P_2 = -345.7/P_2 = -2.4$ ft^5/lbm·lbf
$\partial \mathrm{v}_3/\partial P_3 = -\mathrm{v}_3/P_3 = -15.68/P_3 = 7.97\text{E}{-3}$ ft^5/lbm·lbf
$\partial T_2/\partial h_2 = 1/c_{p,2} = 2.247$ lbm·F/Btu
$\partial T_3/\partial h_3 = 1/c_{p,3} = 4.167$ lbm·F/Btu

Upon substitution, the set of equations for the first time step becomes:

$$\begin{pmatrix} 5785 & 0 & -3.7\text{E}5 & 0 \\ 0 & 1.275\text{E}5 & 0 & -3.7\text{E}5 \\ 7746 & -14360 & -13888 & 1013.4 \\ 2.247 & -4.167 & 0 & 0 \end{pmatrix} \begin{pmatrix} \dot{h}_2 \\ \dot{h}_3 \\ \dot{P}_2 \\ \dot{P}_3 \end{pmatrix} = \begin{pmatrix} 8600 \\ 2760 \\ -33786 \\ 0 \end{pmatrix}$$

we find the four unknowns as $\dot{h}_2$ = 1300 Btu/lbm s, $\dot{h}_3$ = 70 Btu/lbm s, $\dot{P}_2$ = 20.3 psi/s and $\dot{P}_3$ = 24.1 psi/s. Having the derivatives, we find h_2, h_3, P_2, and P_3 at the next time step. The FORTRAN program to solve this problem is included on the accompanying CD-ROM. The results for this problem for temperature and relative humidity are shown in the plots. Containment pressure in 10 minutes reaches 40 psia (2.76 bar).

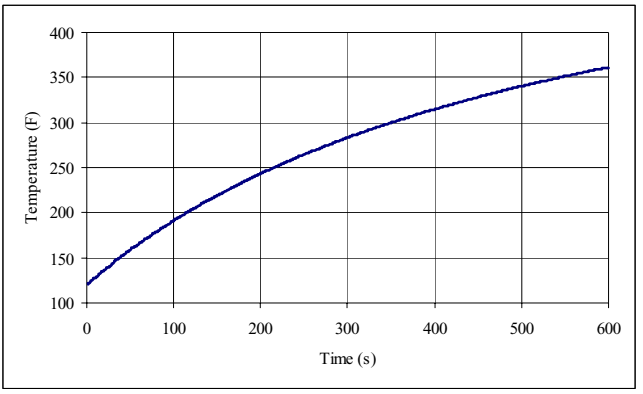

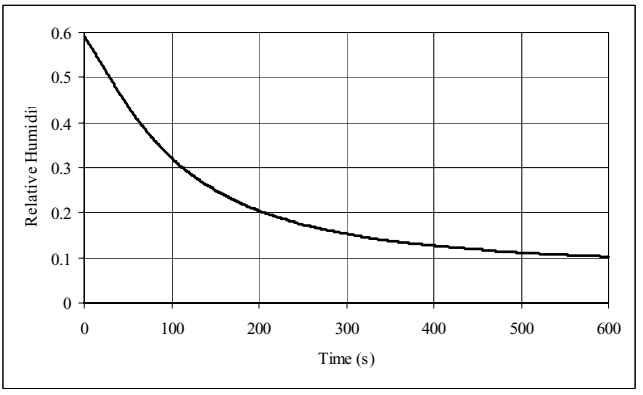

6.1. Break Flow Split

Consider the containment of Figure VId.6.1(b) initially being at P_o and T_o. We now inject saturated water or a two-phase mixture to the vapor region of this containment. The pressure and temperature of the injected flow are greater than those of the containment, $P_m > P_o$ and $T_m > T_o$, where subscript m stand for mixture. Our goal is to find the percentage of the injected flow that becomes steam and joins the vapor region and the portion that becomes water and flows to the pool region. Such injected flow split depends on the conditions at the plane of entrance to the containment. If the injected flow to the vapor region is saturated water for example, the flow partially flashes to steam upon entering the low pressure vapor region. The constitutive equations for determination of the injected flow split into two distinct phases in the containment are known as the *pressure flash* and the *temperature flash* models. Both models assume an isoenthalpic split of the injected flow so that:

$$\dot{m}_m h_m = \dot{m}_f h_f + \dot{m}_g h_g \qquad \text{VId.6.8}$$

However, the difference between the two models lies in the evaluation of the saturated water and saturated steam enthalpies. To elaborate, let's define the fraction of the flow which flashes to steam, χ as:

$$\chi = \frac{h_m - h_f(y_1)}{h_g(y_2) - h_f(y_1)} \qquad \text{VId.6.9}$$

In the pressure flash model, the saturation enthalpies are developed based on pressure. For example, $y_1 = y_2 = P_2$ (i.e. the partial pressure of steam). Another way to calculate the split fraction is to take $y_1 = P_1$ (i.e. total pressure in the containment) and $y_2 = P_2$ or to take $y_1 = y_2 = T_2$, as summarized in Table VId.6.1.

Table VId.6.1. Summary of various break flow split models

Break Flow Split		y_1	y_2
Pressure Flash	Model A	P_1	P_1
	Model B	P_1	P_2
	Model C	P_2	P_2
Temperature Flash		T	T

Note that in some references the temperature flash model is defined differently. In the temperature flash model described by Hargroves for example, the injected flow is instantaneously mixed and reaches equilibrium with the steam in the vapor region.

Example VId.6.2. A high energy pipe break occurs inside containment. Compare the split fraction of the break flow using various models of Table VId.6.1. Data: $P_o = 16.5$ psia, $T_o = 125$ F, $\phi_o = 51.5\%$, $h_m = 550$ Btu/lbm.

Solution: We find $P_2 = 0.515 \times P_{sat}(125\text{ F}) = 1$ psia. Thus, $P_3 = P_1 - P_2 = 16.5 - 1 = 15.5$ psia.

(a) $y_1 = y_2 = 16.5$ psia;
$\chi_a = (550 - 186.11)/(1152.7 - 186.11) = 0.376$ steam and 62.4% water

(b) $y_1 = 16.5$ psia and $y_2 = 1$ psia;
$\chi_b = (550 - 186.11)/(1105.8 - 186.11) = 0.395$ steam and 60.5% water

(c) $y_1 = y_2 = 1$ psia;
$\chi_c = (550 - 69.730)/(1105.8 - 69.730) = 0.463$ steam and 53.7% water

(d) $y_1 = y_2 = 125$ F;
$\chi_d = (550 - 92.960)/(1115.7 - 92.960) = 0.447$ steam and 55.3% water

7. Mathematical Model for PWR Components, Steam Generator

The function of a PWR U-tube steam generator is described in Chapter I. Feedwater entering the downcomer, Figure I.6.6(b) and mixing with the saturated water returning from the separator assembly enters the tube bundle to reach saturation and begins to boil. Heat is transferred from the primary side through the tubes to the two-phase flow, which further increases steam quality. The two-phase flow eventually enters the risers or stand pipes of the moisture separator. The saturated water flows downward to mix with the feedwater while saturated steam enters the dryer and eventually the steam line.

The primary side response was discussed in Section 3. We now discuss mathematical modeling of the secondary side. Figure VId.7.1(a) shows a simple nodalization of the secondary side of the steam generator. We may use this simple nodalization to estimate the mass, enthalpy, pressure, and velocity distribution, which is helpful in refining the nodalization. Like before, we may also apply the simplifying assumption of an integral, loop-wide momentum equation as discussed in Section 3. However, the loop in the case of the secondary side of a steam generator consists of the following flow path; steam generator downcomer, tube bundle, riser, separator, dryer. The flow path then leads to the steam dome and the steam line for the dry saturated steam and back to the downcomer for the saturated recirculation water, as shown in Figure VId.7.1(b).

The one dimensional integral momentum equation for the flow loop in the secondary side of the SG is found by applying Equation VId.3.15 to the various regions shown in Figure VId.7.1(b).

Determination of the Boil Off Rate

To obtain a simple relation for estimation of the boil-off flow rate, we consider a pot-boiler (no circulation) where heat is added to the water region, steam exits the water region and enters the steam region, and feedwater is added to the water region to maintain inventory. The mass flow rate of steam is given by Equation IIa.5.3:

$$\dot{m}_g = \rho_g V_g A_g = \rho_g V_g \left(\alpha_e A_c\right) \qquad \text{VId.7.1}$$

where α_e is the void fraction at the froth level (the interface between the water and the steam region) and A_c is the boiler cross sectional area at the froth level, perpendicular to the flow direction. Also in Equation VId.7.1, ρ_g and V_g are steam saturation density and steam velocity, respectively. Since ρ_g is a function of the operating pressure of the boiler (a known quantity) and A_c is the boiler flow area, also a known quantity, we need to find relations for α_e and V_g in terms of other known quantities. Void fraction is given by Equation IIId.2.2:

$$\alpha_e = \frac{X_e}{C_o[X_e + (\rho_g / \rho_f)(1 - X_e)] + (\rho_g V_{gj} A_c / \dot{m}_{boil})}$$

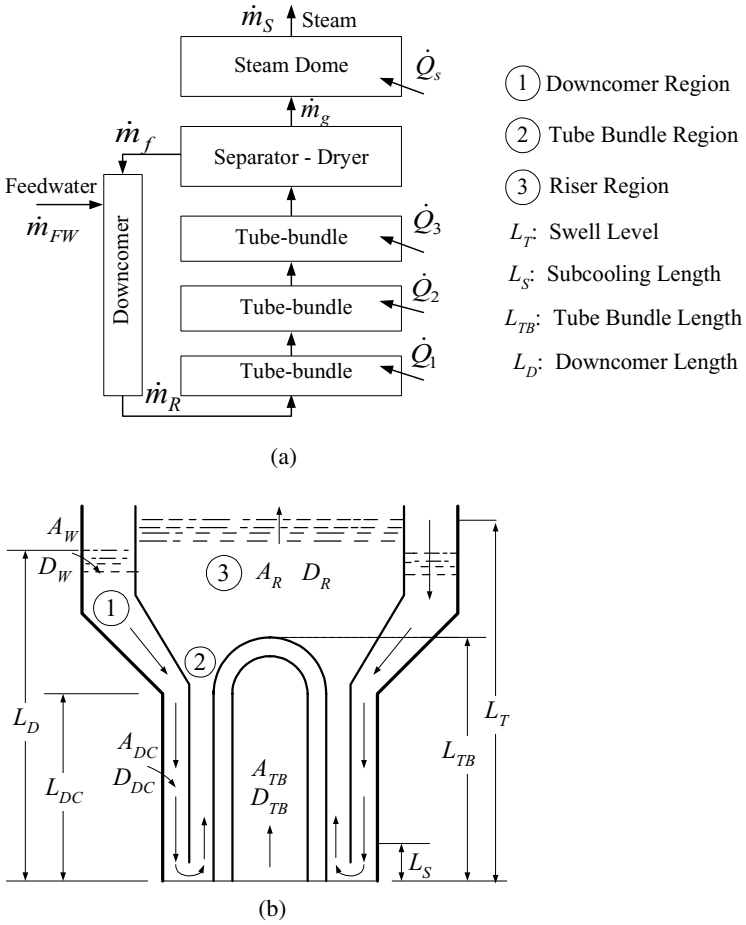

Figure VId.7.1. Mass and energy control volumes and flow paths for conservation equation of momentum

where X_e may be calculated from $X_e = (h_e - h_f)/h_{fg}$ and V_{gj} from Equation IIId.2.4. Finally, we find steam velocity, V_g from $V_g = J + V_{gj}$ where J may be estimated from $J = (\dot{m}_{FW} + \dot{m}_g)/(2\rho_e Ac)$. In this relation, subscript FW stands for feedwater and ρ_e is the mixture density. Substituting for a_e and V_g in Equation VId.7.1, we find an implicit second-order algebraic equation for the boil off mass flow rate.

QUESTIONS

- An electromagnetic pump is used to circulate fluid around a flow loop. Describe the flow trend if the pump is tripped. Compare it with a pump equipped with a flywheel.
- What is the role of the buoyancy head in early flow coastdown of a forced circulation loop?
- Thermal center in Equation VId.3.12 is defined based on T_H. How do you define it based on T_C?
- Can a natural circulation loop operate with the thermal center of the heat sink located slightly below that of the heat source?
- What are the important assumptions made that led to the derivation of Equation VId.3.16, used to estimate the natural circulation mass flow rate?
- What types of work should be considered in the derivation of the pressurizer pressure?
- In the derivation of the pressurizer pressure, only the conservation equations of mass and energy were used. What is the application of the momentum equation in the pressurizer?
- Consider the mass flow rate due to the condensation of steam on the wall of the pressurizer. Can we obtain this term from the conservation equations of mass and energy written for the water and the steam regions?
- Can Equation VIc.6.2 be applied to a three region pressurizer by taking $k = 3$?
- We used one pressure for the pressurizer, taken in the steam region. What assumption makes it possible to apply this same pressure to the water region?
- Plot the in-surge and the out-surge processes of a pressurizer on a *T-s* diagram.

PROBLEMS

1. Use the definition of thermal center and show that for the core, having near linear temperature profile, the thermal center is located at $H_{core}/2$ where H_{core} is the core height.

2. Derive Equation VId.3.13, the thermal center of a U-tube steam generator, where λ_{SG} is measured from the tube sheet. [Hint: Start with Equation VId.3.12. Then use the definition of the thermal expansion coefficient to relate density difference to temperature difference. Find λ_{SG} from:

$$\lambda_{SG} = \frac{\int_0^L [\rho(s) - \rho_H]\vec{g} \cdot d\vec{s}}{(\rho_C - \rho_H)g}$$

where the numerator is given in Example VId.3.1].

3. The following data are given for a U-tube steam generator. Tube mass flow rate $\dot{m} = 70E6$ lbm/h, total number of tubes $N = 8500$, tube outside diameter $d_o =$ 0.75 in, overall heat transfer coefficient $U_o = 1000$ Btu/h ft^2 F, average tube length

L = 60 ft, average tube height l = 28 ft, cold leg temperature T_C = 500 F, hot leg temperature T_H = 570 F, pressure P = 2265 psia. For this steam generator find a) the hydrostatic head and b) the thermal center.

4. The U-tube steam generator of Problem 3 is located in a PWR loop. Use the following data to find the loop hydrostatic head (i.e., the difference in the elevations of the heat source and heat sink thermal centers). Z_{SG} = 45 ft and $(Z_{th})_{core}$ = 30 ft.

5. A PWR is operating at a steady state condition. We now shutdown the plant and want to estimate the natural circulation flow rate. Although the reactor power decays after shutdown, we assume the core power remains steady for the duration of interest. Find the natural circulation flow rate 48 hours after shutdown. Data: Nominal reactor power: 3000 MWth, reactor pressure: 2265 psia, T_C = 550 F, T_H = 610 F, $\Sigma R = 0.28$ ft^{-4}.

6. Show that for large values of l^*, given in Equation VIa.5.8, the thermal center of a U-tube steam generator approaches $Z_{SG} = (1 + \delta)\, l/2$.

7. Derive Equation VId.3.14 by integrating the hydrostatic pressure term around a natural circulation flow loop. In this derivation assume a linear temperature profile over the heat source and apply Equation VId.3.12 for the heat sink. [Hint: Find the density profile in the core and the related hydrostatic head. Take the height from the heat source exit to the heat sink inlet as h_H in which ρ_H remains constant. Take the height from the heat sink exit to the heat source inlet as h_C in which ρ_C remains constant. Then use $h_C - H_{core}/2 = h_H + H_{core}/2$]

8. An experimental flow loop is constructed to study events in a PWR plant. The core consists of electrically heated rods and the two steam generators are simulated by two shell and tube heat exchangers. The vessel is connected to the heat exchangers by two hot legs and four cold legs. Water flows from the hot leg in the tubes while the secondary side water is cooled by a cooling tower. The following flow resistances are measured for this facility R_V = 227 ft^{-4}, R_{HL} = 560 ft^{-4}, R_{HX} = 369 ft^{-4}, R_{CL} = 767 ft^{-4}. Find the natural circulation flow a) assuming no pump exists in the loop and b) considering four non-operating pumps on each cold leg, R_{Pump} = 1793 ft^{-4}. Other design data are: core thermal power = 178 kW, core inlet temperature = 38 C, vertical distance between the core and the heat exchanger thermal centers = 0.75 m, average density = 985 kg/m^3, average specific heat = 4.18 kJ/kg K, and β = 0.37E-3 1/K.

9. Find the hydrostatic pressure in a flow loop operating at 3 MPa with T_C = 150 C and T_H = 175 C. In this loop, the distance between the heat source and heat sink thermal centers is 5 m. [Ans.: 1.6 kPa].

10. Derive the hydrostatic head for a once-through steam generator. Tubes are oriented vertically. Hot water enters the tubes from the top and leaves from the bottom. Water boils in the secondary side.

11. The flow resistance of a flow loop is given as 9.81 m^{-4}. The loop flow rate at steady state condition is 5 m^3/s. Find the total head loss in the loop. Also find the pressure drop in the loop. The average loop pressure and temperature are 2.5 MPa and 95 C, respectively. [Ans.: 12.5 m].

12. Show that the half life of a pump impeller is given by:

$$\left(t_{1/2}\right)_P = I_P \frac{2\eta_o \omega_o^2}{\rho R \dot{V}_o^3}$$

where η is the pump efficiency, R is the loop flow resistance, and $\dot{V}$ is the volumetric flow rate in the loop. Subscript o indicates nominal values.

13. A pump is operating in a flow loop at nominal speed. We now turn off the pump. Find the time it takes the impeller to reach half of its nominal speed. Data: ω_o = 124 s^{-1}, I_o = 2200 slug-ft^2, $\dot{V}$ = 85000 GPM, η_o = 0.78, R = 0.076 ft^{-4}, ρ_o = 38 lbm/ft^3. [Ans.: 2.7 s].

14. A natural circulation loop is shown in the figure. Verify the validity of Equation VId.3.14. Assume that the thermal centers for the heat source and heat sink, in this case, are located at the geometrical center of each source. The vertical distance between the two sources is shown by H_{th}. Elevations L_1, L_2, and L_3 are given.

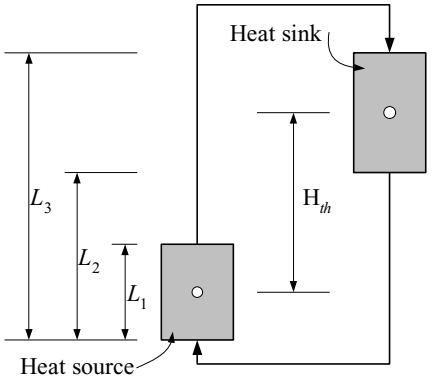

15. Define the system *thermal length* as the vertical distance between the thermal centers of the heat source and heat sink, $H_{th} = (Z_{th})_V - (Z_{th})_{SG}$ where subscript V stands for the heat source vessel and SG stands for the steam generator. In this problem we want to find the effect of the thermal length on the loop flow rate and the loop temperature gradient. Therefore, we keep changing the loop configuration with respect to the heat sink elevation. Due to height limitation of the building housing the loop, we would eventually have to place the steam generator horizontally. Assume all design parameters remain the same except for the increasing thermal length. a) Derive the loop flow rate as a function of the thermal length.

b) Prepare a table of loop flow rate and loop temperature gradient for various values of H_{th}. To do this, start from H_{th} = 0.3 m and conclude at Hth = 15 m using a 1 m height increment. c) Plot the values for $\dot{m}$ and for T_H versus H_{th}. d) Compare the vertical and the horizontal orientation of the heat sink and comment on the advantages and drawbacks of each orientation. Other Data: P = 4.48 MPa, $\overline{T}$ = 243 C, $\dot{Q}$ = 15 MW

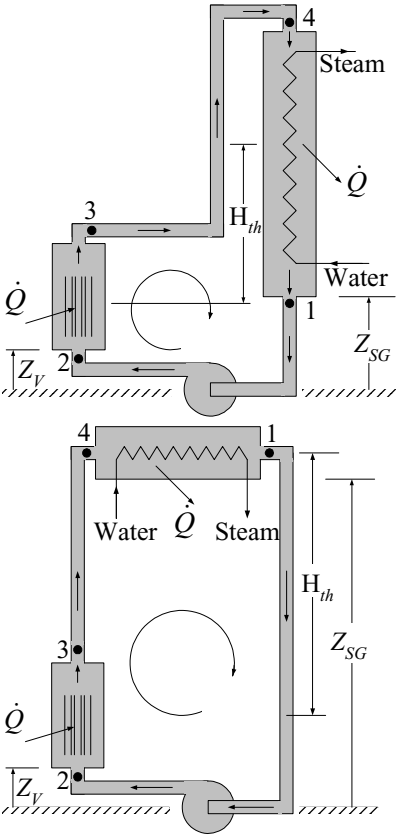

Region	A (m^2)	L (m)	D_e (m)	K
1-2	1.59	13.26	0.71	6
2-3	1.86	17.83	0.013	10
3-4	1.31	10.67	0.91	4
4-1	2.44	16.00	0.014	2

16. An approximate value for the mass flow rate in a natural circulation loop as given by Equation VId.3.18 was derived assuming a constant friction factor. a) By using Equations IIIb.3.2 and IIIb.3.6 show that in general, the mass flow rate is given by:

$$\dot{m}_{NC} = \left(\frac{2\beta g \overline{\rho}^2 H_{th} \dot{Q}_{\text{Core}}}{c_p R} \right)^{\frac{1}{3-n}}$$

where $n = 0.2$ for turbulent flow in all the sections of the flow loop and $n = 1$ for laminar flow in all the sections of the flow loop. b) Show that the maximum power that can be removed from the heat source in a natural circulation loop is given by:

$$\dot{Q} = \left[\frac{2\beta g \overline{\rho}^2 \mathrm{H}_{th}}{R} \right]^{\frac{1}{2-n}} (\Delta T)^{(3-n)/(2-n)} \overline{c}_p$$

where $\overline{\rho}, \overline{c}_p$, and $\overline{T}$ are the loop average density, specific heat, and temperature. Also H_{th} is the system thermal length, as defined in Problem 15.

17. Some nuclear power plants, which are facing space limitation in their spent fuel pool, place older fuel assemblies in steel cylinders, referred to as dry shielded canisters (DSC). The DSC is then hermetically sealed and placed horizontally inside a concrete bunker, known as the horizontal storage module (HSM). Decay heat is removed by natural convection. Colder air entering the HSM through the inlet screen leaves through the vents located at the top of HSM. The loss coefficient and flow area of the inlet and exit ports are as follows:

	$K_{\text{Outer screen}}$	$K_{\text{Inner screen}}$	$K_{\text{Enterance/Exit}}$	Area (m^2)
Inlet port	0.4	0.5	1.4	0.5
Exit port	0.4	0.5	1.0	1.0

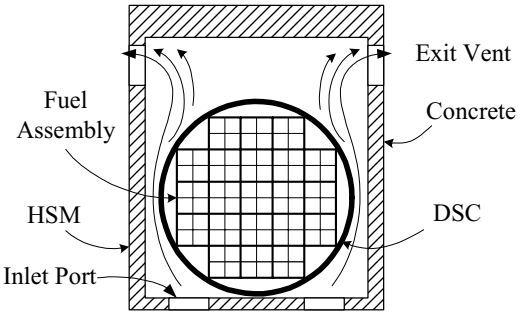

Total loss coefficient and flow area associated with the flow through the HSM are 2.5 and 0.5 m^2, respectively. Total rate of decay heat for the DSC is 15 kW. The system thermal length, as defined in Problem 14 is 3.5 m. Air enters the HSM at a temperature of 22 C. Assume air at exit is well mixed. Use the given data to find a) temperature rise, b) flow rate of air through the HSM, and c) total pressure drop from inlet to exit.

18. A tank containing saturated liquid undergoes a rapid drop in pressure. This results in flashing to take place in the tank. In the absence of any other process, use the conservation equations of mass and energy to derive a relation for the flashing mass flow rate in terms of the depressurization rate.

[Ans.: $\dot{m}_{fl} = -(m_l / h_{fg})[(dh_f / dP) - \mathrm{v}_v](dP / dt)$].

19. A tank containing saturated steam undergoes a rapid drop in pressure. This results in rainout from the steam. In the absence of any other process, use the conservation equations of mass and energy to derive a relation for the rainout mass flow rate in terms of the depressurization rate.
[Ans.: $\dot{m}_{fl} = (m_v / h_{fg})[(dh_g / dP) - \mathrm{v}_v](dP / dt)$].

20. Consider a tank filled with steam at enthalpy h_v. A spray valve is opened allowing water at a rate of $\dot{m}_{sr}$ and at enthalpy of h_{sp} to flow into the vapor space. The rate of steam condensation on the spray droplets is $\dot{m}_{sc}$. Assuming both spray water and the condensate reach saturation, write a steady state energy balance and find the rate of spray condensation.
[Ans.: $\dot{m}_{sc} / \dot{m}_{sp} = (h_f - h_{sp}) / (h_v - h_f)$].

21. Find the spray flow rate into the pressurizer of a PWR by using a force balance around a closed loop. This loop starts from the inlet to the spray line and includes spray line, spray valve, pressurizer, surge line, hot leg, steam generator primary side, reactor coolant pump suction pipe, reactor coolant pump, and reactor coolant pump discharge line. The spray valve flow area and loss coefficient are A_{sp} and K_{sp}, respectively. For given height and elevations, find the spray flow rate and the condition at which there is no spray flow.
{Ans.: $\dot{m}_{sp} = [(\Delta P_{HL} + \Delta P_{SG} + \Delta P_{CL}) + (\rho_{l,P} g / g_c)(L_P + Z_P) - (\rho_{CL} g / g_c) Z_{sp}]^{0.5} (A_{sp} / \mathrm{K}_{sp}^{0.5})$ }.

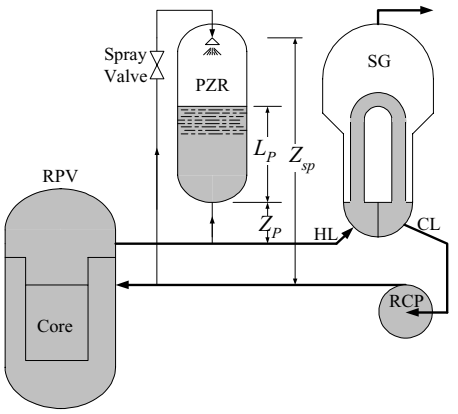

22. Schematics of a PWR reactor coolant system and the secondary side of the steam generator are shown in the figure. The reactor is shutdown and the decay power is being steadily removed by the residual heat removal system (not shown in the figure). At this steady state operation, the average temperature in the primary side is equal to the temperature of water in the secondary side of the steam

generator, hence, there is no heat transfer taking place in the steam generator tubes. At time zero, we lose the cooling of the residual heat removal system, we inject water at a specified flow rate and enthalpy into the primary side, and we turn on the reactor coolant pumps (not shown in the figure). a) Set up the governing differential equations. Use one control volume for the primary side water and one for the secondary side water, b) solve the differential equations to find the primary side and secondary side temperatures as functions of time and other system parameters specified below, c) use the given data and plot the surge flow rate (out of the primary side) as a function of time for the first ten minutes from the start of the event. The primary and the secondary sides are identified with subscripts P and S, respectively.

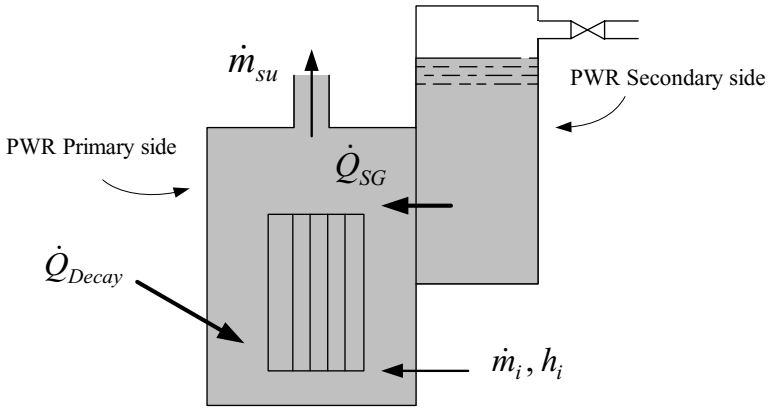

Volume data: $V_P = 260$ m^3 (9,181 ft^3), $V_S = 85$ m^3 (3000 ft^3),
Pressure data: $P_P = 2$ MPa (290 psia), $P_S = 138$ kPa (20 psia),
Injection data: $\dot{V}_i = 8.33$ lit/s (132 GPM), $T_i = 43$ C (110 F),
Heat transfer data: $A_{SG\text{-}tubes} = 8{,}383$ m^2 (90,232 ft^2), $U = 4531$ W/m^2·C (798 Btu/h·ft^2·F)
Power addition data: $\dot{Q}_{decay} = 3$ MW, $\dot{Q}_{pump} = 17$ MW
Initial condition: $T_P = T_S = 105$ C (221 F).
Assumptions:
a) The primary and secondary sides pressures remain constant throughout the event,
b) water in both control volumes remains subcooled for the duration of interest such that $du \cong dh \cong cdT$,
c) the overall heat transfer coefficient U remains constant,
d) no water enters or leaves the secondary side.

23. The steam line in a BWR is equipped with a relief valve to discharge steam to the pressure suppression pool during an emergency. The valve opens upon the

closure of the isolation valve. To prevent overcooling of the reactor pressure vessel, the discharge of steam through the valve must not result in a cooldown rate in excess of 100 F/h. Use the data and the associated simplifying assumptions to find pressure in the reactor pressure vessel (RPV) and temperature in the suppression pool as functions of time for a discharge period of 10 minutes.

RPV initial condition:
Pressure: 1015 psia (7 MPa),
water volume: 14,583 ft^3 (413 m^3),
steam volume: 8370 ft^3 (237 m^3),

RPV injection data:
feedwater flow rate: 1,252,000 lbm/h (32 kg/s), feedwater enthalpy: 335 Btu/lbm (780 kJ/kg),

RPV power addition data:
rate of heat deposition to the mixture from the RPV internal structure: 950 Btu/s (≈ 1 MW), rate of heat deposition to the mixture from radioisotope decay: 1% of the reactor nominal power of 3434 MWth,

Suppression pool initial condition:
Water mass: 7.6E6 lbm (3,447 kg), water temperature: 90 F (32 C), pressure: 14.7 psia (1 atm).

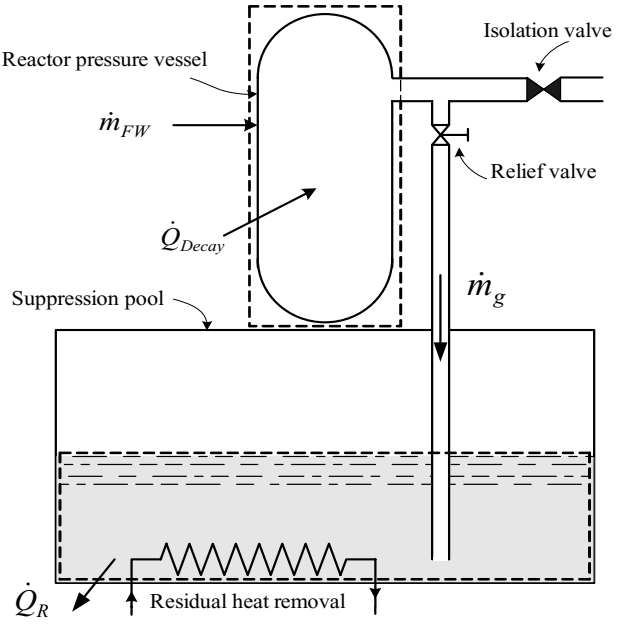

RPV assumptions:
a) water and steam are completely mixed and remain in thermodynamic equilibrium throughout the discharge period,
b) only saturated steam leaves the RPV,
c) the rate of heat deposition to the RPV from both sources remain constant throughout the discharge period.

Suppression pool assumptions:
a) water in the suppression pool remains subcooled at atmospheric pressure throughout the event, and
b) no residual heat removal system is activated for the suppression pool as long as the pool temperature remains below 110 F (43 C).
[Ans.: $P_{RPV} \approx 900$ psia and $T_{Pool} \approx 110$ F].

24. Find the cooldown rate and the suppression pool temperature in Problem 23 for a case that the relief valve has stuck open for five minutes. The valve flow area is 0.1 ft^2 (≈ 0.01 m^2).

25. Our goal in this problem is to find the rate of depressurization in a PWR plant. In this case, the depressurization is due to the pressurizer spray valve failure in the open position. The stuck open spray valve allows colder water from the cold leg to be sprayed into the bulk vapor space. Find the time it takes for pressurizer pressure of 15.5 MPa to drop to 13 MPa. Also calculate the water volume. Assume no other processes take place in the pressurizer. Further assume that the spray flow rate and enthalpy remain constant and $\dot{m}_{sp} = \dot{m}_{out-surge}$.

Data: $\dot{m}_{sp} = 28$ kg/s, $h_{sp} = 1250$ kJ/kg, $(V_l)_{\text{initial}} = 18$ m^3 and $(V_v)_{\text{initial}} = 28$ m^3.

26. A hermetically sealed tank contains a mixture of water and steam at pressure P_1. The tank wall is made of carbon steel. The wall on the inside is covered by a stainless steel cladding and on the outside by a layer of insulation. Use the specified data to find the time it takes for the tank pressure to drop to P_2 MPa.

Pressure data: Initial pressure: 2030.5 psia, final pressure: 1500.0 psia,

Geometry data: tank total volume: 1500 ft^3, water volume fraction: 40%, tank height: 6 ft, cladding thickness: 0.5 in, carbon steel thickness: 5 in, insulation thickness: 3 in,

Heat transfer data: ambient temperature: 85 F, heat transfer coefficient from the mixture to the inside of the tank wall: 150 Btu/h·ft^2·F, heat transfer coefficient from the tank to the ambient: 25 Btu/h·ft^2·F,

Property data: stainless steeel: $k = 8.6$ Btu/h·ft·F, $c_p = 0.123$ Btu/lbm·F, $\rho = 488$ lbm/ft^3,
carbon steel: $k_{carbon\ steel} = 29.6$ Btu/h·ft·F, $c_p = 0.11$ Btu/lbm·F, $\rho = 487$ lbm/ft^3,
insulation: $k = 0.3$ Btu/h·ft·F, $c_p = 0.037$ Btu/lbm·F, and $\rho = 27$ lbm/ft^3

Assumptions:
a) heat loss takes place from all surfaces and
b) heat transfer coefficients remain constant throughout the event.
[Ans.: about 20 hours].

27. A tank contains saturated steam at 10.4 MPa. The height and the inside diameter of the thank are 9 m and 2.5 m, respectively. The bottom of the tank is connected to a supply piping with the admission valve fully closed. We open the admission valve and let water at a rate of 8 lit/s, a pressure of 17 MPa, and a temperature of 275 C enter the tank. We close the admission valve after 20 minutes.

a) Use an isentropic compression assumption for the steam region to find the pressure in the steam dome immediately after the valve is closed.

b) Revise your estimate by considering the effect of heat transfer to the wall and on the water surface.

c) Find the tank pressure 15 minutes after the admission valve is closed. The tank has a wall thickness of 14 cm and is not insulated. The ambient temperature is 45 C and the heat transfer coefficient to ambient is 15 W/m·C.

28. Shown in the figure is a PWR reactor vessel, with the vessel head removed. Initially there are no fuel assemblies in the core and the vessel and pool are full of water. We now place the assemblies in the core. The heat produced in the core, due to the decay of the radio-nuclides must be removed. For this purpose, water from the bottom of the pool is circulated through a heat exchanger and the colder water is returned to the top of the pool. In this way, the core is cooled solely by natural circulation. Use the specified data to estimate the flow rate through the core.
Data: h_{LP} = 3 m, h_C = 3.5 m, h_{UP} = 3.8 m, h_{Pool} = 7 m, D_C = 2.5 m, D_V = 11.3 m, A_{Pool} = 162.5 m^2, $T_{initial}$ = 50 C, Core decay power = 10 MW, Flow rate through the pump = 200 lit/s.

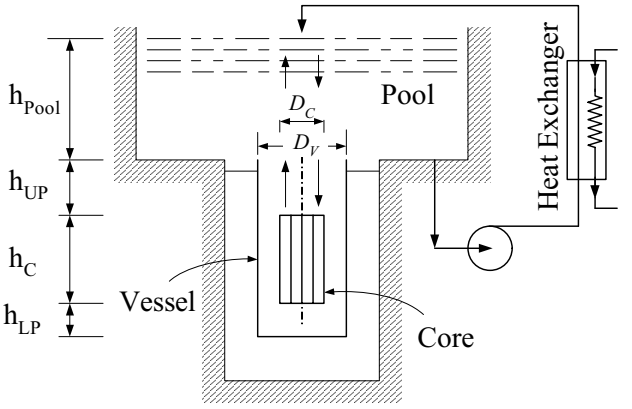

29. A right circular cylinder tank, having a volume of 44 m^3, contains a saturated mixture of water and steam at 15 MPa. The tank has a height of 10 m and a wall thickness of 14 cm. The ambient is quiescent air at 35 C and 1 atm. The initial steam quality is 99%. The tank is fully insulated with negligible heat loss. We now, remove the insulation and let heat loss to ambient take place from the top

and the cylindrical surface. Estimate the value of the following variables after one hour a) steam pressure, b) steam temperature, c) wall temperature facing the steam, d) wall temperature facing the ambient air, e) water level in the tank. [Ans. P_2 = 14.17 MPa, T_2 = 337.5 C, T_{wi} = 337.5 C, T_{wo} = 333.6 C, L_{water} = 13 cm].

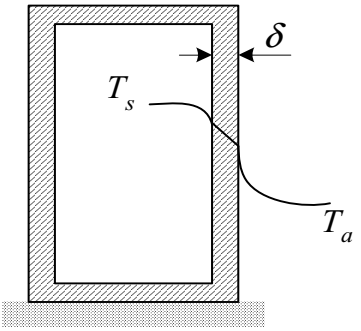

Problem 29

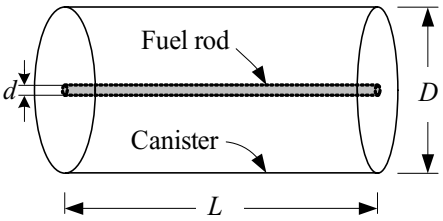

Problem 30

30. A canister of diameter D, length L, and wall thickness δ has an initial temperature of T_c, We now evacuate the air from the canister by using a vacuum pump and place a spent fuel rod while maintaining the wall temperature at T_c. The spent fuel rod produces heat at rate of 5 W. The canister is exposed to air at 35 C and a heat transfer coefficient of 5 W/m^2·C. Plot the spent fuel and the canister wall temperatures versus time for a duration of 18 hours. To simplify the analysis a) assume that the fuel rod is bare UO_2, b) ignore conduction heat transfer between the rod and the canister ends, c) use a lumped capacitance for the fuel as well as the canister wall . Heat transfer takes place at all surfaces. Use, d = 2 mm, D = 10 cm, L = 3 m, ε_{UO2} = 0.8. Canister is made of stainless steel with a wall thickness of 2 cm (ε = 0.4).

31. The models developed in Chapter VId to analyze the primary and the secondary sides of a PWR are based on the thermodynamic equilibrium assumption, except for the pressurizer and the secondary side of the steam generator, which were analyzed based on the thermodynamic non-equilibrium model. In the lumped parameter approach, the perfect mixing assumption is used and only one temperature is allocated to a node. Thus, a multi-node representation was required for regions such as the core and the steam generator primary side in which large temperature gradients exist (Figures VId.2.1, VId.3.2, and VId.7.1).

Another approach, originally developed by Myers and employed by Kao, allocates only one node to a region even if there is a large temperature gradient in the region. For example, one node is used to represent the PWR core despite the large temperature rise over the core. Similarly, the tube bundle region of the steam generator with large density gradient is modeled by only one control volume. This is possible by the introduction of the *linear enthalpy profile* model. In this model a volume-averaged mixture density, ρ^* is defined as:

$$\rho^* = \frac{1}{\mathrm{V}} \int_{\mathrm{V}} \rho_m(P, h_m) d\mathrm{V}$$

Similarly, a volume-averaged mixture enthalpy h^* is defined as:

$$h^* = \frac{1}{\mathrm{V}} \int_{\mathrm{V}} \rho_m(P, h_m) h_m d\mathrm{V}$$

where subscript m stands for mixture. If the volume-averaged mixture density and enthalpy are known, then the mass and energy of a node can be found from $m = \rho^* \mathrm{V}$ and $u = h^* \mathrm{V} - P\mathrm{V}$, respectively. To find the volume-averaged mixture density and enthalpy in closed form, the mixture density profile in terms of pressure and enthalpy is needed to develop the above integrals.

a) To find such profile, show that at a given pressure, density of saubcooled water decreases almost linearly with increasing enthalpy. Also show that the specific volume of a two-phase mixture and of superheated steam increases linearly with enthalpy.

b) Now consider control volume i, connected to the control volumes $i - 1$ and $I + 1$. Show that by a linear transformation, the volume-averaged density and enthalpy become functions of pressure and the inlet and exit mixture enthalpies, given by:

$$\rho_i^* = \frac{\int_{h_{m,i-1}}^{h_{m,i}} \rho_{m,i}(P, h_{m,i}) dh_{m,i}}{h_{m,i} - h_{m,i-1}} \text{ and } h_i^* = \frac{\int_{h_{m,i-1}}^{h_{m,i}} \rho_{m,i}(P, h_{m,i}) h_{m,i} dh_{m,i}}{h_{m,i} - h_{m,i-1}}$$

c) Using the linear enthalpy profile assumption show that in the single-phase region:

$$\rho_{m,i} = \rho_{i-1} + \frac{\partial \rho_{m,i}}{\partial h_{m,i}} \left(h_{m,i} - h_{i-1} \right)$$

where in this region, $\rho_{m,i} / h_{m,i}$ is a constant. Also show that in the two-phase region:

$$\mathrm{v}_{m,i} = \mathrm{v}_{i-1} + \frac{\partial \mathrm{v}_{m,i}}{\partial h_{m,i}} \left(h_{m,i} - h_{i-1} \right)$$

where in this region, $\mathrm{v}_{m,i} / h_{m,i}$ is a constant.

d) Substitute these profiles in the above integrals to obtain expressions for ρ_i^* and h_i^*.

VIe. Nuclear Heat Generation

In Chapter IVa, we treated the volumetric heat generation rate, $\dot{q}'''$ as a known quantity. The internal heat generation in a substance may be due to various processes such as electrical resistance, chemical, or nuclear reactions. If the internal heat generation is due to an electrical resistance, then the calculation of $\dot{q}'''$ is rather trivial. Examples of chemical heat generation include the exothermic reaction of some alloys with water at high temperatures. Zircaloy, for example, reacts with water at elevated temperatures to produce heat and hydrogen gas. In the case of the nuclear reaction, however, calculation of the volumetric heat generation rate is more involved since it requires the study of neutron transport as a result of neutron-nucleus interactions. This is further complicated by the interdependency of neutron populations on the state of the medium, such as the composition, pressure, and temperature. In this chapter we first introduce several key terms that play major roles in nuclear engineering. This is followed by the derivation of the neutron transport equation, which is difficult to solve. Therefore, we introduce the application of Fick's law as our constitutive equation to turn the neutron transport equation into an equation known as the neutron diffusion equation. This is because the neutron diffusion equation provides nearly accurate results for many applications and has the additional advantage of being amenable to even analytical solutions for some familiar geometries. We then proceed to find the rate of nuclear heat generation from fission. Finally, we investigate the effect of the neutron flux on temperature distribution in conventional reactor cores.

1. Definition of Some Nuclear Engineering Terms

1.1. Definitions Pertinent to the Atom and the Nucleus

Atom is defined as the smallest unit of an element that can combine with other elements. Democritus in the fifth century B.C. believed that an atom is the simplest thing from which all other things are made. The Greek word *atomos* means *indivisible*. It was not until the early 20^{th} century that subatomic particles were identified and the structure of the atom was described in terms of the nucleus and electrons. The nucleus consists of positively charged protons and neutral neutrons. The protons and neutrons are tightly clustered in the nucleus. The negatively charged electrons encircle the nucleus on far away orbits. Indeed the distance between the closest electron orbit to the nucleus is about 100,000 times the radius of the nucleus. Even further away is the neighboring nucleus, which is as far away as about 200,000 times the radius of the nucleus. The diameter of an atom is generally expressed in terms of angstrom (A^o), which is 1E–10 m. For example, the diameter of a chlorine atom is 2 A^o. The hydrogen atom has the simplest structure. Its nucleus consists of a proton with one electron in its orbit, which makes the atom neutral. Helium has two protons and two neutrons in the nucleus with two electrons orbiting the nucleus. There are a maximum number of

electrons that each orbit, or shell, can possess. In chemical reactions, electrons of the last shell, which is not filled to capacity, bond with the shells of other atoms to produce a molecule. In this reaction, the nucleus remains intact. In nuclear reactions, the nucleus itself is affected.

Nucleon is referred to a particle that exists in the nucleus. Thus protons and neutrons are *nucleons*.

Nuclide refers to a specific atom or nucleus. If a nuclide is not stable, it is referred to as a *radionuclide*.

Atomic number (Z) represents the number of protons in an atom. If N is the number of neutrons, then the *mass number* (A) is equal to the total number of neutrons and protons, $A = N + Z$. We generally show elements as ${}^{A}_{Z}\mathrm{E}$. For example, natural uranium is shown as ${}^{238}_{92}\mathrm{U}$. There are elements for which we can find various mass numbers. Atoms of these elements have the same number of protons but a different number of neutrons. These are known as *isotopes*. For example, naturally occurring uranium ore has 99.28% atoms of ${}^{238}_{92}\mathrm{U}$, 0.714% atoms of ${}^{235}_{92}\mathrm{U}$, and 0.006% atoms of ${}^{234}_{92}\mathrm{U}$. Thus U-233, U-234, U-235 and U-238 are isotopes of uranium. The effect of isotopes on mass number is shown in Figure VIe.1.1(a). We may enhance the number of atoms in an isotope in the naturally occurring substance; this process is referred to as *enrichment*.

Atomic mass unit (amu) is equal to the one-twelfth of the mass of carbon 12. Since one mole of ${}^{12}_{6}\mathrm{C}$ has 6.023E23 atoms and weighs 12 gram, then 1 amu = (1/12) × (12/6.023E23) = 1.66E–24 gram. On this basis, m_{proton} = 1.007277 amu, $m_{neutron}$ = 1.008665 amu, and $m_{electron}$ = 0.000548597 amu as summarized in Table VIe.1.1. Based on Einstein's equation, the energy equivalent with 1 amu is $E = mc^2$ = (1.66E–27 kg)(3E8 m/s)^2 = 1.49E–10 J. Since 1 MeV = 1.602E–13 J, then 1 amu = 931.5 MeV.

Table VIe.1.1. Approximate classical characteristics of atoms and particles

Object	Mass (amu)	Mass (g)	Charge (coul)	Radius (cm)
Electron	0.000548597	9.11E–28	–1.6E–19	2.822E–13
Proton	1.007277	1.67E–24	+1.6E–19	2.103E–14
Neutron	1.008665	1.67E–24	0.0	2.100E–14
Nucleus	$Zm_p + Nm_n$	$Zm_p + Nm_n$	$Z \times$ 1.6E–19	$(1.2\text{E}{-13})A^{1/3}$
Atom	$Z(m_p + m_e) + Nm_n$	$Z(m_p + m_e) + Nm_n$	$Z \times$ 1.6E–19	1.0E–8

Atom density, N is the number of the atoms of an element per unit volume (#/m^3). Atom density is given by $N = \rho N_A/M$. Atom density is generally a function of space and time, $N = N(\vec{r}, t)$.

Mass defect is defined as the difference in measured mass between the conglomerate mass of a coalesced nucleus and the sum of the masses of the individual

constituent particles of that nucleus. The mass defect for element ${}^{A}_{Z}\mathrm{E}$, for example, is found as $\Delta m = Z(m_{proton}) + N(m_{neutron}) - (M_E - Zm_{electron})$.

Binding energy (*B.E.*) of a nucleus is the energy-equivalent of the mass defect of that nucleus ($B.E. = \Delta mc^2$). The binding energy may be thought of as the energy that would be required to break the nucleus into its individual constituents or as the amount of energy that would be released upon an instantaneous coalescence of all individual constituents to form the nucleus.

Example VIe.1.1. Find the mass defect and the binding energy per nucleon for Beryllium, ${}^{9}_{4}\mathrm{Be}$. The mass of this element is given as 9.01219 amu.

Solution: The mass defect is found as:

$\Delta m = 4 \times 1.007277 + 5 \times 1.008665 - (9.01219 - 4 \times 0.000549) = 0.062439$ amu

The equivalent energy is found as:

$E = mc^2 = (0.062439 \times 1.66\text{E}{-27}\ \text{kg})(3\text{E}8\ \text{m/s})^2 = 9.328\text{E}{-12}\ \text{J} = 58.2\ \text{MeV}.$

The binding energy per nucleon is found as:

58.2/9 = 6.5 MeV/nucleon.

Binding energy per nucleon, Figure VIe.1.1(b) is a minimum for hydrogen and reaches a maximum of about 9 MeV per nucleon for iron. As mass number increases beyond 60, binding energy per nucleon keeps dropping. The slope of the curve is an indication of relative stability and potential sources for energy release. For example, for such heavy elements as Uranium and Plutonium, the binding energy drops to about 7.5 MeV/nucleon. If the atom of such materials split, energy is released and more stable nuclei appear.

Neutron-nucleus interactions are of two types. Consider bombardment of a target material with a beam of neutrons. Depending on the energy and the direction of the neutrons as well as the atoms of the target, we may have an interaction. If an interaction occurs, it results in the neutrons being scattered from the nucleus or absorbed by the nucleus.

Scattering is one of two outcomes resulting from interaction between a target nucleus and the bombarding neutron. If the total kinetic energy of the neutron and the nucleus before and after the scattering event remains the same, the event is referred to as *elastic scattering*. Otherwise, the interaction is known as *inelastic scattering*. For low neutron energies in elastic scattering, the passing neutron is bounced due to the force exerted by the nucleus, hence the process is referred to as *potential scattering*. However, for higher neutron energies, the neutron and nucleus may combine to form a *compound nucleus* from which a neutron emerges. For inelastic scattering to occur, the energy of the neutron must exceed the minimum energy required for a compound nucleus to form.

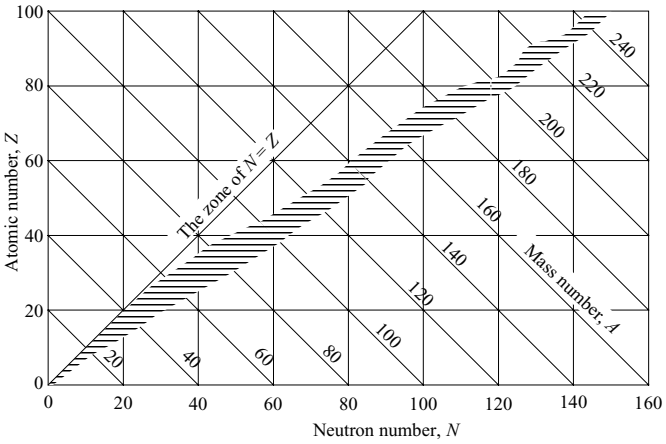

(a)

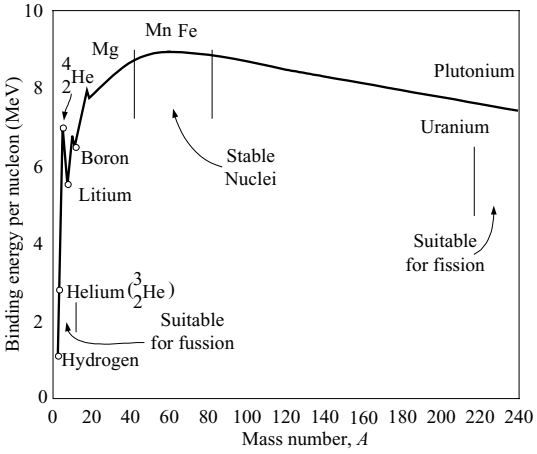

(b)

Figure VIe.1.1. (a) Effect of isotopes on mass number and (b) Binding energy per nucleon

Absorption is the second outcome in a neutron-nucleus interaction. Absorption in turn may lead to several types of interactions. The absorption of a neutron by the nucleus places the resulting compound nucleus is an excited state. The compound nucleus may then break up, leading to fission, or it may de-excite itself by emitting energetic radiation such as alpha (α), gamma (γ), neutron (n), or protons (p). Although the excited state of a nucleus can be as short as 1E–14 seconds, it is considered a well-defined state compared with the approximately 1E–22 seconds it takes for a neutron to travel across the nucleus.

Resonance. Application of the wave or quantum mechanic to the atomic nucleus shows that the internal energy of a nucleus is quantized (see the solution to Equation VIIb.1.32). If a neutron has a sufficient amount of *K.E.* for the creation

of a compound nucleus then the neutron and the nucleus are said to be in resonance.

Microscopic cross section σ_i, represents probability of occurrence of a given type of interaction between an incident neutron and the target nucleus of the medium through which the neutron travels. In this case, the subscripted variable, *i*, represents the type of interaction, whereby the relative probability of occurrence of a scattering reaction would be represented as σ_s (σ_a for absorption and σ_f for fission). This property, which represents probabilities of certain types of interaction, is specific to the target nucleus type (as it is a property) and is also dependent upon incident neutron energy and type of interaction. This probability is generally represented in units of area, cm^2, or barns (b) where 1 barn = 1.0E–24 cm^2.

Macroscopic cross section, Σ_i is the probability of interaction of type *i* per unit length (1/cm) of neutron travel. Thus, the chance of interaction with an atom per unit distance traveled is σ and for *N* atoms is $\Sigma_i = N\sigma_i$.

Resonance cross section refers to the range of neuron energy of 1 eV to 1E5 eV where for many isotopes the absorption cross section of the target nucleus displays extreme variations in magnitude as shown in Figure VIe.1.2(a). The resonance cross section, indicating a high probability of interaction, occurs when the energy quantized or the excited state of the compound nucleus matches the summation of the neutron K.E. and the compound nucleus binding energy.

Fission event. Figure VIe.1.1 shows that, following the stable region, binding energy decreases with increasing number of neutrons. This implies that if we break up heavy nuclei such as uranium, we would end up with two nuclei having mass numbers of about one-half of the original nucleus hence being more stable. This is indeed the case, as the breaking up, referred to as fission, results in lighter and more stable nuclei with respect to fission. The appearance of a fission products is a probabilistic event. For example, the fission of uranium-235 may result in excess of 200 different isotopes of 35 different elements. Examples for fission of a Uranium-235 nucleus include the appearance of Zr, Te, Kr, and Ba:

$$ {}_0^1\mathrm{n} + {}_{92}^{235}\mathrm{U} \rightarrow {}_{40}^{97}\mathrm{Zr} + {}_{52}^{137}\mathrm{Te} + 2\,{}_0^1\mathrm{n} $$

$$ {}_0^1\mathrm{n} + {}_{92}^{235}\mathrm{U} \rightarrow {}_{36}^{91}\mathrm{Kr} + {}_{56}^{142}\mathrm{Ba} + 3\,{}_0^1\mathrm{n} $$

It must be emphasized that the fission products are generally highly radioactive and thus hazardous.

The above reactions indicate that, in a sustained interaction leading to fission, between 2 to 3 neutrons emerge for each neutron that is absorbed to cause fission in U-235. The number of neutrons emerging in a fission is represented by ν. These newly emerged neutrons have a spectrum of energy as shown in Figure VIe.1.2(b) and mathematically described as:

$$ \chi(E) = 0.453 e^{-1.036E} \sinh\sqrt{2.29E} $$

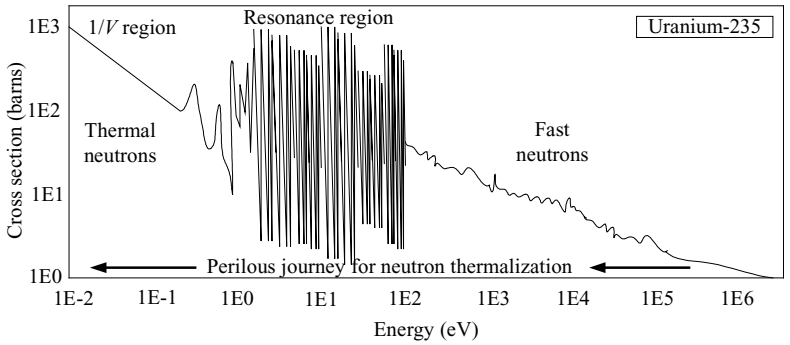

(a)

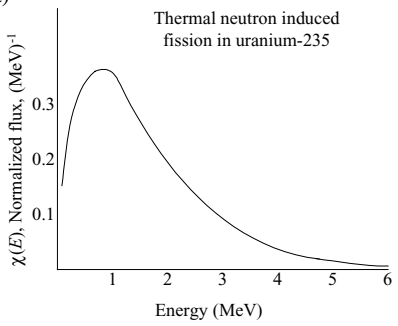

(b)

Figure VIe.1.2. U-235 (a) Fission cross-section and (b) prompt fission neutron spectrum

where E is in MeV. While some newly emerged neutrons have energies as low as a fraction of MeV and a few up to 17 MeV, the most probable energy is found as 0.73 MeV and the average energy as 1.98 MeV. The U-235 isotope has a large fission cross section for slow neutrons, (i.e., neutrons that have energy in the range of 0.025 eV). Hence, we must use some means of slowing down neutrons to such low energies. However, the journey for neutrons from about 2 MeV to about 0.025 eV is quite perilous. This is because the U-235 cross section for fission is highly energy dependent (Figure VIe.1.2(a)). Thus, there is a high probability that the neutron, before being slowed down is captured in the isotope, especially in the resonance region, hence not leading to fission. In the low energy range, referred to as the thermal region, the nucleus cross-section is proportional with the inverse square root of energy, known as the $1/V$ region.

Fissile, fissionable, and fertile isotopes. A fissile material is an isotope that would fission upon the absorption of a neutron of essentially no kinetic energy. In other words, simply the binding energy of that last neutron in the compound system is enough to overcome the critical energy required for fission to occur. This type of isotope proves to be the most useful for producing the neutron chain reaction necessary to produce power with a thermal pressurized water reactor. Fissible isotopes include ^{233}U, ^{236}U, ^{239}Pu, and ^{241}Pu. Plutonium-239 is found in abun-

dance in spent fuel rods and can be recovered in reprocessing facilities. During normal operation of a nuclear reactor, plutonium-239 is produced inside the fuel rod such that towards the end of a fuel cycle, it is one of the major contributors (up to 50%) of the power produced by the reactor. Fissionable materials are isotopes that, like fissile materials, fission, but only with fast or energetic neutrons (energies higher than 2 MeV for U-238). An important fissionable isotope is the naturally occurring U-238. The contribution of this isotope to the power level of a thermal reactor is about 5%. Other fissionable isotopes are ^{232}Th and Pu-240.

Fertile materials are isotopes that do not fission but produce fissile materials as a result of an interaction with neutrons. An example of a fertile isotope is $^{232}_{90}\mathrm{Th}$:

$$^{1}_{0}\mathrm{n} + {}^{232}_{90}\mathrm{Th} \rightarrow {}^{233}_{90}\mathrm{Th} \rightarrow {}^{233}_{91}\mathrm{Pa} + \beta^{-} \rightarrow {}^{233}_{92}\mathrm{U} + \beta^{-}$$

where β^- refers to beta-decay. The most important fertile isotope is uranium-238 resulting in the fissile isotope plutonium-239.

Since there are isotopes that are suited for fission if exposed to fast neutrons and similarly isotopes suited for fission by slow (or thermal) neutrons, there are also two types of reactors, fast and thermal. However, there are many more nuclear reactors based on thermal fission than based on fast fission.

Moderator is used to slow down the newly born fast neutrons in thermal reactors. The moderator in thermal reactors generally has a dual role as it is also used as a coolant. Water (H_2O) is used in "light water reactors" and heavy water (D_2O), using deuterium instead of hydrogen, in "heavy water reactors". The latter reactor is of Canadian design and is known as the Canada Deuterium Uranium or CANDU reactor, for short. Since a neutron loses most of its energy in scattering events with light nuclei, a moderator should be a substance made of light nuclei with low absorption and a high scattering cross section. Properties of widely used moderators are listed in Table VIe.1.2, where D is the diffusion coefficient and Σ_a is the macroscopic absorption cross sections.

Table VIe.1.2. Properties of some moderators (at 20 C) for thermal neutrons (Lamarsh)

Moderator	Density (g/cm^3)	D (cm)	Σ_a (1/cm)
Water (H_2O)	1.00	0.16	1.97E–2
Heavy Water (D_2O)	1.00	0.87	9.3E–5
Beryllium (Be)	1.85	0.50	1.04E–3
Graphite (C)	1.60	0.84	2.4E–4

1.2. Definitions Pertinent to Neutrons

Neutron density, $n(\vec{r}, E, \vec{\Omega}, t)$ as shown in Figure VIe.1.3(a) is the number of neutrons that at time t are at location x, y, z in volume dV, of energy E about dE and travelling in the direction of Ω_x, Ω_y, and Ω_z (or Ω_r, Ω_θ, and Ω_ϕ) in $d\vec{\Omega}$ (the solid angle is shown in Figure IVd.5.1). If, for example, we want to find the num-

ber of neutrons having all ranges of energy and travelling in all directions, we integrate over energy and solid angle*:

$$n(\vec{r},t)=\int_{\Omega}\left(\int_{0}^{\infty} n(\vec{r},\vec{\Omega},E,t)dE\right)d\vec{\Omega} \qquad \text{VIe.1.1}$$

While $n(\vec{r}\ ,\ \vec{\Omega}\ ,E,t)$ has units of $s^{-1}\ cm^{-3}\ eV^{-1}\ sr^{-1}$, $n(\vec{r}\ ,t)$ has units of neutrons/s cm^3.

Neutron velocity, $V(E)$ is the length per unit time traveled by the neutrons, (cm/s). Neutron velocities may range from 8,000 to 80,000,000 km/h. The newly born neutrons due to fission are very energetic (average energy is about 2 MeV but some may emerge with energies up to 20 MeV). Such neutrons lose their energy due to collision with the moderator nuclei. The loss of energy would eventually result in neutrons coming to thermal equilibrium with their surrounding medium. This is why the slowed down neutrons are referred to as being *thermalized*. Energy of neutrons in a neutron population can be approximately obtained from the Maxwell-Boltzmann distribution (see Problem 4). Using the Maxwellian distribution, we can find the most probable velocity in terms of neutron temperature as $V = (2\kappa T/m)^{1/2}$ where κ is the Boltzmann constant, $\kappa = R_u/N_A$ = 8.314/6.023E23 = 1.38E–23 J/K. Thus, neutrons at room temperature of 20 C have a velocity of V = (2 × 1.38E-23 × [20 + 273.16/(1.008665 × 1.66E-27)]$^{1/2}$ ≈ 2200 m/s. The kinetic energy at this velocity is:

$$K.E.=mV^2/2=0.5\times\left[\left(1.008665\times1.66\text{E}-27\right)/\left(1.602\text{E}-13\right)\right](2200)^2$$
$$=\left(5.226\text{E}-15\right)V^2=0.0253\ \text{V}$$

Neutron angular flux, $\phi(\vec{r}\ ,\ E,\ \vec{\Omega}\ ,t)dEd\vec{\Omega}$ is the number of neutrons at location r, energy (E) about dE and traveling at time t through a unit area perpendicular to $\vec{\Omega}$, in the differential solid angle $d\vec{\Omega}$ in the direction of $\vec{\Omega}$. As shown in Figure VIe.1.3(a), $\vec{\Omega}$ is the unit vector of the neutron velocity vector, hence, $\vec{V}=V\vec{\Omega}$. To find the integrated steady state neutron flux, we integrate the steady state angular flux over all solid angles to obtain:

$$\phi(\vec{r},E)=\int_{\Omega}\phi\left(\vec{r},E,\vec{\Omega}\right)d\vec{\Omega} \qquad \text{VIe.1.2}$$

For the special case of isotropic emission of neutrons, where neutrons are distributed uniformly over the surface area of a sphere having a radius of unity, the angular flux is related to the integrated flux through:

$$\phi(\vec{r},E,\vec{\Omega})=\frac{\phi(\vec{r},E)}{4\pi} \qquad \text{VIe.1.3}$$

---

* Another way of representing $n(\vec{r}\ ,\ E,\ \vec{\Omega}\ ,t)$ is to write
$d^6n/dxdydzdEd\vec{\Omega}\,dt = d^7n/dxdydzdE(\sin\varphi d\theta d\varphi)dt$

The integrated flux is shown in Figure VIe.1.3(b). To relate neutron flux to the number density of the neutrons, we may treat neutrons as a fluid and use the similarity between neutron flux (ϕ), neutron density (n), and neutron velocity (V) with mass flux (G), density (ρ) and flow velocity (V) per Equation IIa.5.3, ($G = \rho V$). Thus, for neutron flux we find:

$$\phi(\vec{r}, E) = n(\vec{r}, E)V(E) \qquad \text{VIe.1.4}$$

If the integrated flux over all directions is also integrated over all energies, we find neutron flux $\phi(\vec{r}, t)$ or the steady state flux $\phi(\vec{r})$. This is referred to as the *one-speed neutron flux*.

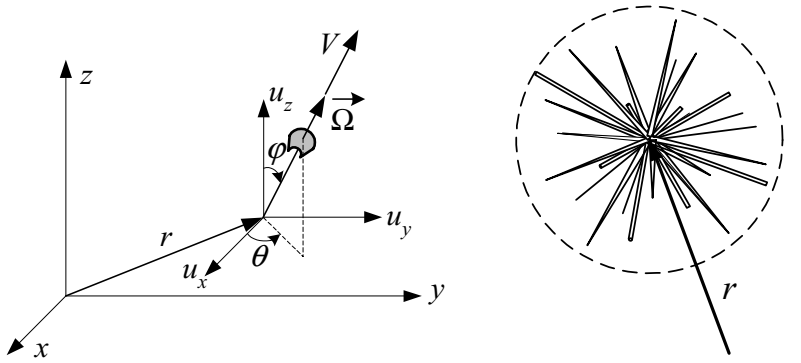

Figure VIe.1.3. (a) Depiction of position and direction of a neutron. (b) Integrated flux over all directions at position $\vec{r}$ (Ott).

Angular current density is a vector defined by the following relation $\vec{J}(\vec{r}, E, \vec{\Omega}, t) = \phi(\vec{r}, E, \vec{\Omega}, t)\vec{\Omega}$, hence, it has an absolute value equal to the angular flux. Thus $\vec{J}(\vec{r}, E, \vec{\Omega}, t)dE\overrightarrow{dS}d\vec{\Omega}$ represents the rate of neutrons at location $\vec{r}$, passing at time t through differential area dS, with an energy (E) in dE and in the direction of $\vec{\Omega}$ in $d\vec{\Omega}$.

Neutron current density or simply neutron current is obtained by the integration of the angular current density over all possible directions:

$$\vec{J}(\vec{r}, E, t) = \int_{\Omega} \vec{J}(\vec{r}, E, \vec{\Omega}, t)d\vec{\Omega} \qquad \text{VIe.1.5}$$

If we integrate the neutron current density over all ranges of energy we obtain the neutron current as $\vec{J}(\vec{r}, t)$. The neutron current, being a vector, is instrumental in describing the leakage of neutron, into or out of a region.

Rate of neutron interaction, is obtained by multiplying the neutron flux by the macroscopic cross section of the nucleus for a specific outcome. Thus $R_i = \phi\Sigma_i$ (neutron/s·cm^2) × (atoms/cm) = interaction/s·cm^3.

Rate of heat generation $\dot{q}'''$ (W/cm^3) is found from the rate of interaction. If we consider the interaction of type i as that leads to fission, then $i = f$ and $R_f = \phi\Sigma_{fr}$, where subscript fr stands for fission in the fuel rod. If the energy produced per fission is E_R, then the total power produced per unit volume is given by:

$$\dot{q}''' = E_R\, \phi\Sigma_{fr} \qquad \text{VIe.1.6}$$

The energy produced per fission, E_R is about 200 MeV (1 eV = 1.6E–19 joules hence E_R = 3.2E–11 J). When the nucleus of a heavy element undergoes fission, most of the resulting energy is due to the kinetic energy of the fission fragments as shown in Table VIe.1.2. Note that the deposited energy is E_d = 90% E_R = 180 MeV.

Table VIe.1.2 Approximate distribution and deposition of fission energy (El-Wakil)

Type	Process	Percent of total energy	Energy deposition
Fission (prompt)	Kinetic energy of fission fragments	80.5	Fuel material
	Kinetic energy of the emergent fast neutrons	2.5	Moderator
	γ Energy associated with fission	2.5	Fuel & structure
Fission (delayed)	Kinetic energy of delayed neutrons	0.02	Moderator
	β^--decay energy of fission products	3.0	Fuel material
	Neutrinos from β^-	5.0	Nonrecoverable
	γ-decay of fission products	3.0	Fuel & structure
Capture	β^- and γ-decay energy of (n, γ) product	3.5	Fuel & structure
Total		100	

Example VIe.1.2. Find the prompt energy of U-235 fission resulting in the appearance of Xe and Sr:

$$^{235}_{92}\mathrm{U} + {}^{1}_{0}\mathrm{n} \rightarrow {}^{140}_{54}\mathrm{Xe}^{*} + {}^{96}_{38}\mathrm{Sr}^{*} \rightarrow {}^{139}_{54}\mathrm{Xe} + {}^{95}_{38}\mathrm{Sr} + 2\left({}^{1}_{0}\mathrm{n}\right) + 7(\gamma)$$

Solution: The prompt energy related to the mass defect is found from:

$$E_p = [M\left({}^{235}_{92}\mathrm{U}\right) + m_n - M\left({}^{139}_{54}\mathrm{Xe}\right) - M\left({}^{95}_{38}\mathrm{Sr}\right) - 2m_n]c^2$$
$$= [235.043923 + 1.008665 - 138.918787 - 94.919358 - 2(1.008665)]$$

Thus E_p = 0.197113 amu = 0.197113 × 931.5 MeV/amu= 183.61 MeV. This includes 5.2 MeV kinetic energy of the two prompt neutrons and 6.7 MeV energy of the emerging gamma rays.

The six factor formula. Earlier we discussed that the emerging fast neutrons from the fission of U-235 have a perilous journey from the fast to the thermal region before being used for the next fission cycle. Aside from being absorbed in the nucleus (fuel) without causing fission, they may leak out of our control volume or may be absorbed by elements other than the fuel, such as the reactor structure (Table VIe.3.1). To formulate this verbal discussion in mathematical terms, we consider two cases of infinite and finite media. The infinite medium consists of fuel, structure, and neutrons. In such a medium, no neutron can be lost to leakage. However, for the finite medium case, we do lose neutrons to leakage. Such leakage is due to scattering out of the region of interest. To keep track of the neutron inventory in each cycle, we define k, *the multiplication factor*, as the ratio of the number of neutrons in the new cycle to the number of neutrons in the previous cycle. We represent this ratio by k_∞ for the infinite and by k_{eff} for the finite medium. If we divide the energy spectrum to fast and thermal, we may lose neutrons to leakage in both energy regions. The relation between the ratios is:

$$k_{eff} = k_\infty P_{FNL} P_{TNL}$$

were P_{FNL} is the probability that a fast neutron not leak out and P_{TNL} is the probability that a thermal neutron does not leak out. Having taken care of the leakage term for now, we begin to focus on k_∞. By definition, in an infinite medium, the ratio of neutrons in the present cycle to that of the previous cycle is:

$$k_\infty = \frac{\int_{medium} dV \int_0^\infty \nu\Sigma_f(\vec{r},E)\phi(\vec{r},E)}{\int_{medium} dV \int_0^\infty \Sigma_a(\vec{r},E)\phi(\vec{r},E)} = \frac{\int_{fuel} dV \int_0^\infty \nu\Sigma_f(\vec{r},E)\phi(\vec{r},E)}{\int_{medium} dV \int_0^\infty \Sigma_a(\vec{r},E)\phi(\vec{r},E)}$$

where we changed the numerator to an integral over the fuel region, as there is no fission anywhere else in the medium. We further break down the above ratio by introducing terms in the numerator and denominator.

$$k_\infty = \frac{\int_{fuel} dV \int_0^\infty \nu\Sigma_f(\vec{r},E)\phi(\vec{r},E)}{\int_{fuel} dV \int_0^{E_T} \nu\Sigma_f(\vec{r},E)\phi(\vec{r},E)} \times \frac{\int_{fuel} dV \int_0^{E_T} \nu\Sigma_f(\vec{r},E)\phi(\vec{r},E)}{\int_{fuel} dV \int_0^{E_T} \Sigma_a(\vec{r},E)\phi(\vec{r},E)} \times \frac{\int_{fuel} dV \int_0^{E_T} \Sigma_a(\vec{r},E)\phi(\vec{r},E)}{\int_{medium} dV \int_0^{E_T} \Sigma_a(\vec{r},E)\phi(\vec{r},E)} \times \frac{\int_{medium} dV \int_0^{E_T} \Sigma_a(\vec{r},E)\phi(\vec{r},E)}{\int_{medium} dV \int_0^\infty \Sigma_a(\vec{r},E)\phi(\vec{r},E)} \qquad \text{VIe.1.7}$$

where $E_T \cong 1$ eV is a cutoff energy separating the thermal region from the slowing down region. The first ratio represents the neutron production rate as a result of both fast and thermal fission to the neutron production rate due only to thermal fission. This ratio is shown by ε and referred to as the *fast fission factor*:

$$\varepsilon = \frac{\text{No. of neutrons produced in fast and thermal fission}}{\text{No. of neutrons produced in thermal fission}} = \frac{\int_{fuel} dV \int_0^\infty \nu\Sigma_f(\vec{r},E)\phi(\vec{r},E)}{\int_{fuel} dV \int_0^{E_T} \nu\Sigma_f(\vec{r},E)\phi(\vec{r},E)}$$

The second ratio in Equation VIe.1.7 represents the rate of neutron production due to thermal fission to the rate of absorption of thermal neutrons:

$$\eta = \frac{\text{No. of neutrons produced in thermal fission}}{\text{No. of thermal neutrons absorbed in fuel}} = \frac{\int_{fuel} dV \int_0^{E_T} \nu\Sigma_f(\vec{r},E)\phi(\vec{r},E)}{\int_{fuel} dV \int_0^{E_T} \Sigma_a(\vec{r},E)\phi(\vec{r},E)}$$

$$\cong \frac{\nu\Sigma_f}{\Sigma_{aF}}$$

where Σ_{aF} is the macroscopic cross section for absorption of the fuel material. This ratio is referred to as the *eta factor*. The third ratio in Equation VIe.1.7 is the rate of thermal neutrons absorbed in the fuel to the rate of thermal neutrons absorbed in the entire medium:

$$f = \frac{\text{No. of thermal neutrons absorbeded in fuel}}{\text{No. of thermal neutrons absorbed in medium}} = \frac{\int_{fuel} dV \int_0^{E_T} \Sigma_a(\vec{r},E)\phi(\vec{r},E)}{\int_{medium} dV \int_0^{E_T} \Sigma_a(\vec{r},E)\phi(\vec{r},E)}$$

$$\cong \frac{\Sigma_{aF}}{\Sigma_a}$$

where Σ_a is the macroscopic cross section for absorption of the entire medium. This ratio is known as the *thermal utilization factor*. Finally, the last ratio in Equation VIe.1.7 represents the absorption rate of thermal neutrons to the absorption rate of all neutrons in the medium:

$$p = \frac{\text{No. of thermal neutrons absorbed in medium}}{\text{No. of all neutrons absored in medium}} = \frac{\int_{medium} dV \int_0^{E_T} \Sigma_a(\vec{r},E)\phi(\vec{r},E)}{\int_{medium} dV \int_0^{\infty} \Sigma_a(\vec{r},E)\phi(\vec{r},E)}$$

This ratio is known as the resonance escape probability. Therefore, we can write the multiplication factor of the infinite medium as $k_\infty = \varepsilon\eta fp$. Upon substitution, the six-factor formula then becomes:

$$k_{eff} = \varepsilon\eta fp P_{FNL} P_{TNL}$$

Some one-group key constants for fast reactors are shown in Table VIe.1.3.

Table VIe.1.3 Nominal one-group constants for a fast reactor (Lamarsh)

Element	σ_f	σ_a	σ_{tr}	ν	η
Na	0	0.0008	3.3	–	–
Al	0	0.0020	3.1	–	–
Fe	0	0.0060	2.7	–	–
U-235	1.4	1.6500	6.8	2.6	2.2
U-238	0.095	0.2550	6.9	2.6	0.97
Pu-239	1.85	2.1100	6.8	2.98	2.61

Cross sections are in barn (i.e., 1E–24 cm^2)

2. Neutron Transport Equation

The neutron transport equation is the mathematical expression of the following fact:

rate of change of neutron population in a control volume =
rate of neutron appearance in the control volume –
rate of neutron disappearance in the control volume

We now evaluate each term in this neutron balance statement for a differential control volume $d\mathrm{V}$ and integrate over the volume of interest:

– Rate of change of neutron population in a control volume:
$\int_{\mathrm{V}} \left(dn(\vec{r}, E, \vec{\Omega}, t) / dt\right) d\mathrm{V}$

– Rate of neutron production by the source*. If by fission then:
$\int_{\mathrm{V}} s d\mathrm{V} = \int_{\mathrm{V}} \nu \Sigma_f(\vec{r}, E) \phi(\vec{r}, E, \vec{\Omega}, t) d\mathrm{V}$

– Rate of neutron production due to scattering from all energy groups and all directions into the differential control volume:
$\int_{\mathrm{V}} \left\{ \int_0^{\infty} \int_{4\pi} \left[\phi(\vec{r}, E', \Omega', t) \Sigma_s(E' \to E, \vec{\Omega}' \to \vec{\Omega})\right] dE' d\vec{\Omega}' \right\} d\mathrm{V}$

– Rate of net neutron leakage into or out of $d\mathrm{V}$:
$\int_{\mathrm{S}} \vec{J}(\vec{r}, E, \vec{\Omega}, t) \cdot dS = \int_{\mathrm{V}} \vec{\nabla} \cdot \vec{J}(\vec{r}, E, \vec{\Omega}, t) d\mathrm{V}$

– Rate of neutron scattering out of $d\mathrm{V}$ and absorption in $d\mathrm{V}$:
$\int_{\mathrm{V}} \left[\phi(\vec{r}, E, \vec{\Omega}, t) \Sigma_t(\vec{r}, E) d\mathrm{V}\right] dE d\vec{\Omega}$

where the divergence theorem related the surface to volume integral, $\oint_A \left[\vec{J}(r,t) \cdot \vec{n}\right] dA = \iiint_{\mathrm{V}} \left[\vec{\nabla} \cdot \vec{J}(r,t)\right] d\mathrm{V}$. Substituting these in the above statement for neutron balance and dropping the integral over V, gives:

$$\frac{1}{V} \frac{\partial \phi}{\partial t} + \vec{\nabla} \cdot \vec{J}(\vec{r}, E, \vec{\Omega}, t) + \phi(\vec{r}, E, \vec{\Omega}, t) \Sigma_t(\vec{r}, E)$$
$$= \nu \phi(\vec{r}, E, \vec{\Omega}, t) \Sigma_f(\vec{r}, E) + \int_0^{\infty} \int_{4\pi} \phi(\vec{r}, E', \vec{\Omega}', t) \Sigma_t(E' \to E, \Omega' \to \vec{\Omega}) dE' d\Omega' \qquad \text{VIe.2.1}$$

where we also substituted for n in terms of ϕ from Equation VIe.1.4. Equation VIe.2.1, known as the neutron transport equation, is a linear partial differential equation. The angular flux in this equation is a function of seven variable; $\vec{r}$ (x, y, z), $\vec{\Omega}$ (θ, φ), E, and t. Since both space and time derivatives of the angular flux, as well as integrals over energy and solid angle, appear together in Equation VIe.2.1, the neutron transport equation is considered an integrodifferential equation. Appearance of both flux and current in Equation VIe.2.1 further complicates finding a solution. It is, therefore, important to find a more useful expression for

* See Section 2.2 and Problem 42 for the discussion on the type of neutron source.

neutron current in terms of neutron flux than the one we already have, $\vec{J} = \phi\vec{\Omega}$. Introduction of any type of simplification to allow us deal with Equation VIe.2.1 undoubtedly requires introduction of assumptions. One of the most important assumptions is the scattering-dominant reaction as discussed next.

2.1. Neutron Current In Weakly Absorbing Media

To express neutron current density, appearing in Equation VIe.2.1 in terms of neutron flux, we consider isotropic scattering of neutrons in a weakly absorbing medium. Figure VIe.2.1(a) shows neutrons being scattered isotropically out of the differential control volume dV. We want to find the neutron current density arriving at the differential surface dS at the origin located at a distance r from dV. If the macroscopic scattering of the nuclei located in volume dV is Σ_s and the flux of neutron in dV is ϕ, then the rate of neutrons scattered out of dV in all directions is $(\phi\Sigma_s)d$V. Thus, neutrons streaming out of dV are distributed over a sphere centered at dV at a rate of $(\phi\Sigma_s)d\text{V}/(4\pi r^2)$. The fraction of these neutrons that should reach dS at the origin should be $[(\phi\Sigma_s)d\text{V}/(4\pi r^2)]dS\cos\varphi$. However, neutron interaction with nuclei in the medium attenuates the rate of neutrons (see Problem 30) arriving at dS by a factor of $\exp(-\Sigma r)$. This factor is the probability of no collision between position r and the origin. In this relation, $\Sigma = \Sigma_a + \Sigma_s$. Since we considered weakly absorbing medium $\Sigma_a \approx 0$ we may then use $\Sigma \approx \Sigma_s$. As a result, the rate of neutrons arriving per unit area of the differential surface dS at the origin due to the neutrons streaming out of dV is:

$$[(\phi\Sigma_s)d\text{V}/(4\pi r^2)]dS\cos\varphi\exp(-\Sigma_s r)$$

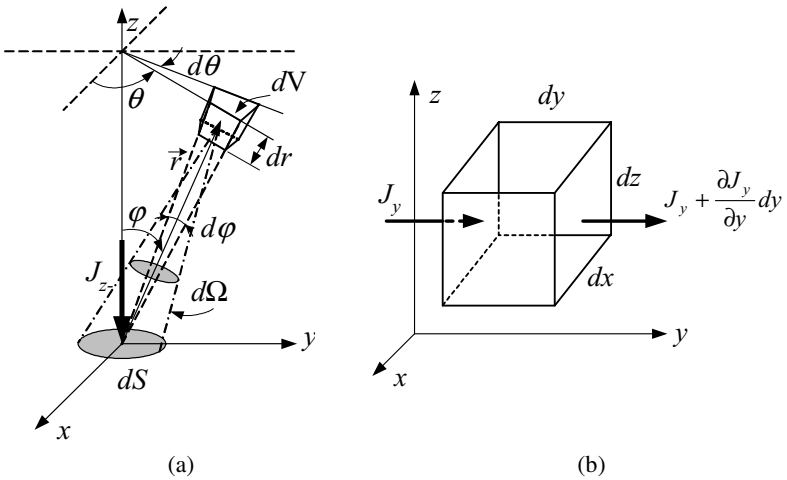

Figure VIe.2.1. (a) Neutron scattering in dV and (b) Neutron leakage from dV

The resulting neutron current in the direction shown in Figure VIe.2.1(a) is:

$$\overrightarrow{dJ}_{z-} \cdot \overrightarrow{dS} = dJ_{z-}dS = \left(\phi\Sigma_s\right) d\mathrm{V} e^{-\Sigma_s r} \frac{\cos\varphi dS}{4\pi r^2}$$

Substituting for differential volume $d\mathrm{V} = (dr)(r\sin\varphi d\theta)(rd\varphi)$ and integrating, we get:

$$J_{z-} = \int_{\theta=0}^{2\pi}\int_{\varphi=0}^{\pi}\int_0^{\infty} \frac{\Sigma_s}{4\pi}\left[\phi(x,y,z)e^{-\Sigma_s} \cos\varphi\sin\varphi d\theta d\varphi dr\right] \qquad \text{VIe.2.2}$$

We now expand $\phi(x, y, z)$ using the Maclaurin series in terms of flux at the origin, $\phi_o = \phi_o(x_o, y_o, z_o)$:

$$\phi(x,y,z) = \phi_o + x\left(\frac{\partial\phi}{\partial x}\right)_o + y\left(\frac{\partial\phi}{\partial y}\right)_o + z\left(\frac{\partial\phi}{\partial z}\right)_o + \frac{x^2}{2}\left(\frac{\partial^2\phi}{\partial x^2}\right)_o + \frac{y^2}{2}\left(\frac{\partial^2\phi}{\partial y^2}\right)_o + \frac{z^2}{2}\left(\frac{\partial^2\phi}{\partial z^2}\right)_o + \cdots$$

Ignoring the higher order terms and substituting flux in Equation VIe.2.2, we obtain:

$$J_{z-} = \phi_o\int_{\vartheta=0}^{2\pi}\int_{\varphi=0}^{\pi/2}\int_0^{\infty}\frac{\Sigma_s}{4\pi}\left[e^{-\Sigma_s r}\cos\varphi\sin\varphi d\theta d\varphi dr\right] + \frac{\partial\phi_o}{\partial z}\int_{\theta=0}^{2\pi}\int_{\varphi=0}^{\pi/2}\int_0^{\infty}\frac{\Sigma_s}{4\pi}\left[\left(r\cos\varphi\right)e^{-\Sigma_s r}\cos\varphi\sin\varphi d\theta d\varphi dr\right]$$

where we have also substituted for $z = r\cos\varphi$ and noted that the integral over $x(\partial\phi/\partial x)_o$ and $y(\partial\phi/\partial y)_o$ vanishes (see Problem 31). Integrating this equation results in:

$$J_{z-} = \frac{\Sigma_s\phi_o}{4\pi}\left[\frac{-e^{-\Sigma_s r}}{\Sigma_s}\right]_0^{\infty}\left[\frac{\sin^2\varphi}{2}\right]_0^{\pi/2}\left[\theta\right]_0^{2\pi} + \frac{\Sigma_s\phi_o}{4\pi}\left(\frac{\partial\phi}{\partial z}\right)_o\left[\frac{-e^{-\Sigma_s r}}{\Sigma_s}\left(-\Sigma_s r-1\right)\right]_0^{\infty}\left[\frac{\sin^2\varphi}{3}\right]_0^{\pi/2}\left[\theta\right]_0^{2\pi}$$

After the substitution of the integral limits we obtain:

$$J_{z-} = \frac{\phi}{4} + \frac{1}{6\Sigma_s}\left(\frac{\partial\phi}{\partial z}\right)_o \qquad \text{VIe.2.3}$$

In order to find the net current in the z-direction at the origin due to the neutrons scattered from dV, we also need to find J_{z+}. This component is easily obtained by integrating Equation VIe.2.4 for $\pi/2 \le \varphi \le \pi$:

$$J_{z+} = \frac{\phi}{4} - \frac{1}{6\Sigma_s}\left(\frac{\partial \phi}{\partial z}\right)_o \qquad \text{VIe.2.4}$$

Thus the net neutron current at the origin in the z-direction becomes:

$$\overrightarrow{J_z} = \overrightarrow{J_{z+}} - \overrightarrow{J_{z-}} = -\frac{1}{3\Sigma_s}\left(\frac{\partial \phi}{\partial z}\right)_o \qquad \text{VIe.2.5}$$

Similar analyses can be performed for the x and y directions. Thus the total neutron current becomes:

$$\vec{J} = -\frac{1}{3\Sigma_s}\left(\frac{\partial \phi}{\partial x} + \frac{\partial \phi}{\partial y} + \frac{\partial \phi}{\partial z}\right) \qquad \text{VIe.2.6}$$

Note that in Equation VIe.2.6 we dropped subscript o (i.e., the reference to the origin). This is because we can carry out similar analyses for any other point, taken as the origin of the coordinate system, in space. We may further simplify Equation VIe.2.6 as:

$$\vec{J}(\vec{r}, E) = -D(\vec{r})\vec{\nabla}\phi(\vec{r}, E) \qquad \text{VIe.2.7}$$

where D in Equation VIe.2.7, is known as the diffusion coefficient (Table VIe.1.2) and is given by $D = 1/3\Sigma_s$. Recall that we derived Equation VIe.2.7 assuming isotropic scattering in a weakly absorbing medium. We may still apply Equation VIe.2.7 to cases where scattering is not isotropic by including the mass number of the moderating nuclei and using $D = A/(3A + 2)\Sigma_s$. In a homogeneous medium Σ_s and D are constant values independent of location. Thus Equation VIe.2.7 in the thermal region, for example, simply becomes $\vec{J}(\vec{r}) = -D\vec{\nabla}\phi(\vec{r})$. This is known as *Fick's law* expressing the fact that in weakly absorbing media, the current of neutrons is from the highly populated region to the sparsely populated region simply due to the net diffusion of the neutrons.

2.2. The One-Speed Neutron Diffusion Equation

The neutron diffusion equation may be obtained from the neutron transport equation or derived directly by applying the balance of neutrons for the control volume of Figure VIe.2.1(b). Choosing the latter method, we find the net rate of leakage into the differential volume in the y-direction as:

$$J_y(dxdz) - \left[J_y + \frac{\partial J_y}{\partial y}dy\right](dxdz) = -\frac{\partial J_y}{\partial y}dxdydz$$

Adding the leakage terms in the *x*- and *z*- directions, we find the total leakage for the control volume *d*V as $-\vec{\nabla}\cdot\vec{J}$. Thus the rate of change of neutrons in the control volume, $(1/V)(\partial\phi/\partial t)$ is equal to the rate of production from a neutron source such as *s* and the net in-leakage minus the net absorption or removal. Expressed mathematically;

$$\frac{1}{V}\frac{\partial\phi(\vec{r},t)}{\partial t}=s(\vec{r},t)-\vec{\nabla}\cdot\vec{J}(\vec{r},t)-\Sigma_a(\vec{r})\phi(\vec{r},t) \qquad \text{VIe.2.8}$$

Substituting for the neutron current density from Fick's law given by Equation VIe.2.7, we find:

$$\frac{1}{V}\frac{\partial\phi(\vec{r},t)}{\partial t}=s(\vec{r},t)-\left[\Sigma_a(\vec{r})\phi(\vec{r},t)+\vec{\nabla}\cdot[-D(\vec{r})\vec{\nabla}\phi(\vec{r},t)]\right] \qquad \text{VIe.2.9}$$

Expectedly, Equation VIe.2.9 is similar to Equation IVa.2.1 as it was derived for diffusion of heat in solids. For a homogeneous medium, *D* can be treated as a constant and the diffusion equation is obtained as:

$$\frac{1}{V}\frac{\partial\phi(\vec{r},t)}{\partial t}=s(\vec{r},t)-\Sigma_a(\vec{r})\phi(\vec{r},t)+D\nabla^2\phi(\vec{r},t) \qquad \text{VIe.2.10}$$

Note that in the derivation of the neutron diffusion equation we assumed that the flux of neutrons is isotropic (i.e., with no directional preference), otherwise the diffusion model does not apply. For example, while the diffusion model is applicable in water, it breaks down at the water-air boundary. This is due to the fact that water is much denser than air hence more neutrons move from water to air than from air to water. If we are interested only in the steady state solution, the diffusion equation further simplifies to:

$$D\nabla^2\phi(\vec{r})-\Sigma_a\phi(\vec{r})=-s(\vec{r}) \qquad \text{VIe.2.11}$$

In Equation VIe.2.11, the Laplacian operator for a rectangular parallelepiped, a cylinder, or a sphere is given by Equation VIIc.1.9, VIIc.1.10, or VIIc.1.11, respectively. For example, neutron flux in a slab is only a function of *x*, thus Equation VIe.2.11 simplifies to:

$$\frac{d^2\phi(x)}{dx^2}-\frac{\Sigma_a}{D}\phi(x)=-\frac{s(x)}{D} \qquad \text{VIe.2.12}$$

Since Σ_a/D is referred to as the diffusion area $L^2=\Sigma_a/D$ then *L* is known as the *diffusion length*. In cylindrical coordinates, assuming flux varies only in the *r*-direction, Equation VIe.2.11 simplifies to:

$$\frac{1}{r}\frac{d}{dr}\left[r\frac{d\phi(r)}{dr}\right]-\frac{\Sigma_a}{D}\phi(r)=-\frac{s(r)}{D} \qquad \text{VIe.2.13}$$

and in spherical coordinates, assuming flux varies only in the *r*-direction, Equation VIe.2.11 becomes:

$$\frac{1}{r^2}\frac{d}{dr}\left[r^2\frac{d\phi(r)}{dr}\right]-\frac{\Sigma_a}{D}\phi(r)=-\frac{s(r)}{D} \qquad \text{VIe.2.14}$$

To find neutron flux we need two boundary conditions for the second order differential equation VIe.2.11. These boundary conditions depend not only on the geometry of the medium but also on the type of the neutron source. These are discussed next.

Medium geometry: The simplest geometry for Equations IVe.2.11 through IVe.2.14 is an infinite medium. Other geometries include infinite slab, finite slab, parallelepiped, infinite cylinder, finite cylinder, and sphere.

Type of source: Neutron sources may be of flux-dependent or flux-independent types. Flux dependent sources are due to fission. Flux-independent sources are sources that emit neutrons at a constant rate and are the driving force for the existence of neutron flux in a medium such as a moderator. The flux-independent sources may either be of a localized or distributed type. We can find analytical solutions for flux-independent sources of point, line, or planar types located in a sphere, cylinder, or slab (See Problems 32 through 41). If we are solving Equations VIe.2.11 through VIe.2.14 for flux-independent localized sources, *s* in these equations should be set to zero, as the neutron source would appear in the boundary condition.

Type of boundary condition: If we are dealing with an infinite medium, one boundary condition is obtained by the fact that as the variable approaches infinity, the flux must become zero. On the other hand, if we are dealing with finite medium, the flux must be zero at the extent of the medium.

The second boundary condition is obtained from the type of the neutron source. For example, the neutron current is generally known as the independent variable approaches the source. For a distributed neutron source, we can take advantage of symmetry if the source is distributed uniformly. If a medium is one that is covered by a blanket, also known as a reflector (see Problem 35), then at the interface between two regions *A* and *B*, we must satisfy:

$$\phi_A = \phi_B \quad \& \quad J_A\cdot\vec{n}=J_B\cdot\vec{n} \qquad \text{VIe.2.15}$$

For the continuity of current in a reflected slab, for example;

$$-D_A(\partial\phi_A/\partial x)_{\text{boundary}} = -D_B(\partial\phi_B/\partial x)_{\text{boundary}}$$

For flux-dependent distributed sources, where the neutron flux and the neutron source are intertwined, we can write:

$$s=\eta\Sigma_{aF}\phi=\eta\frac{\Sigma_{aF}}{\Sigma_a}\Sigma_a\phi = \eta f\Sigma_a\phi$$

where *f*, the fuel utilization factor, is simply given as $f = \Sigma_{aF} / \Sigma_a$ and the multiplication factor k_∞:

$$k_\infty = \frac{\eta f \Sigma_a \phi}{\Sigma_a \phi}$$

Table VIe.1.3 gives useful data such as σ_f, σ_a, v, and η for various materials, where η is the average number of fission neutrons emitted per neutron absorbed. Substituting k_∞ into the diffusion equation, we find:

$$D\nabla^2\phi - \Sigma_a\phi = -k_\infty \Sigma_a \phi$$

Dividing through by the diffusion coefficient, we get:

$$\nabla^2\phi + \frac{\Sigma_a}{D}(k_\infty - 1)\phi = 0$$

Defining $L^2 = D/\Sigma_a$ as *the diffusion area*, we find:

$$\nabla^2\phi + B^2\phi = 0 \qquad \text{VIe.2.16}$$

where $B^2 = (k_\infty - 1)/L^2$ is known as *Material Buckling*. Equation VIe.2.16 is a one-group (i.e., one-energy group) diffusion equation. We can express the one group diffusion equation for a variety of sources such as infinite planar source, point source, and bare slab. However, we are more interested in reactor cores having such familiar geometries as parallelepiped, cylindrical, and spherical. All we need to do is to express the Laplacian operator for the specified core geometry as discussed next.

3. Determination of Neutron Flux in an Infinite Cylindrical Core

Since the cylindrical geometry is most applicable to actual reactor cores, we begin with an infinite circular cylinder and then reduce the solution to the finite right circular cylinder.

Flux in infinite cylindrical core. An infinite cylindrical core is a theoretical concept. We analyze it to eliminate the variation of neutron flux in the *z*-direction, which will be considered later. Assuming symmetry in the θ-direction, neutron flux becomes only a function of *r*. The diffusion equation then becomes:

$$\frac{1}{r}\frac{d}{dr}\left(r\frac{d\phi(r)}{dr}\right) + B^2\phi(r) = 0$$

If we compare this equation with Equation VIIb.1.13, we note that we are dealing with a Bessel differential equation of order zero ($v = 0$) with m also being zero. The solution is given by Equation VIIb.1.14:

$$\phi = c_1 J_0(Br) + c_2 Y_o(Br)$$

where we must find constants c_1 and c_2 from the following boundary conditions:

at $r = 0$, $\phi =$ finite and at $r = R$, $\phi \cong 0$

From the first boundary condition and Figure VIIb.3.1, we conclude that $c_2 = 0$ hence, $\phi = c_1 J_o(Br)$. The second boundary condition is even more interesting, as we get a host of answers. Figure VIIb.3.1 shows that function $J_o(x)$ goes to zero for three values of x when x ranges only from 0 to 8. This indicates that we are dealing with a Sturm-Liouville problem. The diffusion equation is a boundary-value problem having two homogenous boundary conditions. The Sturm-Liouville problem is discussed in Chapter VIIb. Hence, from the second boundary condition we find the n answers that satisfy the secondary boundary conditions as:

$$B_n R = x_n$$

where x_n stands for all n zeros of $J_o(x)$, the Bessel function of the first kind of order zero. As seen from Figure VIIb.3.1, the first zero occurs at 2.405. Hence, $B_1 R = 2.405$ and $B_1 = 2.405/R$. Thus the flux becomes:

$$\phi = c_1 J_o\left(\frac{2.405r}{R}\right)$$

Although we were not able to find c_1, we managed to find the square root of the buckling term. To find coefficient c_1, we use the power produced by the reactor. The power produced per unit volume is given by Equation VIe.1.5 as $\dot{q}''' = E_R \phi \Sigma_f$. Thus, power produced by a unit length of the infinite cylinder reactor is found as:

$$\dot{Q} = \int_V E_R(\phi\Sigma_f)dV = \int_0^R E_R(\phi\Sigma_f)(2\pi r dr)$$

$$= \int_0^R E_R\left[c_1 J_o\left(\frac{2.405r}{R}\right)\Sigma_f\right](2\pi r dr) = \left(2\pi c_1 E_R \Sigma_f\right)\int_0^R J_o\left(\frac{2.405r}{R}\right) r dr$$

In Chapter VIIb the above integral is carried out so that:

$$\int_0^R J_o\left(\frac{2.405r}{R}\right) r dr = \frac{R}{2.405}\left[r J_1\left(\frac{2.405r}{R}\right)\right]_{r=0}^{r=R}$$

$$= \frac{R}{2.405}\left[R J_1(2.405) - 0 \times \cancel{J_1(0)}\right] = \frac{0.51911 R^2}{2.405} = 0.2158 R^2$$

Substituting for the integral and solving for c_1, neutron flux distribution in an infinite cylinder core becomes:

$$\phi = \frac{\dot{Q}}{1.356 E_R R^2 \Sigma_f} J_o\left(\frac{2.405r}{R}\right) \qquad \text{VIe.3.1}$$

Flux in a finite cylinder core. Having solved the infinite cylinder core, we may apply the same method of solution to other geometries such as an infinite slab, rectangular parallelepiped or a spherical core. The results for all these cases are summarized in Table VIe.3.1. Note that the solution for a rectangular parallelepiped is obtained from the solution for an infinite slab. Similarly, the solution for a finite cylinder is obtained from the solutions for an infinite slab and an infinite cylinder. This is the same method we used for the determination of temperature distribution in these geometries, as shown in Table IVa.9.2. The reason for the similarity in mathematical solution is the fact that diffusion is the mechanism for both heat and flux transfer. As seen from Table VIe.3.1, for a finite cylinder, which resembles actual nuclear reactor cores, neutron flux varies as a cosine function in the axial and as the Bessel function of the first kind of order zero in the radial direction. Hence, maximum flux occurs in the center of the reactor. As will be discussed later in this chapter, neutron flux should be as uniform as possible in nuclear reactors. In practice this goal is approached by variety of means including the arrangement of higher power fuel assemblies in the core periphery. From Table VIe.3.1, neutron flux in a finite cylinder and homogenous core is then given as:

$$\phi(r, z) = \left(\frac{3.63\dot{Q}}{\mathrm{V}E_R\Sigma_f}\right) J_o\left(\frac{2.405r}{R}\right) \cos\left(\frac{\pi z}{\mathrm{H}}\right) \qquad \text{VIe.3.2}$$

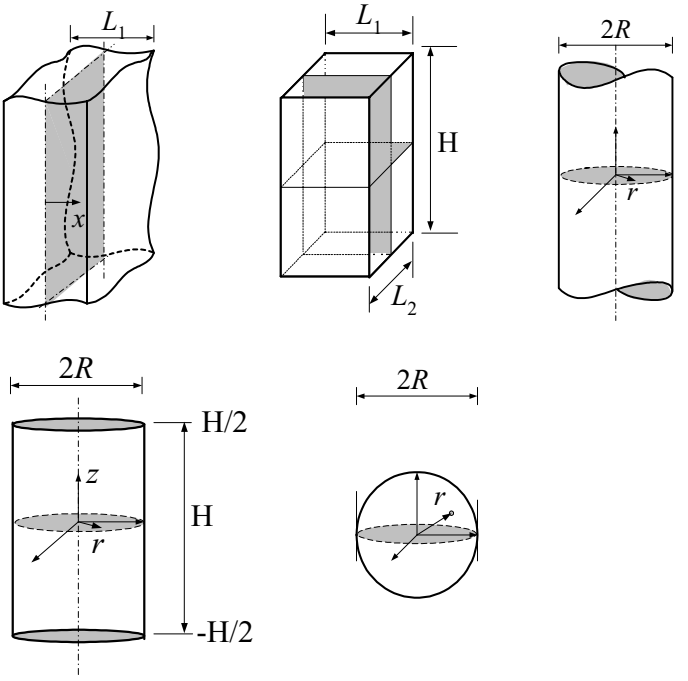

Figure VIe.3.1. Infinite slab, rectangular parallelepiped, infinite cylinder, finite cylinder and sphere

Table VIe.3.1. Flux and geometrical buckling for various critical core geometries

Type	Geometrical Buckling	ϕ	$\zeta = \phi_{max}/\phi_{av}$
Infinite Slab	$\left(\frac{\pi}{L_1}\right)^2$	$\left(\frac{1.57\dot{Q}}{L_1 E_R \Sigma_f}\right)\cos\left(\frac{\pi x}{L_1}\right)$	$\pi/2 = 1.57$
Parallelepiped	$\left(\frac{\pi}{L_1}\right)^2+\left(\frac{\pi}{L_2}\right)^2+\left(\frac{\pi}{\mathrm{H}}\right)^2$	$\left(\frac{3.87\dot{Q}}{\mathrm{V}E_R\Sigma_f}\right)\cos\left(\frac{\pi x}{L_1}\right)\cos\left(\frac{\pi y}{L_2}\right)\cos\left(\frac{\pi z}{\mathrm{H}}\right)$	$(\pi/2)^3 = 3.88$
Infinite Cylinde	$\left(\frac{2.405}{R}\right)^2$	$\left(\frac{0.738\dot{Q}}{R^2 E_R \Sigma_f}\right) J_o\left(\frac{2.405r}{R}\right)$	2.32
Finite Cylinder	$\left(\frac{2.405}{R}\right)^2+\left(\frac{\pi}{\mathrm{H}}\right)^2$	$\left(\frac{3.63\dot{Q}}{\mathrm{V}E_R\Sigma_f}\right) J_o\left(\frac{2.405r}{R}\right)\cos\left(\frac{\pi z}{\mathrm{H}}\right)$	3.64
Sphere	$\left(\frac{\pi}{R}\right)^2$	$\left(\frac{\dot{Q}}{4R^2 E_R \Sigma_f}\right)\frac{1}{r}\sin\left(\frac{\pi r}{R}\right)$	3.29

where H is the total height of the core, as shown in Figure VIe.3.1. Reactor cores consist of thousands of fuel rods. To be able to apply Equation VIe.3.2 to reactors, we relate Σ_f for the entire core to that of the fuel rods by:

$$[(\pi a^2 \mathrm{H}) N_{rod}]\Sigma_{fr} = \pi R^2 \mathrm{H}\Sigma_f$$

where N_{rod} is the number of fuel rods in the core. Solving for Σ_f, we find:

$$\Sigma_f = [a^2 \mathrm{N_{rod}}]\Sigma_{fr} / R^2.$$

where a is the fuel rod radius. Substituting Σ_{aF} in Equation VIe.3.1.2, we get:

$$\phi(r, z) = \left(\frac{3.63\dot{Q}R^2}{\mathrm{V}E_R\Sigma_{fr}N_{rod}a^2}\right) J_o\left(\frac{2.405r}{R}\right)\cos\left(\frac{\pi}{\mathrm{H}}\right)$$

$$= \left(\frac{1.16\dot{Q}}{E_R\Sigma_{fr}N_{rod}a^2\mathrm{H}}\right) J_o\left(\frac{2.405r}{R}\right)\cos\left(\frac{\pi z}{\mathrm{H}}\right)$$

Multiplying $\phi(r, z)$ by energy deposited per fission (E_d) and substitute from Equation VIe.1.5, we obtain:

$$\dot{q}'''(r, z) = \left(\frac{1.16E_d\dot{Q}}{E_R N_{rod} a^2 \mathrm{H}}\right) J_o\left(\frac{2.405r}{R}\right)\cos\left(\frac{\pi z}{\mathrm{H}}\right) \qquad \text{VIe.3.3}$$

Equation VIe.3.3 gives the distribution of the volumetric heat generation rate in reactor cores of finite cylinder. Since $[J_0(x)]_{\max} = 1$ and $[\cos(x)]_{\max} = 1$, the maximum volumetric heat generation rate occurs at the center of the cylinder where $r = z = 0$. Hence, Equation VIe.3.3 can be expressed as:

$$\dot{q}'''(r, z) = \dot{q}'''_{\max} J_o\left(\frac{2.405r}{R}\right)\cos\left(\frac{\pi z}{\mathrm{H}}\right) \qquad \text{VIe.3.4}$$

Example VIe.3.1. A reactor core contains 41,000 fuel rods. The nuclear plant is operating at 1000 MWe and 29% thermal efficiency. Fuel pellet diameter is 0.44 in. Core dimensions are, D = H = 4 m. Find the volumetric heat generation rate at z = H/3 and $r = R/2$.

Solution: We find the maximum volumetric heat generation rate occurring at z = r = 0 from:

$$\dot{q}'''_{\max} = \left(\frac{1.16E_d\dot{Q}}{E_R N_{rod} a^2 \mathrm{H}}\right) = \frac{1.16\times180\times(1000/29\%)}{200\times41000\times[(0.44/2)/12]^2\times4} = 65.31 \text{ MW/ft}^3$$
$$= 2.23\text{E8 Btu/h·ft}^3$$

Therefore, $\dot{q}'''(r, z)$ = 2.23E8 [J_0(2.405 × R/2R) cos(π× H/3H)] = 2.23E8 × 0.67 × 0.5 = 0.75E8 Btu/h·ft^3.

Actual versus bare reactor cores. In actual reactor cores the maximum volumetric heat generation rate, is less than that calculated in the above example. To find $\dot{q}'''_{\max}$ in actual cores, we write:

$$\left(\dot{q}'''_{\max}\right)_{actual} = \Sigma_{fr} E_d \phi_{\max} = \Sigma_{fr} E_d (\phi_{\text{av}}\, \zeta) = \Sigma_{fr} E_d \left(\frac{\dot{Q}\zeta}{\Sigma_f E_R \mathrm{V}}\right)$$

$$= \Sigma_{fr} E_d \left(\frac{\dot{Q}\zeta}{(\Sigma_{fr} N_{rod} a^2 / R_2) E_R \mathrm{V}}\right)$$

or alternatively;

$$\left(\dot{q}'''_{\max}\right)_{actual} = \frac{\dot{Q}E_d\zeta}{\pi \mathrm{H} a^2 N_{rod} E_R}$$

Heat flux distribution. We obtained the volumetric heat generation rate in a cylindrical core in Equation VIe.3.4. To obtain similar distribution, but for core heat flux, we write the relation between power, linear heat generation rate, heat flux and volumetric heat generation rate for a fuel rod as:

$$\dot{Q} = \dot{q}'\mathrm{H} = \dot{q}''\mathrm{P}_F\mathrm{H} = \dot{q}'''A_F\mathrm{H} \qquad \text{VIe.3.5}$$

where H is the rod length, P_F is the fuel pellet perimeter, and A_F is the fuel pellet cross sectional area. Thus, Equation VIe.3.4 can also be written as:

$$\dot{q}''(r, z) = \dot{q}''_{\max} J_o\left(\frac{2.405r}{R}\right)\cos\left(\frac{\pi z}{\mathrm{H}}\right) \qquad \text{VIe.3.6}$$

where $\dot{q}''$ is the local and $\dot{q}''_{\max}$ is the maximum fuel rod heat flux.

Example VIe.3.2. Data for a BWR core, bundle, and rod are given as follows:

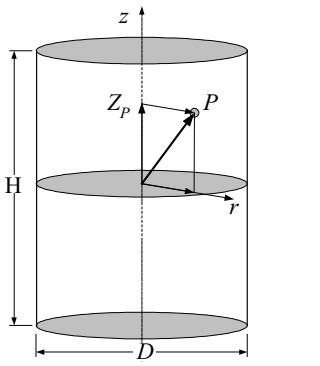

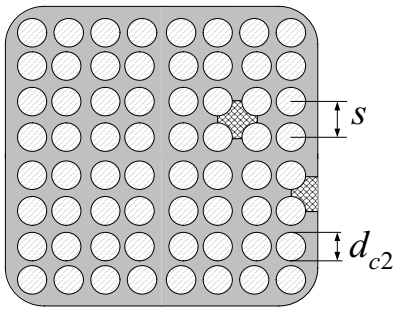

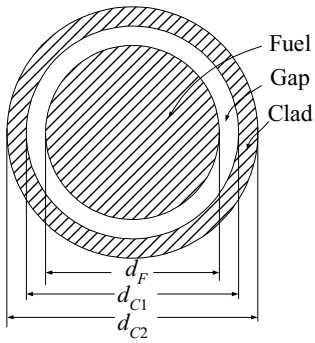

D: Core diameter (ft):	16	H: Core height (ft):	12
n: Rods per bundle:	64	s: Pitch (in):	0.74
d_{C1}: Clad in-dia. (in):	0.50	d_{C2}: Clad out-dia. (in):	0.56
$\dot{Q}$: Core power (MWth):	3,300	ρ: UO_2 density (lbm/ft^3):	644
N: Number of fuel bundles:	585		
d_F: Pellet diameter (in):	0.48		
δ: Clad thickness (in):	0.03		
Ω: $\dot{q}'''_{\max} / \dot{q}'''_{av}$:	2.5		

Find,
a) total weight of UO_2 in kg,
b) core average power density in kW/lit,
c) specific power in kW/kg,
d) average linear heat generation rate in kW/ft,
e) average heat flux in kW/ft^2,
f) the maximum volumetric heat generation rate in kW/ft^3, and g) the volumetric heat generation rate at $r = R/2$ and $z = H/3$.

Solution:
a) We first find total volume and mass of UO_2:

$$\mathrm{V}_{\mathrm{UO}_2} = \pi d_F^2 \mathrm{H}/4 = \pi \times (0.48/12)^2 \times (12/4) \times (8 \times 8 \times 585) = 564.58 \text{ ft}^3$$

$$M_{\mathrm{UO}_2} = \rho \mathrm{V} = 643.85 \times 564.58 = 363{,}505 \text{ lbm} = 164{,}667.7 \text{ kg} \cong 165 \text{ tons}$$

b) We now calculate core volume:

$$\mathrm{V}_{Core} = \pi D^2 \mathrm{H}/4 = \pi \times (16/3.2808)^2 \times (12/3.2808)/4] = 68.32\text{E}3 \text{ lit}$$

By definition: $\overline{P.D.} = \dot{Q}_{Core} / \mathrm{V}_{Core} = 3{,}300 \times 1000/68.32\text{E}3 = 48.3$ kW/lit

c) By definition: $S.P. = \dot{Q}_{Core} / M_{\mathrm{UO}_2} = 3{,}300 \times 1000/164{,}667.7 = 20$ kW/kg

d) By definition: $\bar{\dot{q}}' = \dot{Q}_{Core} / (N_{Rod} \times \mathrm{H}) = 3{,}300 \times 1000 / [(585 \times 8 \times 8) \times 12] =$ 7.3 kW/ft

e) $\bar{\dot{q}}'' = \dot{Q}_{Core} / (N_{Rod} \times \pi d_{C2} \mathrm{H}) = 3{,}300 \times 1000 / [(585 \times 8 \times 8) \times \pi \times (0.56/12) \times 12]$
= 50 kW/ft^2

f) $$\left(\dot{q}'''_{\max}\right)_{Bare} = \frac{1.16 P E_d}{\mathrm{H} a^2 N_{Rod} E_R} = \frac{1.16 \times 3{,}300 \times 1000 \times 180}{12 \times (0.48/12)^2 \times (64 \times 585) \times 200}$$
= 4792.67 kW/ft^3

$$\dot{q}'''_{\max} = \frac{1.16 P E_d}{\mathrm{H} a^2 N_{Rod} E_R} \left(\frac{\zeta}{1.16\pi} \right) = 4792.67 \times \frac{2.5}{1.16\pi} = 3287.83 \text{ kW/ft}^3$$

g) Since $\dot{q}'''(r,z) = \dot{q}'''_{\max} J_o\left(\frac{2.405 r}{R}\right) \cos\left(\frac{\pi z}{\mathrm{H}}\right)$

then $\dot{q}'''(r,z) = 3287.83 \times J_o[(2.405 \times R/2)/R] \times \cos[(\pi \times \mathrm{H}/3)/\mathrm{H}] = 3287.83 \times 0.669 \times 0.5 = 1099.78$ kW/ft^3

Average heat generation rate. We find the core average heat generation rate from:

$$\overline{\dot{q}'''} = \frac{\int_N \dot{q}'''(r,z)d\mathrm{V}}{\mathrm{V}} = \left(\frac{1}{\pi R^2 H}\right)\left(\frac{1.16E_d\dot{Q}}{E_R N_{rod} a^2 \mathrm{H}}\right)$$

$$\left[\int_0^R J_o\left(\frac{2.405r}{R}\right)(2\pi r dr)\right]\left[\int_{-\mathrm{H}/2}^{\mathrm{H}/2}\cos\left(\frac{\pi z}{H}\right)dz\right]$$

If we carryout the integrals in the radial and the axial directions, we find $\overline{\dot{q}'''} = \dot{q}'''_{\max}/(2.316 \times 1.57)$. Writing in terms of heat flux by using Equation VIe.3.5 and representing $F_N = 2.316 \times 1.57$ we obtain:

$$\dot{q}''_{\max} = \overline{\dot{q}''} \times F_N \qquad \text{VIe.3.7}$$

where in Equation VIe.3.7, F_N is known as the *nuclear peaking factor*. The first multiplier, $F_N^{axial} = 2.316$, is the axial peaking sub-factor and the second multiplier, $F_N^{radial} = 1.57$, is the radial peaking sub-factor.

3.1. Axial Temperature Distribution

We use the volumetric heat generation rate, as given by Equation VIe.3.3 to determine the axial temperature distribution in the reactor core. To limit the analysis to only one variable, we choose the central channel for which $r = 0$ hence $J_o = 1$. We also limit the analysis to PWRs* where coolant entering and leaving the core remains subcooled. This assumption allows us to write $dh = c_p dT$. Using subscript f for the bulk coolant, F for the fuel, and applying Equation IIa.6.6 to an elemental control volume taken at axial location z (Figure VIe.3.2(c)), yields:

$$\dot{m}h + d\dot{Q} = \dot{m}(h + dh)$$

Simplifying, we find $\dot{m}c_p dT_f = d\dot{Q}$. For the fuel rod of Figure VIe.3.2, $\dot{Q} = \dot{q}'\mathrm{H} = \dot{q}''\mathrm{P}_{C2}\mathrm{H} = \dot{q}'''A_F\mathrm{H}$ where $\mathrm{P}_{C2} = \pi d_{C2}$, and $A_F = \pi d_F^2/4$. Substituting for total rate of heat generation we get:

$$\dot{m}c_p dT_f = d\dot{q} = \dot{q}'''(z)A_F dz$$

We now substitute from Equation VIe.3.3 and integrate from the core inlet to any elevation:

---

* Note we are assuming that boiling does not occur even in the hot channel.

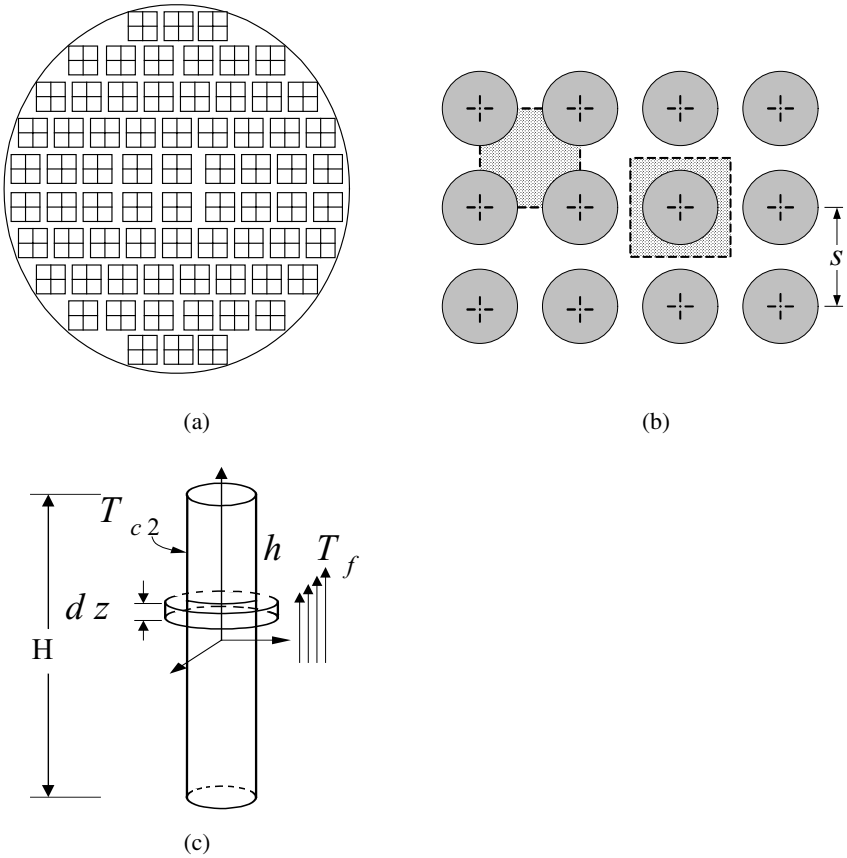

Figure VIe.3.2. (a) Core, (b) Fuel rods, and (c) Central rod and channel

$$\int_{-\mathrm{H}/2}^{z} \dot{m} c_p dT_f = A_F \dot{q}'''_{\max} \int_{-\mathrm{H}/2}^{z} \cos\left(\frac{\pi z}{\mathrm{H}}\right) dz$$

Carrying out the integral and simplifying, we obtain the coolant temperature as:

$$T_f(z) = T_{f,in} + \frac{\dot{q}'''_{\max} A_F \mathrm{H}}{\pi \dot{m} c_p}\left[1 + \sin\left(\frac{\pi z}{\mathrm{H}}\right)\right] \qquad \text{VIe.3.8}$$

Having the coolant temperature, we can find the clad outside temperature from a steady state heat balance:

$$d\dot{Q} = h\left(\mathrm{P}_{C2} dz\right)\left(T_{C2} - T_f\right)$$

Substituting for the rate of heat transfer and for fluid temperature and solving for clad temperature, we get:

$$T_{C2}(z) = T_{f,in} + \frac{\dot{q}'''_{\max} \mathrm{V}_F}{\pi \dot{m} c_p}\left[1 + \sin\left(\frac{\pi z}{\mathrm{H}}\right)\right] + \frac{\dot{q}'''_{\max} A_F}{h \mathrm{P}_{C2}} \cos\left(\frac{\pi z}{\mathrm{H}}\right) \qquad \text{VIe.3.9}$$

In this equation, we assumed that the heat transfer coefficient, h, remains constant from inlet to any elevation. Having the clad outside temperature, we can find clad inside temperature, T_{C1}, fuel surface temperature, T_{F2}, and fuel centerline temperature by using the corresponding thermal resistances. Following the procedure that led to derivation of Equation IVa.6.15, we can find each temperature in terms of $T_{f,\,in}$, $\dot{m}$, and $\dot{q}'''_{\max}$ as:

$$T_{c1}(z) = T_{f,in} + \frac{\dot{q}'''_{\max} \mathrm{V}_F}{\pi \dot{m} c_p}\left[1 + \sin\left(\frac{\pi z}{\mathrm{H}}\right)\right] + \mathrm{V}_F (R_f + R_C)\dot{q}'''_{\max} \cos\left(\frac{\pi z}{\mathrm{H}}\right) \qquad \text{VIe.3.10}$$

$$T_{F2}(z) = T_{f,in} + \frac{\dot{q}'''_{\max} \mathrm{V}_F}{\pi \dot{m} c_p}\left[1 + \sin\left(\frac{\pi z}{\mathrm{H}}\right)\right] + \mathrm{V}_F (R_f + R_C + R_G)\dot{q}'''_{\max} \cos\left(\frac{\pi z}{\mathrm{H}}\right) \qquad \text{VIe.3.11}$$

$$T_{F1}(z) = T_{f,in} + \frac{\dot{q}'''_{\max} \mathrm{V}_F}{\pi \dot{m} c_p}\left[1 + \sin\left(\frac{\pi z}{\mathrm{H}}\right)\right] + \mathrm{V}_F (R_f + R_C + R_G + R_F)\dot{q}'''_{\max} \cos\left(\frac{\pi z}{\mathrm{H}}\right) \qquad \text{VIe.3.12}$$

where the thermal resistance of fuel (R_F), gap (R_G), clad (R_C), and flow (R_f) are the terms in the denominator of Equation IVa.6.15. Temperature distributions of the coolant, clad, and fuel are shown in Figure VIe.3.3.

As we expect, the coolant temperature peaks at the channel exit due to the accumulation of heat. However, the fuel rod temperature is a function of both coolant temperature and the volumetric heat generation rate. While the coolant temperature keeps increasing along the channel, the volumetric heat generation rate is at its maximum at the center and then keeps decreasing, due to the $\cos(\pi z/\mathrm{H})$ multiplier. Therefore, the axial fuel rod temperature increases until a maximum temperature is reached, the location of which is expectedly above the core centerplane and below the channel exit.

Now that we evaluated the axial temperature distribution of the fuel rod at a given radius, let's evaluate the radial temperature distribution of the fuel rod at a given axial location. By expressing fuel rod temperature at various radial locations (Equations VIe.3.9 through VIe.3.12) with temperature at each location being a function of z, we have used a two-dimensional approach for the fuel rod temperature, albeit for selected nodes. Note that by using a single control volume for the coolant, its temperature in the radial direction is lumped. Since at any axial location, fuel rod temperature is a function of both T_f and $\dot{q}'''_{\max}$, it is then expected that temperature further inside the fuel rod is influenced more by $\dot{q}'''_{\max}$ and less by

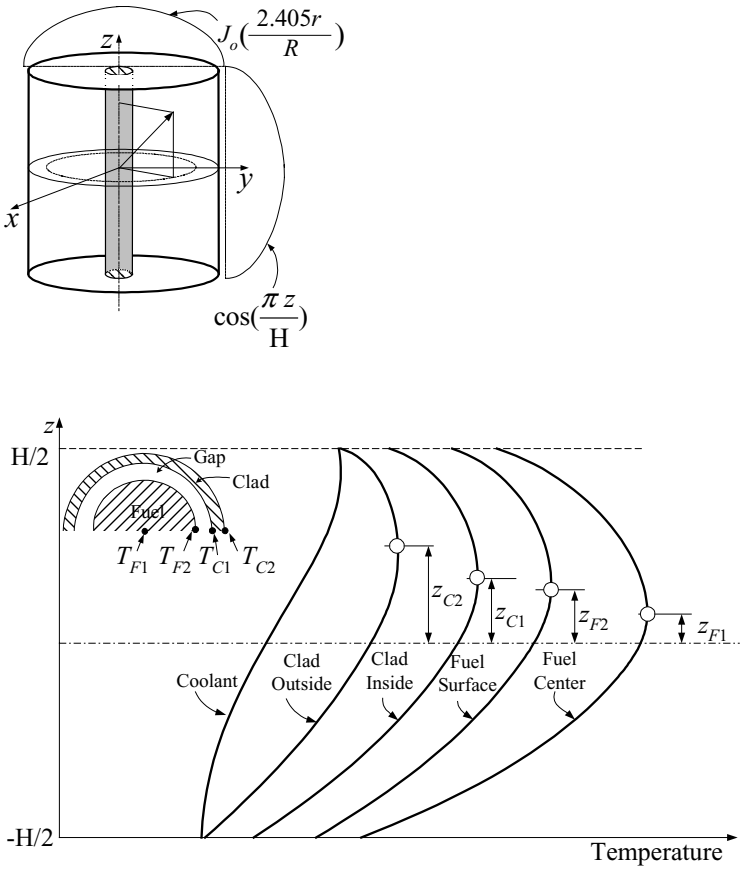

Figure VIe.3.3. Two dimensional temperature distribution of a fuel rod in the hot channel of a PWR

T_f . This is shown by the elevations from the point of maximum temperature to the core center-plane for various radial location as clad outside (z_{C2}), clad inside (z_{C1}), fuel surface (z_{F2}), and fuel centerline (z_{F1}).

To find the location of the maximum temperatures, we take the derivative of the related equation for temperature and set it equal to zero. By substituting the location at which temperature is maximum, we can obtain the value of T_{max} in terms of all the known variables for any radial location of the fuel rod. For example, for clad outside temperature, we take the derivative of Equation VIe.3.9 and set it equal to zero:

$$z_{c2,\max} = \left(\mathrm{H}/\pi\right)/\tan^{-1}\left(\pi \dot{m} c_p R_f\right)$$

Example VIe.3.3. A PWR core contains 217 fuel assemblies, each on the average containing 176 fuel rods, operating at 2700 MWth.. Use the data given below and find the location and the value of the peak clad outside temperature. Data: H = 12 ft, $\dot{m}$ = 138.5E6 lbm/h, d_{F2} = 0.377 in, d_{C2} = 0.44 in, h = 4000 Btu/h·ft^2 F, c_p = 1.392 Btu/lbm·F, $T_{f,\,in}$ = 550 F, and Ω = 2.56.

Solution: We first find the number and volume of the rods:
$N_{rod} = 217 \times 176 = 38{,}192$
$V_F = \pi(d_{F2})^2/4 \times H = \pi(0.377/12)^2 \times 12/4 =$ 9.3E–3 ft^3

We now find thermal resistance of the coolant film:
$R_f = (\pi d_{C2}H)h = 1/[\pi \times (0.44/12) \times 12 \times 4000] =$
1.81E–4 h·ft^2·F/Btu (3.186E–5 m^2·K/W)
$Z_{C2,\,max} = (12/\pi)/\tan^{-1}[\pi \times (138.5E6/38{,}192) \times 1.392 \times 1.81E{-}4] = (12/\pi)/1.235 =$
3.1 ft (1 m)

The maximum volumetric heat generation rate is found from:

$$\dot{q}'''_{\max} = \left(\frac{E_d \dot{Q}\zeta}{\pi E_R N_{rod} a^2 H}\right) = \frac{180 \times 2700 \times 2.56}{\pi \times 200 \times 38{,}192 \times [(0.377/2)/12]^2 \times 12} = 17.51 \text{ W/ft}^3$$

= 5.97E7 Btu/h·ft^3

The peak clad outside temperature is found from Equation VIe.3.9 by substituting for $z = z_{c2,\max} = 3.1$:

$$T_{C2,\,\max} = 550 + \frac{5.97E7 \times 9.3E-3}{\pi \times (138.5E6/38{,}192) \times 1.392}\left(1 + \sin\frac{\pi \times 3.1}{12}\right) +$$

$$\frac{5.97E7 \times 9.3E-3}{1/181E-4}\cos\frac{\pi \times 3.1}{12} = 680 \text{ F}$$

Example VIe.3.4. Shown in the figure is the surface heat flux of a rod in an experimental reactor. Use the given data and find a) coolant temperature, b) clad surface temperature, and c) fuel centerline temperature at z = H/2. Data: H = 6 ft, $d_{F2} = d_{C1}$ = 0.4 in, d_{C2} = 0.5 in, $T_{f,in}$ = 155 F, $\dot{m}$ = 375 lb/hr per rod, h = 2000 Btu/h·ft^2·F, k_F = 1 and k_C = 3 Btu/h·ft·F, $\dot{q}''_1$ = 120,000 Btu/hr ft^2, $\dot{q}''_1$ = 250,000 Btu/hr·ft^2.

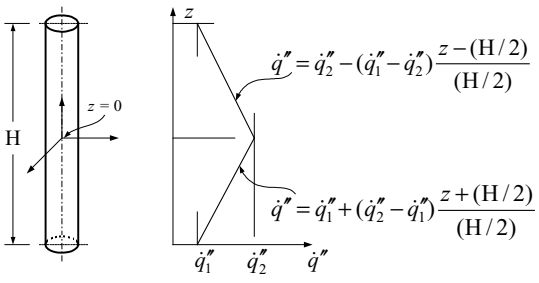

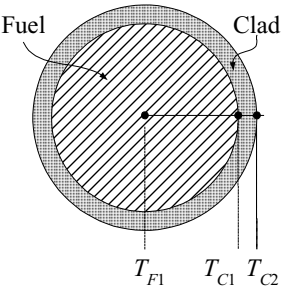

Solution:
a) We write an energy balance for an elemental control volume and integrate:

$$\dot{m}c_p\left[T_f(z)-T_{f,in}\right]=\int_{-\mathrm{H}/2}^{0}\dot{q}''(z)(\pi d)dz+\int_{0}^{z}\dot{q}''(z)(\pi d)dz$$

We then substitute for heat flux and carrying out the integral:

$$\dot{m}c_p\left[T_f(z)-T_{f,in}\right]=$$

$$\pi d\left[\left(\dot{q}_1''z+(\dot{q}_2''-\dot{q}_1'')\frac{(z^2/2)+(\mathrm{H}/2)z}{\mathrm{H}/2}\right)_{-\mathrm{H}/2}^{0}+\left(\dot{q}_1''-(\dot{q}_2''-\dot{q}_1'')\frac{(z^2/2)-(\mathrm{H}/2)z}{\mathrm{H}/2}\right)_{0}^{z}\right]$$

Solving for $T_f(z)$ and substituting values, we find:

$$T_f(z)=T_{f,in}+\frac{\pi d\mathrm{H}}{2\dot{m}c_p}\left(\dot{q}_1''+\dot{q}_2''\right)=155+\frac{\pi\times(0.5/12)\times6}{2\times375\times1}\left(1.2\mathrm{E}5+2.5\mathrm{E}5\right)$$

$$=542.5\ \mathrm{F}$$

b) From a transverse heat balance we also find:

$$T_{C2}(z)=T_f(z)+\left[\dot{q}''(z)/h\right]$$

Substituting values to get:

$$T_{C2}=T_f(z)+\left[\dot{q}_1''-(\dot{q}_2''-\dot{q}_1'')\frac{z-(\mathrm{H}/2)}{\mathrm{H}/2}\right]/h=542.5+\frac{1.2\mathrm{E}5}{2000}=602.5\ \mathrm{F}$$

c) We find, T_{F1} from another energy balance:

$$\dot{Q}(z)=\dot{q}''(z)(\pi d_{C2}z)=\left[T_{F1}(z)-T_{C2}(z)\right]/\Sigma R$$

$$T_{F1}=T_{C2}+d_{C2}\left[\frac{1}{4k_F}+\frac{\ln(d_{C2}/d_{C1})}{2k_C}\right]\left(\dot{q}_1''\right)$$

$$=\ T_{F1}=474+\frac{0.5}{12}\left[\frac{1}{4\times1}+\frac{\ln(0.5/0.4)}{2\times3}\right]\times1.2\mathrm{E}5=\ 1910\ \mathrm{F}$$

3.2. Determination of Incipient Boiling

In BWRs we often need to find the surface temperature and its location corresponding to the inception of subcooled boiling. As was discussed in Chapter Vb, such local temperature is not a single fixed temperature. Still, we can estimate a value for it from the following relation:

$$T_{SB} = T_{sat} + (T_{C2} - T_{sat})_{\text{J-L}} - (\dot{q}''/h) \qquad \text{VIe.3.13}$$

where $(\Delta T_{sat})_{\text{J-L}}$ is given by the Jens-Lottes correlation, for example:

$$T_{C2} - T_{sat} = \frac{60(\dot{q}''/1\text{E}6)^{1/4}}{e^{P/900}}$$

In British units, P is in psia, temperatures are in F, $\dot{q}''$ is in Btu/h·ft^2 and h is in Btu/h·ft^2·F. In general, the heat flux is given as a function of elevation, based on $\dot{q}''' = \dot{q}'''_{\max}\cos(\pi z/\text{H})$, where the clad surface temperature is given by Equation VIe.3.9. Thus, $T_{SB} = T_{C2}$ and Z_{SB} are found by solving Equations VIe.3.9 and VIe.3.13 simultaneously. We may solve the resultant set by plotting each equation and finding the intersection. Or we set these equations equal and solve the resultant nonlinear equation by numerical means. Using the second method, the equation becomes:

$$T_{f,in} + \frac{\dot{q}'''_{\max}\text{V}_F}{\pi \dot{m} c_p}\left[1 + \sin\left(\frac{\pi z}{\text{H}}\right)\right] + \frac{\dot{q}'''_{\max} A_F}{h\text{P}_{C2}}\cos\left(\frac{\pi z}{\text{H}}\right) =$$
$$T_{sat} + \frac{60(\dot{q}''/1\text{E}6)^{1/4}}{e^{P/900}} - \frac{\dot{q}''}{h}$$

We now substitute for $\dot{q}'' = \dot{q}'''_{\max}(A_F/\text{P}_{C2})\cos(\pi z/\text{H})$ and rearrange the above relation to get:

$$\lambda_1 \text{Y} - \lambda_2(1 - \text{Y}^2)^{1/2} - \lambda_3 \text{Y}^{1/4} + \lambda_4 = 0$$

where, in this relation, Y = cos(πz/H), and coefficients λ_1 through λ_4 are given as $\lambda_1 = 2(A_F/\text{P}_{C2})\,\dot{q}'''_{\max}/h$, $\lambda_2 = \dot{q}'''_{\max}\text{V}_F/(\pi c_p \dot{m})$, $\lambda_3 = 60[(A_F/\text{P}_{C2})\,\dot{q}'''_{\max}/1\text{E}6]^{1/4}/\text{e}^{P/900}$, and $\lambda_4 = T_{f,in} + \lambda_2 - T_{sat}$.

Example VIe.3.5. Water enters the hot channel of a BWR at a velocity of V = 8 ft/s, temperature of 525 F, and pressure of 1020 psia. Fuel rods are arranged in square array on a pitch of 0.738 in. Heat flux can be closely represented as $\dot{q}'' = \dot{q}''_{\max}\cos(\pi z/12)$ where z is in ft. Find the clad temperature and its location of the inception of subcooled boiling. Data: $\dot{q}'''_{\max} = 1.28\text{E}7$ Btu/h·ft^3, d_{C2} = 0.563 in and d_F = 0.487 in.

Solution: At 1020 psia & 525 F, ρ = 47.6 lbm/ft^3, c_p = 1.24 Btu/lbm·F, μ = 6.6E-5 lbm·ft/s, k = 0.3 Btu/h·ft·F

$A_F = \pi d_F^2/4 = \pi(0.487)^2/4 = 1.293\text{E-}3$ ft^2, $\text{P}_{C2} = \pi d_{C2} = 0.147$ ft, $\text{V}_F = A_F\text{H} = 1.293\text{E-}3 \times 12 = 0.0155$ ft^3

$A_{Flow} = p^2 - \pi d_{C2}^2/4 = (0.738/12)^2 - \pi(0.563)^2/4 = 2.05\text{E-}3$ ft^2 (1.9 cm^2)

$D_e = 4A_{Flow}/P_{C2} = 4 \times 2.05\text{E-}3/(\pi \times 0.563/12) = 5.58\text{E-}2$ ft (1.7 cm)
$\dot{m} = \rho \times V \times A_{Flow} = 47.6 \times 8 \times 2.05\text{E-}3 = 0.78$ lbm/s = 2810 lbm/h (0.354 kg/s)

Calculate h from Equation IVb.3.6 for forced single phase flow:
$C = 0.042(0.7382/0.563) - 0.024 = 0.031$
$\text{Nu} = hD_e/k_{Water} = 0.031\text{Re}^{0.8}\text{Pr}^{1/3} = 0.031[47.6 \times 8 \times 5.58\text{E-}2/6.6\text{E-}5]^{0.8}(0.873)^{1/3}$
$= 754$

Hence, $h = 754 \times 0.3377/5.58\text{E-}2 = 4563$ Btu/h·ft^2·F (25.91 kW/m^2·K)

$\lambda_1 = 2(A_F/P_{C2})\ \dot{q}'''_{\max}/h = 2(1.293\text{E-}3/0.147) \times 1.28\text{E}7/4563 = 49.35$ F (9.6 C)
$\lambda_2 = \dot{q}''_{\max} V_F/(\pi c_p \dot{m}) = 1.28\text{E}7 \times 0.0155/(\pi \times 1.24 \times 2810) = 18.12$ F (–7.7 C)
$\lambda_3 = 60[(A_F/P_{C2})\ \dot{q}'''_{\max}/1\text{E}6]^{1/4}/e^{P/900} = 60(8.78\text{E-}3 \times 1.28\text{E}7/1\text{E}6)^{1/4}/e^{1020/900} = 11.18$
F (–11.56 C)
$\lambda_4 = T_{f,in} + C_2 - T_{sat} = 525 + 18.12 - 546.99 = -3.87$ F (–15.63 C)

$49.35\text{`Y} - 18.12(1 - \text{Y}^2)^{1/2} - 11.18\text{Y}^{1/4} - 3.87 = 0$

By iteration we find $\text{Y} = \cos(\pi z/\text{H}) = 0.5732$

Hence, $z_{SB} = -44$ in (i.e., 44 in below the core centerline or (144/2) – 44 = 28 in from the core inlet). Upon substitution in either Equation VIe.3.9 or VIe.3.12, we find $T_{SB} = 542.4$ F (283.5 C). Note, T_{sat} (1020 psia) = 547 F (286 C).

In the above example we determined incipient boiling in a BWR. Let us now investigate a similar question for a PWR. Although there is no bulk boiling under normal operation, during certain transients or for the hot-channel even at steady state, local boiling may take place. While PWR channels are interconnected and heat flux profile is not uniform, we still consider fluid flow in a single vertical channel, subject to uniform heating to characterize flow in a PWR hot channel. For this channel, the temperature profiles of water and of channel surface as well as the void fraction profile versus the flow quality, X are shown in Figure VIe.3.4. Water enters this heated channel and flows upward. Heat transfer takes place from the channel wall to the single phase water in forced convection. Somewhere along the channel, at the point of the incipient boiling, the first bubble appears. As discussed in Chapter Vb, the surface temperature would remain nearly unchanged subsequent to the inception of subcooled boiling. The bubbles eventually manage to leave the surface, migrate into the bulk liquid, and collapse to heat up water, which is eventually brought to saturation.

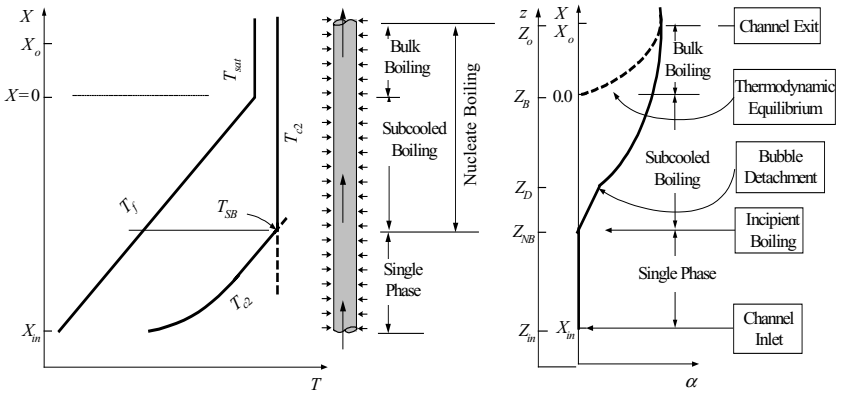

Figure VIe.3.4. Incipient boiling and void-quality profile for uniform heating of water

As the void-flow quality profile of Figure VIe.3.4 indicates, void fraction remain zero as long as water remains subcooled. At the incipient boiling, void fraction becomes nonzero and rises steadily. Upon more vigorous bubble production, which then results in bubble detachment, the increase in void fraction occurs at a larger slope, which continues up to the channel exit. The dotted curve shows void fraction starting from $X = 0$, which conforms to the assumption of thermodynamic equilibrium.

3.3. Margin for Thermal Design

Nuclear peaking factors. We derived the nuclear peaking factor, F_N in Equation VIe.3.7 for a right circular cylinder core using assemblies that produce equal power and are distributed uniformly in the core. These peaking factors are shown in Table VIe.3.1 for various core geometries. Equation VIe.3.3 shows that the maximum heat flux for a set of operational conditions is a fixed value and to increase the core average heat flux, we must reduce the nuclear peaking factors. Thus, for the same $\dot{q}'''_{\max}$, the flatter the neutron flux, the smaller the nuclear peaking factors and the larger the core average heat flux. In practice, there are various means of flattening the neutron flux in the core. For example, to flatten the radial distribution of neutron flux, fuel assemblies with higher enrichment are placed in the core periphery and less enriched assemblies in the center of the core. Instead of using higher enrichment, we may place older assemblies closer to the center and fresh assemblies in the core periphery during the plant scheduled shutdown for reload. The same goal may also be achieved by using burnable poisons or chemical shim (neutron absorbing material such as boron). However, placing higher enrichment or fresh assemblies at the core periphery would also increase neutron leakage. In the axial direction, fuel rods are loaded with less enriched fuel or even fuel mixed with burnable poison in the center of the rod. Figure VIe.3.5 shows two axial distributions. Figure VIe.3.5(a) shows the flux profile with cosine distribution at the beginning of cycle (BOC) and dipping in the central region to-

wards the end of cycle (EOC) due to higher flux. Figure VIe.3.5(b) shows the effect of burnable poison on flattening the neutron flux profile, hence, reducing the axial peaking factor.

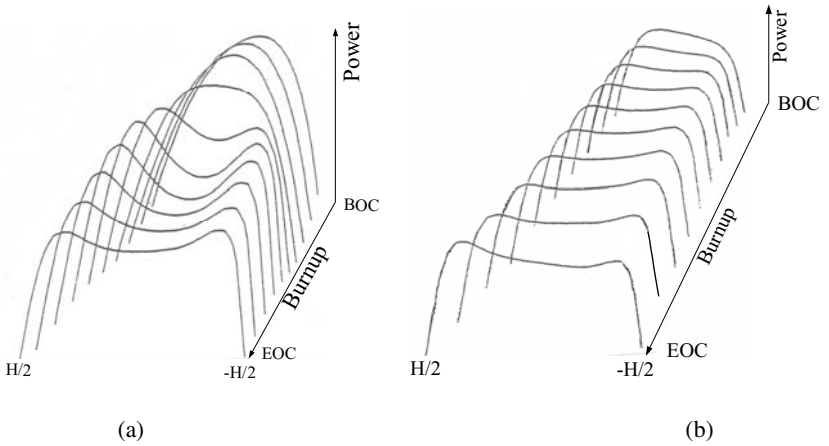

Figure VIe.3.5. Axial power distribution (a) Uniformly loaded rod and (b) rod loaded with poison

Engineering peaking factors, F_E, enhance the total peaking factor, $F = F_N \times F_E$ and further reduce the core average heat flux. The engineering peaking factors are those that affect the temperatures of clad and fuel centerline. These can be easily identified from Equations VIe.3.9 through VIe.3.12 as follows:

- *channel flow rate* ($\dot{m}$). Reduction in flow rate to the central channel increases bulk temperature.
- *heat transfer coefficient* (h). Reduction in flow rate would adversely affect h through the Reynolds number.
- *clad thickness* ($d_{C2} - d_{C1}$). Increase in clad thickness increases thermal resistance to the flow of heat
- *pellet diameter* (d_{F2}). Larger fuel diameter than nominal increases pellet/clad interaction.
- *gap heat transfer coefficient* (h_G). Reduction in h_G increases thermal resistance to the flow of heat.
- *clad thermal conductivity* (k_C). Reduction in k_C increases thermal resistance to the flow of heat.
- *fuel thermal conductivity* (k_F). Reduction in k_F increases thermal resistance to the flow of heat.
- *fuel density*. Increase in fuel density increases neutron flux, hence, the linear heat generation rate.

Examples for such engineering sub-factors include: heat flux; 1.03, hot channel; 1.02, rod bowing; 1.065, axial fuel densification; 1.002, and azimuth power tilt;

1.03. The engineering peaking factors are primarily due to the manufacturing tolerances resulting in the finished product slightly deviating from the specified nominal value. The deviation from the nominal is a probabilistic event. Hence, the deviation can be higher or lower than the nominal value. However, to be conservative, we may consider only deviations that result in undesirable outcome. In this case, deviations that result in the fuel rod temperature to increase. For example, for the specified nominal value of 0.42 for clad outside diameter, the finished product may be $d_{C2} = 0.42 \pm 0.005$ inch. It is conservative to use $d_{C2} = 0.425$ in.

We may calculate the engineering peaking factor F_E from the various peaking sub-factors (itemized above) in two ways. The most conservative method is to assume that all sub-factors occur for the most limiting, or the hottest channel. Mathematically, this is equivalent to:

$$F_E = F_E^{\dot{m}} \times F_E^{d_{C2}} \times F_E^{d_{F2}} \times F_E^{k_C} \times F_E^{k_F} \times \cdots$$

In this method, F_E is a maximum, $\overline{\dot{q}''}$ is a minimum, and, economically, the operation of the reactor is least desirable. Obviously, such a doomsday scenario does not occur in practice. A reasonable way to account for all the engineering sub-factors is to use a method based on statistical combination of uncertainties.

Transient peaking factors. So far, we discussed nuclear and engineering peaking factors. These are applicable when plant is operating at steady state condition and producing nominal power. Two more sets of peaking factors are also considered. The first sub-factor (F_P), accounts for deviations from nominal power during normal operation and second peaking sub-factor (F_T) accounts for such conditions as the build up of thermal stresses in the clad due to plant transients. The result is to further increase the safety factor:

$$F = F_N \times F_E \times F_P \times F_T$$

Figure VIe.3.7 shows the effect of various peaking factors on core heat flux. In addition to the above mentioned factors, we need to consider another safety factor to provide margin to the critical heat flux as discussed next.

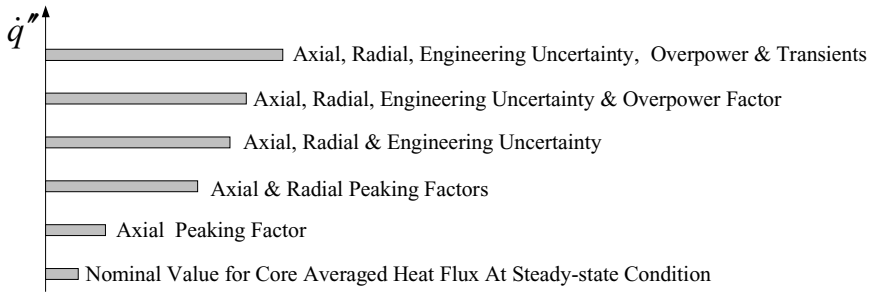

Figure VIe.3.7. Determination of peaking factors for reactor thermal design (Todreas)

4. Reactor Thermal Design

In the design of a power plant, many aspects must be evaluated and several constraints must be met. Some of the aspects that must be evaluated include federal, state, and local regulations, economical and environmental considerations, site suitability, structural, electrical, thermal, and hydraulic constraints. Focusing only on the thermalhydraulics of a water-cooled nuclear power plant, we start from the electric power demand that should be met by the utility. The balance of plant is designed based on the demand on the electric grid. This design consists of the steam cycle including turbine, steam extraction, feedwater heaters, and other heat exchangers. The site selected for the power plant determines the ultimate heat sink. If located on sites close to a bay, a lake, or other large bodies of water, selection of a condenser is warranted. Otherwise, cooling ponds or cooling towers should be used. If a condenser is used, the appropriate condensate pumps and condensate booster pumps to provide the design head and flow rate must be selected. This is also applied to such other pumps as the main feedwater and the feedwater heater pump.

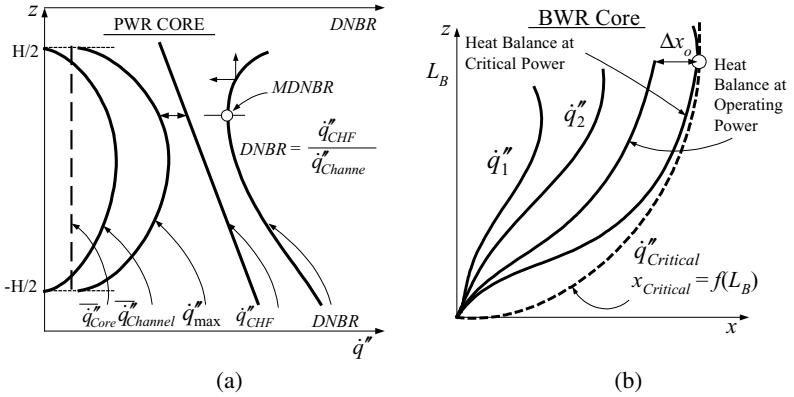

Figure VIe.4.1. Determination of CHFR in (a) PWRs and (b) BWRs

The selection of the steam supply system is the most crucial decision. For nuclear plants the choice in the United States is primarily between a PWR or a BWR, although, gas cooled reactors may also be an alternative. To determine the required thermal power of the reactor core, we need to first calculate thermal efficiency of the steam cycle. Having thermal efficiency, we then design the core.

It is important to note that according to Carnot's efficiency, Equation IIa.9.2, the higher the heat source temperature, the higher the thermal efficiency. In BWRs, this is the core exit temperature and in PWRs this is the steam temperature in the steam dome. The highest temperature, being directly related to the integrity of the fuel rods, must remain well below the melting temperature of the cladding metal. The Code of Federal Regulations (10 CFR 50-46) requires the peak clad temperature not to exceed 2200 F (1500 K) during design basis events, as described later in this Chapter. If a nuclear reactor was a temperature-controlled sys-

tem, we could have defined a safety factor for the maximum temperature and operate the plant such that temperature does not exceed the calculated value. However, as Equation VIe.3.2 shows, reactors are flux-controlled systems. In such systems as Figure VIe.4.1 shows, the CHF point must not be approached since temperature jumps from the value corresponding to nucleate boiling to the elevated value corresponding to the film-boiling region. Thus, to ensure fuel rod temperature remains below limit, a regulatory approved correlation is first used to calculate critical heat flux. A safety factor, F_{CHF}, is then applied for conservatism. This safety factor is the critical heat flux ratio (CHFR).

The CHF in PWRs is due to the departure from nucleate boiling (DNB), which is a local phenomenon. Therefore, in PWRs this safety factor is referred to as the DNBR (departure from nucleate boiling ratio). To demonstrate this graphically, let's evaluate the plots of Figure VIe.4.1(a). The dashed line shows the core average heat flux. Note that the core average heat flux is related to the fuel rod surface area according to:

$$\overline{\dot{q}''_{av}} = \frac{\dot{Q}}{\mathrm{P}_F \mathrm{H} N_{rod}} = \frac{\dot{W}}{(\mathrm{P}_F \mathrm{H} N_{rod})\eta} \qquad \text{VIe.4.1}$$

where $\dot{W}$ is the required power on the grid (MWe), $\dot{Q} = \dot{W}/\eta$ is core thermal power (MWth), and η is plant thermal efficiency. The first cosine curve in Figure VIe.4.1(a) shows the axial heat flux distribution in an average channel. The second cosine curve shows the axial heat flux distribution in the hot channel. Note that, similar to Equation VIe.3.7 and from our earlier discussion, the relationship between heat flux in an average channel to the heat flux in the hot channel is in the form of:

$$\overline{\dot{q}''_{av}} = \frac{\dot{q}''_{\max}}{F} \qquad \text{VIe.4.2}$$

In Figure VIe.4.1(a), $\overline{\dot{q}''}$ is followed by the axial critical heat flux distribution, $\dot{q}''_{CHF}(z)$. The last curve on the right side shows the plot of:

$$DNBR(z) = \frac{\dot{q}''_{CHF}(z)}{\dot{q}''_{\max} \cos(\pi z / \mathrm{H})}$$

which is the departure from nucleate boiling ratios for various points along the hot channel. The minimum point on this plot is the minimum departure from nucleate boiling ratio, *MDNBR*:

$$MDNBR = \frac{\dot{q}''_{CHF}(z_{DNB})}{\dot{q}''_{\max} \cos(\pi z_{DNB} / \mathrm{H})} \qquad \text{VIe.4.3}$$

If we substitute from Equation VIe.4.3 into Equation VIe.4.2 and subsequently in Equation VIe.4.1, we find:

$$N_{rod} = \left[\frac{\cos(\pi z_{DNB}/\mathrm{H})}{(\mathrm{P}_F \mathrm{H}\eta)}\right] F \times MDNBR \times \frac{\dot{W}}{\dot{q}''_{CHF}(z_{DNB})} \qquad \text{VIe.4.4}$$

Equation VIe.4.4 shows the intricate relationship between power production, hot channel factor, and the minimum departure from nucleate boiling ratio. Economically, for the same core design parameters, higher power is obtained when the *MDNBR* and the hot channel factor are minimized.

Example VIe.4.1. The axial power distribution in a PWR core is represented as $\dot{q}''' = C\cos(\pi z/12)$ where z is in ft. Use the given data and the Bernath correlation for CHF to find the *MDNBR*.

Data: $\dot{Q}_{core}$ = 2700 MWth, P = 2250 psia (15.5 MPa), $T_{f,in}$ = 550 F (560.7 K), $\dot{m}_{core}$ = 138.5E6 lbm/h (62.82 kg/h), N_{Rod} = 38,000, $\mathrm{H_{core}}$ = 12 ft (3.66 m), d_F = 0.38 in (0.96 cm), d_{C1} = 0.39 in (0.99 cm), d_{C2} = 0.45 in (1.14 cm), s = 0.588 in (1.493 cm), c_p = 1.3 Btu/lbm·F (5.44 kJ/kg·K), N_{Rod} = 38,000.

Solution: Find $\dot{q}'''_{\max} = \left(\frac{1.16\dot{Q}_{core}E_d}{\mathrm{H}N_{rod}a^2E_R}\right) = \frac{1.16\times 2700\times 3412{,}000\times 180}{12\times(0.38/2\times 12)^2\times 38{,}000\times 200} =$ 84.13E6 Btu/h·ft^3 (870.7 MW/m^3)

$(\dot{q}'''_{\max})_{actual} = 2\dot{q}'''_{\max}/3 =$ 56E6 Btu/h·ft^3 (579.6 MW/m^3)

$A_F = \pi d_F^2/4$ = 7.87E-4 ft^2. We also find the channel flow area $A_{Flow} = s^2 - \pi d_{C2}^2/4$ = 1.296E-3 ft^2 (1.2 cm^2)

$D_e = 4A_{Flow}/\mathrm{P}_{C2} = 4\times 1.296\text{E-}3/(\pi\times 0.45/12) = 0.044$ ft (1.34 cm)

$\dot{m} = 135.5\text{E}6/38000$ = 3565.8 lbm/h (0.45 kg/s)

$\dot{q}''(z) = \left(d_F^2/4d_{C2}\right)\dot{q}'''_{\max}\cos(\pi z/\mathrm{H})$ = [(0.38/12)^2/(4 × 0.45/12)] × 56E6 cos(πz/H) = 0.374E6 cos(πz/H)

$$T_f(z) = T_{f,in} + \frac{\dot{q}'''_{\max}A_F\mathrm{H}}{\pi\dot{m}c_p}\left[1+\sin\left(\frac{\pi z}{\mathrm{H}}\right)\right] =$$

$$550 + \frac{56\text{E}6\times 7.87\text{E}-4\times 12}{\pi\times 3565.8\times 1.3}\left[1+\sin\left(\frac{\pi z}{\mathrm{H}}\right)\right] = 550 + 36\left[1+\sin\left(\frac{\pi z}{\mathrm{H}}\right)\right]$$

We now set up the following table for the hot channel in the core:

z	−5H/10	−4H/10	−3H/10	−2H/10	−H/10	0.0	H/10	2H/10	3H/10	4H/10	5H/10
$T_f(z)$	550.0	551.8	556.9	563.5	575.0	586.3	597.5	607.6	615.6	620.8	622.6
$\rho(z)$	47.17	46.95	46.73	46.08	45.25	44.44	43.48	42.55	41.67	41.15	40.98
$V(z)$	16.19	16.27	16.35	16.58	16.88	17.19	17.57	17.95	18.33	18.56	18.64
$\dot{q}''_{DNB}$	1.36	1.35	1.32	1.27	1.19	1.11	1.03	0.98	0.90	0.86	0.850
$\dot{q}''$	0.00	0.116	0.220	0.303	0.356	0.374	0.356	0.303	0.220	0.116	0.000
DNBR	-	11.6	6.0	4.2	3.3	2.9	2.7	3.2	4.1	7.4	-

z: ft, T_f: F, ρ: lbm/ft^3, V: ft/s, heat flux: MBtu/h·ft^2.
Note that we have assumed flux at $z = 0$ and $z = L$ is zero. In reality, flux goes to zero at *extrapolation lengths*

where $\dot{q}''_{DNB}$ is calculated from:

$$\dot{q}''_{CHF} = h_{CHF}\left(T_{s,CHF} - T_f\right)$$

In this equation, h_{CHF} and $T_{s,CHF}$ are obtained from (the Bernoth correlation):

$$h_{CHF} = 10{,}890\frac{1}{1+(\mathrm{P}_h/\pi D_e)} + \frac{48V}{D_e^{0.6}}$$

and $T_{s,CHF} = 32 + 102.6\ln P - \dfrac{97.2}{1+(15/P)} - 0.45V$, respectively.

More accurate results are obtained if we use smaller increments from $z = 0.0$ to $z =$ 2H/10. According to the Bernath correlation, the *MDNBR* = 2.7. Expectedly, the determination of the *MDNBR* strongly depends on the correlation used to predict CHF in the hot channel. Note that we ignored small changes in pressure due to friction, elevation, and acceleration pressure drops. In this table, water temperature at each node is calculated from Equation VIe.3.9, which is used in turn to find water density and to obtain water velocity in the channel from Equation IIa.5.2.

As discussed in Chapter Vb, the critical heat flux in BWRs is due to the total heat deposited in the channel resulting in an annular flow regime and eventually leading to dryout. For this reason, in BWRs the CHFR is referred to as the critical power ratio, CPR. Shown in Figure VIe.4(b), the first curve on the left side is the flux distribution in a channel. The second shows the increased heat flux from $\dot{q}''_1$ to $\dot{q}''_2$. We may keep increasing the heat flux and obtaining similar curves. The third plot, for example, shows the curve corresponding to the normal operational condition. The heat flux may be further increased so that the corresponding curve is tangent to the curve representing the critical condition. This is the limiting power that must not be approached. The curve representing CHF, in terms of critical quality versus boiling length, is known as GEXL and is obtained by General Electric (GE) from proprietary data.

Example VIe.4.2. The axial power distribution in a PWR core is represented as $\dot{q}''' = \dot{q}'''_{\max} \cos(\pi z/12)$ where z is in ft. The core active length is 12 ft. The *MDNBR* of 2.0 occurs 20 inches from the core mid-plane where the critical heat flux is calculated as 1.2E6 Btu/h·ft^2. Find a) $\dot{q}''_{\max}$, b) $\dot{q}''_{av}$, and c) total fuel rod surface area. Data: Hot channel factor: 2.8, Required power on grid: 1000 MWe, $\eta = 29\%$.

Solution: We find the heat flux profile from $\dot{q}'''$ profile since $\dot{q}'''(\pi d_F^2/4)\mathrm{H} = \dot{q}''(\pi d_{C2})\mathrm{H}$. Therefore, we find $\dot{q}'' = \dot{q}'''$ (A_F/P$_{C2}$) where A_F and P are the fuel cross sectional area and perimeter, respectively. The heat flux profile becomes:

$$\dot{q}''(z) = (A_F/\mathrm{P}_{C2})\dot{q}'''_{\max}\cos\left(\frac{\pi z}{12}\right) = \dot{q}''_{\max}\cos\left(\frac{\pi z}{12}\right)$$

a) The maximum heat flux is found from the fact that at z = 20 in, *MDNBR* = 2.0

$$\dot{q}''(20) = \dot{q}''_{\max}\cos\left(\frac{20\pi}{144}\right) = \frac{\dot{q}''_{CHF}}{MDNBR} = \frac{1.2\mathrm{E}6}{2.0} = 600{,}000 \text{ Btu/h·ft}^2$$

Therefore, the maximum heat flux is found as,

$$\dot{q}''_{\max} = \frac{600{,}000}{\cos(20\pi/144)} = \frac{600{,}000}{0.906} = 662026.75 \text{ Btu/h·ft}^2$$

b) The average heat flux is found as $\dot{q}''_{av} = \dfrac{\dot{q}''_{\max}}{F} = \dfrac{662{,}026.75}{2.8} = 236{,}438$ Btu/h·ft^2.

c) The required surface area is found from, $A = \dot{Q}_{Core}/\dot{q}''_{av}$ where $\dot{Q}_{Core} = (\dot{W}/\eta_{th})$. Hence, we find total fuel rod surface area from A = (1000 × 3412,000/0.29)/236,438 = 50,000 ft^2.

Example VIe.4.3. Use the following data and plot the temperature profile of water in a PWR.

Data: $\dot{Q} = 2700$ MWth, $\dot{m}_{Core} = 138\mathrm{E}6$ lbm/h, T_{CL} = 550 F, T_{FW} = 430 F, P_{Core} = 2250 psia, P_{SG} = 900 psia, $P_{Condenser}$ = 1 psia, $\dot{m}_{Heat\ Sink}$ = lbm/h, d_{C2} = 0.45 in, H$_{Core}$ = 12 ft, F = 2.5, $T_{sink,in}$ = 70 F, and $T_{sink,o}$ = 80 F.

Solution: To find the plant temperature profile, we assume pipe runs are fully insulated. Then find

– core exit temperature by applying Equation IIa.6.6 to the core:

$h_e = h_i + (\dot{Q}/\dot{m})$ = 547.15 + (2700 × 3412000/138E6) = 614 Btu/lbm

Hence, $T_{HL} \cong 600$ F

- the profile of the water temperature in the average channel from Equation VIe.3.8
- steam generator inlet temperature from $T_{h,in} = T_{HL} = 600$ F
- the profile of water in the steam generator tubes from Equation VIa.6.8. Note, $T_{h,o} = T_{CL} = 550$ F
- steam generator secondary-side inlet temperature, $T_{c,i} = T_{FW} = 430$ F.
- turbine exit temperature from the condenser pressure, $T_{turbine,o} = 100$ F.

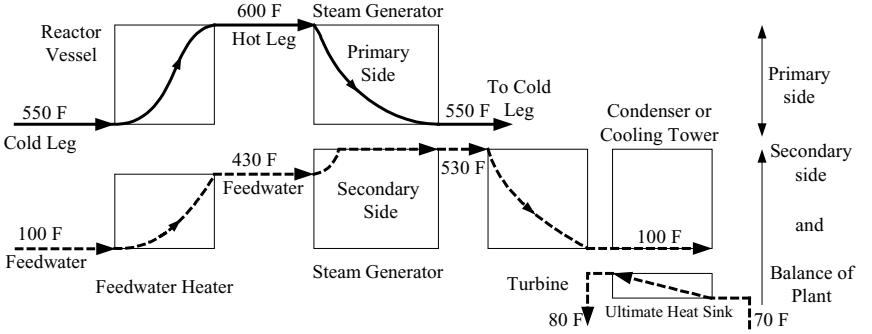

5. Shutdown Power Production

Unlike other power producing systems, nuclear reactors continue to produce power, albeit at a much smaller rate, even after being shutdown. Power generation in nuclear reactors following shutdown is due to two sources: the power produced by fission caused by the delayed neutrons and the power due to β and γ decays of radioisotopes. Power produced by delayed neutrons is short lived. It can be calculated by solving the neutron kinetic equation with the insertion of a large negative reactivity (–0.09). Such solution would show that the reactor power due to delayed neutrons would decrease exponentially over a period of about 80 seconds (the half-life of the longest lived delayed neutron precursor). Hence, the most dominant source of power following a reactor shutdown is the decay of radioisotopes.

The rate of decay heat, as shown in Figure VIe.5.1 is generally obtained from the models developed by the American Nuclear Society (ANS). In this figure, ANS 1971_1 refers to the nominal value for the decay of fission products. ANS 1971_2 refers to the nominal value plus the decay of the heavy elements (U-239 and NP-239). ANS 1971_3 is the same as ANS 1971_2 but it accounts for 20% uncertainty in the nominal and 10% uncertainty in the decay of the heavy elements. ANS 1971_4 applies 20% instead of 10% uncertainty to the decay of the heavy elements.

ANS 1979_1 refers to the nominal value for the decay of fission products plus the decay of the heavy elements. The ANS 1979_2 model also accounts for 2σ

uncertainty. The Branch Technical Position (BTP) in this figure is similar to ANS 1971_3. To highlight the differences between these model, the bottom figure focuses on the first 1000 seconds after shutdown.

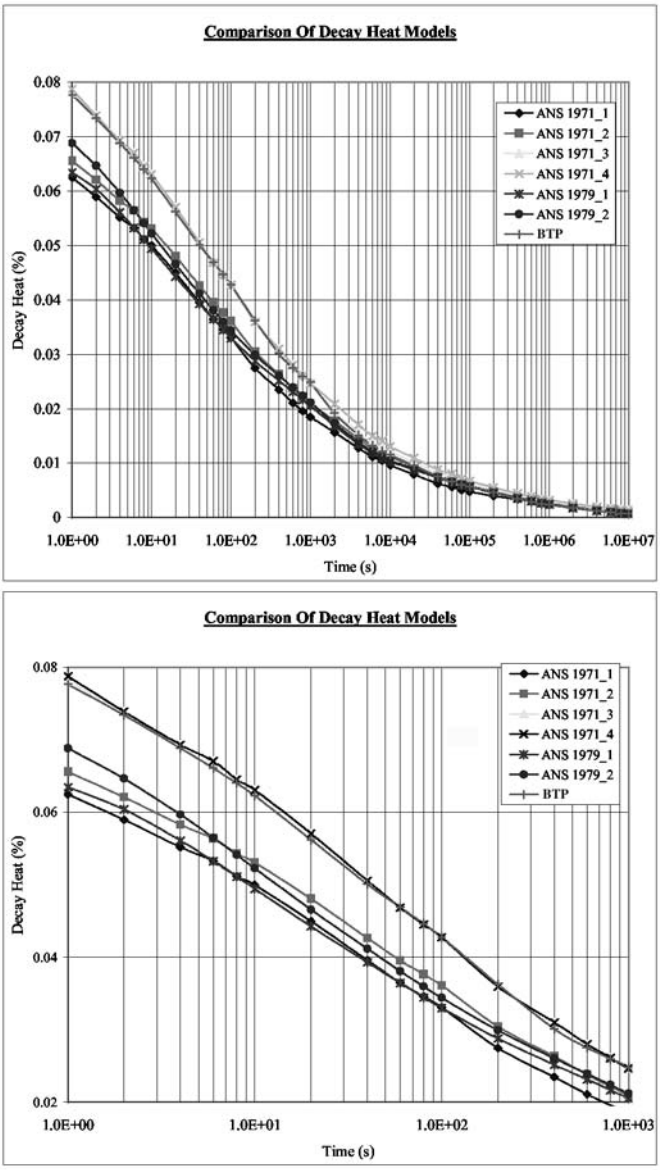

Figure VIe.5.1. Various models for the estimation of decay power

As shown in Figure VIe.5.1, reactor decay power following shutdown drops rapidly in the short term (about 1000 s) and in the long term approaches zero asymptotically. Obtaining a general formula for decay power is difficult due to such factors as dependency on the fuel cycle and duration of operation (resulting in differences in heavy nuclide concentration and their decay characteristics). See Problem 55 for a best estimate prediction of decay heat as recommended by El-Wakil. This correlation is applicable for time greater than 200 s after shutdown.

QUESTIONS

- What is the diameter of the chlorine atom?
- What are *subatomic* particles?
- What is an isotope? What are the isotopes of uranium?
- Define atomic mass unit. How much energy in MeV is associated with 1 amu?
- Explain the difference between a chemical and a nuclear reaction
- What is the abundance of the U-235 isotope in naturally occurring uranium?
- What is the process by which we increase the mass of certain isotopes in naturally occurring substance?
- What is mass defect? Why is the mass of a nucleus less than the total mass of its constituents?
- Why are heavy elements such as uranium and plutonium more amenable to fission?
- In how many ways may a neutron interact with a nucleus?
- What are the differences between elastic and inelastic scattering?
- Are microscopic and macroscopic cross sections properties of the neutron or of the nucleus?
- What does the macroscopic cross section physically represent?
- Why do we refer to slow neutrons as thermal neutrons?
- What major assumption constitutes the basis of the diffusion equation?
- Mathematically speaking, what do temperature distribution in a rectangular plate (Figure VIIb.2.1) and neutron flux distribution in a cylindrical core have in common?
- Why, in an elastic scattering between a fast neutron and a nucleus, is most energy lost in collision with light nuclei than with heavier nuclei?

PROBLEMS

1. The atomic nucleus contains protons and neutrons while the electrons are orbiting the nucleus on specific shells or orbits. Each shell is filled with a certain number of electrons. The shells are identified with quantum numbers 1, 2, 3, …, etc. The shell with the quantum number 1 is the closest orbit to the nucleus. These are also referred to as orbits *K*, *L*, *M*, N, etc. Usually the shells closest to the nucleus are filled first. The number of electrons each shell is filled is given by $2n^2$. Thus, shell *K* is filled with 2, shell *L* with 8, shell *M* with 18, and shell *N* with 32 electrons. Electrons that orbit in the outermost shell of an atom are called

the valance electrons. Shown in the figure are the structure and the valance electrons for hydrogen, helium, lithium, and neon. Draw similar atomic structures for sodium, phosphorous, and xenon.

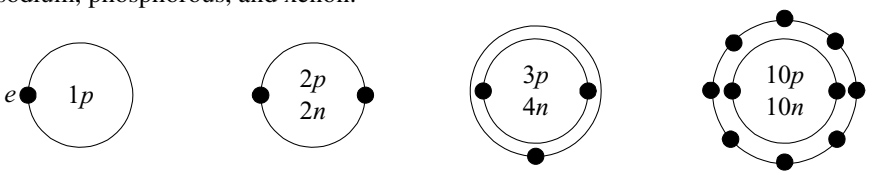

2. How much energy corresponds to 1 lbm?

3. If the energy released by the Hoover dam in 2.5 days is 2.7E14 J, find the equivalent mass associated with this amount of energy. [Ans. 3 grams].

4. Treating neutrons as a gas, we may describe the total number of neutrons per unit volume by the Maxwellian distribution. If $n(E)$ is the number of neutrons per unit volume having energy E per unit energy, then $n(E)dE$ is the number of neutrons per unit volume having energies in the range of E and $E + dE$ so that:

$$n(E) = \frac{2\pi n}{(\pi\kappa T)^{3/2}} E^{1/2} e^{-E/\kappa T}$$

where N is the total number of neutrons and T is the absolute temperature of the medium. In this relation, κ is Boltzmann's constant κ = 1.3806E–23 kJ/K = 8.617E –5 eV/K. Use the above information and find:

a) similar distribution for neutron velocity. [Hint: Substitute for E from the *K.E.*]
b) the most probable energy, the most probable velocity, and the energy corresponding to the most probable velocity.
c) the average energy

[Hint: use the averaging method given by $\overline{E} = \left(\int_0^E n(E)EdE\right)/n$].

[Ans.: a) $E_p = \kappa T/2$, b) $V_p = (2\kappa T/m)^{1/2}$, and c) $\overline{E} = 3\kappa T/2$].

5. Calculate the most probable neutron velocity and the neutron energy corresponding to the most probable velocity. Use room temperature of 20 C. [Ans.: V_p = 2200 m/s, and E = 0.0253 eV].

6. Steady state neutron flux in a bare spherical reactor of radius R is approximately expressed as:

$$\phi(\vec{r}, E, \vec{\Omega}) = \frac{\phi_o}{4\pi} E \exp\left(-\frac{E}{\kappa T}\right) \frac{\sin(\pi r / R)}{r}$$

where φ_o is the maximum flux at the center of the reactor. Use Equation VIe.1.4 and the relation between energy and velocity to find the number of neutrons in the reactor. Gamma function properties are given in Chapter VIIb. [Ans. $\phi_o(2\pi n)^{1/2}(\kappa T)^{3/2}R^2$].

7. Show that the atom density of an element is given by $N = \rho N_A/\mathrm{M}$ where N_A is Avogadro's number (6.023E23) and M is the molecular weight. Find the atom density of C-12. Use the data for scattering and absorption cross sections and find the total macroscopic cross section of C-12. Since the mean free path is $\lambda = 1/\Sigma$, show that C-12 is an excellent moderator.

8. Collision between neutrons and nucleus of the moderator results in slowing down the newly born fast neutrons. Such a collision is depicted in the figure. The striking fast neutron has an initial energy E_n and an initial momentum p_n. The target nucleus is initially at rest. Considering an elastic scattering, following the collision, the scattered neutron has an energy of $E_n^{'}$ and momentum of $p_n^{'}$ while the recoiling nucleus has an energy of $E_N^{'}$ and momentum of $p_N^{'}$. Use the conservation of momentum and energy to drive a relation for energy of the scattered neutron in terms of the initial neutron energy and mass number of the target nucleus. [Hint: Find the momentum of the recoiling nucleus in terms of the momentum of the initial and the scattered neutron. Substitute for momentum terms ($p^2 = 2mE$) and for the recoiling energy from the energy balance].

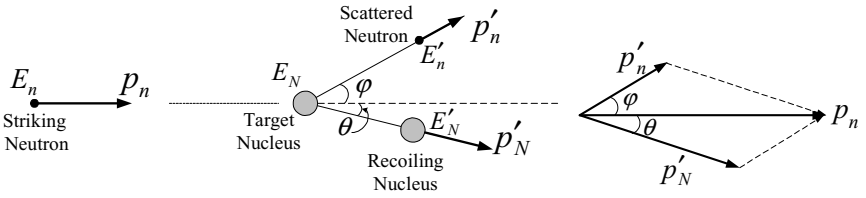

9. The energy of the scattered neutron following an elastic scattering between the neutron and the target atom is given as (note that the molecular mass of the nucleus, M divided by the mass of neutron, m is $M/m = A$):

$$E_n' = \frac{E_n}{(A+1)^2}\left[\cos\varphi + \sqrt{A^2 - \sin^2\varphi}\right]^2$$

Find the minimum energy of the scattered neutron following a collision with the atom of C-12. The striking neutron has an initial energy of 5 MeV.

10. An isotropic neutron source emitting S_o neutrons/s·cm^2 is located on the surface of a sphere of radius R. Find a) neutron flux at the center of the sphere and b) neutron current at the center of the sphere through a mid plane. [Ans.: $S_o/2$ and $S_o/4$ downward].

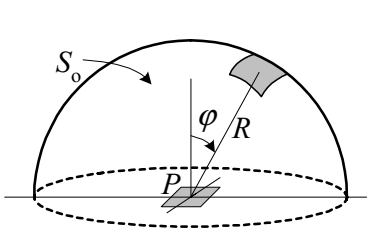

Problem 10

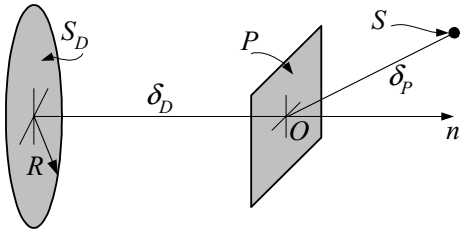

Problem 11

11. A plane (P) is located between a disk (D) and a point source. The disk emits S_D particles isotropically and is located at a distance δ_D from plane P. The point source emits S particles isotropically and is located at a distance δP from point O on plane P. Find neutron flux and current at point O.

12. The collision in Problems 8 and 9 is described from the point of view of a stationary observer, referred to as the laboratory (LAB) system. Now, consider a case were the observer is instead located at the center of momentum of the neutron and nucleus, referred to as the center of momentum (COM) system. In this case the total momentum before and after the collision is zero. Show that the velocity of the center of momentum (which for non-relativistic events is the same as the center of mass) for the stationary nucleus is given by $V_{COM} = V_{n,LAB}/(A + 1)$ where $V_{n,LAB}$ is the neutron velocity in the LAB system before collision. Also show that $V_{n,COM} = A\ V_{n,LAB}/(A + 1)$ and $V_{N,COM} = -\ V_{n,LAB}/(A + 1)$ where $V_{N,COM}$ is the velocity of the nucleus before the collision in the COM system.

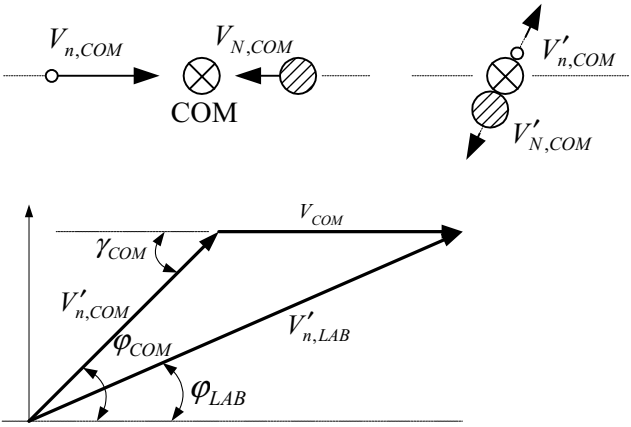

Problems 12, 13, and 15

13. Use the diagram showing neutron velocity before and after a collision to conclude that:

$$\frac{E_n'}{E_n} = \frac{A^2 + 2A\cos(\varphi_{COM}) + 1}{(A+1)^2} = \frac{1+\alpha}{2} + \frac{1-\alpha}{2}\cos\varphi_{COM}$$

where $a = [(A - 1)/(A + 1)]^2$ is known as the *collision parameter*. Use this relation to:

a) find the angle corresponding to the minimum energy of the emerging neutron ($E'_{\min}$)

b) find $E'_{\min}$, the minimum energy of the emerging neutron

14. Neutron lethargy is defied as $\lambda = \overline{\ln E - \ln E'} = -\ln(\overline{E'/E})$. Use the result of Problem 13 and show that neutron lethargy in terms of the nucleus mass number may be expressed as $\lambda \approx 2/(A + 2/3)$. [Hint: Finde an energy-averaged lethargy. The probability distribution function for elastic scattering and isotropic in the center of mass is $1/(1 - \alpha)E$].

15. Use the diagram to conclude that the cosine of the scattering angle in the LAB system in terms of the cosine of the scattering angle in the COM system is given as:

$$\cos(\varphi_{LAB}) = \frac{A\cos(\varphi_{COM})}{\sqrt{A^2 + 2A\cos(\varphi_{COM}) + 1}}$$

16. Use the results of Problems 13 and 15 to plot E'/E as a function of both φ_{LAB} and φ_{COM}.

17. Consider the case of linearly anisotropic elastic scattering in the COM system $\sigma_s(\mu_{COM}) = \sigma_0 + \sigma_1\mu_{COM}$ where σ_0 and σ_1 are known constants. Find and plot the distribution of the nuclear recoil energies

18. Find the probability of isotropic scattering into a differential solid angle is $d\Omega/4\pi r^2$ where the differential solid angle $d\Omega$ is given as $2\pi r\sin(\varphi_{COM})(rd\varphi_{COM})$. [Hint: Integrate over θ to get scattering in the segment]

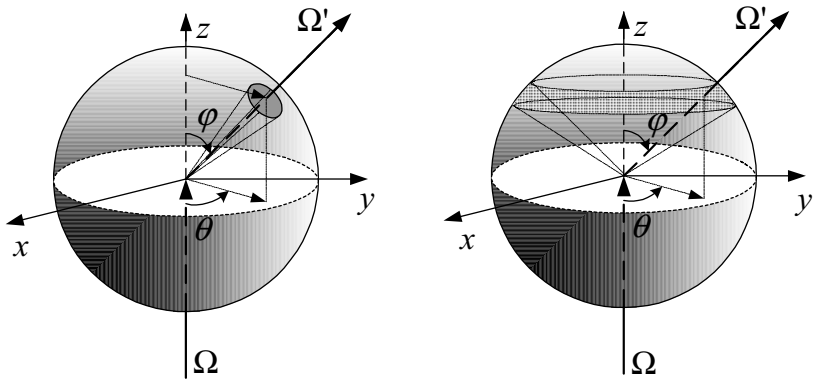

19. Show that scattering in the COM system is isotropic. For this purpose, find $\overline{\cos(\varphi_{COM})}$ and interpret the result. [Hint: Multiply the cosine of the scattering angle in the COM by the probability of scattering and integrate from 0 to π].

20. Use the result of Problem 15 and the method of Problem 18 to find the cosine of the scattering angle in the LAB system, $\overline{\cos(\varphi_{LAB})}$. Does the result show that scattering in the LAB system is backward, isotropic, or forward scattering? [Ans.: $2/(3A)$].

21. In Problem 13 it is shown that there is a one-to-one relation between the change in neutron energy and the change in the scattering angle. Thus, it can be concluded that $p(E \rightarrow E')dE' = -p(\Omega \rightarrow \Omega')d\Omega'$ where p is probability and the minus sign reflects the fact that the larger the scattering angle, the lower the energy of the scattered neutron. We represent $p(\Omega \rightarrow \Omega') = 4\pi\sigma_s(\Omega \rightarrow \Omega')/\sigma_s$ where $\sigma_s(\Omega \rightarrow \Omega')$ is the differential scattering cross section and $\int_{\Omega'}\sigma_s(\Omega \rightarrow \Omega')d\Omega' = \sigma_s$. Use this information and find $p(E \rightarrow E')$ for an elastic scattering and isotropic in the COM where $\sigma_s(\Omega \rightarrow \Omega') = \sigma_s/4\pi$. [Ans.: $p(E \rightarrow E') = 1/(1-\alpha)E$].

22. Use the result of Problem 21to find the *average fractional energy loss* in an elastic scattering collision. The average fractional energy loss is defined as $\overline{\Delta E}/E$. [Ans. $(1-\alpha)/2$].

23. Regarding neutron-nucleus interaction, so far we dealt with elastic collision for *isotropic* and *anisotropic* scatterings. In this problem, we want to find E'/E for an inelastic scattering in which the target nucleus absorbs an amount of energy Q. Use the energy equation, which now accounts for Q and the velocity diagram of Problem 12 to show that:

$$\frac{E'}{E} = \frac{A^2\xi^2 + 2A\xi\cos\varphi_{COM} + 1}{(1+A)^2};\ \xi = \left(1 - \frac{1+A}{EA}Q\right)^{1/2}$$

24. Consider two groups of isotopes. Group A consisting of U-233, U-235, Pu-239, Pu-241 and group B of Th-232, U-238, Pu-240, and Pu-242. Identify the group that represents fissile and the group that represents fissionable nuclides.

25. Find velocity (m/s) and kinetic energy (eV) of a thermal neutron at a temperature of 500 F. [Ans.: 2964].

26. Find the temperature of a thermal neutron having energy of 0.11 eV. [Ans.: 1000 C].

27. Start with the one-group neutron diffusion equation and derive the relation for neutron flux in a bare critical slab reactor. Find the maximum to average flux for this reactor.

28. An isotropic surface source of S_o neutrons/s·cm^2 is located on the surface of a sphere of radius R. The sphere consists of a non-absorbing material. Find a) the

flux density at the center of the sphere and b) the net current of neutrons at the center of the sphere through a mid plane. [Ans.: a) S_o and b) 0].

29. An isotropic surface source emits S_o neutrons/s·cm^2 and is distributed on the surface of a hemisphere of radius R. The hemisphere consists of a non- absorbing material. a) Find the flux density at the center of the hemisphere. b) Find the net current of neutrons at the center of the hemisphere through a mid plane. [Ans.: $S_o/2$ and $S_o/4$].

30. The left side of the slab shown in the figure is exposed to a monoenergetic neutron beam of an intensity I_o neutrons/s cm^2. The slab material is homogenously distributed and has an atom density of N atoms/cm^3 and a cross section of σt for interactions with incident neutrons. Show that the neutron distribution inside the slab is given by $I(x) = I_o\exp(-\Sigma_t x)$ where $\Sigma_t = N\sigma_t$. Find a) the probability that a neutron does not have an interaction when moves a distance dx, b) the fraction of neutrons without any interaction at $x = L$, and c) the average distance a neutron travels before interacting with a nucleus located in dx.

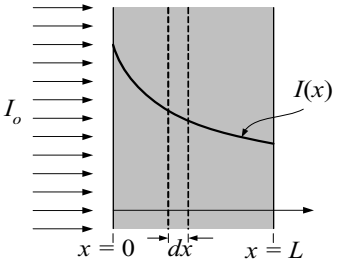

31. Show that the following integral is zero:

$$\frac{\partial \phi_o}{\partial x}\int_{\alpha=0}^{2\pi}\int_{\beta=0}^{\pi}\int_{0}^{\infty}\frac{\Sigma_s}{4\pi}\left[\left(r\sin\beta\cos\alpha\right)e^{-\Sigma_s r}\cos\beta d\alpha d\beta dr\right]=0$$

32. Consider a plane neutron source emitting S_o neutrons/s·cm^2 in a non-multiplying, infinite, homogenous medium. The material of the medium has high scattering and low absorption cross section for neutrons. Find an expression for neutron flux in terms of D and L of the medium. [Hint: Solve Equation VIe.2.12 in the x-direction with $s = 0$ subject to the boundary conditions given by VIe.2.15]. [Ans.: $\phi(x) = (S_oL/2D)e^{-|x|/L}$].

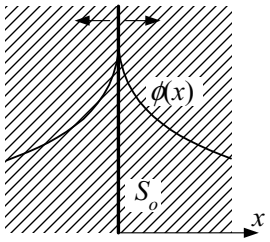

33. An isotropic point source emits S_o neutrons per second in an infinite non-multiplying weakly absorbing medium. Find neutron flux as a function of r, D, and L of the medium. [Ans.: $\phi(x) = (S_o/4\pi Dr)e^{-r/L}$].

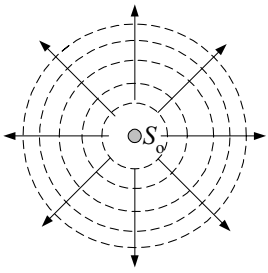

34. A plane neutron source emitting S_o neutrons/s·cm^2 is located at the center of a non-multiplying homogenous bare slab. The material of the medium has high scattering and low absorption cross section for neutrons. Find an expression for the neutron flux in the slab. [Ans.: $\phi(x) = (S_oL/2D)\ \sinh(c_1)/\cosh(c_2)$ where $c_1 = (b - 2x)/2L$ and $c_2 = b/2L$ with $b = \delta + a/2$].

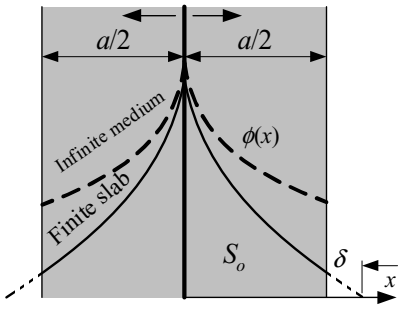

35. The slab of Problem 32 is now placed between two slabs of weakly absorbing materials. Find the neutron flux profile in each slab. Slab 2, which is blanketing slab 1 is referred to as a blanket or reflector.

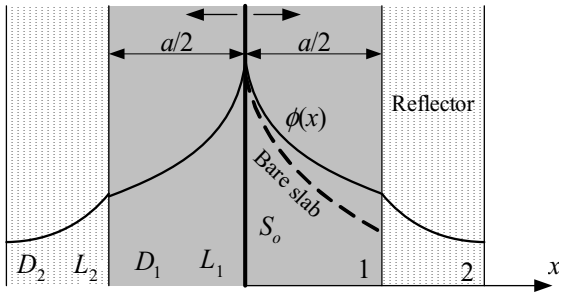

36. Consider the slab of Problem 34. However, in this case the localized planar source is replaced with a uniformly distributed neutron source emitting S_o neutrons/s cm^2. Find the flux in the slab. [Ans.: $\{1 - (\cosh x/L)/\cosh a/L\}(S_o/\Sigma_a)$].

37. Albedo, or the reflection coefficient (α), is defined as the ratio of the reflected to the incident current, $\alpha = J_{out}/J_{in}$. Derive the albedo expression for a slab of thickness a. [Ans.: $\alpha = (1 - b)/(1 + b)$ where $b = (2D/L)\coth(a/L)$]. [Hint: Use Equations VIe.2.3 and VIe.2.4].

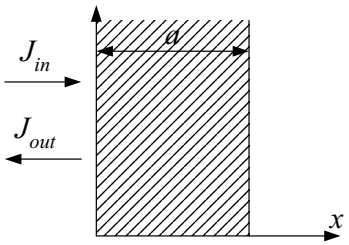

38. Consider an infinite medium through which monoenergetic sources of neutron emitting S_o neutrons/s cm^2 are uniformly distributed. Find neutron flux in this medium. [Ans.: $\phi = S_o/\Sigma_a$].

39. An isotropic point source emitting S_o neutrons/s is placed in the center of a bare sphere of radius R. The sphere is made up of carbon ($L^2 = D/\Sigma_a$). Show that the general solution for flux inside the sphere is given by:

$$\phi(r) = \frac{C_1}{r} e^{-r/L} + \frac{C_2}{r} e^{r/L}$$

where C_1 and C_2 are constants of integration. Apply the boundary conditions and find the neutron flux anywhere at $r = R/2$. [Hint: Start with Equation VIe.2.14 and make a change of function; $\phi = \varphi/r$].

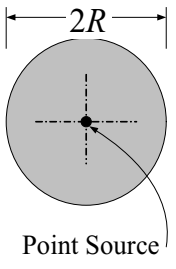

Problem 39

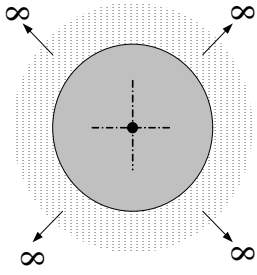

Problem 40

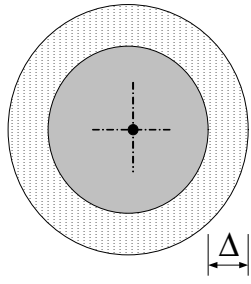

Problem 41

40. Solve problem 39 considering the sphere is located in an infinite medium made up of water.

41. Solve problem 40 considering the thickness of the water region is Δ and beyond $2R + \Delta$ is vacuum.

42. Start with the one-group neutron diffusion equation and derive the relation for neutron flux in a bare critical parallelepiped reactor. Find the maximum to average flux for this reactor.

43. Start with the one-group neutron diffusion equation and derive the relation for neutron flux in a bare critical spherical reactor. Find the maximum to average flux for this reactor.

44. Categorize the type of neutron source used in problems 32 through 43. For this purpose, use the flow chart as shown below and find the box that best matches the source of neutron used in the above problems. In this figure, 1-D for example, stands for neutron diffusion equation in a one dimensional medium.

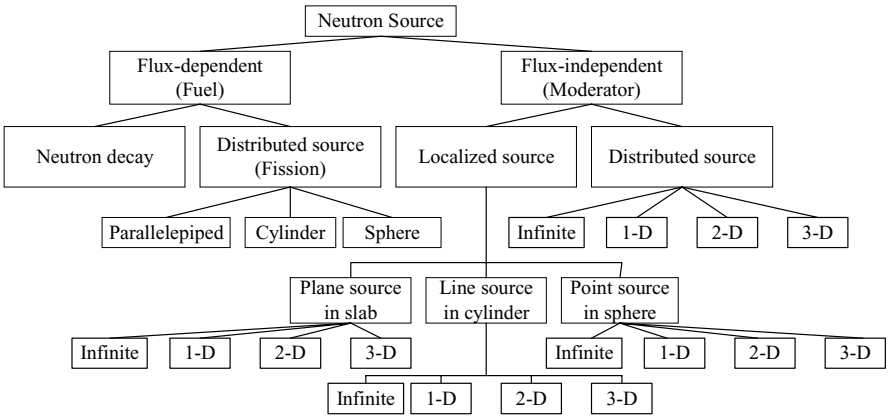

45. Determine the maximum linear heat generation rate to limit the average exit void fraction of a BWR to 0.60. Use the power profile of $\dot{q}'(z) = \dot{q}'_{\max} \sin(\pi z / L)$ where z is the distance from the assembly inlet and L is the assembly length. Use both homogeneous and drift flux models for void fraction. H = 12 ft, P = 1000 psia, $T_{f,in}$ = 530 F, $(A_{Flow})_{\text{Assembly}}$ = 15 in^2, $\dot{m}$ = 68E6 lbm/h.

46. Water flows in a uniformly heated tube. At the entrance to the tube, water is subcooled at system pressure. Water leaves the tube as a saturated two-phase mixture. The figure below shows the heated tube and the plots of temperature versus quality. Match a) numbers with the lower case letters and b) temperatures with the upper case letters.

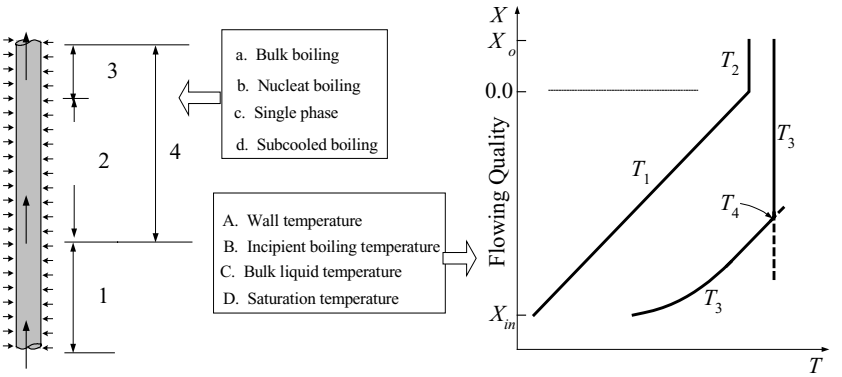

47. Water enters a BWR channel. Use the following data and find the location of the incipient boiling and the clad temperature corresponding to the incipient boiling.
Data: Pellet diameter: 0.45 in, Rod diameter: 0.55 in, Square array pitch: 0.8 in, core height = 12 ft, flow velocity: 8.5 ft/s, water inlet temperature: 530 F, system pressure: 1035 psia, $\dot{q}'''_{\max} = 1.25\text{E}7$ Btu/h·ft^3.
[Ans.: Nu = 1239, h = 5355 Btu/h·ft^2·F, Y = 0.7, z_{SB} = –36.2 in, and T_{SB} = 545.6 F].

48. Water enters a BWR channel. Use the following data and find the location of the incipient boiling and the clad temperature corresponding to the incipient boiling.
Data: Pellet diameter: 0.5 in, Rod diameter: 0.6 in, Square array pitch: 0.9 in, core height = 12 ft, flow velocity: 9 ft/s, water inlet temperature: 550 F, system pressure: 1050 psia, $\dot{q}'''_{\max} = 1.3\text{E}7$ Btu/h·ft^3.
[Ans.: z_{SB} = –63.72 in and T_{SB} = 553.77 F].

49. In this problem we want to find the bulk temperature corresponding to the incipient boiling temperature of the surface. Use the data of Example VIe.3.5 and find $T_f(Z_{SB})$. [Ans.: $T_f(Z_{SB})$ = 528.3 F].

50. Find the bulk temperature corresponding to the incipient boiling temperature of problem 45.

51. Use the Bowring correlation for the calculation of CHF and solve Example VIe.4.1. Plot the results and find the *MDNBR*. [Ans.: CHF in MBtu/h·ft^2 for various nodes: 1.85, 1.388, 0.11, 0.9251, 0.7929, 0.6937, 0.6166, 0.5549, 0.504, 0.4624, 0.4268. The *MDNBR* = 1.5].

52. Find the required number of rods for a PWR producing 1200 MWe having an efficiency of 30%. Other pertinent data at steady state operation are as follows: *MDNBR* = 2.5, F = 2.3, z_{DNB} = 25" from the core mid-plane, H = 12 ft, d_{c2} = 0.45 in, $\dot{q}'''_{CHF}(z_{DNB}) = 1.5\text{E}6$ Btu/h·ft^2. [Ans.: N_{Rod} = 31,638].

53. We would like to load a core with fuel rods in which fuel pellet enrichment is such that the neutron flux increases linearly along the vertical axis as shown in the figure. Water is used as coolant. Use the given data

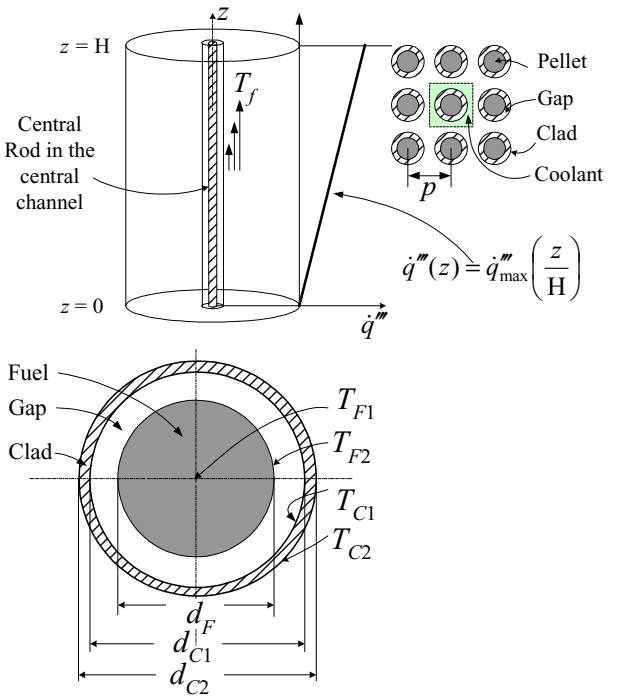

and find a) water temperature at the exit of the channel, b) peak temperatures of clad outside, clad inside, fuel surface, and fuel center, c) the incipient boiling temperature, and d) critical heat flux at the channel exit.

Data:

d_F (in):	0.38	P (psia):	1000
d_{C1} (in)	0.39	T_{in} (F):	500
d_{C2} (in):	0.44	$\dot{m}$ (lbm/s):	1.00 (per rod)
p (in):	0.59	$\dot{q}'''$ (Btu/h ft^3):	0.01E6

54. The fuel assembly shown in the left figure consists of periodic arrays of annular bare fuel rods, which are cooled by passing water through the center of the rods as well as over the outer surface. We want to analyze the thermal performance of the fuel rods by dividing the assembly into a number of unit cells (control volumes) and evaluating the performance of a cell, as shown in the right figure.

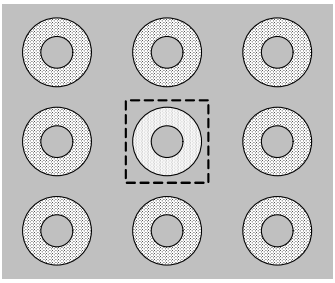

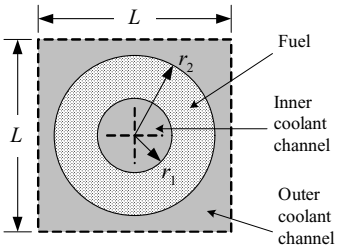

a) Find the ratio of the average coolant velocities in the inner and outer channels at the axial level z. At this level, the pressure drop per unit length is the same in both channels and the bulk coolant temperature is 293 C. Assume that the flow is turbulent and fully developed in both channels.
b) Find the maximum temperature in the rod, and the radius at which the maximum temperature occurs, for a particular axial location where the inner and outer surface temperatures of the rod are 371 C. At that level the volumetric heat generation rate may be assumed to be uniform and equal to 0.1 MW/m^3. Assume constant fuel conductivity for the fuel.
c) Find the mean temperature of the coolant at the core exit (i.e., the mixture of the coolant passing through the inner channel and that passing through the outer channel). The fuel rod is 4.3 m long and the axial power profile along the channel is give by:

$$\dot{q}'''(z) = \dot{q}'''_o \cos\left(\frac{\pi z}{4.3}\right)$$

where z is in m and $\dot{q}'''_o = 0.52$ MW/m^3. Other pertinent data: Inlet water temperature = 293 C, water pressure at the outlet = 14 MPa, water flow rate per unit cell = 18.37 kg/s, unit cell side (L) = 6.35 cm, fuel inner radius (r_1) = 1.27 cm, and fuel outer radius (r_2) = 2.54 cm.

55. A reactor that has been operating at nominal power level of 2700 MWth for 2 years is shut down. The decay power from this reactor, for any time after shutdown, can be fairly well estimated from:

$$\frac{\dot{Q}(t)}{\dot{Q}_{\text{nominal}}} = 0.095 t^{-0.26}$$

where t in this formula is the time after reactor shutdown in seconds. Find a) the power obtained from the reactor 1 day after shutdown, and b) the amount of energy produced by the decay power in a period of 24 hours. [Ans.: 13.35 MWth and 1.56E6 MJ].

56. A curve fit to the rate of the decay heat data of a typical PWR fuel cycle resulted in the following equation:

$$\frac{\dot{Q}(t)}{\dot{Q}_{\text{nominal}}} = A + \sum_{i=1}^{6} \frac{B_i}{t^i}$$

where $\dot{Q}(t)$ is the decay power at time t, $\dot{Q}_{\text{nominal}}$ is the nominal reactor power, and t is the time after reactor shutdown. Coefficients A and B_i are: A = 0.3826033E-2, B_1 = 276.6013, B_2 = -5,124,569, B_3 = 0.6344872E11, B_4 = -0.4427653E15, B_5 = 0.1551979E19, and B_6 = -0.2086165E22. Evaluate the accuuracy of the formula given in Problem 55 by plotting both equations and comparing the results.

57. This problem deals with a CE-designed 2 × 4 PWR (i.e., 2 hot legs and 4 cold legs as shown in Figures I.6.2(b), I.6.4(CE), I.6.5, I.6.6(a), and I.6.6(b)). Use the given data to find the answers to the questions that follow the set of data.

Primary side data (BU - SI):	
Core power (Btu/h - MWth):	9.2124E9 - 2700
Pressure in lower plenum (psia - MPa):	2595 - 18
Core pressure drop (psia - kPa):	14 - 100
Vessel pressure drop (psia - kPa)	37.1 - 256
Cold leg temperature (F - C):	550 - 288
Mass flow rate through core (lbm/h - kg/s):	138.5E6 - 17451
Number of fuel assemblies:	217
Number of rods per assembly:	14 × 14 (square array)
Fuel rod (Core) length (ft – m):	12 – 3.657
Fuel rod outside diameter (in - cm):	0.44 - 1.12
Fuel rod inside diameter (in - cm):	0.388 - 0.98
Fuel pellet diameter (in - cm):	0.377 - 0.96
Fuel pellet length (in - cm):	0.45 - 1.14
Fuel rod pitch (in - cm)	0.58 - 1.473
Gap heat transfer coefficient (Btu/h·ft^2·F - W/m^2·K):	1000 - 5678
Thermal conductivity of fuel pellet, UO_2 (Btu/h·ft·F - W/m·K):	1.5 - 2.6
Thermal conductivity of Zircaloy (Btu/h·ft·F - W/m·K):	3.0 - 5.2
Hot leg inside diameter (ft - m):	3.5 - 1.067
Cold leg inside diameter (ft - m):	2.5 - 0.762
Volume of one hot leg (ft^3 - m^3):	138 - 3.9078
Volume of one cold leg (ft^3 - m^3):	224 - 6.343
Total peaking factor:	1.15

Steam generator (SG) data (BU - SI):	
Number of steam generators:	2
Number of tubes per SG:	8485
Tube inside diameter (in - cm):	0.654 - 1.66

Tube outside diameter (in - cm):	0.750 - 1.905
Volume of the SG inlet plenum (ft^3 - m^3):	250 -7.079
Volume of the SG outlet plenum (ft^3 - m^3):	250 - 7.079
Inlet plenum hydraulic diameter (ft - m):	7.6 - 2.316
Outlet plenum hydraulic diameter (ft - m):	7.6 - 2.316
Steam dome pressure (psia - MPa):	880 - 6.067
Feedwater pressure (psia - MPa):	1095 - 7.5
Feedwater temperature (F - C):	440 - 227
Tube material:	Stainless steel
Boiling heat transfer coefficient ($Btu/h{\cdot}ft^2{\cdot}F$ - $W/m^2{\cdot}K$):	6400 - 36340

Pressurizer data (BU - SI):

Geometry:	Circular cylinder
Steam dome Pressure (psia - MPa):	2250 - 15.51
Volume (ft^3 - m^3):	1500 - 42.477
Height (ft - m):	30 - 9.15
Water level (ft - m):	18 - 5.486
Wall thickness (in - cm):	4.5 - 11.43
Insulation thickness (in - cm):	0.00
Wall material:	Carbon Steel
Number of Relief Valves:	2
Relief valve flow area (ft^2 - cm^2):	0.01 - 0.01
Relief valve discharge coefficient	0.61
Ambient temperature (F - C):	90 - 32
Ambient pressure (psia - kPa):	14.7 - 101.35

Balance of plant data (BU - SI):

Total pumping power (condensate, booster, heater, and feewater) (MW):	190
Condenser Pressure (in Hg - mm Hg):	26 - 660
Circulating water inlet temperature (F - C):	60
Circulating water flow rate (lbm/h - kg/s):	5.2E8 - 65,520

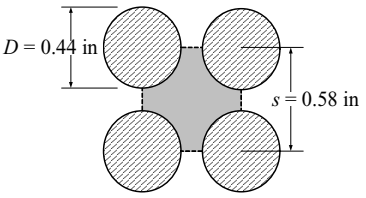

Find the answer to the following questions:

1. The centerline temperature in an average fuel rod
2. The centerline temperature in the fuel rod located in the hot assembly

3. Total power developed by the turbine (MW). Assume $\eta_{turbine} = 100\%$
4. The core total ΔP due to skin friction and the core total loss coefficient ($K = \Sigma K_i$)
5. The overall heat transfer coefficient in SG (a: assume feedwater is saturated, b: fouling = 0)
6. The average tube length of one SG (for questions 5 and 6 use Equations VIa.1.1 and VIa.2.12)
7. Pressure drop across the primary side of the SG (i.e., from the hot leg inlet to the outlet to cold leg)
8. The ΔP across the reactor coolant pump and the total power used by a reactor coolant pump
9. The temperature rise of the circulating water
10. We open one of the pressurizer relief valves. Find the maximum flow rate through the valve if one of the pressurizer relief valves is lifted.
11. Find the steam mass flow rate through the relief valve and the pressurizer pressure versus time if the relief valve is stuck open for one minute. Assume that the pressurizer is isolated from the rest of the reactor.